การหาอายุรอยทางการแบ่งแยกนิวเคลียสของอะพาไทต์หินตะกอนเนื้อเศษหินซิลิกามีโซโซอิกจากกลุ่มหินโคราชในเทือกเขาภูพาน ภาคตะวันออกเฉียงเหนือของประเทศไทย

นายอภิวุฒิ วีรวินันทนกุล

วิทยานิพนธ์นี้เป็นส่วนหนึ่งของการศึกษาตามหลักสูตรปริญญาวิทยาศาสตรมหาบัณฑิต
สาขาวิชาธรณีวิทยา ภาควิชาธรณีวิทยา
คณะวิทยาศาสตร์ จุฬาลงกรณ์มหาวิทยาลัย
ปีการศึกษา 2560

APATITE FISSION TRACK DATING OF MESOZOIC SILICICLASTIC ROCKS FROM KHORAT GROUP IN PHU PHAN MOUNTAIN RANGE, NORTHEASTERN THAILAND

Mr. Apivut Veeravinantanakul

A Thesis Submitted in Partial Fulfillment of the Requirements
for the Degree of Master of Science Program in Geology
Department of Geology
Faculty of Science
Chulalongkorn University
Academic Year 2017

Thesis Title	APATITE FISSION TRACK DATING OF MESOZOIC SILICICLASTIC ROCKS FROM KHORAT GROUP IN PHU PHAN MOUNTAIN RANGE, NORTHEASTERN THAILAND
By	Mr. Apivut Veeravinantanakul
Field of Study	Geology
Thesis Advisor	Associate Professor Pitsanupong Kanjanapayont, Dr.rer.nat.
Thesis Co-Advisor	Professor Punya Charusiri, Ph.D.

Accepted by the Faculty of Science, Chulalongkorn University in Partial Fulfillment of the Requirements for the Master's Degree

.....Dean of the Faculty of Science

(Professor Polkit Sangvanich, Ph.D.)

THESIS COMMITTEE

.....Chairman

(Professor Montri Choowong, Ph.D.)

.....Thesis Advisor

(Associate Professor Pitsanupong Kanjanapayont, Dr.rer.nat.)

.....Thesis Co-Advisor

(Professor Punya Charusiri, Ph.D.)

.....Examiner

(Assistant Professor Vichai Chutakositkanon, Ph.D.)

.....External Examiner

(Prinya Putthapiban, Ph.D.)

อภิวุฒิ วีรวินันทนกุล : การหาอายุรอยทางการแบ่งแยกนิวเคลียสของอะพาไทต์หินตะกอนเนื้อเศษหินซิลิกามีโซโซอิกจากกลุ่มหินโคราชในเทือกเขาภูพาน ภาคตะวันออกเฉียงเหนือของประเทศไทย (APATITE FISSION TRACK DATING OF MESOZOIC SILICICLASTIC ROCKS FROM KHORAT GROUP IN PHU PHAN MOUNTAIN RANGE, NORTHEASTERN THAILAND) อ.ที่ปรึกษาวิทยานิพนธ์หลัก: รศ. ดร. พิษณุพงศ์ กาญจนพยนต์, อ.ที่ปรึกษาวิทยานิพนธ์ร่วม: ศ. ดร. ปัญญา จารุศิริ, หน้า.

การสำรวจภาคสนามและการรับรู้ระยะไกลได้ถูกนำมาใช้ในการทำแผนที่หินตะกอนเนื้อเศษหินซิลิกามีโซโซอิกของเทือกเขาภูพานทางภาคตะวันออกเฉียงเหนือของประเทศไทย โดยผลจากการทำลำดับชั้นหินพบว่าเทือกเขาภูพานประกอบด้วย 5 หมวดหิน ได้แก่หมวดหินภูกระดึงที่มีความหนาเฉลี่ย 93 เมตร หมวดหินพระวิหารที่มีความหนาเฉลี่ย 64 เมตร หมวดหินเสาขัวที่มีความหนาเฉลี่ย 63 เมตร หมวดหินภูพานที่มีความหนาเฉลี่ย 84 และหมวดหินโคกกรวดที่มีความหนาเฉลี่ย 49 เมตร และนอกจากนี้ข้อมูลจากสนามและการรับรู้ระยะไกลแสดงให้เห็นว่าชั้นหินมีการเปลี่ยนแปลงโครงสร้างเป็นชุดของชั้นหินโค้งรูปประทุนและชั้นหินโค้งรูปประทุนหงายที่มีแนวการวางตัวในทิศตะวันตกเฉียงเหนือ-ตะวันออกเฉียงใต้ และในขณะเดียวกันภาคตัดขวางทางธรณีวิทยาในพื้นที่ศึกษาได้แสดงให้เห็นว่าชั้นหินคดโค้งขนาดใหญ่ถูกแทนที่ด้วยรอยเลื่อนตามแนวระดับขนาดเล็กที่มีการเลื่อนแบบซ้ายเข้า จากตัวอย่างหินกลุ่มหินโคราชทั้งหมด 21 ตัวอย่าง ได้ถูกเก็บมาเพื่อวิเคราะห์ศิลาวรรณาและหาอายุรอยทางการแบ่งแยกนิวเคลียของอะพาไทต์ โดยที่ผลจากการศึกษาศิลาวรรณาพบว่าเป็นหินทรายที่เนื้อละเอียดมากจนถึงเนื้อปานกลางชนิดเฟลด์สปาร์ติกลิทอารีไนท์ ซับลิทอารีไนท์ และลิทอารีไนท์ และจากข้อมูลศิลาวรรณาร่วมกับการวิเคราะห์ส่วนประกอบทางแร่ของหินจากควอตซ์ เฟลด์สปาร์ และเศษหินบ่งบอกถึงต้นกำเนิดของตะกอนว่ามาจากการสึกกร่อนของภูเขาที่ยกตัว ซึ่งคาดว่าแหล่งต้นกำเนิดของตะกอนมาจากแนวคดโค้งเลย-เพชรบูรณ์ และแนวคดโค้งตรังซอน สำหรับตัวอย่างที่นำมาศึกษามีลักษณะเป็นหินตะกอนเนื้อเม็ดที่มีตัวเชื่อมประสานคือซิลิกาและแคลเซียม ที่ประกอบด้วยควอตซ์ประมาณ 72.7% เฟลด์สปาร์ประมาณ 3.6% และเศษหินประมาณ 23.7% และมีแร่ประกอบหินอันดับรองที่สำคัญคือ อะพาไทต์ และเซอร์คอน โดยที่อะพาไทต์มีลักษณะเป็นแท่งยาวและปรากฏเป็นเม็ดแร่กระจัดกระจายในหิน จากอะพาไทต์ประมาณ 120 เม็ดจาก 6 ตัวอย่างได้ถูกนำมาวิเคราะห์หาอายุรอยทางการแบ่งแยกนิวเคลียส เมื่อนำผลอายุที่ได้จากการศึกษานี้ร่วมกับการงานวิจัยเก่าแสดงให้เห็นสิ่งที่น่าสนใจ และสามารถจำแนกอายุรอยทางการแบ่งแยกนิวเคลียสของอะพาไทต์จากเทือกเขาภูพานและพื้นที่ข้างเคียงได้สามช่วง ได้แก่ 78 ถึง 60 ล้านปี 55 ถึง 42 ล้านปี และอ่อนกว่า 37 ล้านปี โดยช่วงแรก 78 ถึง 60 ล้านปี โดยช่วงแรก 78 ถึง 60 ล้านปี ซึ่งเป็นช่วงที่เกิดเหตุการณ์ธรณีแปรสัณฐานแบบบีบอัดในทิศตะวันออกเฉียงเหนือและตะวันตกเฉียงใต้ที่กระทำต่อที่ภูมิภาคโคราชอันก่อให้เกิดโครงสร้างแปลงรูปในพื้นที่ศึกษา ในบางครั้งโครงสร้างประทุนภูพานได้เกิดขึ้นและอาจทำให้เกิดแอ่งตะกอนสองแอ่งบนภูมิภาคโคราชในช่วงเวลานี้ ช่วงที่สอง 55 ถึง 42 ล้านปี ซึ่งสอดคล้องกับเหตุการณ์การยกตัวและสึกกร่อนทั้งภูมิภาคโคราช และยกตัวขึ้นมาเป็นที่ราบสูงโคราช และช่วงที่สาม อ่อนกว่า 37 ล้านปี ซึ่งสอดคล้องกับการเกิดรอยเลื่อนแนวระดับที่เกิดขึ้นซ้อนทับบนโครงสร้างประทุนภูพานจากการหมุนตามเข็มนาฬิกาของแผ่นอนุทวีปอินโดจีน จากผลการศึกษานี้ร่วมกับงานวิจัยเก่าแสดงให้ว่าเทือกเขาภูพานยังมีอัตราการยกตัวประมาณ 0.0139 มิลลิเมตรต่อปี (หรือ 13.9 เมตรต่อล้านปี)

ภาควิชา ธรณีวิทยา	ลายมือชื่อนิสิต .....
สาขาวิชา ธรณีวิทยา	ลายมือชื่อ อ.ที่ปรึกษาหลัก .....
ปีการศึกษา 2560	ลายมือชื่อ อ.ที่ปรึกษาร่วม .....

5772206923 : MAJOR GEOLOGY
KEYWORDS: APATITE FISSION TRACK DATING / SANDSTONE / KHORAT GROUP / EXHUMATION / PHU PHAN RANGES

APIVUT VEERAVINANTANAKUL: APATITE FISSION TRACK DATING OF MESOZOIC SILICICLASTIC ROCKS FROM KHORAT GROUP IN PHU PHAN MOUNTAIN RANGE, NORTHEASTERN THAILAND. ADVISOR: ASSOC. PROF. PITSANUPONG KANJANAPAYONT, Dr.rer.nat., CO-ADVISOR: PROF. PUNYA CHARUSIRI, Ph.D., pp.

Field and remote-sensing investigations have been performed for mapping the Mesozoic siliciclastic rocks of the Phu Phan Ranges (PPR), northeastern Thailand. Stratigraphically, the PPR study area has been remapped and is occupied by 5 distinct successive formations, including the Phu Kradung Formation with the average thickness of 93 m, the Phra Wihan Formation with the average thickness of 64 m, the Sao Khua Formation with the average thickness of 63 m, the Phu Phan with the average thickness of 84 m, and the Khok Kruat with the average thickness of 49 m. Results on field and remote sensing analyses reveal that the PPR rocks are structurally deformed into series of anticlines and synclines with the NW-SE trend. Geological transects have been performed over the PPR study area. It has been recognized that the major fold has been displaced by NE-SW, short left-lateral strike slip faults. A total of 21 samples of the Khorat Group rocks have been collected for petrographic and apatite fission track (AFT) analyses. Petrographically, all the samples are very fine- to medium-grained sandstones, viz. feldspathic litharenite and litharenite. The sandstone petrography and modal analysis of quartz, feldspar, and lithic fragments points to the provenance of recycled orogen. It is considered that the source regions are the Loei-Phetchabun and the Truong Son Belts. The studied samples have essentially clastic textures with siliceous and calcareous cements and contain abundant quartz (av. 72.7%) with minor feldspar (av. 3.6%) and rock fragments (av. 23.7%). Apatite and zircon are significant accessories. Apatite invariably forms long prismatic habits and occurs as discrete detrital grains. About 120 grains from qualified 6 samples have been analyzed for fission track dating. The current AFT result from this study along with those of the previous studies reveals an interesting scenario. Three age ranges of the PPR and surrounding regions have been recognized viz., 78 to 60 Ma, 55 to 42 Ma, and younger than 37 Ma. The first episode (78 – 60 Ma) corresponds to the tectonic movement in response to the NE–SW compressive stress within the Khorat region, giving rise to the major deformed structure in the study area. Perhaps the Phu Phan anticlinal structures have been formed. Two successive basins within the Khorat region may have been developed at this stage. The second episode (55 – 42 Ma) indicates an extensive exhumation (major uplift and erosion) developed within the whole Khorat region, becoming a Khorat Plateau. The final episode (<37 Ma) is marked by the minor movement along the strike-slip fault which slightly displaced the Phu Phan anticlinal structure in response to the clock-wise rotation of the Indochina block. The AFT results from this current and previous studies advocate an average exhumation rate of the Phu Phan Mountain range to be *ca.* 0.0139 mm/yr (or 13.9 m/Ma).

Department:	Geology	Student's Signature	.....
Field of Study:	Geology	Advisor's Signature	.....
Academic Year:	2017	Co-Advisor's Signature	.....

ACKNOWLEDGEMENTS

This research would not have been possible without the help of a number of people. I would like to express my sincere thanks and gratefulness to everyone involving in this thesis.

First of all, I would like to thank my thesis advisor Associate Professor Pitsanupong Kanjanapayont, Dr.rer.nat. and co-advisor Professor Punya Charusiri, Ph.D. for outstanding advice, suggestions, kind supports and treasured guidance throughout the study. Besides, I would like to appreciate the thesis committees for their recommendations to improve this thesis. The Department of geology, Chulalongkorn University should also be recognized for furnishing facilities for the study.

Secondly, I sincerely thank PTTEP to fund the research grant for supporting field investigation and collection, chemicals, and travelling expenses to Kanazawa University, Japan.

For the laboratory work during in Japan, I would like to appreciate to Prof. Noriko Hasebe, Ph.D., specialist in geochronology from Institute of Nature and Environmental Technology, Kanazawa University, Japan, to provide a scholarship (JASSO) for the accommodation in Japan and teach about the fission track dating theory and procedure to do for this thesis with kindness.

Furthermore, I also would like to thank to Department of Mining and Petroleum Engineering, Faculty of Engineering, Chulalongkorn University for mineral separation processes.

Moreover, I am thankful to Mr. Arak Sangsomphong, Mr. Sitichok Kamrungwat, Mr. Norarat Boonkanpai, and Ms. Chonnipha Fakseangsa for providing geological data and supporting me during in field work. I am grateful Mr. Preeda Tapiang to help the mineral separation process, Mr. Pannaruj Akephattharaphaibul for giving me advices in petrography, and other seniors and friends studying in the master degree of science in geology and earth sciences program at Chulalongkorn University for helping in preparation all documents.

Finally and most importantly, I am appreciative to my parents and my elder brother without who's moral and work support, this work would not have been successfully finished.

CONTENTS

Page

Page

Page

Page

LIST OF TABLES

Page

LIST OF FIGURES

Page

Chapter 1 Introduction

1.1 Rational

This thesis investigates the Mesozoic – Cenozoic exhumation history of Khorat Plateau in northeastern Thailand. This area is one of the significant parts of tectonism in Thailand and is the part of Indochina block. Thailand is a structurally complex region that has been deeply affected by the Late Cretaceous/Early Tertiary Himalayan Orogeny. As a distal response to this major mountain building event, Thailand has developed a numerous of both offshore and onshore Tertiary basins that being exploited for their hydrocarbon and gas resources. The timing of basin formation and subsequent inversion is, therefore, of relevance to the petroleum industry for future exploration.

Khorat Plateau is an area which was affected from the tectonic events that created many folding structures and faults and exhumed later in Cretaceous and Cenozoic. Phu Phan Mountain Range which is located in the north-center of Khorat Plateau, contains plentiful folding like anticlinal and synclinal structure. Besides, the area has exhumation histories after many uplift events. An apatite fission-track (AFT) study has been carried out to provide an insight into the timing and mechanism that drove basin formation during the Tertiary.

Fission track dating is the radiometric dating technique used to understand the thermal history of the area which was affected from tectonism or burial metamorphism. This method involves using the spontaneous tracks decay of U-238 in common accessory minerals to date the time of rock cooling below the closure temperature (Gleadow et al., 1986). For fission track dating, the common minerals which currently use for analysis are apatite, zircon, and sphene (Fleischer and Price, 1964; Gleadow et al., 2002; Tagami et al., 1988) that can be found in the various kinds of rocks. Generally, they have different temperature of partial annealing, that is to say, 60-120 °C for apatite, 230-250 °C for zircon and 300 °C for sphene.

Carter et al. (1995) is the first person who started investigating the thermal history of sandstone on Khorat Plateau by using apatite and zircon fission track. His

ZFT study revealed the maximum age of possibly stratigraphic age of Phra Wihan Formation which ranged from 125 to 160 Ma. However, his AFT study is still going on. After that, Racey et al. (1997) and Upton (1999) continued studying the AFT in Khorat Group sandstone, mainly in Huai Hin Lat, Nam Phong, Phu Kradung, Phra Wihan, Sao Khua, Phu Phan, and Khok Kraut Formation, and some of the granite on the western edge of Khorat Plateau and northwestern part of Phu Phan Mountain Range.

The studies found that the ages obtained from AFT were younger than their biostratigraphic age. Therefore, their study was expected that the AFT age should provide the history of exhumation (uplift and erosion) and contribute the AFT age range from 31±3 ma from Triassic granite to 84±8 ma from Khorat Group sandstone with denuded at 45-62m Ma^{-1} following 275-440 m of tectonic uplift on Phu Phan Mountain. Moreover, Carter and Moss (1999) and Carter and Bristow (2003) continued studying on ZFT dating together with U-Pb zircon dating.

Their studies show the relationship of two methods for providing unique provenance information in Khorat Plateau where the Khorat Plateau Basin sediments might have originated from a reactivate event that affected a mature orogenic hinterland that exhumed slowly and reached shallow crustal levels by the Early to Middle Jurassic, then exposed to an Early Cretaceous event that invigorated erosion to create a period of enhanced sediment supply to the basin.

In this study, apatite will be used for fission track dating in order to know the youngest possible age in Khorat Group sandstone.

1.2 The study area

The location of study area covers on Phu Phan Mountain Range where the Khorat Plateau, Northeastern Thailand is located. The area under investigation lies within the latitudes 17°10’03” N to 15°59’41” N and 16°40’16” N to 15°28’51” N and longitudes 104°00’31” E to 105°38’04” E and 103°36’12” E to 105°13’46” E (black box in Figure 1.1) which investigates only in Thailand. The study area is approximately 500 km northeast of Bangkok, the capital city of Thailand.

1.3 Objectives

1. To determine ages of apatite fission track dating method and

2. To compare the age obtained from apatite fission track dating results with the geological events.

1.4 Scope of study

This study is based solely upon the result of the interpreted AFT dating data. With this result in conjunction with those of the previous studies, Carter et al. (1995), Racey et al. (1997), and Upton (1999), the tectonic uplift of the study area has been delineated. Because the stratigraphy of the area under the investigation is complicated and its ages have not been consensus yet; therefore, in this study, only stratigraphy used by DMR (1999; 2000; 2001; 2004; 2007; 2008) has been applied.

1.5 Methodology

The methodology of the study is divided into 4 main steps, viz, planning and preparation of significant data, field investigation, laboratory analysis, and discussion and conclusion from the results. A flow chart of methodology for this study is presented in Figure 1.2.

1.5.1 Planning and preparation

The first step involves with data collection in order to contribute preliminarily available data about the regional study area and to prepare essential data for following steps. This step includes literature reviews from previous works, finding base maps (topographic map, geological maps 1:50,000, 1:250,000, 1:2,500,000, and lineament map), and obtaining the satellite images for selecting the study area and investigating route condition, and the other related to technical and nontechnical documents.

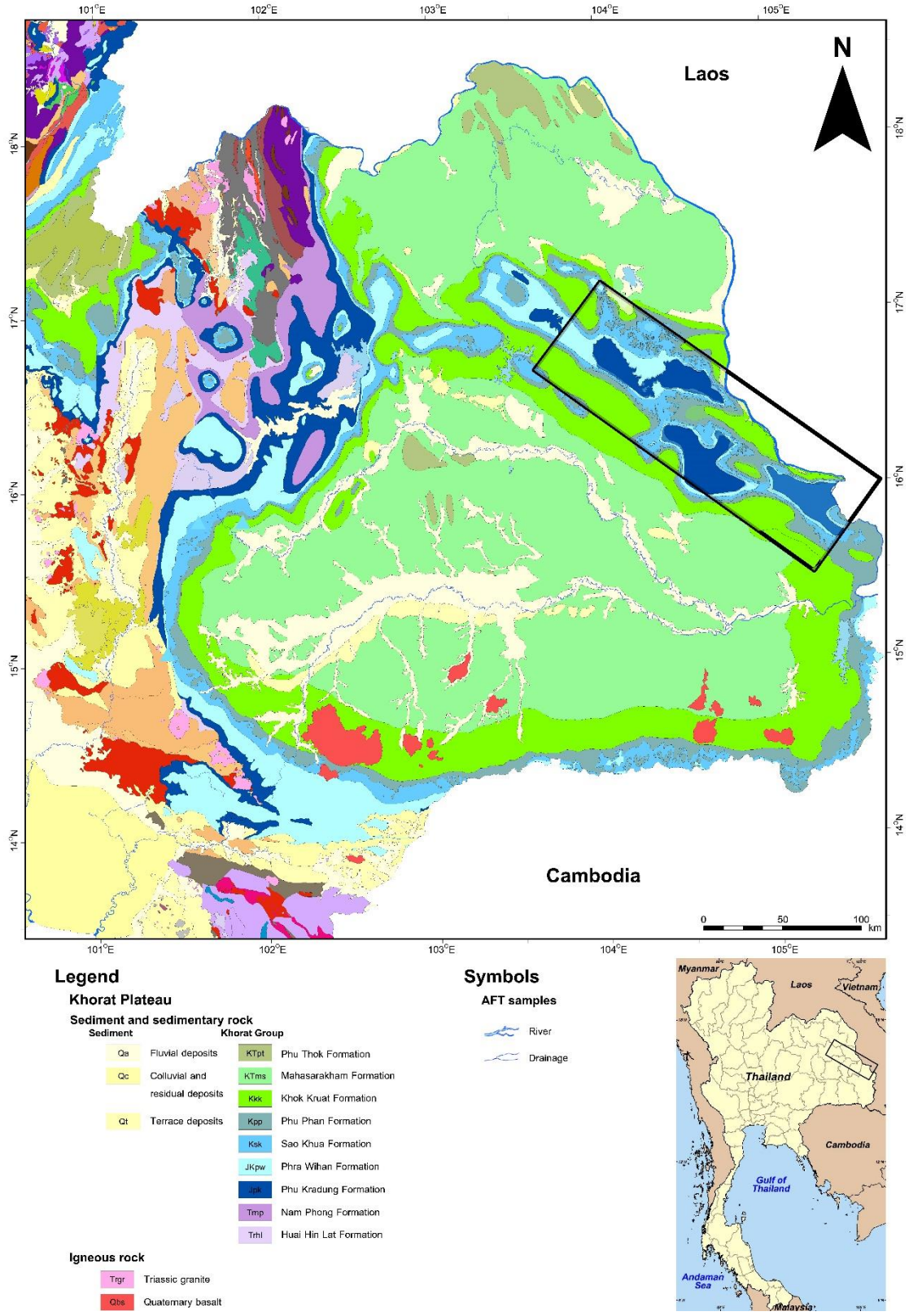

Figure 1.1 *A simplified geological map of northeastern Thailand based on 1:250,000 geological map of DMR (Department of Mineral Resources, 2007). The black box is the study area.*

1.5.2 Field investigation

This step begins after observing the conditions of study area from the first step. Basic geological data such as strike and dip angle of bed, cross-bed, rock strata, and sandstone samples from outcrops at the Phu Phan Mountain Range are collected for analyses and interpretation.

1.5.3 Laboratory analysis

Laboratory analysis is the third step with the main purpose of collecting sandstone samples for petrography and apatite fission track dating by Laser ablation induced couple plasma mass spectrometer (LA-ICP-MS) method following that of Hasebe et al. (2004), Hasebe et al. (2013) and Donelick et al. (2005). For more detail of apatite fission track dating procedure is in Chapter 3.

1.5.4 Discussion and conclusion

This stage includes unification of all results, including combining the previous works of geological structure, stratigraphic columns, paleocurrent data, on the Phu Phan Mountain Range and apatite fission track data on the whole Khorat Plateau in order to understand source of rock, the timing and rate of exhumation with geological structure events of the Phu Phan Mountain Range. Moreover, the previous geochronological data from apatite fission track dating, Ar-Ar dating, Rb-Sr dating, U-Pb dating, and U-Th/He dating after the late cretaceous to the present day along the major fault zone in Thailand are used for interpretation and discussion in order to know the tectonic implication.

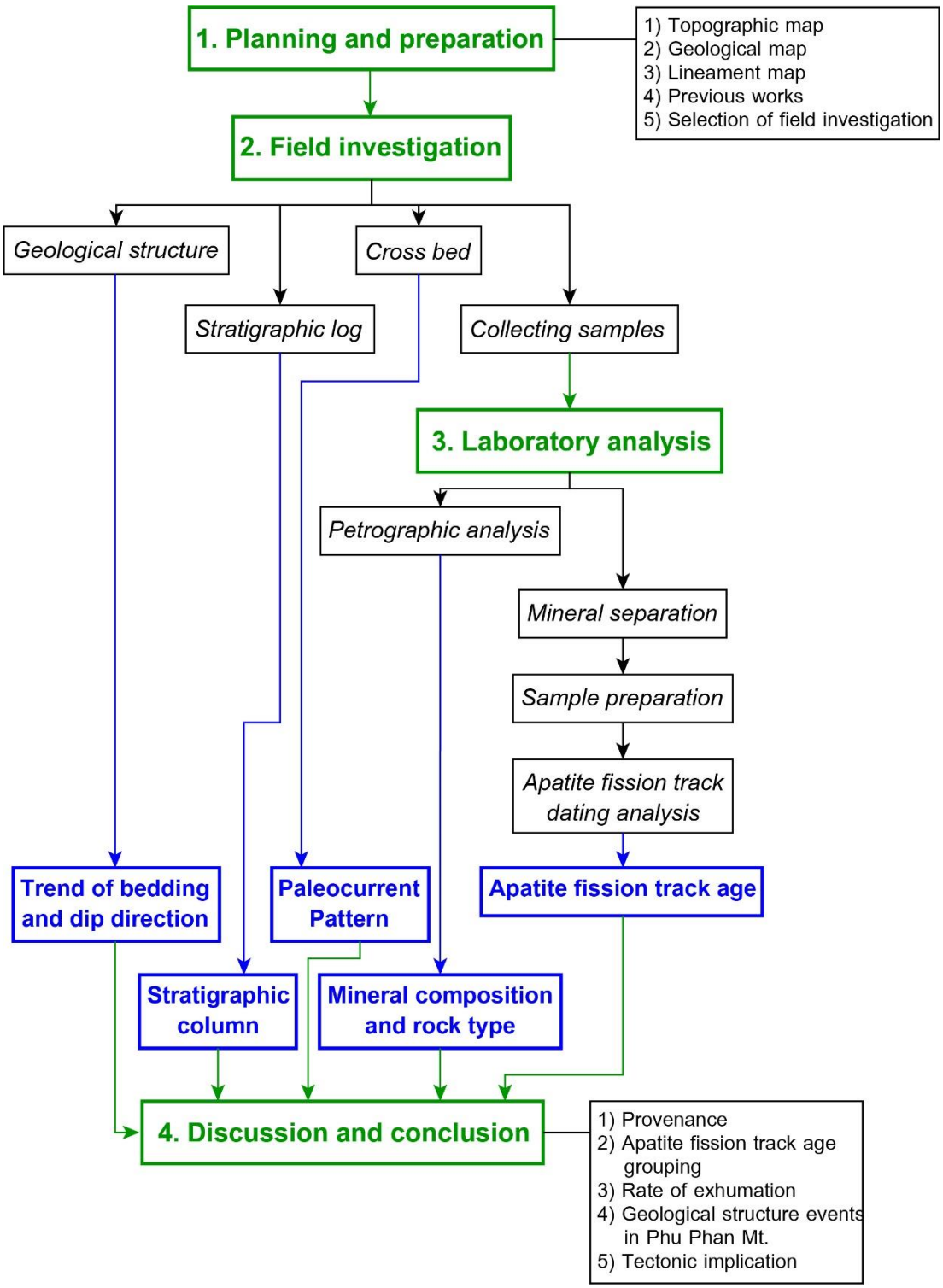

Figure 1.2 *Simplified flow chart showing investigation procedures for this study.*

1.6 Literature reviews

Carter et al. (1995) studied zircon fission track (ZFT) from sandstone in the western edge of the Khorat Plaeau to know the maximum depositional age of Phra Wihan Formation, Sao Khua Formation, and Khok Kruat Formation, which contributed 125±18 Ma, 160±6 Ma, and 133±13 Ma, respectively. Therefore, these 3 formations should be in Early Cretaceous rather than Middle Jurassic that was obtained from stratigraphy and fossil age. Moreover, apatite fission track (AFT) was performed in Phra Wihan Formation which provided the ages of 50±5 Ma, 53±6Ma, and 58±5 Ma.

Racey et al. (1997) investigated AFT dating from Phu Kradung Formation, Phra Wihan Formation, and Phu Phan Formation sandstone of the Khorat Group on the Khorat Plateau. The burial temperature of the area is above 120°C in 65 – 45 Ma (early to middle Tertiary) and 50 - 90°C in 35 – 20 Ma (late Tertiary) for the latest cooling temperature.

Upton (1999) observed the AFT dating from sandstone of Hua Hin Lat Formation, Nam Phong Formation, Phu Kradung Formation, Phra Wihan Formation, Sao Khua Formation, and Phu Phan Formation in the Khorat Group. The results, were interpreted with the data from Racey et al. (1997), provided AFT age range from ~70-50 Ma (late Cretaceous to early Tertiary) that is younger than depositional age and stratigraphical age which is the same period of Himalayan Orogeny. Moreover, the rate of cooling is 1.5±0.5°C per year and the rate of exhumation on western edge of the Khorat Plateau is 50 – 68 meters per year and 35 – 20 meters per year and the Phu Phan Mountain Range is 45 – 62 meters per year.

Carter and Moss (1999) acquired the ages of ZFT from Phra Wihan Formation and Phu Kradung Formation are 114±6 Ma and 141±17 Ma, respectively which informed the sediment on the Khorat Plateau possibly came from the Qinling Belt and the large basin parallel to the Mountain Range in the Lasa Plate and Eurasia Plate collision event during late Jurassic to early Cretaceous.

Carter and Bristow (2003) obtained ZFT age from Phu Kradung Formation sandstone on the Khorat Plateau equal to 141±17 Ma and 210±24 Ma that are in the timing of metamorphism of rock. Moreover, the U-Pb zircon dating was performed in

order to know the source of sediment that contributed the age equal to 2,456±4 Ma, 2001±4 Ma, 251±3 Ma, and 168±2 Ma that associated with the age of Qinling Belt in China.

Putthapiban (1984) reported fission track dating by using apatite, zircon, and sphene extracted from granitic rock in Phuket area. The fission track ages obtained from sphene and zircon contributed older ages than fission track age from apatite. Fission track age of the granite suites range from 57 to 53 Ma. The AFT analysis are from 3 samples containing sphene, 2 samples for zircon, and 5 samples for apatite. In addition, zircon fission track age obtained from 1 samples of granite pebble in Permo-Carboniferous pebbly mudstone is 64 Ma. Furthermore, apatite fission track ages from granite suites and granite pebble in Permo-Carboniferous pebbly mudstone range from 48 to 43 Ma.

Chapter 2 Geological Backgrounds

This chapter is divided into 3 parts, including physiography, regional structures and regional stratigraphy. Each part has been compiled using pre-existing data, the current remote-sensing, and airborne geophysical investigations.

2.1 Regional Physiography

The northeast Thailand (Figure 2.1) is a large area occupying an aerial extent of about 150,000 sq. km. It is a large plateau with an elevation ranging from 130 to 250 m above mean sea level. To the west of the plateau its physiography is bordered by the north-south trending Phetchabun Ranges. In the south the plateau is bordered by San Khampaeng and Phanom Dongrak Ranges with the main area tilting to the north. Regionally, the Khorat Plateau has the shape like a large basin and is separated by the long NW-trending Phu Phan Range. The Plateau is also subdivided into 2 sub-basins, namely Sakon Nakhon basin and Khorat basin (Figure 2.1).

Phu Phan Range

The Phu Pan Range is the long and narrow range almost in the middle portion of the Khorat Plateau and trends in the NW-SE direction. The range also extends to Savannakhet and Salavan in southern Lao PDR. Generally, it is a range of hills dividing the Khorat Plateau of the Esan region into two basins: the northern Sakhon Nakhon Basin, and the southern Khorat Basin. The Phu Phan Mountains rise above the Plateau and are not prominent. They straddle most of the Provinces of northern and eastern Isan, including Khon Kaen, Nong Bua Lamphu, Udon Thani, Sakon Nakhon, Nakhon Phanom, Kalasin, Roi Et, Maha Sarakham, Mukdahan, Amnat Charoen, and Ubon Ratchathani province (Figures 2.2 and 2.3).

The highest elevation of the Phu Phan Range is the 641-m high summit known as Phu Lang Ka. It is located in Nakhon Phanom Province. Other important peaks are 624 m high Phu Mai Hia in Mukdahan Province and the 563-m high summit known as Phu Langka Nuea in Nakhon Phanom Province.

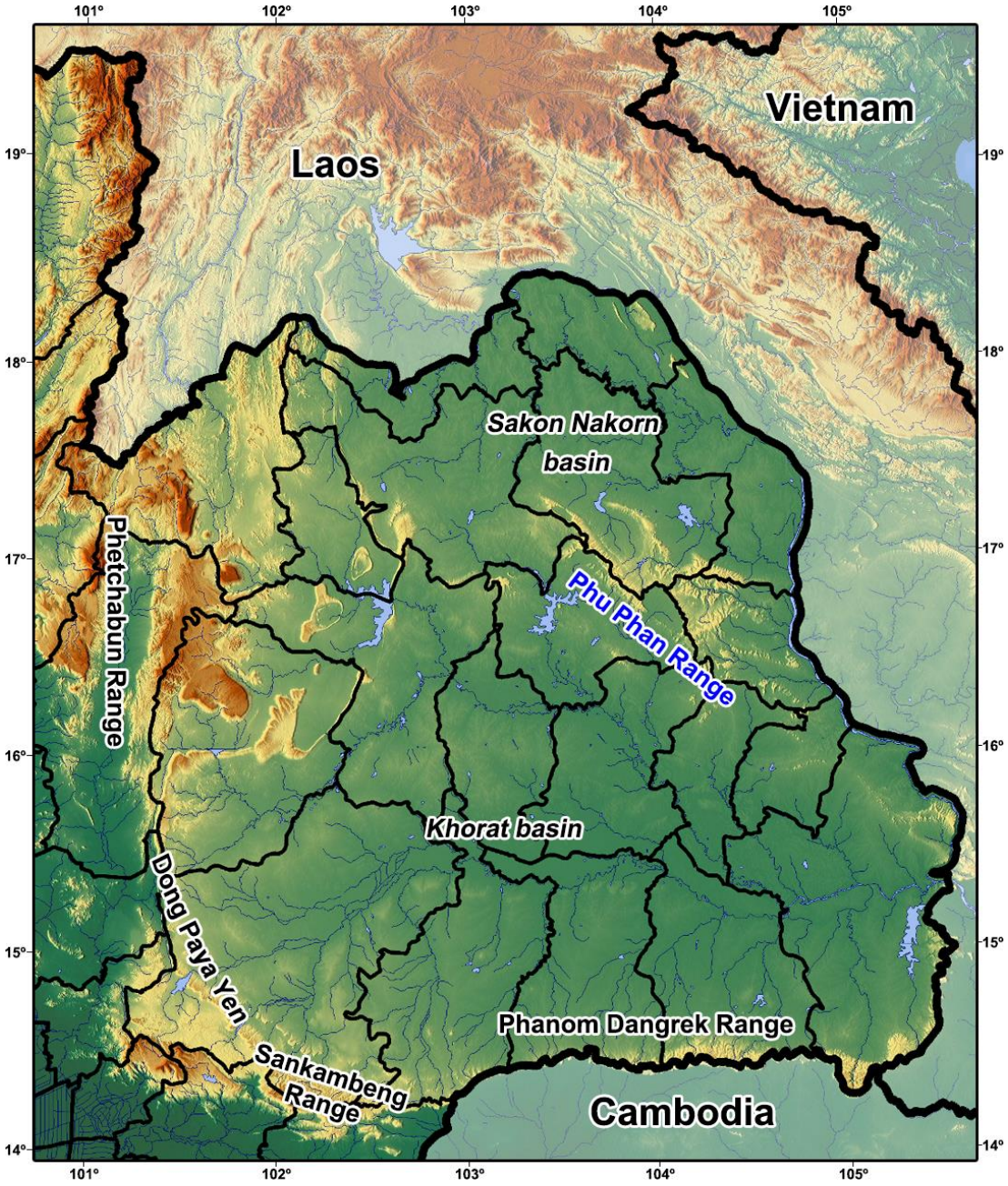

Figure 2.1 *Geographical map of Khorat Plateau, northeastern Thailand showing 2 basins are divided by Phu Phan Mountain Range on the center of plateau. (modified from http://www.freemapviewer.com/th/map/แผนที่-ประเทศไทย_795.html)*

Figure 2.2 *Phu Phan Mountains, Northeastern Thailand have been taken from Wat Tham Kham, Phannanikhom District, Sakonna Sakon Nakon Province. (http://en.wikipedia.org/wiki/Phu_Phan_Mountains).*

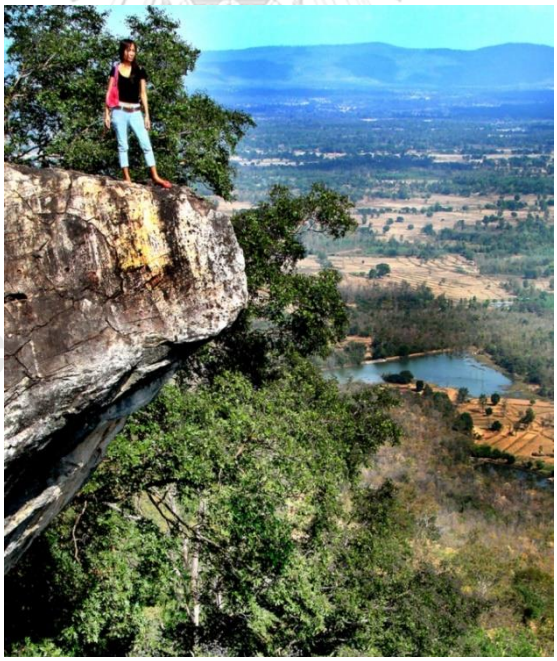

Figure 2.3 *The Phu Phan Range, and a beautiful lake, Nong Bua Lampu is rich of cultural attractions. The name Nong Bua Lampu appears in historical records as a rest venue for the Siamese Army during their march to fight against Vientiane in both the Ayuthaya and the Rattanakosin eras.*

2.2 Regional Stratigraphy

Northeastern Thailand (or the so-called “Isan” or “Esan” in some literatures) region is herein called the Khorat Plateau (or Esan) which occupies 200,000 km^2, or one third of the whole country. In general, the topography of the Khorat Plateau consists of low rolling hills bounded by mountains to the west, south and the middle of the region (Figure 2.1).

The surface data indicate the most area is covered by the Mesozoic sequence (the Khorat Group). Only the western rim, the outcrops, consists of Triassic (Huai Hin Lat Formationor Kuchinarai Group) and Permian rocks (Saraburi Group). The Khorat Group is a greater thickness unit, which is also found the continental sediments. The Huai Hin Lat Group is the fluvio-lacustrine clastics sediment, which seal the Triassic half-graben. The Kuchinarai Group is defined for the fluvio-lacustrine sediments, which deposited in the Triassic half-graben. The Saraburi Group comprises the sediments of shallow to deep marine depositional environments during the Permian (Figure 2.6 and 2.7). Figures 2.4 and 2.5 displays a geological map in the area of Khorat Plateau.

An unpublished report by Department of Mineral Resources (1999) on the petroleum potential assessment of northeastern Thailand divided the Mesozoic thick sedimentary pile of the Khorat Plateau region into 6 main groups or mega-sequences (Figure 2.8, 2.9 and 2.10).

The stratigraphic divisions are based almost entirely on bounding major unconformity surfaces and may be referred to as the tectono-stratigraphic units. The six groups are as follows:

Group VI Post-Himalayan Mega-sequences: Tha Chang Formation.

Group V Pre-Himalayan Mega-sequences: Phu Tok Formation, Maha Sarakham Formationand Khorat Group.

Group IV Pre-Indosinian II Mega-sequences: Huai Hin Lat Formation.

Group III Pre-Indosinian I Mega-sequences: Saraburi Group and Wang Saphung Formation.

Group II Pre-Variscan Mega-sequence Pak ChomGroup.

Group I Pre-Caledonian Mega-sequences: Na Mo Group.

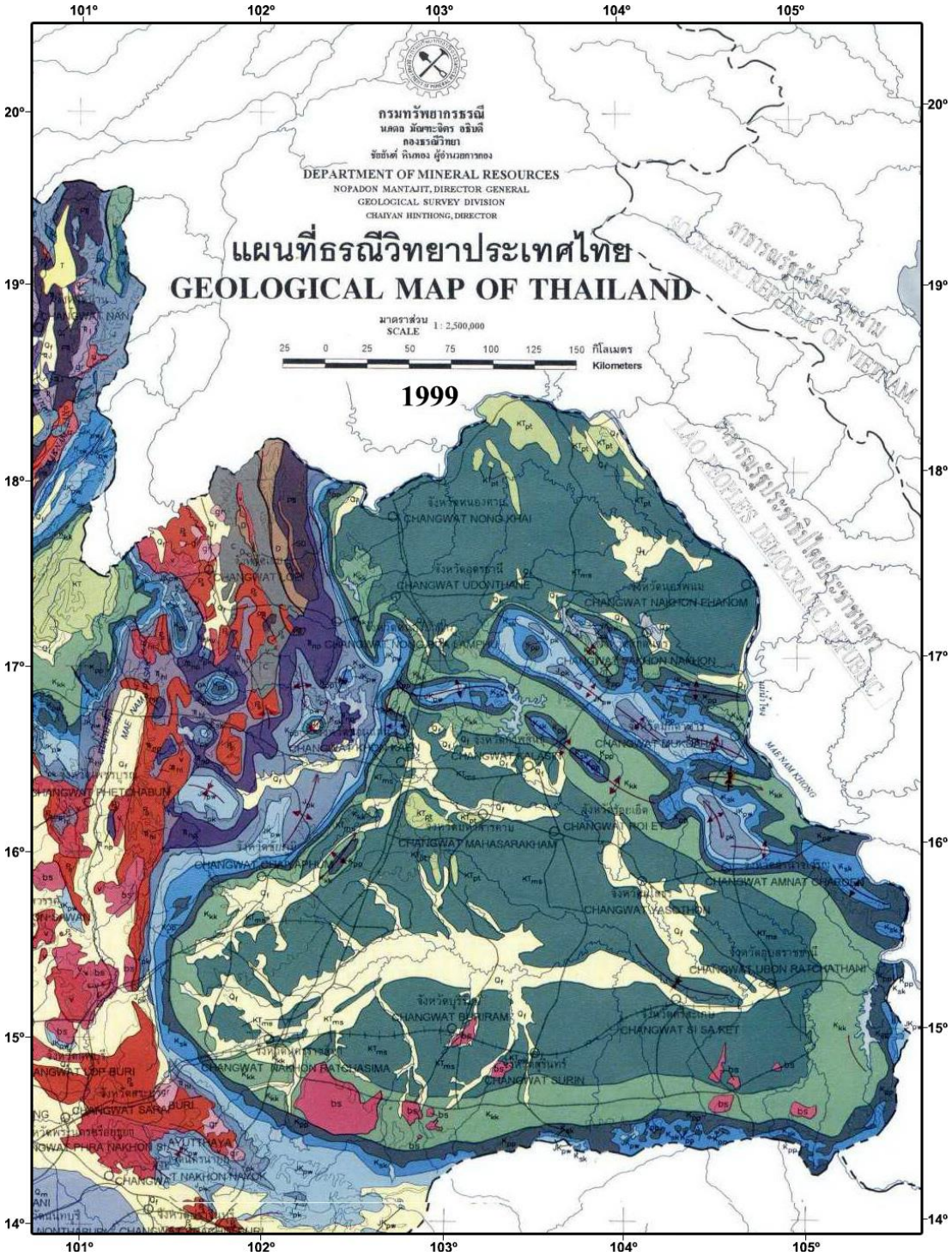

Figure 2.4 *Geological map based on Department of Mineral Resource geological map 1:2,500,000 of Northeast Thailand.*

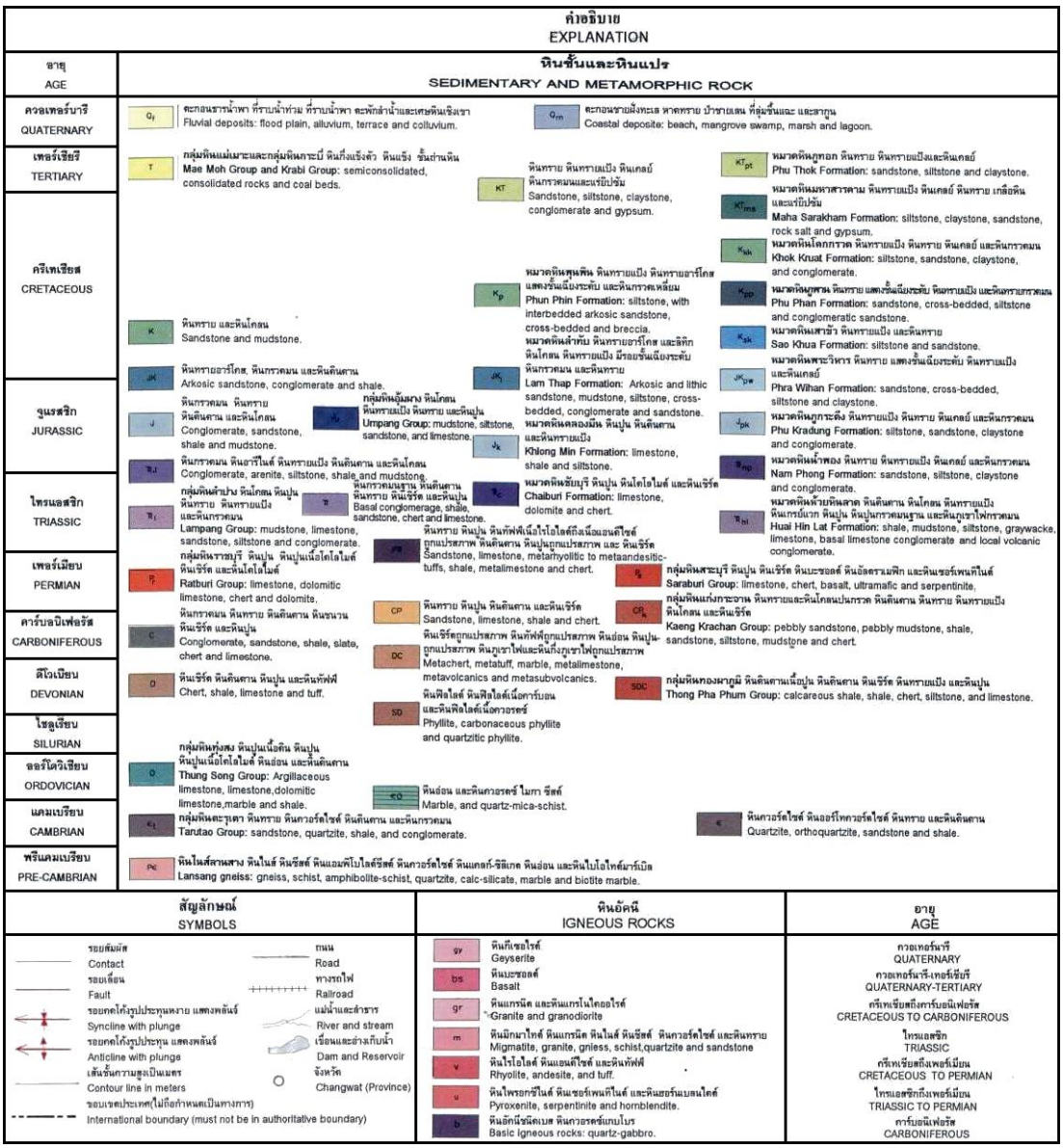

Figure 2.5 *The explanation of the geological map of Northeast Thailand for Figure 2.4.*

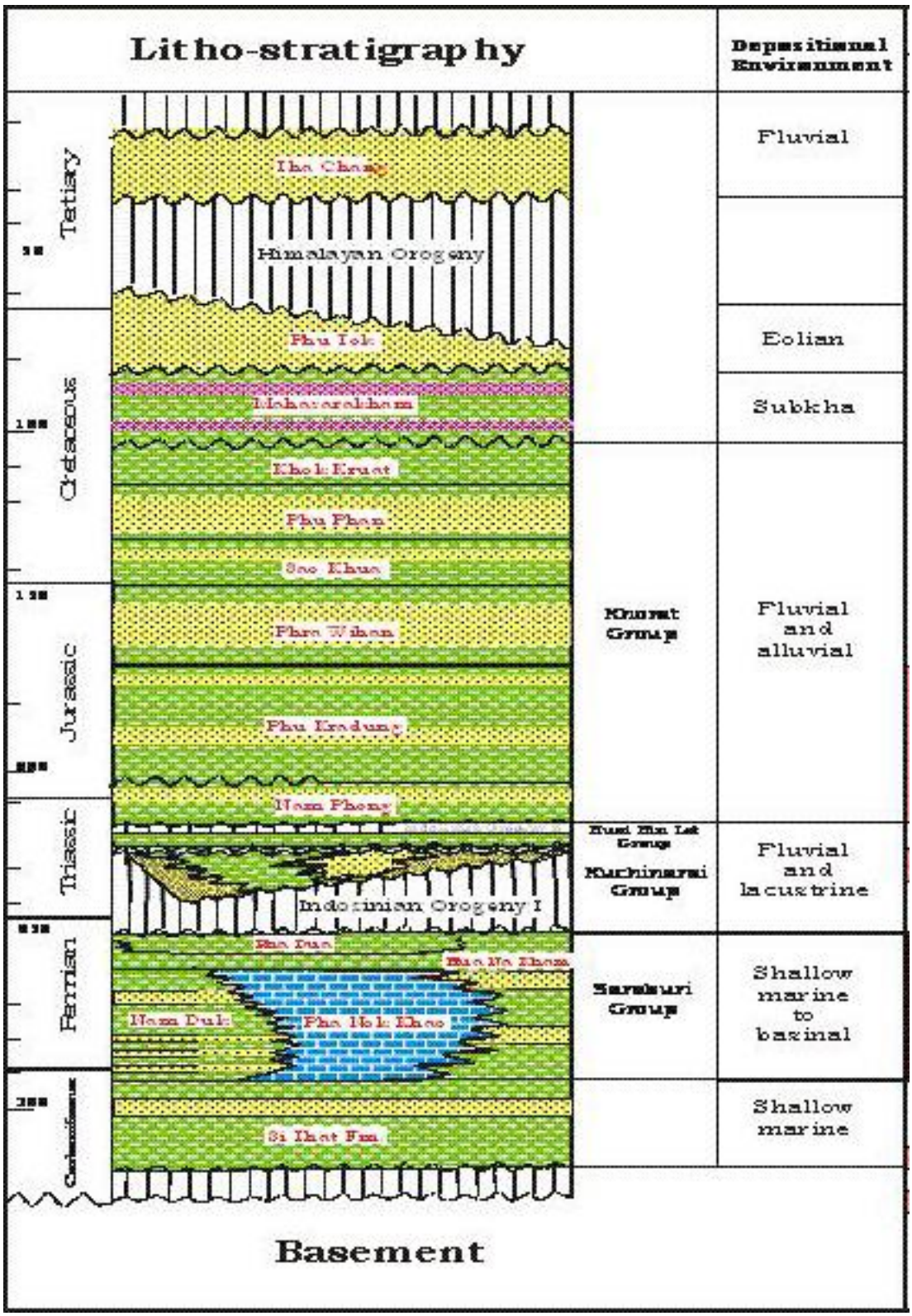

Figure 2 6 *Lithostratigraphy of the Khorat Plateau (modified from Sattayarak, 2005, Department of Mineral Fuel, 2005, Chantong, 2005 and Wanida 2006).*

Period		Lee (1923)	Brawn et al., (1953)	La Moreaux et al., (1956)	Ward and Bunnag (1964)		Iwai et al.,(1964; 1966)	Kobayashi et., al (1964)	Gardner et al., (1967)	Bunopas (1971)	DMR (1997)
Tertiary								Upper Khorat Series	(Salt F)		
Cretaceous	L		Khorat Series		Unnamed Rk		Lom Sak F		Maha Sarakham F		Phu Thok F
				Phu Phan m	The Khorat Group	Khok Kruat F					Maha Sarakham F
				Phra Vihan m			Ban Na Yo F	Middle Khorat Series			Khok Kruat F
	E			Phu Kradung m		Phu Phan F					Phu Phan F
			(Including marine Triassic limestone)			Sao Khua F	Phu Phan F	Lowest Khorat Series			Sao Khua F
Jurassic	U					Phra Vihan F					Phra Wihan F
	M						Phra Wihan F				Phu Kradung F
	L					Phu Kradung F	Phu Kra Dung F			Phu Kradung F (3 members)	
Triassic		Upper non-marine				Nam Phong F	Huai Hin Lat F			Nam Pha F	Nam Phong F
		Lower non-marine									Huai Hin Lat F

Figure 2.7 *Evolution of stratigraphic correlation of Khorat Group (DMR, 2011).*

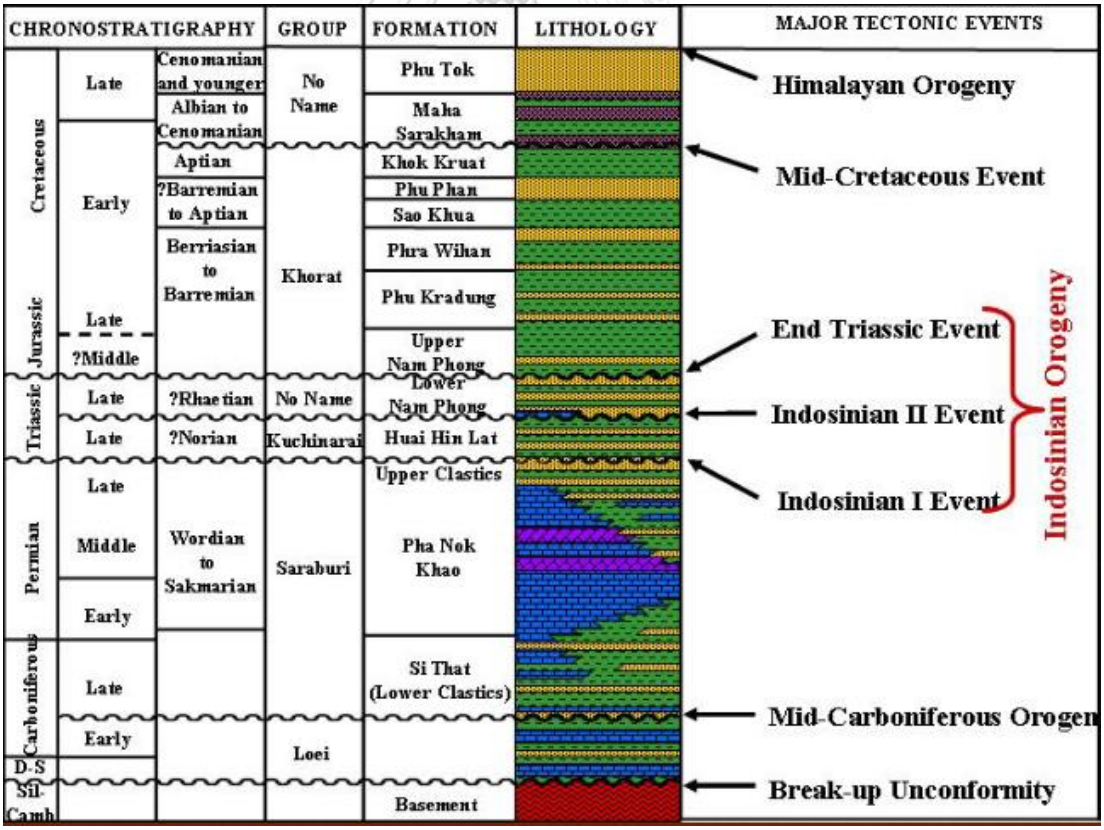

Figure 2.8 *Stratigraphy in the Khorat Plateau Region (Booth and Sattayarak, 2011).*

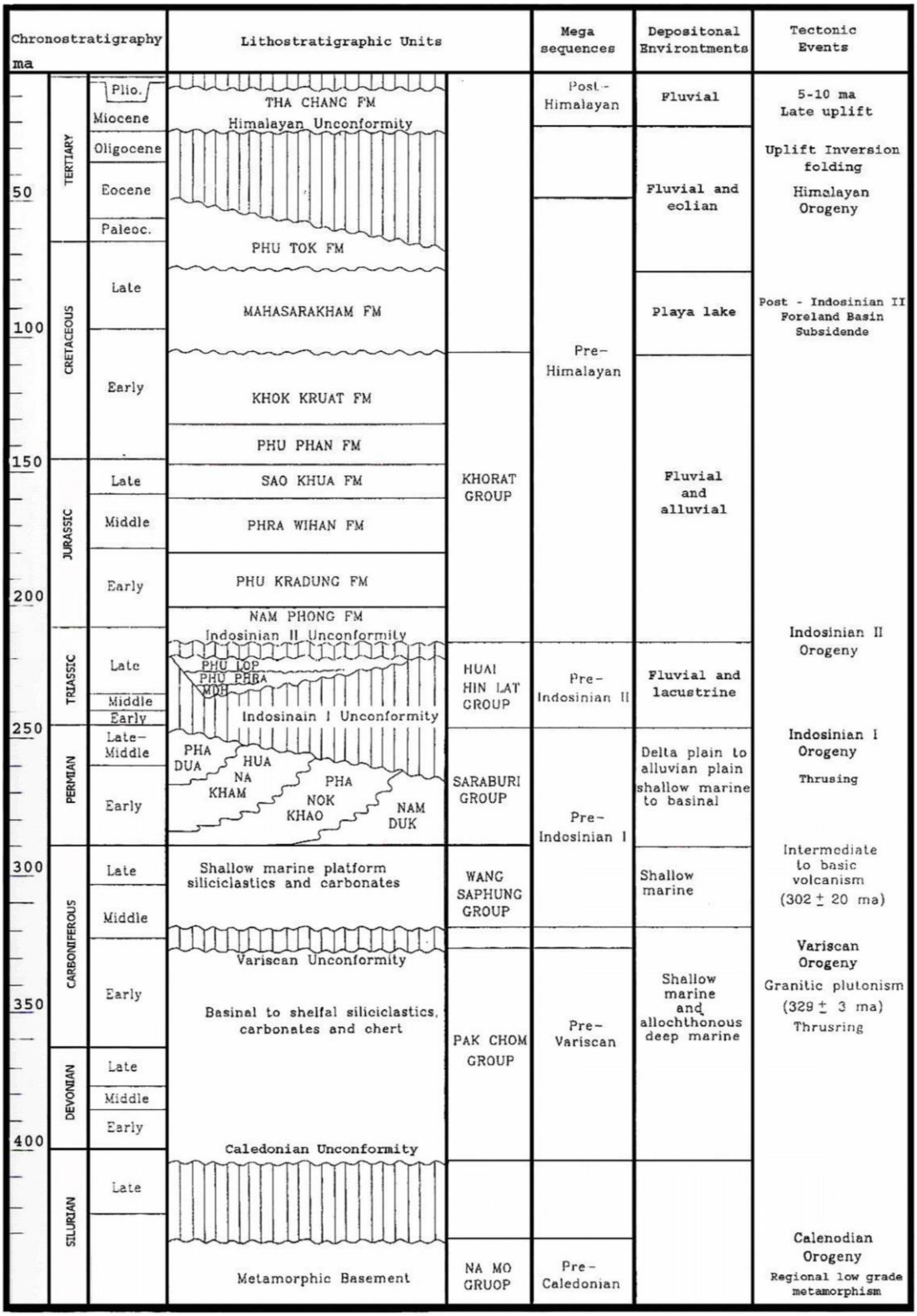

Figure 2.9 *Stratigraphy of the Khorat Plateau and related tectonic events (DMR, 1999).*

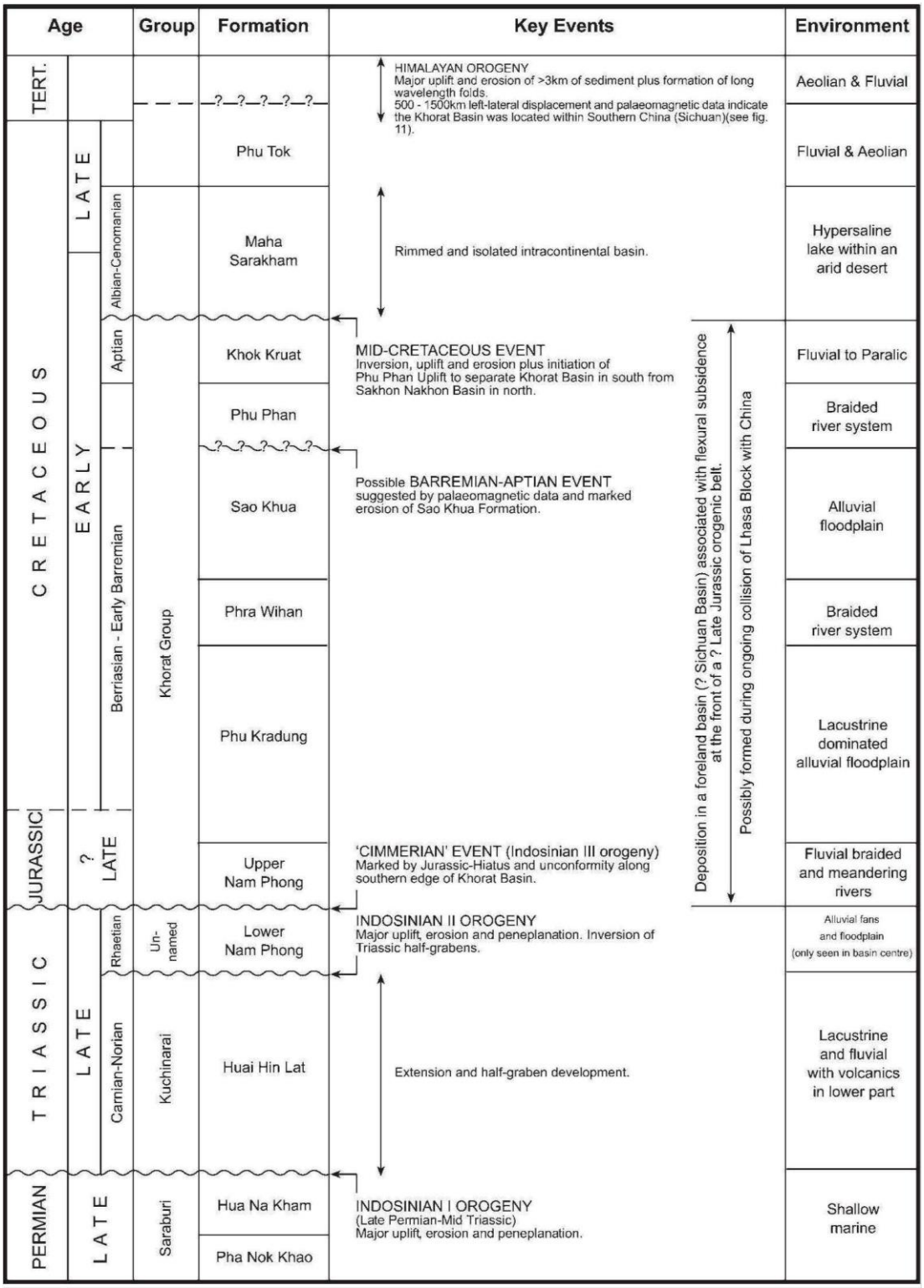

Figure 2.10 *Stratigraphic column for the Mesozoic of NE Thailand with the main depositional environments and key tectonic events (Racey, 2009)*

2.2.1 Na Mo Group

The Na Mo Group forms the metamorphic basement exposed in the Loei area, on the northwestern margin of the Khorat Plateau. It consists of low grade metamorphic rocks of the upper greenschist facies (phyllite, chlorite and pelitic schist, metatuff, and quartzite). The metamorphism is dated stratigraphically as resulting from the pre-Late Silurian (Caledonian) Orogeny.

2.2.2 Pre-Mesozoic Sequences

2.2.2.1 Pak Chom Group

The Pak Chom Group consists mainly of shallow marine sediments of diverse lithologies (such as limestone, greywacke, shale, conglomerate, and tuff). The Pak Chom Group unconformably overlies the Na Mo Group. It contains a prolific fauna indicating ages ranging from the Late Silurian to Serpukhovian (Early Carboniferous see Workman, 1975). The Pak Chom Group can be frequently detected in the subsurface below the Variscan Unconformity on seismic profiles.

2.2.2.2 Saraburi Group

The Saraburi Group can be subdivided into 4 units (in descending order): the Pha Dua, the Hua Na Kham, the Pha Nok Khao, and the Nam Duk Formations. These formations are partly coeval and represent sediments deposited in different environments ranging from delta plain, shelf platform, to deep basin.

The *Pha Dua Formation* consists of thin-bedded fine grained clastic sequence with dark shale and siltstone.

The *Hua Na Kham Formation* consists of intercalated light and dark gray siltstone, sandstone, claystone, and limestone.

The *Pha Nok Khao Formation* consists predominantly of massive to thick-bedded gray limestone and dolomite, and thin-bedded gray shale and black, nodular or thin-bedded chert may occur locally.

The *Nam Duk Formation* consists mainly of pelagic shale, clastic turbidites, and thin- bedded allodapic limestone.

2.2.2.3 Wang Saphung Formation

The Wang Saphung Formation conformably underlies the massive Permian Pa Nok Khao Formation. It has been informally called the “Lower Clastics” of the “Ratburi Group”. It can be delineated from the seismic profiles and commonly occupies a section between the base of the Pha Nok Khao Formation and the Variscan Unconformity. In the Loei area the Wang Saphung Formation unconformably overlies the Pak Chom Group in outcrop. Subsurface data on seismic profiles reveal that the base of the Wang Saphung Formation is marked by a major unconformity above either the Pak Chomor economic basement (metamorphic rocks). The Wang Saphung Formation consists largely of siliclastics (mainly conglomerate, shale, and sandstone) interbedded with limestones and volcanic rock.The rocks of this group are well exposed in the northwestern margin of the Khorat Plateau.

2.2.4 Huai Hin Lat Formation

Rocks of this mega-sequence unconformably overlies those of the Wang Saphung Formation. It is (the Huai Hin Lat Formation) unconformably overlain by mega-sequences of the Khorat Group. It consists mainly of clastics with minor intercalations of limestones and has been called the “Huai Hin Lat Formation”. Its age is Late Triassic based on invertebrates, vertebrates and plant fossils. Data from drilling wells in the northern Khorat Basin by oil companies indicate that the Huai Hin Lat Formation contains two intraformational unconformities. Hence the formation is raised to the Group status for subsurface workers and for oil companies. Three formations which are almost equivalent to the Huai Hin Lat Formation are also recognized. They are Phu Lop Formation, Phu Phra Formation and Mukdahan Formation.

The Phu Lop Formation consists mainly of siltstone sand shale, with a few sandstones. The interpretation of seismic profiles in the Phu Phra area indicates that the Phu Lop Formation overlies the undifferentiated unit of Phu Phra and Mukdahan Formations. The Phu Phra Formation consists predominantly of dark shale with minor amounts of sandstones and siltstones. The fine-grained sediments show varves, coaly plant remains, ripples and occasional sand-filled mud-cracks.

The Mukdahan Formation is considered to be the basal unit of the Huai Hin Lat Group. It consists largely of green to greenish gray volcanogenic sandstone and poorly sorted sandy conglomerate with intercalations of green siliceous tuff and tuffaceous shale.

2.2.5 Khorat Group

The Mega-sequence or the more famous name “the Khorat Group” consists of thick sequences of sedimentary units between the Indosinian II and the Himalayan Unconformity. The Himalayan Orogeny which caused the major unconformity in Northeastern Thailand is dated as Late Cretaceous to Miocene. The Pre-Himalayan Mega-sequence overlies the Pre-Indosinian II or older Mega-sequences. It comprises the Khorat Group, the Maha Sarakham Formation and the Phu Thok Formation respectively in ascending order. The total thickness of the Pre-Himalayan Mega-sequence is over 5,000 m.

The Khorat Group has been interpreted to represent Mesozoic non-marine deposition in an intracontinental basin, during a period of thermal subsidence that followed rifting and sediment deposition of Triassic rocks. Six formations constitute the Khorat group. It is estimated by DMR (1999) that the total original thickness is about 5 kilometers. The formations, from base to top, are the Nam Phong, Phu Kradung, Phra Wihan, Sao Khua, Phu Phan, and Khok Kruat Formations.

The Nam Phong Formation is characterized by thick to massive resistant beds of reddish brown sandstone, conglomerate and interbedded shale and reddish-brown claystone. It was deposited by meandering rivers with associated floodplain and over bank deposits. The age of this formation is Rhaetian (Upper Triassic). The thickness is 100-1,500 meters.

The Phu Kradung Formation is composed of reddish to grey or white thick bed calcareous mudstone/siltstone, limestone, high radioactive reddish-brown claystone, siltstone and sandstone. Its paleoenvironment is interpreted as deposition in a meandering channel system environment. The age of this formation is Middle Jurassic to Upper Jurassic. The thickness is 800-1,200 meters.

The Phra Wihan Formation is composed of white, thick and massive bedded, arkosic to orthoquartzitic and cross-bedded sandstone, interbedded with reddish brown and grey claystone. Small quartz and chert pebble oriented along cross bedding and bedding plane are normally found in the upper- most part of the formation. It was deposited by an extensive semi-distal braided river system. The age of this formation is Upper Jurassic to Lower Cretaceous. The thickness is 100-250 meters.

The Sao Khua Formation consists of reddish brown and greenish grey claystone, siltstone, sandstone and calcareous caliche-siltstone-pebble conglomerate. The depositional environment was a flood plain associated with low energy meandering system. The age of this formation is Lower Cretaceous. The thickness is 200-760 meters.

The Phu Phan Formation is characterized by thick-bedded, and cross bedded conglomeratic sandstone, yellowish grey to pinkish grey sandstone interbedded with siltstone and shale. The depositional environment of the formation is interpreted as strong, low-sinuosity braided river system. The age of this formation is Lower Cretaceous. The thickness is 80-140 meters.

The Khok Kraut Formation comprises fluviatile red bed, sandstone, siltstone, claystone and interbedded conglomerate. The depositional environment of the formation was the flood plain with interbedded low energy meandering river. The age of this formation is Upper Cretaceous. The thickness is estimated to be within the range of 430-700 meters.

The Maha Sarakham Formation overlies the Khok Kruat Formation with a very sharp boundary at the bottom of the basal anhydrite (Hite and Japakasetr, 1979). The Maha Sarakham Formation is preserved within the northern Sakon Nakhon Basin and the southern Khorat Basin. The two basins are separated by the Phu Phan Range. The Formation averages 250 m thick at the type locality (Gardner et al., 1967). The sequence comprises claystone, siltstone, and three rock salt beds; the Lower, the Middle and the Upper salt members which are the main sources of soil and groundwater salinization in the Khorat Plateau (Figure. 2.10). Most of the current margins of the basins are dissolution, as are the upper and lower contacts of the salt units (Warren, 1999). Salt domes and salt anticline of the Maha Sarakham Formation occur in several places.

The Phu Tok Formation consists mainly of massive red sandstone with very large cross-beds interbedded with channelized fine-grained, red to purple sandstone and siltstone with red clay horizons.

2.3 Regional Structures

2.3.1 Reviews on tectonic structures

Major structural elements of the Khorat Plateau Basin run almost parallel to the sutures at the northern and western margin of Indochina. Northwest-southeast trending inversions such as the Khammouane and Namleuk Uplifts of the Phu Luang Terrane or (Annamictic Fold Belt) in Laos and Phu Phan Uplift in Thailand (Figure 2.11) are parallel to the Song Masuture to the north (see Figure 2.12). This trend predominates in the central and eastern parts of the basin and controlled extensional and flexural depocenters since the Devonian (at least) and into the Late Triassic. It is alsocontrolled by compression-related deformations and wrenching up the Early Cenozoic. The N-S trending Phetchabun Foldbelt is associated with the Nan-Uttaradit suture in the west, which is highly tectonised and eroded. N-S trends have been reported in the Devonian (Chairangsee et al., 1990), and control the Permian Nam Duk Basin in the west of the Phetchabun Fold Belt. Kozar et al. (1992) shows this trend to control basin development during the Late Carboniferous to Permian times. There is evidence that structures seen at the surface in the Khorat Plateau Basin are basement controlled. The density of faults affecting the Cretaceous sediments is much lower than the density offaultsseen both onseismic sections and in outcrops of basement around the basin margins. Satellite imagery clearly shows that theCenozoic faults have inherited their orientation fromthe pre-existing structural grain.

Chuaviroj (1997) interpreted lineations of the Khorat Plateau from Landsat TM5 imagery as displayed in Figure 2.13, and he also suggested 3 deformations of the Mesozoic rocks as briefly explained below.

- **F1** is the oldest deformation with N-S fold axes trends inherited from the suturing of Shan Thai to Indochina. It is possibly Late Cretaceous in age. This trend is seen at Phu Luang (Loei) and Phu Wiang (Khon Kaen).

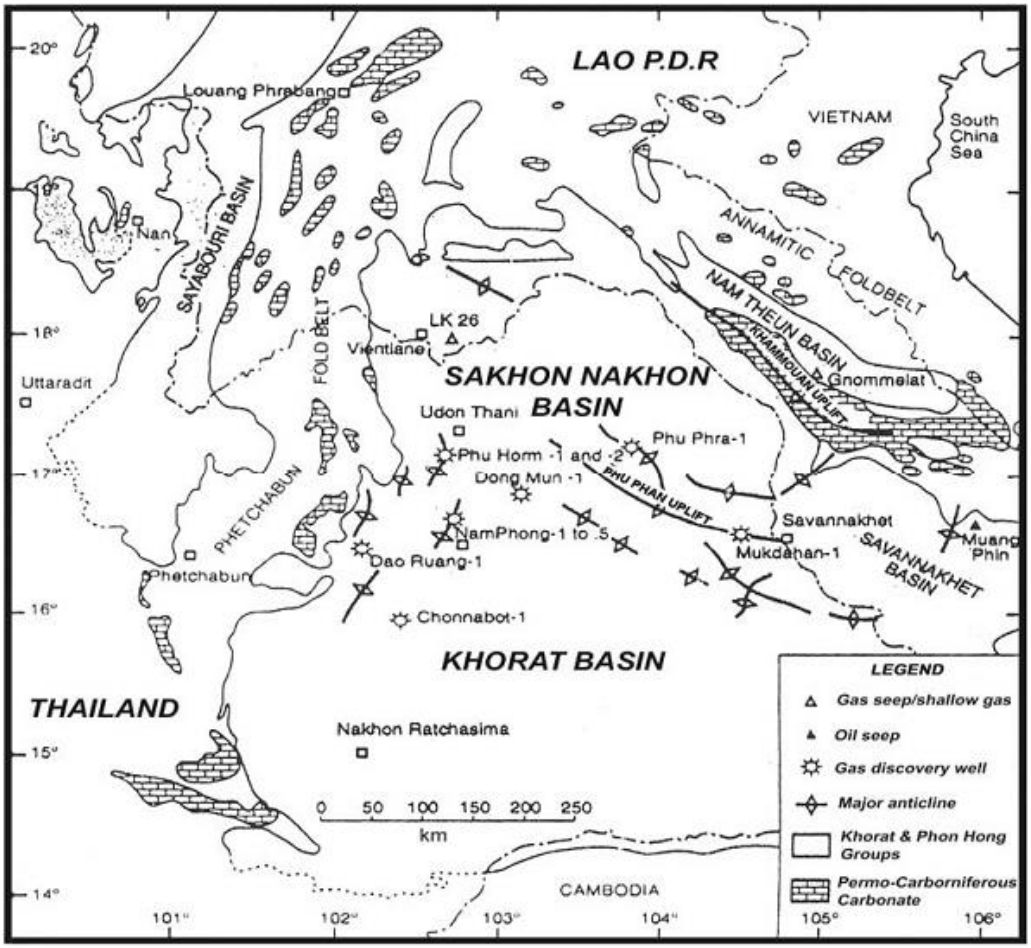

Figure 2.11 *Surface geological elements of the Khorat Plateau and hydrocarbon discoveries (after Smith and Stokes, 1997)*

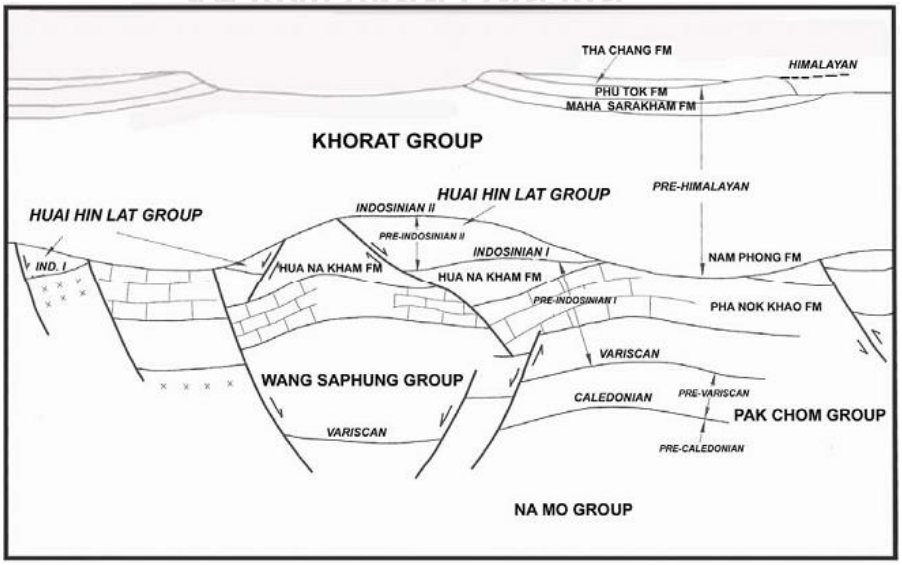

Figure 2.12 *Lithostratigraphic units of rock sequences of Khorat Plateau and their structural setting (after DMR, 1999).*

- **F2** resultedfromthe collision betweenIndia and Eurasia and produced the Phu Phan Range. The NW-SE trend was interpretedas the consequence of NE-SW compression. This trend is seen at The Phu Wiang Syncline, the Si Saket Syncline, the Khon Kaen Syncline, and the Ubon Anticline.

- **F3** was probably produced during the later stages of the Himalayan Orogeny, which caused up-doming in the Neogene/Pleistocene. Compression was believed to be NW-SE causing the axes of F3 folds to be almost parallel to the Kumpawapee Syncline.

2.3.2 Regional structures based on previous remote-sensing interpretation of the Khorat Plateau

The Khorat Basin is covered most of the northeastern Provinces of Thailand except Loei Province and also extends into Laos covered Vientiane and Suvan-nakhet.

Phu Phan Mountain Structural Domain is NW-SE trending sub-basin, elongated, most of the basin is confined in Thailand, and only the southeastern end is extended into Laos PDR at Muang Tha Khek. The northeastern flank is followed the Mae Khong River. The basement of basin is formed as a half garben with boundary fault along Mae Khong River.

2.3.3 Regional structures based on airborne geophysical interpretation of the Khorat Plateau

The RTP magnetic map of Phu Phan Mountain shows circular and flat magnetic features and general high magnetic response (Figure 2.14 and 2.16). Rose plots deduced from the RTP magnetic map shows the NW-SE trending structure as the major structure (Figure 2.16) in Mukdahan area. The NW-SE trending structure is interpreted to have both dextral and sinistral fault movements (as shown in Figure 2.16) in SW of Sakon Nakhon Province. The NW-SE structure is cross-cut by the NE-SW sinistral and dextral fault well presented in N of Kalasin Province and S of Mudahan Province. Therefore, the NW-SE trending structure is represented as major structure and oldest structure in the area.

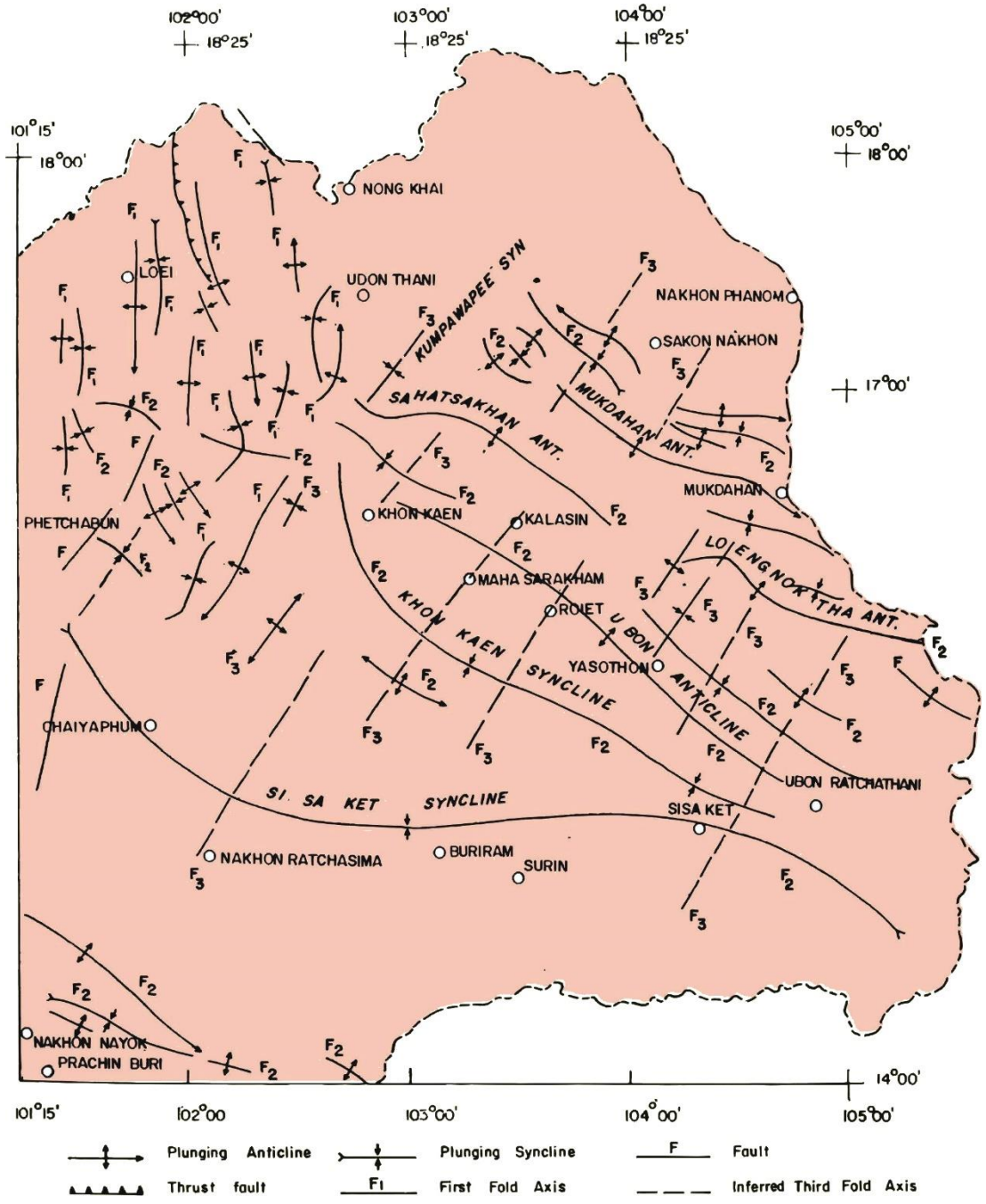

Figure 2.13 *Map illustrating geological structure of of Mesozoic sedimentary rocks in the northeast Thailand (Chuaviroj, 1997).*

In summary, based on magnetic data interpretation, the sequences of structures in Mukdahan area can be visualized from older to younger. Major NW-SE trending sinistral and dextral faults may have occurred first and predate the NE-SW

trending dextral and sinistral faults, respectively. Gravity data (Figure 2.17) shows a circular feature with high intensity in the NW of area and moderate intensity with flat gravity feature in the SE of the area. Major structure is represented by the NW-SE trending structure based on magnetic data. Radiometric data interpretation map (Figure 2.18) shows high intensity and major NW-SE trending surface structure in Mesozoic rocks and conformable with the deep structure interpreted from the magnetic data.

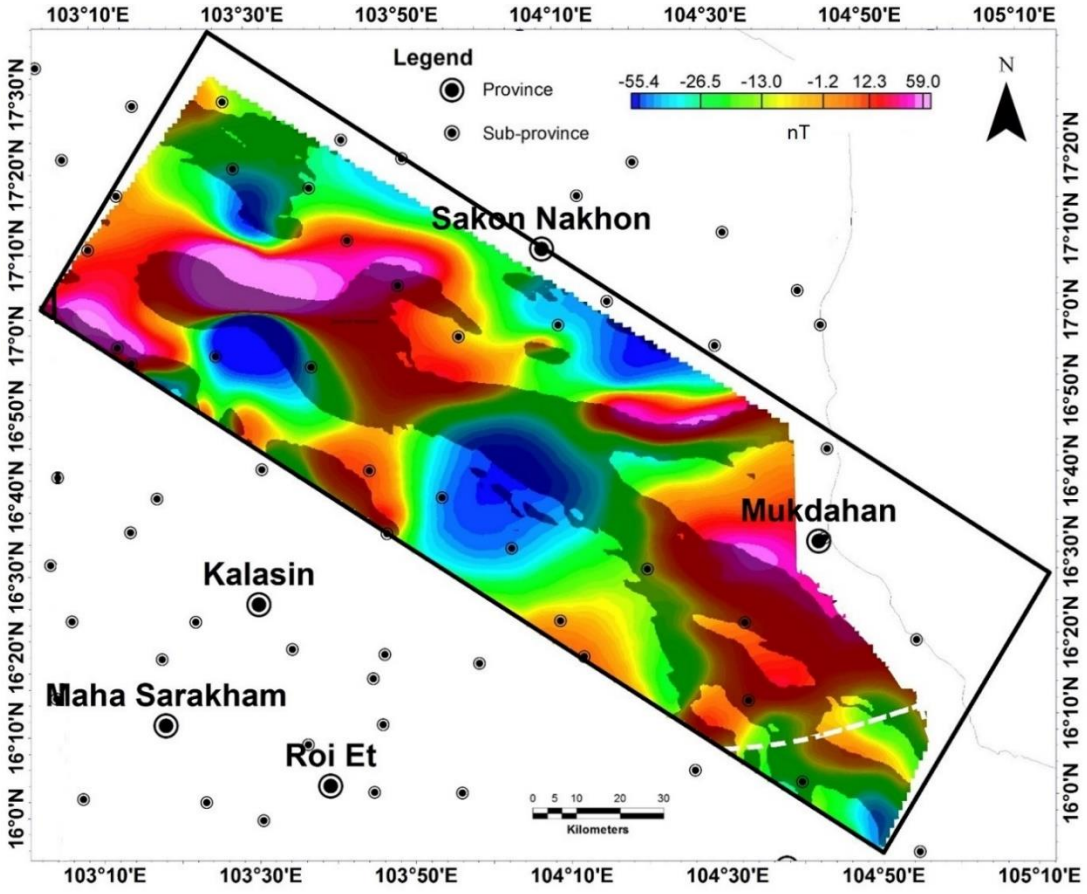

Figure 2.14*. Airborne magnetic map using RTP enhancement in the Phu Phan Mountain Range. (Charusiri et al., 2018)*

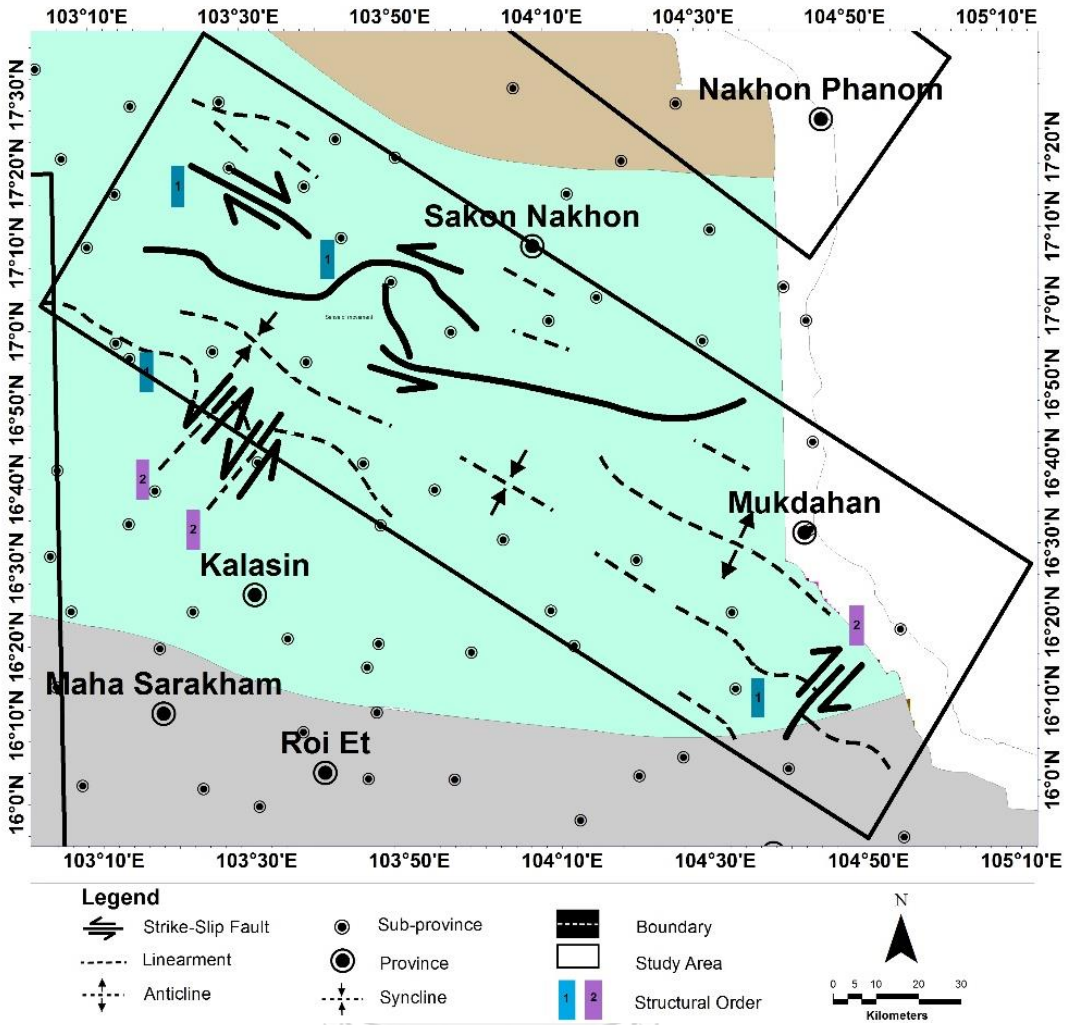

Figure 2.15 *Airborne magnetic interpretation map of the Phu Phan Mountain Range. (Charusiri et al., 2018).*

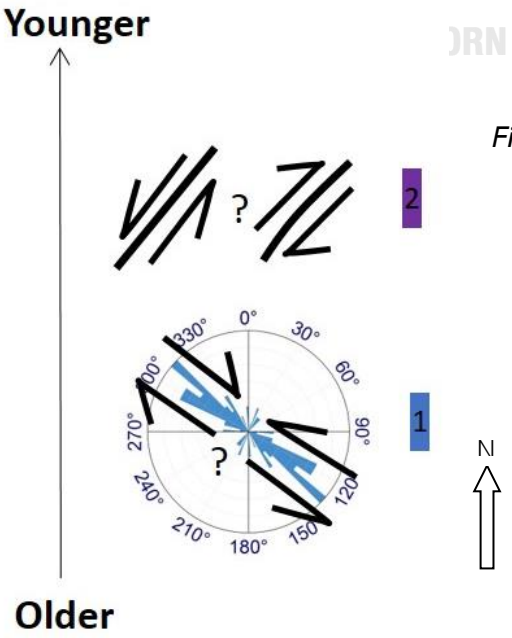

Figure 2.16 *Structural relationship based on airborne magnetic interpretation of the Phu Phan Mountain Range (Charusiri et al., 2018).*

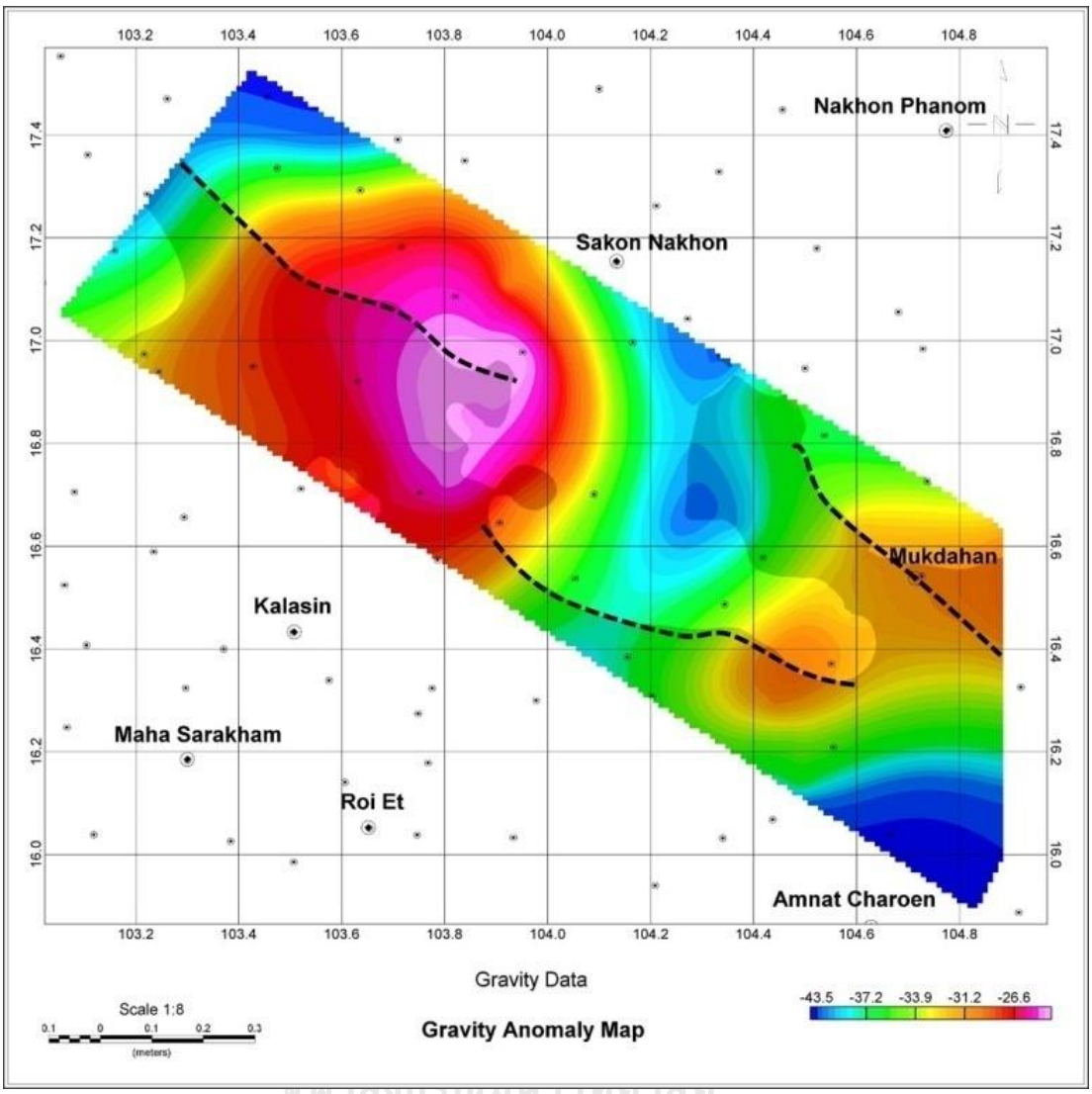

Figure 2.17. *Gravity map showing a major linear structure of the Phu Phan Mountain Range (Charusiri et al., 2018).*

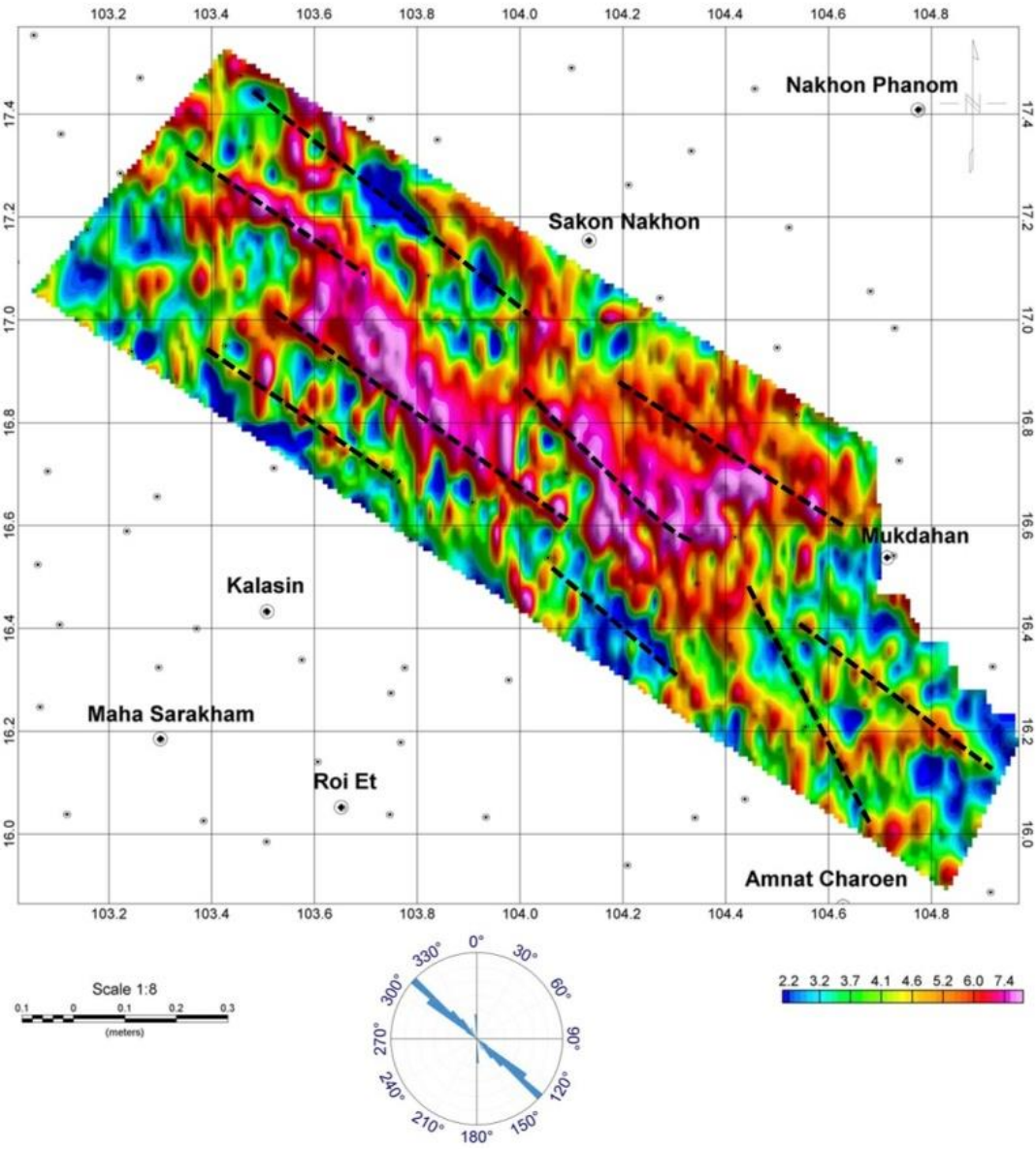

Figure 2.17. *Airborne radiometric map with total count data and a rose diagram of the Phu Phan Mountain Range (Charusiri et al., 2018).*

Chapter 3 Apatite fission track dating

3.1 Introduction

Apatite fission track (AFT) dating is a method of the low-temperature thermochronology that has been widely used for constraining low-temperature thermal histories over four decades ago The application of the method is to investigate the history of many igneous, metamorphic, and sedimentary rocks in an extensively range of geological setting, such as the orogenic belt, rifted margins, faults, sedimentary basins, cratons, and mineral deposits, for solving the geological problems that are provenance studies, rates of tectonic events, thermal history analysis in sedimentary basins, sedimentary basin evolution, the timing of hydrocarbon generation and ore mineralization, the absolute age of volcanic deposits, the effects of major climatic changes on the near-surface geothermal gradient, long-term landscape evolution, evolution of orogenic or mountain belts, and applications in non-orogenic settings. (Donelick et al., 2005; Gallagher et al., 1998). Naeser (1967) and Wagner (1968) provide the first basic procedures of AFT-dating and later, this technique has been exceeding developed. While mentioning the history of technique, this review will discuss on the latest method.

3.2 Track formation

The method of AFT dating is hinged mainly on the fission track accumulation in the crystal lattice composed of apatite crystals. Fission track is one type of ion tracks (commonly known as damage trails) which were induced by penetration of swift heavy ions through solids. In general, there have been many literatures which contains several models to describe ion track formations including fission tracks. For example, the ion explosion spike model of Fleischer et al. (1975) (Figure 3.1) illustrated the electron collision cascade model and the thermal spike model. During spontaneous radioactive ^{238}U nuclei fission, the atomic structures cause its fission to be unstable and produce two highly charged heavy particles which approximately emit 200 MeV (milli-electron volt) of energy in the movement of the two fragments (Friedlander et al., 1981).

Charged particles are recoiled because of Coulomb repulsion and stripping electrons (ionization) away transpire in order that the interaction with other atoms will be happened in the crystal lattice which result in further deformation because of repelling each other of ionized atoms in the lattice (Gallagher et al., 1998) (Figure 3.1). In parallel, this interaction and the electron capturing lead to the loss of kinetic energy and therefore the particles cease moving and leave the obvious defects in the crystal lattice technically termed fission tracks (Gallagher et al., 1998).

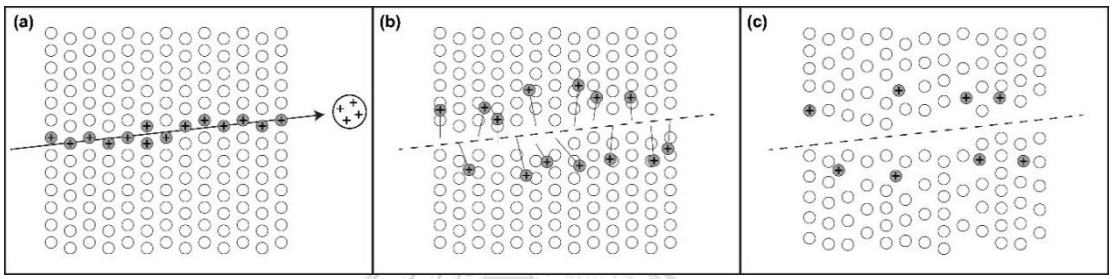

Figure 3.1 Picture showing three major stages of ion explosion spike conducted by Fleischer et al. (1975). (a) The highly charged fission fragment ionizes lattice atoms along its trajectory. (b) Electrostatic repulsion causes displacement of lattice atoms along fragment path. (c) The matrix is strained elastically in proximity to defects and defect clusters. Some of the relaxation takes place in the lattice.

The defects approximately vary from 3 to 14 nanometers (nm) in width (Paul and Fitzgerald, 1992). Chemically etching is operated on apatite grain surfaces in order to see these defects under an optical microscope (Figure 3.2). In this study, the etching "recipe" of Carlson et al. (1999), which consisted of 5 mol of HNO_3 for 20.0s (± 0.5s) at 20°C (± 1°C), is used to etch fission tracks, as most modern fission-track annealing protocols are calibrated against this and similar etching protocols (Ketcham et al., 2007a, b; Ketcham et al., 1999). Fission tracks in apatite were etched up to 16.3 μm long and ~2 μm wide (Fleischer et al., 1975) and can be petrologically detected under a microscope at high resolution. On account of far fewer spontaneous fission reactions with time of ^{235}U and ^{232}Th; therefore, their contribution to the density of total accumulated fission track in a mineral can be ignored.

3.3 Track counting

The AFT ages of the samples are determined by counting the spontaneous tracks within an area. The measurement is carried out with the optical microscope (Eclipse E600, Nikon) at a magnification of 1000x (10x eye piece and 100x objective lens magnification). The software used for observing track is NIS-Elements Microscope Imaging Software.

First step, the surface area wherein the fission tracks are counted is known. Apatite grains has to be at least 40 μm in diameter to avoid measuring too close to the rim as the outermost 10 μm represent a transition zone from 2π geometry to 4π geometry and the cracks or lots of defects with in crystal. Furthermore, the counted area or the region of interest (ROI) (Figure 3.2) should be selected carefully to the spontaneous track distribution which should not be defined an area of high spontaneous track density within a crystal. The apatite grain should have the distribution of uranium is homogeneity within grain (Donelick et al., 2005) and to simplify a 20 μm laser spot. Importantly, the counted area should be clear as possible to avoid misinterpretation of defects, such as inclusions and cracks hamper the track counting. The ROI should be representative of the spontaneous track density of the entire crystal or a large area within the crystal (Figure 3.2). In case of 20 μm spot size of LA-ICP-MS is not located perfectly, caused of minor stage shift on laser ablation system, it still yields a representative uranium concentration of counted area. Therefore, the counted area and beamed spot position need to be considered. Any confined tracks show in the counted area also counted.

A total of 100 confined tracks were aimed. If confined tracks were not reached to 100 tracks, more examine on c-axis would be required. Detailed of track length measurement is in section 3.5 The laser ablation is a destructive method. Therefore, it might be important to reinvestigate the counted grain in the even that grains yield anomalous AFT age.

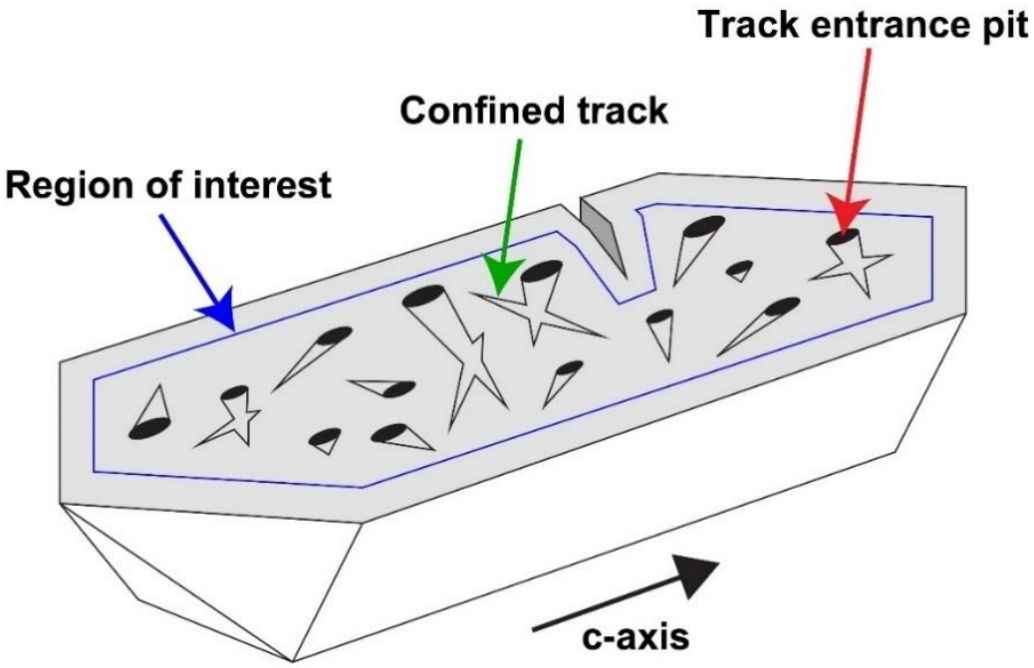

Figure 3.2 *Schematic image of a polished and etched apatite crystal. Red line indicates the region of interest or the area counted for AFT analysis (Doepke, 2017)*

3.4 Thermal annealing of fission tracks

There are three successive annealing behavior of the spontaneous fission of ^{238}U results that effect to the crystal lattice in apatite that can be repaired (or annealed) at temperatures above the closure temperature.

The first zone is above ~120℃ (on average), all spontaneous fission tracks anneal rapidly and are removed over geological timescales (Figure 3.3). For cooling temperature below 120℃, the spontaneous tracks in crystal lattice become short and annealing of tracks is slower than the track forming. These new tracks are also subject to shortening until the sample cools below the lower limit of the zone of track annealing at ~60℃ (Gleadow and Duddy, 1981). This zone between ~60 – 120℃ where shortening of fission tracks takes place is termed the “partial annealing zone” or PAZ (Wagner, 1979). The last zone below ~60℃ are nearly unaffected by partial annealing (Figure 3.3). Nevertheless, Green (1988) recognized a systematic length of track, it is difference between natural occurring fission tracks and fresh or latent fission tracks (induced tracks produced in a nuclear reactor) which are usually 1 to 1.5 μm longer. Induced tracks in apatite are typically 16.3 ± 0.9 μm long (Fleischer et al., 1975) while

spontaneous tracks rarely surpass 15 μm (Green, 1988). This shortening clearly indicates that some annealing occurs between ~60°C and surface temperatures over geological time scales (Gallagher et al., 1998).

Moreover, the behaviour of track annealing in apatite also depends on chemical composition and crystallographic orientation (Donelick et al., 2005; Gallagher et al., 1998). The most common variety of apatite in the crust is near end-member fluorapatite (F- rich). However, there are two different kind of apatite that are chloroapatite (Cl- rich) and hydroxyapatite (OH- rich). F- can be substituted by other anions such as Cl- or OH-. Generally, Chlorine-rich apatite is the most resistant to annealing than pure end-member fluroapatites (Barbarand et al., 2003a; Donelick, 1991; Donelick et al., 2005; Gleadow and Duddy, 1981; Green et al., 1986; O'Sullivan and Parrish, 1995). Thus, chlorine content (Cl wt%) is very important for annealing behaviour of apatite and has implications for the resultant thermal history models (Donelick et al., 2005). Other chemical compositions Ca within the apatite crystal lattice such as Mn, Sr or coupled substitutions of Ca with the rare earth elements (REE) or P with Si are less prevalent and their role in the annealing behaviour is less well understood and not included in any annealing models thus far (Barbarand et al., 2003a; Barbarand and Pagel, 2001; Bergman and Corrigan, 1996; Brown et al., 1994; Crowley et al., 1991; Gallagher et al., 1998; O'Sullivan and Parrish, 1995; Ravenhurst et al., 1992; Spiegel et al., 2007)

Other factor that effects to the annealing behaviour of apatite is the crystallographic orientation. The process of etching and annealing in apatite crystal is anisotropic in relation to their crystallographic orientation (Donelick, 1991; Donelick et al., 2005; Ketcham et al., 2007a). Tracks which are parallel to the crystallographic c-axis commonly etch faster than tracks perpendicular to the c-axis (Gallagher et al., 1998), whereas annealing of tracks parallel to the c-axis is slower than tracks perpendicular to the c-axis (Green et al., 1986). Therefore, the suitable apatite grains for AFT analysis (both fission-track age and track-length determinations) should be parallel to the crystallographic c-axis (Figure 3.4).

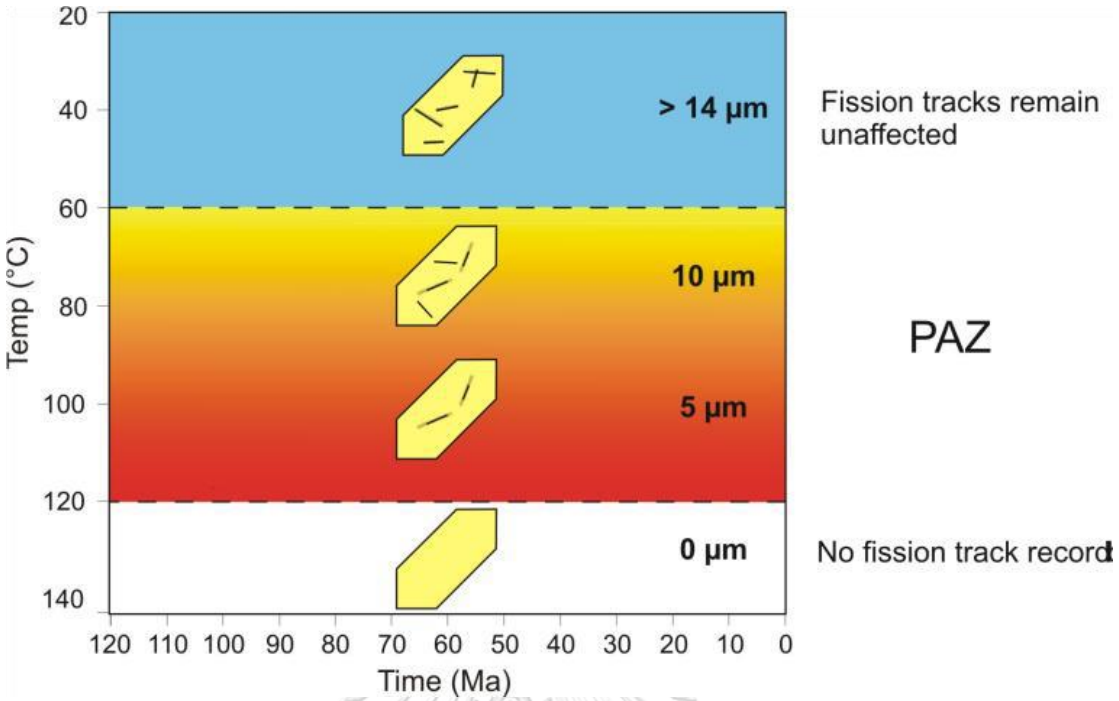

Figure 3.3 *Schematic diagram showing three successive annealing behavior zone of apatite fission tracks with temperature. Above 120°C the fission tracks will completely anneal. Between 120°C and 60°C the fission tracks will partially anneal (PAZ: partial annealing zone) resulting in the tracks shrinking by time and temperature. The higher temperature, the track become shorter. And below 60°C the tracks are nearly "frozen", which means partially annealed tracks (short tracks) and newly formed tracks were kept their initial length (Doepke, 2017).*

3.5 Track length measurement and distribution

AFT dating provides an AFT age and the distribution of a fission-track length (TLD) which importantly documents the cooling historic progression of a sample through the PAZ. AFT system's ability can provide continual thermal histories which can be regarded as a major advantage over other radiometric dating methods and also provide an age of cooling below their consecutive closure temperatures. The distribution of the track length contains "confined tracks" which are completely etched fission tracks beneath the crystal surface and horizontal to the polished surface (Bhandari et al., 1971). They are intersected by other etchable features such as other fission tracks or defects (Donelick and Miller, 1991) which penetrate the surface and thus act as conduits for the etching acid to penetrate and etch the confined track (Figure 3.4).

Only confined tracks which are approximately within ±10° of the horizontal of the polished surface should be measured (Donelick, 1991). The ratio of the measured (apparent) confined track length to the true confined track length is equivalent to the cosine of the angle of the confined track makes to the horizontal polished surface. Cosine (10°) equals 0.985 (i.e. close to unity) and thus within the measurement uncertainty of a single fission-track length (Donelick, 1991; Donelick et al., 2005).

In this study, the Pythagorean theorem ($a^2+b^2 = c^2$) is used for measuring length of incline or decline confined track to the surface, where a means the measured length of the track parallel to the polished grain surface, b refers to the vertical distance from tip to tip of the inclined fission track and c indicates the true length of the confined track (Figure 3.4). Length b is determined by focusing on the tip ends and using the vertical difference in stage heights recorded by the microscope and also takes into account the refractive index of apatite.

Only confined tracks which are fully etched with both ends clearly visible should be measured. In addition, there is two different types of confined tracks; TINTs (Track IN Track) which are intersected by another fission track and TINCLEs (Track IN CLEavage) which are intersected by defects called (Donelick and Miller, 1991). Generally only TINTs should be included within the distribution of track length because TINCLE tracks can display abnormal annealing behavior (Barbarand et al., 2003b; Donelick et al., 2005). There is only TINCLE tracks which can be measured under certain circumstance and can be measured if it was intersected by a polishing scratch mark. Therefore, there was no reason to believe that the TINCLE track would have either annealed abnormally or that the confined track had opened up by movement on a cleavage or fracture plane. Furthermore, the number of TINCLE tracks is typically very small per sample (less than 3), indicating that exclusion would not materially change the distributions of track length.

At least 100 track lengths should be measured for statistically viable TLD data. Nonetheless, as explained in Section 3.4, the annealing and etching behavior of fission tracks are dependent on the orientation to the crystallographic c-axis. Confined tracks at the high angle to the c-axis anneal faster than tracks parallel to the c-axis. In order to receive cooling data from the TLD, it is essential that the track length is independent

of the annealing behavior and therefore only tracks with nearly the same crystallographic orientation (±15° by convention; Gallagher et al., 1998) should be measured for individual sample. Nevertheless, it is very hard to probe the number of tracks with the same orientation, thus a transformation of randomly oriented tracks to their equivalent "projected" track lengths parallel to the c-axis is undertaken (Donelick, 1991; Donelick et al., 2005). The use of projected track lengths productively raises the number of tracks with the same orientation and the projected track-length algorithm is included in the annealing model of (Ketcham et al., 2007b) which is used in this study.

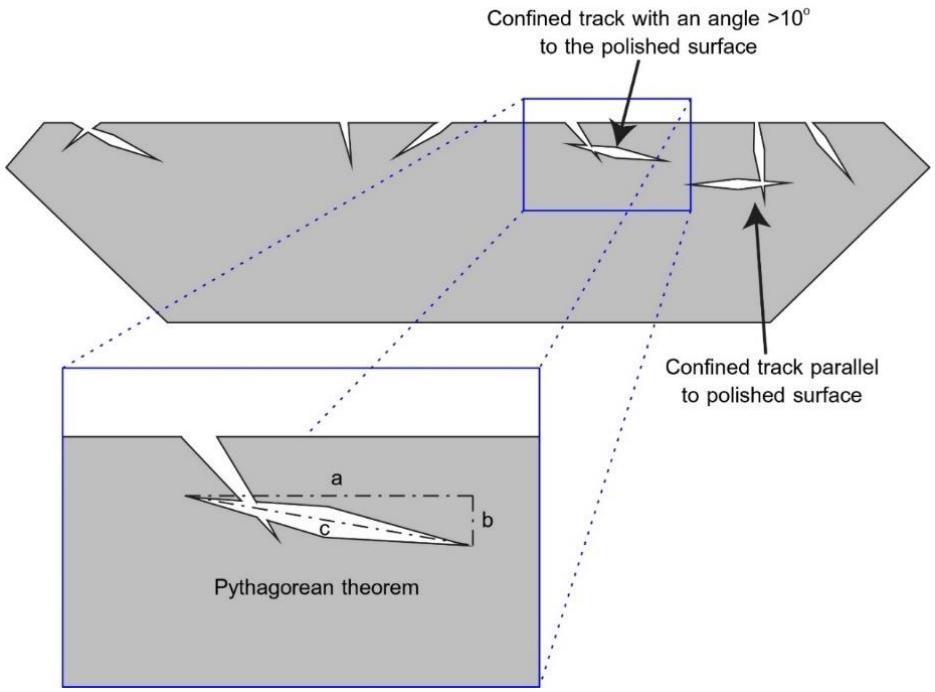

Figure 3.4 *Determination of confined track lengths making an angle of >10° to the counting surface (Doepke, 2017).*

For each AFT sample, I attempted to count at least 100 confined track lengths and subsequently plot them in a histogram with 1 μm intervals (Figure 3.5). The TLD is usually biased towards the longer tracks because (1), longer tracks have a higher probability of being intersected by a track connected to the surface and (2), longer tracks are easier to detect than short tracks. However, the TLD still contains more detailed information about the thermal history of a sample than nearly all of the other thermochronometers (Laslett et al., 1987).

The crucial parameter controlling the distribution of track length is the cooling rate as passing through the PAZ (Figure 3.5). Samples entered the PAZ at the same time, but cool at different rates will be recorded a different TLD and a different age. For instance, a sample passing very quickly through the PAZ (high cooling rate) will have a narrow TLD and a long mean track length (MTL) (Figure 3.5a), whereas samples that cool slowly through the PAZ (low cooling rate) will exhibit a broad TLD skewed towards long track lengths with a long tail of short tracks (Figure 3.5b). A bimodal TLD might indicate a reheating event into the PAZ after the sample has already cooled below ~60°C (Figure 3.5c) or a change in the cooling rate while the sample was still in the PAZ. This last example also reveals that thermal histories based on TLDs are non-unique. Several different cooling histories through the PAZ could yield similar TLDs and without additional information which is impossible to determine that which one is the most realistic cooling history.

3.6 Dpar parameter

The kinetic parameter Dpar is the etch-pit figure of fission tracks intersecting the polished surface of an apatite grain measured parallel to the crystallographic c-axis (Donelick et al., 2005). Dpar is the length which is measured from tip to tip of the hexagonal shaped etch figure (Figure 3.6). Under sturdily controlled etching conditions, Dpar represents an independent parameter for the annealing behaviour of apatites and is commonly used in annealing models for thermal modelling such as in QTQt (Gallagher, 2012) and HeFty (Ketcham, 2005). Dpar typically correlates positively with Cl wt% and OH wt% and negatively with F wt%. Nevertheless, it is not a proxy for Cl content in apatites, the reason is, the geometry of Dpar is not only dependent on the Cl/F ratio, but includes a number of chemical compositions and potentially some other variables as yet not fully investigated (Donelick, 1993; Donelick et al., 2005).

A relatively low value for Dpar (<1.75 μm) shows fast annealing and can be considered a near end-member fluorapatite whereas apatites with Dpar with high values (>1.75 μm) usually anneal slower (Carlson et al., 1999).

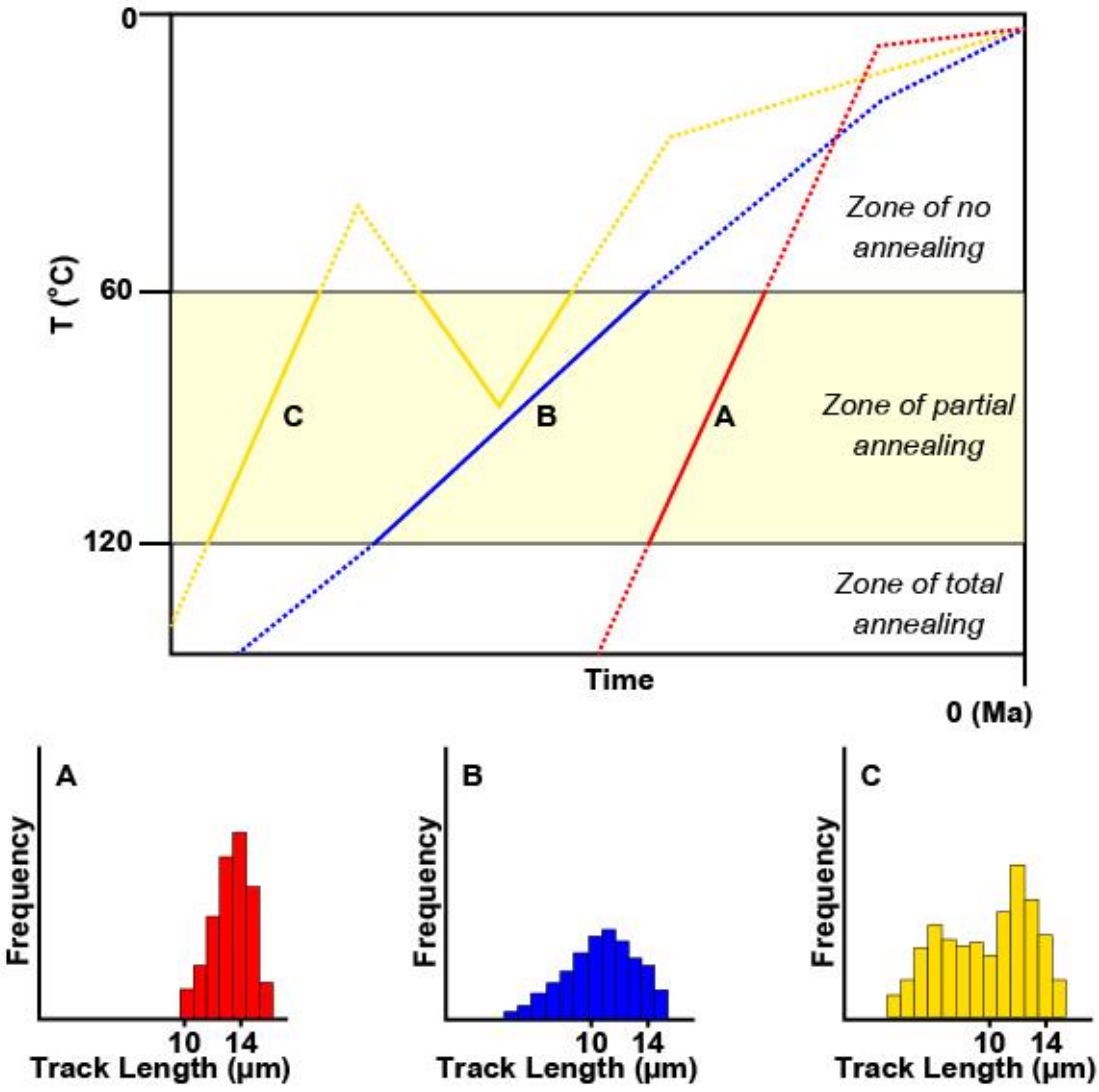

Figure 3.5 *The time-temperature graph showing three possible paths resulting in three different track length distributions as shown at the bottom of figure. A: The narrow track length distribution indicates a rapid cooling of the sample through the PAZ. B: A wide distribution indicates slow cooling through the PAZ. The bimodal distribution indicates reheating of the sample into the temperature range of the PAZ. The pre-existing length population gets annealed and shortened while a younger track length population forms, recording the recent cooling path (Doepke, 2017).*

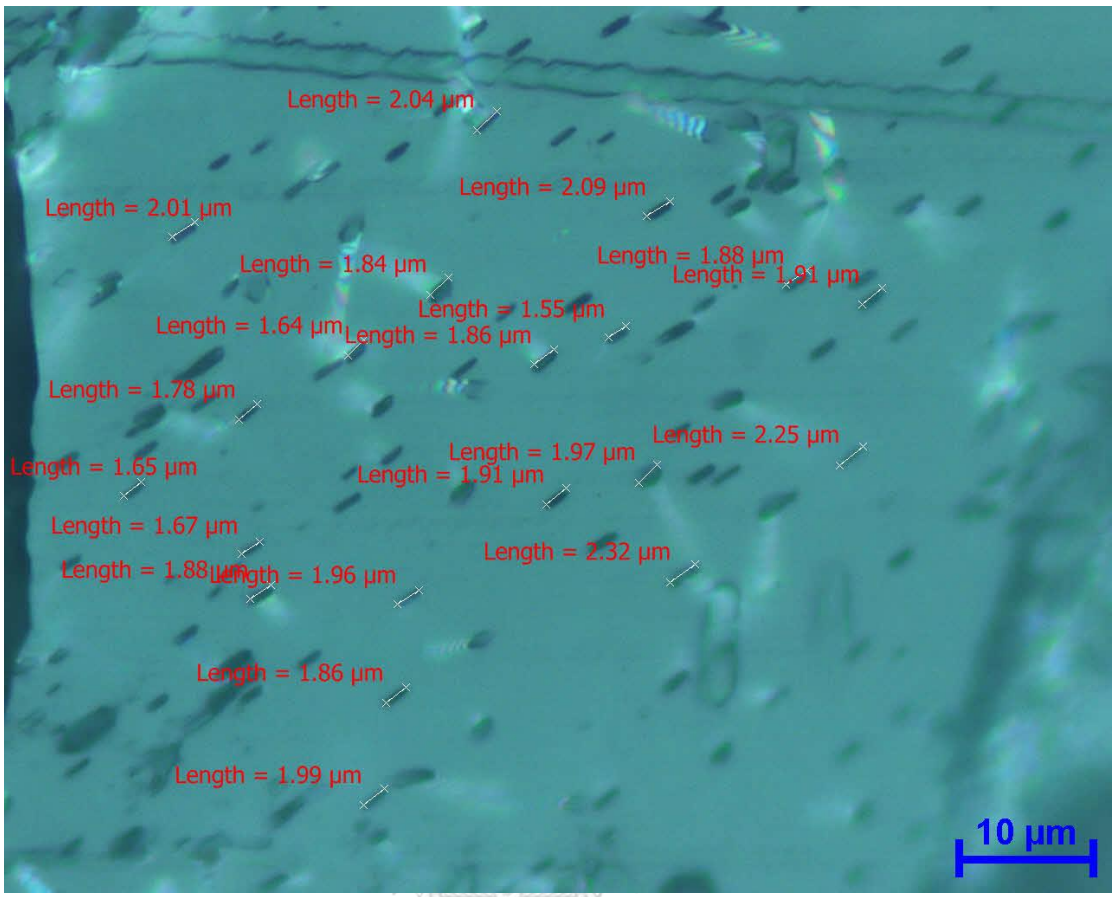

Figure 3.6 *A photograph showing nature of apatite tracks and with their etch pit entrance diameter (Dpar).*

3.7 Types of fission track dating method

3.7.1 External detector method (EDM)

The application of the AFT method was being developed in the early 1980s. In that time the instrumentation was absent. Determining amount of ^{238}U in the analyzed crystal was used in a novel approach which is called as the external detector method (EDM) (Green and Hurford, 1984; Hurford and Green, 1982) which placed the polished grain surfaces of the counted apatite crystals in the close contact with low-U bearing "detector" mica, and bombarded with thermal (slow-moving or low-energy) neutrons in a nuclear reactor (Figure 3.7). This influences on fission of ^{235}U in the apatite lattice, whereas ^{238}U induced fission is impossible because the energy emitted by 238U thermal neutron bombardment is less than the critical energy. Induced fission of ^{235}U atoms in half of a track length of the apatite grain surface can be registered in the mica

detector. The content of induced ^{235}U on the mica and the 238U content tracks can be associated by employing the natural $^{238}U/^{235}U$ ratio of 137.88 (Steiger and Jäger, 1977).

The induced track density (ρ_i) is balanced to ^{235}U content in the apatite, the neutron flux per unit volume (Φ) from the irradiation and the thermal neutron fission cross-section of ^{235}U (σ = 580.2 x 10-24 cm-2; Green and Hurford, 1984; Hanna et al., 1969) and can be computed by using Equation 3.1.

$$\rho_i = q^{235}U\phi\sigma \qquad \textbf{Equation 3.1}$$

where q indicates a plane lined through a given volume where the induced fission tracks are counted (Galbraith, 2005). The neutron flux in the research reactor can be modelled by determining the place of dosimeter glasses (of known U content) in contact with low-U micas in the reactor which are in turn interspersed with the apatite samples (Hurford and Green, 1982). The neutron flux in the time of each irradiation duration is stable, as a consequence it is possible to compute ^{235}U content in a sample by using Equation 3.2.

$$^{235}U_{sample} = \frac{\rho_i}{\rho_D}\,^{235}U_{glass} \qquad \textbf{Equation 3.2}$$

where ρ_D indicates the induced track density in a standard (dosimeter) glass of known ^{235}U concentration and ^{235}U glass is the ^{235}U concentration in the dosimeter glass.

By applying the natural $^{235}U/^{238}U$ isotope ratio to the ^{235}U concentration in a sample, it is possible to determine the ^{238}U concentration and can calculate the AFT age with the EDM method (tEDM) using Equation 3.3.

$$t_{EDM} = \frac{1}{\lambda} ln\left(1 + \frac{\lambda}{\lambda_{fission}}\frac{\rho_s\phi\sigma Ig}{\rho_i}\right) \qquad \textbf{Equation 3.3}$$

where "I" refers to the $^{235}U/^{238}U$ isotope ratio (7.253 x 10^{-3}; Galbraith, 2005), σ is the thermal neutron fission cross-section (Hanna et al., 1969) and g means the geometry factor representative of a 2π (g=1) versus 4π geometry (g=0.5 in equation 3) caused by polishing into the apatite grain (Figure 3.2). Thus, the counted surface within the apatite (4π geometry) contain spontaneous tracks descent from ^{238}U fission from both sides of the counted grain surface, but induced tracks are obtained from the side of

the apatite in contact with the external detector mica only (Figure 3.7) (Donelick et al., 2005; Gallagher et al., 1998; Green and Hurford, 1984).

Evaluating Equation 3 unveil some complexity in terms of calculating the AFT age with the EDM because some parameters are subject to analytical bias and the accuracy value for spontaneous fission decay constant ($\lambda_{fission}$) is not certain. Consequently, a calibration factor is used to the AFT age equation, known as the zeta-calibration factor (ζ), which is described below.

3.7.2 Apatite fission track age determination via LA-ICP-MS

Principally, AFT dating used LA-ICP-MS need the same parameters as the EDM to compute the age are:

(1) the ^{238}U content per unit area

(2) the content spontaneous fission tracks per unit area,

(3) the decay constant of ^{238}U (Table 3.1) and modified zeta calibration factor.

In any case, using laser ablation by passes the requirement to determine the induced track density and instead directly measures the $^{238}U/^{43}Ca$ ratio which replace the induced track density (Figure 3.7). Equation 3.4 is the age calculation for a single fission track age using the LA-ICP-MS method:

$$t_j = \frac{1}{\lambda_D} ln\left(1 + \lambda_D \zeta_{MS} \frac{\rho_j}{m_j}\right) \qquad \textbf{Equation 3.4}$$

where,

- t_p is FT age of the jth grain;
- ρ_j is the spontaneous FT density at the observed surface of the jth grain (μm^{-2}), calculated as $\frac{N_j}{A_j}$;
- N_j is the number of spontaneous tracks counted for the jth grain in a counted area;
- A_j is the counted area for the jth grain (cm^2);
- λ_D is the total decay constant of ^{238}U (1.552 x 10-10/yr, Jaffey et al., 1971);

- m_j is the ratio of mass of uranium divided by internal standard (^{43}Ca) of the unknown sample and mass of uranium divided by internal standard (^{43}Ca) of the external standard (NIST SRM610 glass), calculated as $\left(\frac{^{238}U_j}{^{43}Ca_j}\right) / \left(\frac{^{238}U_{exist-j}}{^{43}Ca_{exist-j}}\right)$;
- $exist - j$ denotes the value for the external standard to the jth measurement of the unknown sample; and
- ζ_{MS} represents the adjusted calibration factor zeta for conventional U concentration measurement by LA-ICP-MS which is calculated in Equation 3.8

The error of the grain age (σ j) is given by Equation 3.5.

$$\sigma_j = t\sqrt{\frac{1}{N_j} + \left(\frac{\sigma_{m_j}}{m_j}\right)^2 + \left(\frac{\sigma_{\zeta_{MS}}}{\zeta_{MS}}\right)^2} \qquad \textbf{Equation 3.5}$$

Where

- σ_{m_j} is uncertainty in the LA-ICP-MS signal intensity (or intensity ratio) related to ^{238}U concentration and
- $\sigma_{\zeta_{MS}}$ is the uncertainty in ζ_{MS}.

The abundant ^{238}U is determined by employing the depth-weighted ^{238}U/43Ca ratio measured by LA-ICP-MS spot analysis in order that the ^{238}U/^{43}Ca contents in contact with the surface of grain (which contributes more fission tracks to the spontaneous track density) are weighted more heavily than ^{238}U/^{43}Ca content at depth.

The depth-weighted ^{238}U/^{43}Ca ratio is computed during the step of data reduction in Iolite, but is imperatively relied on the rate of ablation, which is computed from the depth of ~16 μm laser pit (as determined by in-house measurement after ablation) and the settings of laser (295 shots of the laser in 45 seconds) and the dimensions of the laser spot which is half a sphere obtained from the 20 μm laser spot size and ~16 μm pit depth (Figure 3.8). Because the depth-weighted ^{238}U/^{43}Ca ratio is merely determined for the laser spot position, hence it is necessary to intimately match the laser spot position to the counted area (A_j). Otherwise, probable variations

in the $^{238}U/^{43}Ca$ ratio (e.g. zonation in the apatite grain) might have an influence on the computed AFT age.

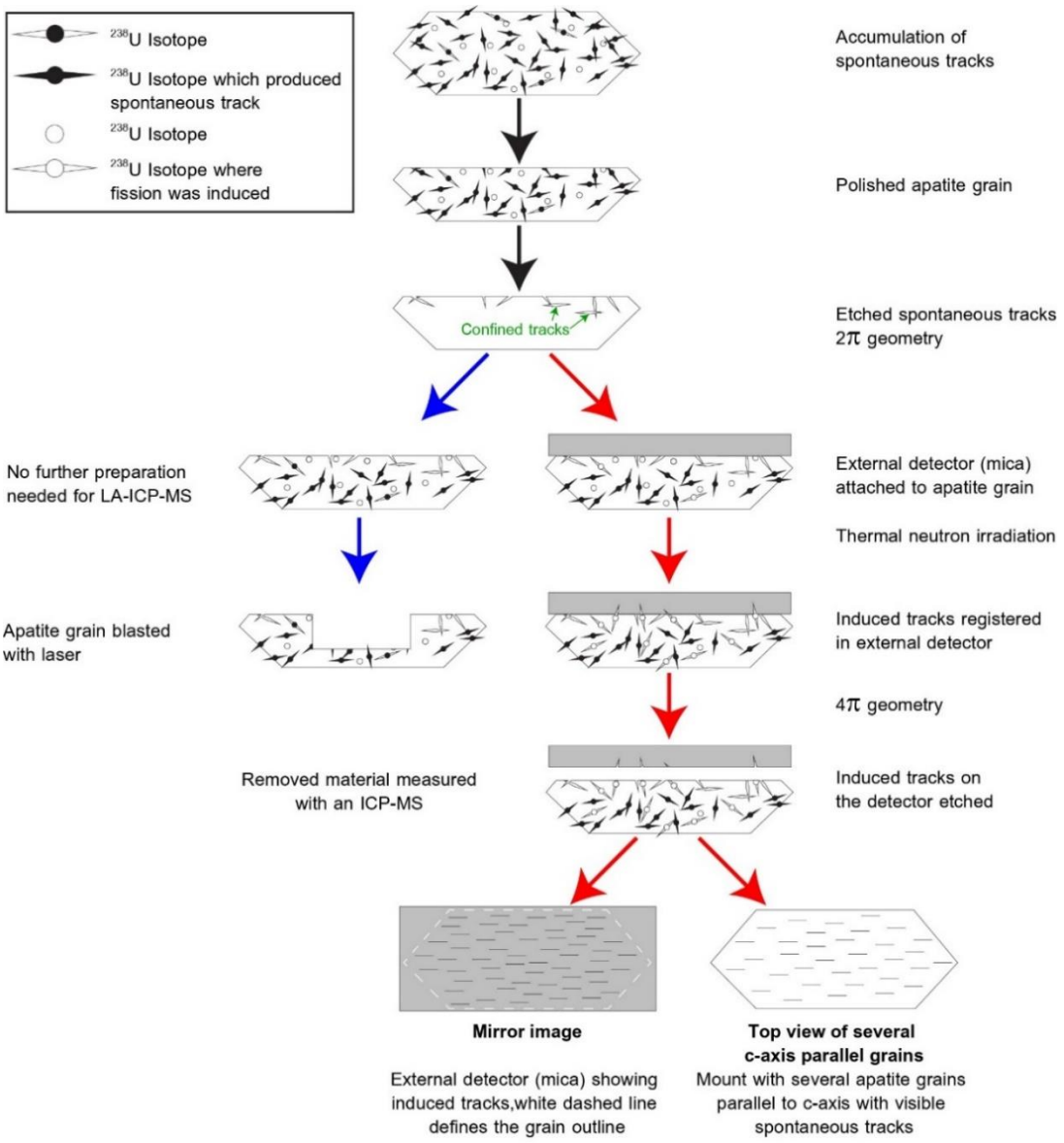

Figure 3.7 *Schematic diagram showing the preparation of an apatite grain for AFT analysis via the external detector method (Hurford and Green, 1982) and the LA-ICP-MS method (Doepke, 2017).*

Table 3.1 Decay constants of the U-Th-Sm decay systems employed in low-temperature thermochronology (Friedlander et al., 1981; Jaffey et al., 1971; Lederer et al., 1967; Steiger and Jäger, 1977; Wagner and Van den Haute, 1992).

Isotope	Decay Constant (yr^{-1})
^{238}U	1.552 x 10-10 yr^{-1} (α)
	~7.5 x 10-17 yr^{-1} (s.f.)
^{235}U	9.848 x 10-10 yr^{-1} (α)
^{232}Th	4.947 x 10-11 yr^{-1} (α)
^{147}Sm	6.538 x 10-12 yr^{-1} (α)

Notes:

α: alpha-decay series

s.f.: spontaneous fission decay

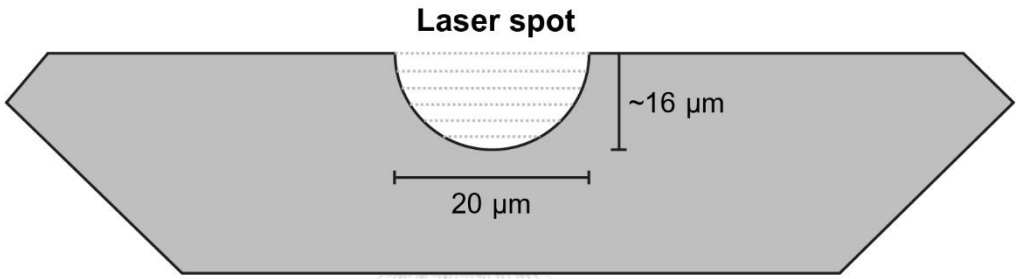

Figure 3.8 *Apatite grains with 20 µm laser spot. Dotted line shows ablations intervals for calculation of depth-weighted $^{238}U/^{43}Ca$ ratio (modified from Doepke, 2017).*

3.8 Zeta calibration

Hurford and Green (1982) established the zeta calibration factor that rectified for several parameters which are not well-known or are subjected to change as mentioned above. While the total decay constant for ^{238}U is well known (λ_D = 1.552 x 10-10 y^{-1}, Jaffey et al., 1971), the spontaneous fission decay constant is uncertain and only estimated at 7.5 x 10-17 y^{-1} (Roberts et al., 1968; Wagner and Van den Haute, 1992). Each analysts differently count fission tracks (i.e. sometimes they may disagree on what is a track and what is not) and thus the spontaneous (ρ_s) and induced (ρ_i) track densities are different from analyst to analyst. Therefore, a correction factor has to account for the analyst bias to ensure that each AFT age is independent from the analyst who is responsible for counting the tracks.

3.8.1 Zeta calibration for EDM

The zeta factor used in EDM involves placing both counted unknowns and known age standards (e.g. Durango or Fish Canyon tuff apatite) into the similar irradiation package. Because standards and unknowns have an identical spontaneous fission decay constant which experienced the same neutron flux and are subjected to the same ambivalence in track identification. These uncertainties are removed and thus the zeta-factor can be defined based on the result shown in Equation 3.6.

$$\zeta = \frac{(e^{\lambda t_{std}} - 1)}{\lambda (\rho_s/\rho_i)_{std} g \rho_d} \qquad \textbf{Equation 3.6}$$

where, t_{std} refers to a well-known and characterized age standard, $(\rho_s/\rho_i)_{std}$ the ratio of spontaneous to induced track densities in the standard and g indicates the geometry factor. By including the zeta calibration factor ζ into Equation 5, the EDM age calculation can be simplified using Equation 3.7.

$$t_{EDM} = \frac{1}{\lambda} ln\left(1 + \lambda \zeta g \left(\frac{\rho_s}{\rho_i}\right) \rho_D\right) \qquad \textbf{Equation 3.7}$$

3.8.2 Zeta calibration for LA-ICP-MS

As mentioned previously (section 3.7), the EDM was created due to the difficulties in the measurement of U content and counting apatite grains. These days, because of enhanced mass spectrometry instrumentation, this is probable to measure the ^{238}U content in situ in an apatite crystal which eliminates the need for the EDM and correction for the neutron flux in the reactor. Anyway, the zeta calibration factor is still used in the LA-ICP-MS method (Donelick et al., 2005) owing to the uncertainties in the $\lambda_{\mathbf{fission}}$ constant and in analyst bias (e.g. uncertainties in counting). As a consequence, the modified zeta-calibration factor for the LA-ICP-MS method removes the neutron flux and replaces the ρ_s/ρ_i ratio of the standard with the spontaneous tracks (N_s) per ^{238}U/^{43}Ca ratio in the counted area A_j (in μm^2). Zeta calibration for LA-ICP-MS can be calculated using equation 3.8.

$$\zeta_{MS} = \frac{aM}{\lambda_f N_A d R_{sp} k I S \left(\frac{j}{exist}\right)^{238} U_{exist} \times 10^{-6}} \qquad \textbf{Equation 3.8}$$

Where

- λ_f is ^{238}U spontaneous fission decay constant (8.46 × 10−17/a Spadavecchia and Hahn, 1967);
- M is the mass of ^{238}U (g);
- N_A is Avogadro's number;
- d is specific density (3.19 g/cm^3 for apatite);
- R_{sp} is a registration factor, by which ^{238}U in a unit volume would leave spontaneous tracks on an observed surface that is half of the mean etchable spontaneous fission track length (cm); and
- k is an experimental factor which varies depending on, for example, the etching and observation conditions

Generally, ζ_{MS} varies depending on the LA-ICP-MS system (a), observation system (k), external standard ($IS_{\left(\frac{j}{exist}\right)}$ and $^{238}U_{exist}$) and mineral species (d and R_{sp}) (Hasebe et al., 2013).

For this study, AFT analysis was performed at Kanazawa University. LA-ICP-MS was completed on an Agilent 7500 instrument equipped with a Microlas Excimer laser ablation system (Ishida et al., 2004; Morishita et al., 2005). The operating conditions for the apatite uranium measurements are summarized in Table 3.2. NIST SRM610 standard glass was used as an external standard, and the internal standards were ^{43}Ca for apatite.

In all studies of LA-ICP-MS fission-track dating, the background-corrected ^{238}U abundance is normalized to the ^{43}Ca content of the apatite (Donelick et al., 2005; Hasebe et al., 2004). Ca is presumed to be stoichiometric in apatite and employed ^{43}Ca as an internal standard for explaining the variation in the quality of the ablation or long-term variations within a session in signal intensities (session drift). Minor session drift in ^{238}U/^{43}Ca ratios is also probable and hence an initial zeta-factor is computed during an extensive LA-ICP-MS period where individual counted standard grain (normally Durango apatites) is analyzed many times. In each following ICP-MS session with unknowns, a secondary zeta calibration factor is subsequently determined and normalized to the primary session value to describe the variations in ICP-MS sensitivity

between different period resulted from differing in instrument of tuning parameters (Donelick et al., 2005; Hasebe et al., 2004). For this study, the value of zeta (ζ_{MS}) is 0.928±0.022 (Hasebe et al., 2013) for pooled AFT age calculation and 1.8560±0.044 for central AFT age calculation in IsoPlotR program (Vermeesch, 2018, in press).

In addition, using LA-ICP-MS instead of the EDM method improve the speed of data acquisition because there is need to be irradiated in the samples and cool-down after irradiation. It also subtracts the need to count the induced tracks on external detector micas and on unknowns as well as dosimeter glasses.

Table 3.2 Operating conditions for the LA-ICP-MS analyses at Kanazawa University (Hasebe et al., 2013)

ICP-MS		**Laser**	
Model	7500 s (Agilent)	Model	GeoLas Q + (Microlas)
Forward power	1200 W	Wavelength	193 nm (Excimer ArF)
Reflected power	1 W	Repetition rate	5 Hz
Carrier gas flow	1.20 L/min (Ar)	Energy density at target	8 J/cm2
	0.3 L/min (He)		
Auxiliary gas flow	1.0 L/min	Spot diameter	20 μm
Plasma gas flow	15 L/min (Ar)		
Cones	Pt sample cone		
	Pt skimmer cone		

3.9 Age Derivation

In order to determine an AFT age, there are three commonly used methods to acquire an AFT age, are the pooled, central, and mean age (Galbraith, 2005). Generally, the mean age is basically statistical arithmetic mean of the single grain ages.

The FT method can provide an individual age for a single grain. To represent 'the sample age' from multiple grain ages, either a weighted mean age or a pooled age is calculated in conventional FT dating (Gleadow, 1981; Green, 1981). For LA-ICP-MS FT dating, a pooled age can be calculated from the sum of the spontaneous track count divided by the sum of the weighted $(U/Ca)_j$ ratio multiplied by the counted area on each apatite grain (Donelick et al., 2005) by using Equation 3.9.

$$t_p = \frac{1}{\lambda} ln \left[1 + \lambda_D \zeta_{MS} \frac{\rho_p}{m_p}\right] \quad \text{Equation 3.9}$$

Where

- t_p is the pooled age.
- $\rho_p = \frac{N_p}{A_p} = \frac{\sum_j N_j}{\sum_j A_j}$ **Equation 3.10**
- $m_p = \sum_j \frac{A_j}{A_p} m_j$ **Equation 3.11**

The error estimate for the pooled ^{238}U concentration using the counted area-weighted $\boldsymbol{\sigma}$ of the grains is suggested by Donelick et al. (2005) in Equation 3.12. This error is used in the age error estimate.

$$\delta_p^2 = \frac{\sigma_{U_p}^2}{^{238}U_p^2} = \frac{\sum_j \left(\frac{A_j}{A_p}\sigma_{U_j}\right)^2}{^{238}U_p^2} \quad \text{Equation 3.12}$$

Where the subscript $\mathbf{p}$ symbolizes the pooled values, and σ_U is an error in the ^{238}U concentration.

However, the statistical meaning of the error of the ^{238}U concentration (or a representative value of ^{238}U concentration) by using the counted area-weight is not clear.

The error of the sample LA-ICP-MS data (m_p) can be calculated from the general Equation 3.13.

$$\sigma_{m_p} \approx m_p \sqrt{\frac{1}{\sum_j \left(\frac{m_j}{\sigma_{m_j}}\right)^2}} \quad \text{Equation 3.13}$$

In general, the pooled age can be allowed when the apatite grains derive from the same source and have a similar chemical composition (i.e. crystalline basement samples or volcanic apatites). Therefore, they should show the same annealing behaviour and yield a similar age. Unless the slowly cooled samples which have spent a long time in the PAZ can show different single grain AFT ages despite being from the same source rock.

In case of detrital samples in sedimentary basins can have multiple source areas that can show a wide spread in AFT ages because of variations in apatite chemistry which may influence annealing behaviour. Galbraith (2005) proposed a Poissonian distribution to test samples. If the sampled grains derived from a single source, a $P(\chi)^2$ test should contribute upper than 5% level (Yates, 1934). In contrast, if grains of sample fail in test (lower than 5%), it would indicate that either the grains are from different populations (such as in detrital samples) or that the U distribution is inhomogeneous in a grain which can influence the track measurement (Galbraith, 1981). However, very slow-cooled samples also can also show large age dispersion since slightly changes in chemistry and temperature can affect the annealing behavior. Therefore, the sample that failed in the $P(\chi)^2$ test, the central age is preferred.

The central age was established by Galbraith and Laslett (1993) and is the weighted mean of the log normal distribution of the single grain ages (Gallagher et al., 1998). The central age is weighted for the precision of track counts from each grain, providing a geometric mean age (Gallagher et al., 1998). The central age can be calculated from Equation 3.14:

$$t_c = \frac{1}{\lambda} log \left[1 + \lambda \zeta g \frac{\eta}{(1-\eta)}\right] \qquad \textbf{Equation 3.14}$$

where η is the weighted average of single-grain variance and $\eta/(1-\eta)$ the equivalent of Ns/Ni. In this study, the central age is calculated by IsoPlotR (Vermeesch, 2018) which shows as a radial plot with central age, $P(\chi)^2$, MSWD, and age dispersion (%).

3.10 Apatite fission track standard samples

Durango apatite (DUR)

Durango apatite is almost definitely the best-characterized fluorapatite, and has been commonly analyzed for AFT annealing and length studies (Green et al., 1986; Laslett et al., 1984) and widely used as standard in AFT dating. Durango apatites are naturally coarse-grained (> 1 cm), euhedral crystals that formed in an ore deposit at Cerro de Mercado near Durango City, Mexico (Young et al., 1969). The iron ore deposit is bracketed by two ignimbrite eruptions which have been dated by the $^{40}Ar/^{39}Ar$

method, yielding an age of 31.4 ± 0.5 Ma (2**σ**) for the Durango apatite itself (Green, 1985). Durango apatite usually has a relatively high chlorine content (0.43 Cl wt%) compared to most natural occurring apatites. These compositional differences mean that the chemical composition (including the chlorine content) and / or the kinetic parameter Dpar should be analysed in apatite unknowns. These data are then incorporated into the thermal history models in order to account for the compositional differences and thus the different annealing behaviour between apatite unknowns and Durango apatite.

Durango apatite is used as standard sample of this study, yields pooled AFT age analysis as 35.6±2 Ma (Table 3.2), where analyses from 2 pieces of large apatite crystals were crushed. The total number of track is 268 tracks in the counted area is 155,600 μm^2. (see more detail in Table 1, Appendix D).

Table 3.2 illustrates AFT ages from pooled age comparing with reference age (Green, 1985) at Kanazawa University laboratory. The pooled age is older than reference age from Green (1985) about 4.2 Ma (13.2%)

Table 3.3 Apatite fission track age obtained from standard sample Durango apatite (DUR).

Sample No.	This study		Number of Grains	Reference age* (Ma)
	Pooled age (Ma)	Central age (Ma)		
DUR	35.6±2.4	-	2 (pieces)	31.4±0.5

*DUR = Durango Apatite (Green, 1985)

Fish Canyon Tuff apatite (FCT)

The Fish Canyon Tuff (FCT) is a voluminous crystal-rich ignimbrite sheet erupted over a relatively short period during the late Oligocene from the ca. 2500 km^2 La Garita Caldera in the San Juan volcanic field, southern Colorado. The FCT contains many of dating standard material in that that it has an excellent assemblage of dateable accessory minerals, such as plagioclase, sanidine, biotite, hornblende, titanite, apatite and zircon. For fission track dating method, apatite and zircon from FCT are commonly

used as a laboratory standard, which has the reference age of 27.8 ± 0.2 Ma obtained from K-Ar and $^{40}Ar/^{39}Ar$ dating results from several minerals from FCT (Bachmann et al., 2007; Green, 1985; Lanphere and Baadsgaard, 2001).

The Fish Canyon Tuff standard sample yields the AFT age using central AFT age model and pooled AFT age model to be 37.9±2.3 Ma and 37.1±2.4 Ma, respectively, which has number of grain is 16 grains. Data distribution is quite low 10% and $P(\chi)^2$ equals to 14% (see Figure 3.9) with number of track ranging from 3 to 56 in area of 21 to 200 μm^2. The total number of track and area of this sample analysis is 319 tracks and 128,586 μm^2. U/Ca ratio of this apatite standard divided by U/Ca of external standard (NIST SRM610) falls within 0.0007 to 0.1. Error of ratio U/Ca of apatite standard divided by error of U/Ca of external standard (NIST SRM610) is in the 0.00002 to 0.00004. (see more detail in Table 2, Appendix D).

Table 3.3 illustrates AFT ages from pooled age and central age comparing with reference age (Bachmann et al., 2007; Green, 1985; Lanphere and Baadsgaard, 2001) at Kanazawa University laboratory. Both pooled age and central age provide similar age but their ages are older than reference age from Green (1985), Lanphere and Baadsgaard (2001), and Bachmann et al. (2007) about 10 Ma (36.1%)

Table 3.4 Apatite fission track age obtained from standard sample Fish Canyon Tuff apatite (FCT).

Sample No.	This study		Number of Grains	Reference age* (Ma)
	Pooled age (Ma)	Central age (Ma)		
FCT	37.9±2.3	37.1±2.4	16	27.7±0.2

*FCT = Fish Canyon Tuff apatite (Bachmann et al., 2007; Green, 1985; Lanphere and Baadsgaard, 2001)

For this study, only the Durango apatite is performed as the standard sample because the percentages of error from an experiment of DUR is less than the percentage of error from an experiment of FCT.

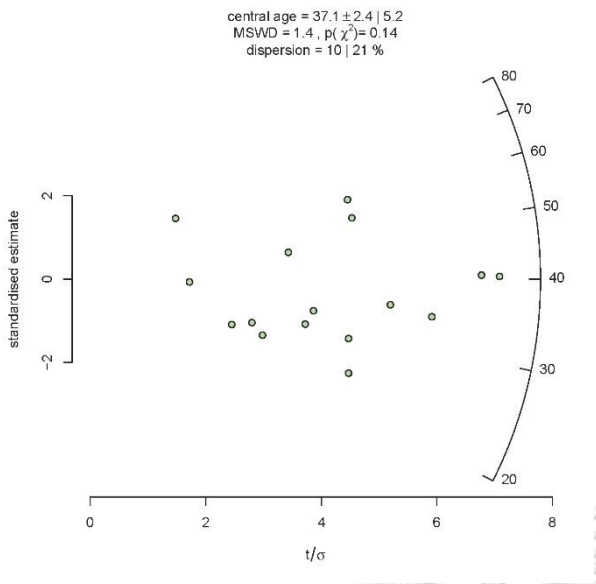

Figure 3.9 *Radial plots to illustrate the relationship between apatite single grain ages assigned to the Fish Canyon Tuff apatite (FCT) standard sample*

3.11 Sample preparation procedures

For apatite fission track dating, it is necessary to separate apatite from their host rocks using their characteristic properties of size, magnetism and density. The examination of petrographic thin sections is sometimes convenient to observe the presence of apatite in sample before starting the separation procedure. Figure 3.10 displays several steps of mineral separation procedure (Tagami et al., 1988).

3.11.1 Mineral separation

3.11.1.1 Crushing

This procedure will do with hard rock for resize the large rocks into small rock chips (3-5 cm-dimension) by using a rock trimmer, a jaw crusher and, a disc mill, respectively.

3.11.1.2 Sieving and Panning

After rock was crushed into small rock chips, the amount of non-using mineral should be discarded and collected only heavy mineral as much as possible. For this procedure, the sample will be washed and separated by wet sieving with mesh no. 60. Normally, the heavy minerals for AFT, such as apatite, zircon, and sphene, has about less than 0.250 mm-diameter-size that can collect them from the particles that pass through a mesh no.60. In case of a lot of unnecessary mineral, like quartz, feldspar,

or mica, Panning will be useful to reduce the amount of sample to reduce the sieving time. After this process, the sample will be dried in the oven with less or equal 60°C for 1 day.

3.11.1.3 Heavy liquid separation (LST: Lithium Sodium Tungstate)

In this process, the dried sample will be separated by using the LST in a separatory funnel, which is non-toxic heavy liquid with density of 2.87 g/cm^3. The heavy particles will sink to the bottom and the light particle will be float. The heavy particle will be collected and washed until it clean and keep it dry in the fume hood.

3.11.1.4 Magnetic separation

The dry heavy portion was mixing of non-magnetic minerals and magnetic minerals. Apatite, zircon, and sphene which are commonly required in FT dating, are non-magnetic mineral, so the magnetic minerals should be removed by using Nd magnet which is a permanent magnet.

3.11.1.5 Heavy liquid separation (Diiodomethane)

For AFT dating is required only an apatite, therefore other non-magnetic heavy mineral, such as zircon and sphene should be taken away. Diiodomethane is toxic heavy liquid which is the density of 3.32 g/cm^3. This procedure must do carefully in fume hood and use it less possible. After mixing of the liquid and heavy minerals, the lighter minerals, such as apatite and tourmaline, will float but zircon, sphene which has more density than the liquid, will sink at the bottom of beaker. Then, the floated mineral is garnered and washed by acetone. The final product will keep in fume hood again about 1-2 hours.

3.11.2 Sample preparation

After mineral separation processes are done, it is importantly to prepare the sample before AFT dating. For doing sample preparation, Tagami et al. (1988) proposed three necessary steps would be done before doing AFT analysis. (Figure 3.11).

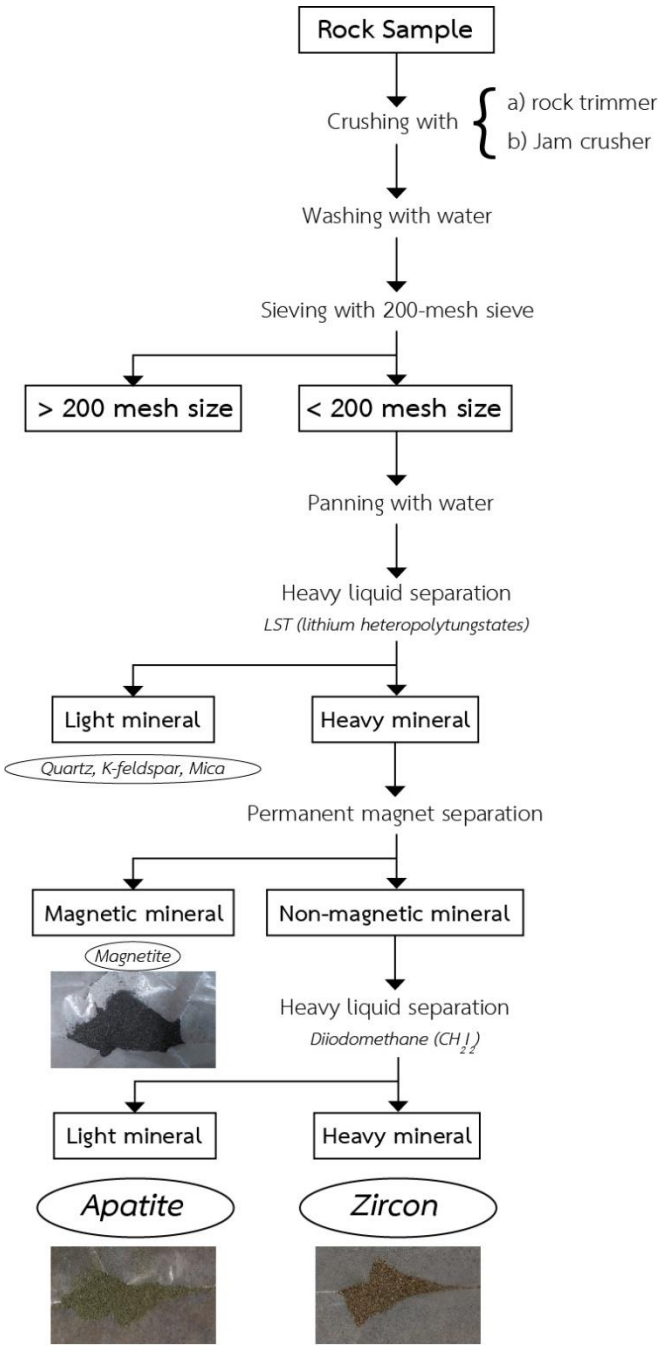

Figure 3.10 *Flow chart for mineral separation (modified from Tagami et al., 1988).*

3.11.2.1 Handpicking and mounting

In this method, 25 apatite grains in array of 5x5 or 36 apatite grains in array of 6x6 are placed on the teflon slide. The c-axis of apatite grain must be parallel with the slide. Then, the epoxy resin of fixed a mount is poured on the grains carefully so that the grain arrangement is not disturbed. Next, the amount of epoxy resin is covered by

another Teflon slide on the glass spacer (Figure 3.11). The resin should be kept for about 24 hours at room temperature to be solid. After that, it is slightly heat, which should be kept below 60℃ for 1-2 hours. The resin will accelerate the solidification that is removed easily. Finally, the sample must be written the code on the backside of a mount.

3.11.2.2 Grinding and polishing

This process is essential to remove a certain thickness to expose 4π geometry for observing spontaneous track density. The thickness corresponds to half of etchable track length of apatite which is about 8 μm (Gleadow et al., 1986). For opening surface of grains, mount must be grinded with the emery paper of 1500 mesh size (wetted with water) till maximum possible area expose. (This step will be called as "pre-grinding").

After pre-grinding, mount will be removed to expose 4π geometry. The mount is ground perpendicular to the direction of pre-grinding until all of the previous grinding scratches disappear. This ensure that all the exposed surface area has been ground and remove for at least 1 μm. Next step of grinding is repeating perpendicular to previous direction of scratches and makes new scratches of all surface area to confirm the removal of another 1 μm. Hence, each step of grinding must repeat for 8 times.

After the grinding, the mount is polished successively to remove preceding grinding scratches with 15 μm and then 3 μm diamond paste.

3.11.2.3 Etching

This procedure is to enlarge fission tracks to be visible. The etching of apatite uses 5 HNO_3 at 20℃ for 20 second. After the experiment is done, mount must clean rapidly by distilled water 2-3 times to avoid the corrosion of acid which continue enlarge the tracks.

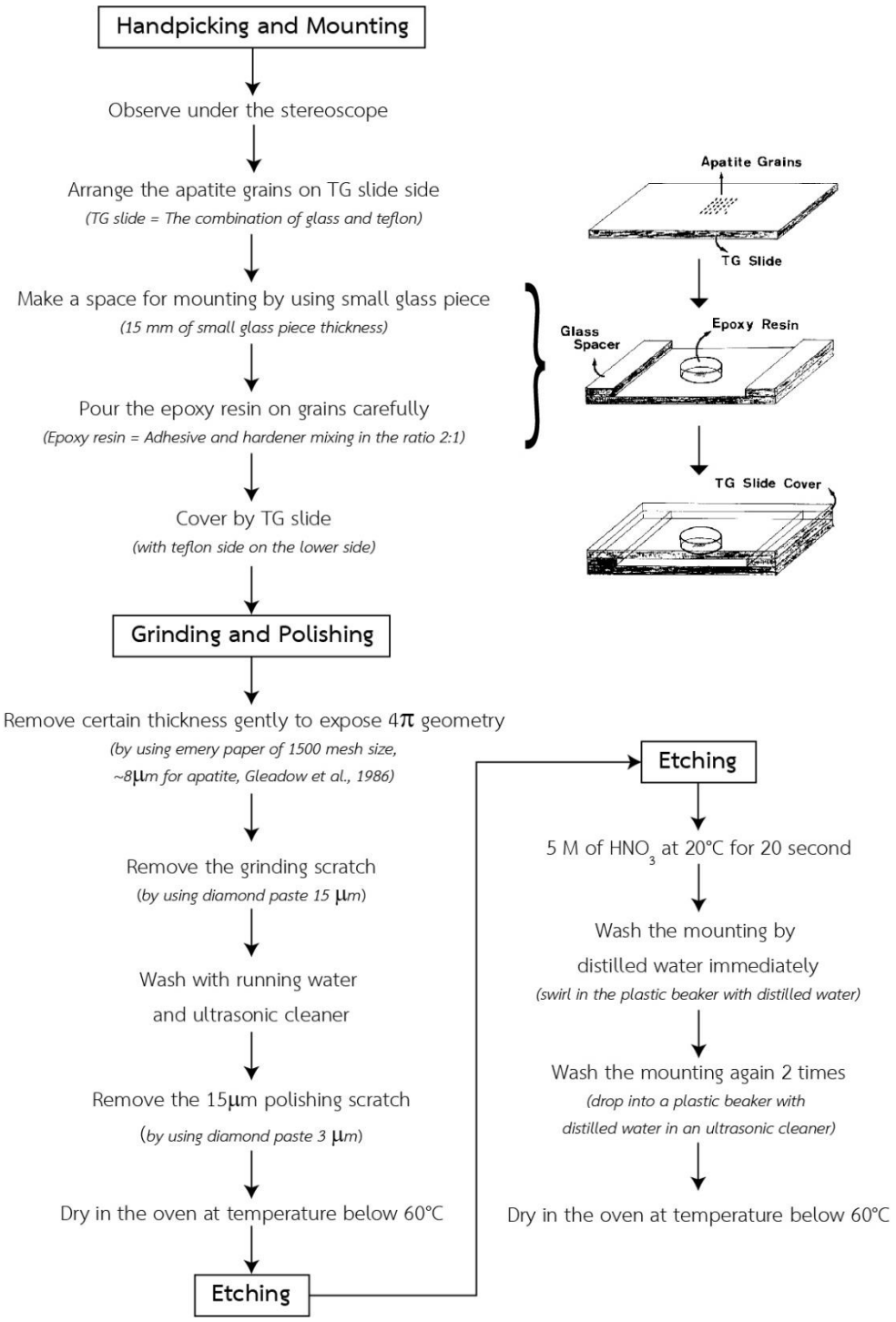

Figure 3.11 *Flow chart for sample preparation (modified from Tagami et al., 1988).*

Chapter 4 Results

In order to fulfill the objectives of this thesis. Not only the results of AFT dating data of the Khorat sedimentary rocks are present but also their structures and stratigraphic sequences are displayed herein.

4.1 Structural analysis

Remote sensing image (from Google Earth) of the PPR study area (Figure 4.1) have been interpreted using visual interpretation. The lineament map of the study area in Figure 4.2 indicates a series of interpreted synclinal and anticlinal structures as well as fractures and joints. Figure 4.3 is a simplified geological map showing structural data from the current and previous field data together with those interpreted from Google Earth image.

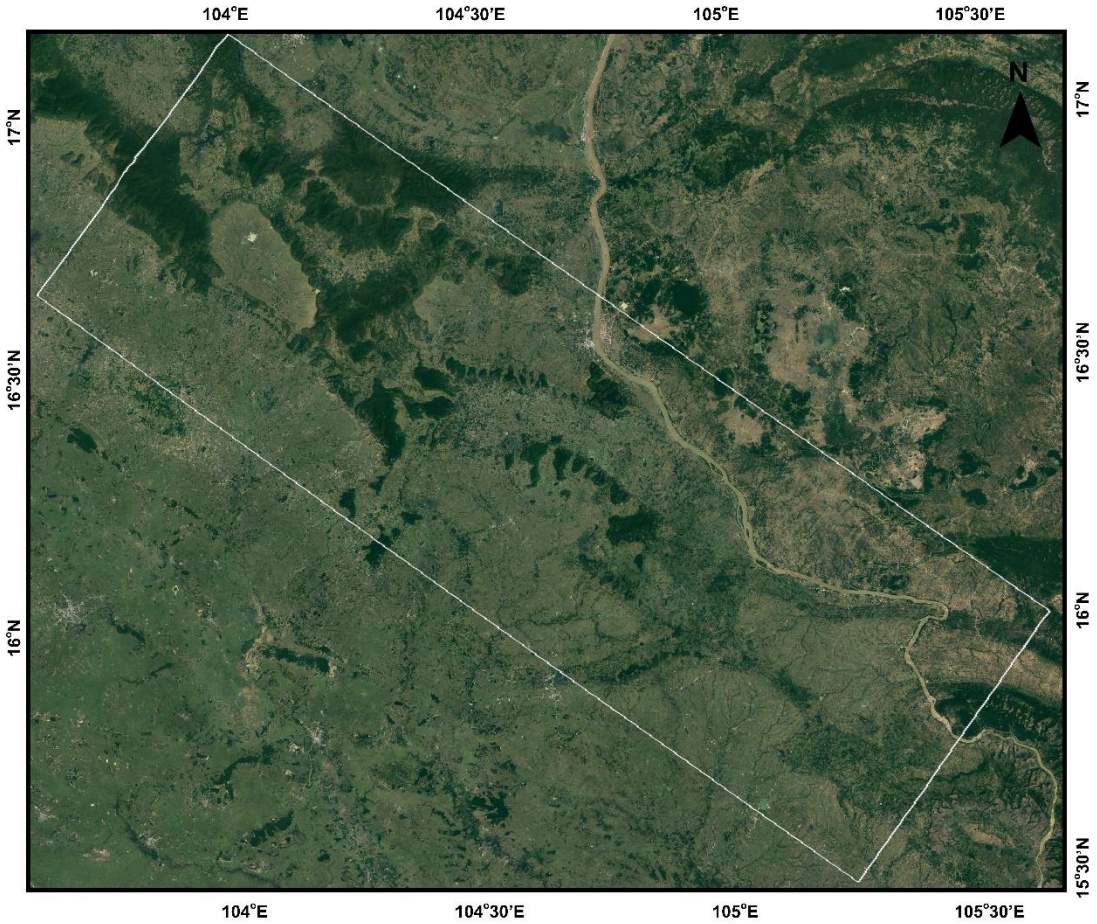

Figure 4.1 *Google image data of the study (white box) and nearby areas in the Phu Phan Ranges.*

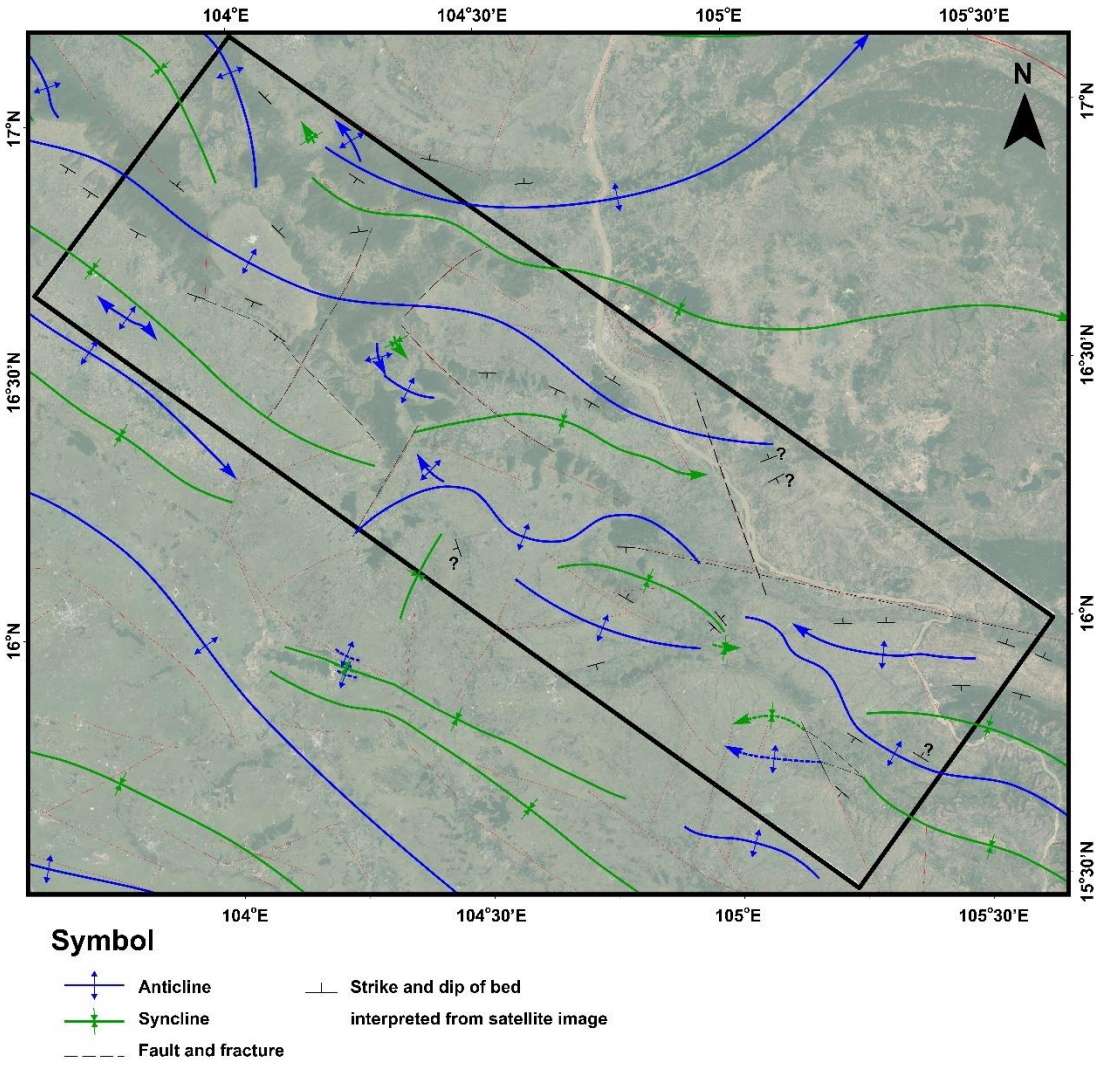

Figure 4.2 *Google map showing lineaments with interpreted fold structures using bedding traces.*

Several outcrops in the Phu Phan Mountain Range were visited and a total of 25 measurements were recorded (Table 4.1). They are 619 points for the attitudes of bedding from measured outcrop in field and attitude of bedding in geological map based on 1:50,000 from DMR (1999; 2000; 2001; 2004; 2008). All structural data are shown in Figure 4.3. A rose diagram reveals that the principle trend in the Phu Phan Mountain area is the NW-SE (Figure 4.4). In addition, trending of dip direction for the Phu Phan Mountain area is shown two directions, they are NE and SE direction (Figure 4.5). In conclusion, the geological structural result of this study harmonizes with the lineament map by Sangsomphong et al. (2018). It is inferred that the Phu Phan Range has a complex compressive structural area, like anticlinal and synclinal structures

(Figure 4.6). Moreover, joints are also measured in individual outcrops. The attitude of joint is displayed in appendix A. Figures 4.5 and 4.6 show cross-sections of study area which cut through the main structure of the area with the elevation of sample. Zoomed picture of each section in Figure 4.8 are in appendix A. It can be clearly seen (as shown in Figure 4.8A) that the Phu Phan Range structure is dominated by a series of broad syncline and anticline. The anticlinal structures of the Phu Phan Mountain area have the wavelength vary from 2 to 26 km and the amplitude of folds from about 200 meters to 300 meters.

Table 4.1 Attitude of bedding in this study

Site	Strike/Dip	Site	Strike/Dip	Site	Strike/Dip	Site	Strike/Dip
PP01	313/02	**PP05-2**	127/05	**PP08**	306/08,	**PP13**	254/06
PP02	290/10	**PP05-3**	182/02,		306/04	**PP14**	071/09
PP03	276/18		172/06	**PP09**	107/10	**PP15**	051/05
PP04	199/04,	**PP06**	020/04,	**PP10**	121/06	**PP16**	005/22
	203/03		017/04	**PP11**	179/06	**PTT14**	218/10
PP05-1	166/04,	**PP07**	342/04	**PP12**	255/10	**PTT15**	139/09
	171/04						

4.2 Stratigraphy

Based upon the current lithological and stratigraphical investigations, the Phu Phan Mountain Range study area consists of 5 formations, from old to young, are Phu Kradung, Phra Wihan, Sao Khua, Phu Phan, and Khok Kruat Formations, respectively. Figure 4.13 shows the comparison of stratigraphic column of each cross-section line. The composite lithostratigraphic column of Phu Phan Mountain Range is illustrated in Figure 4.14. The correlation of the lithostratigraphic column between Khorat Group (Department of Mineral Resources, 2014; Racey, 2009) and Phu Phan Mountain from this study is shown in Figure 4.15.

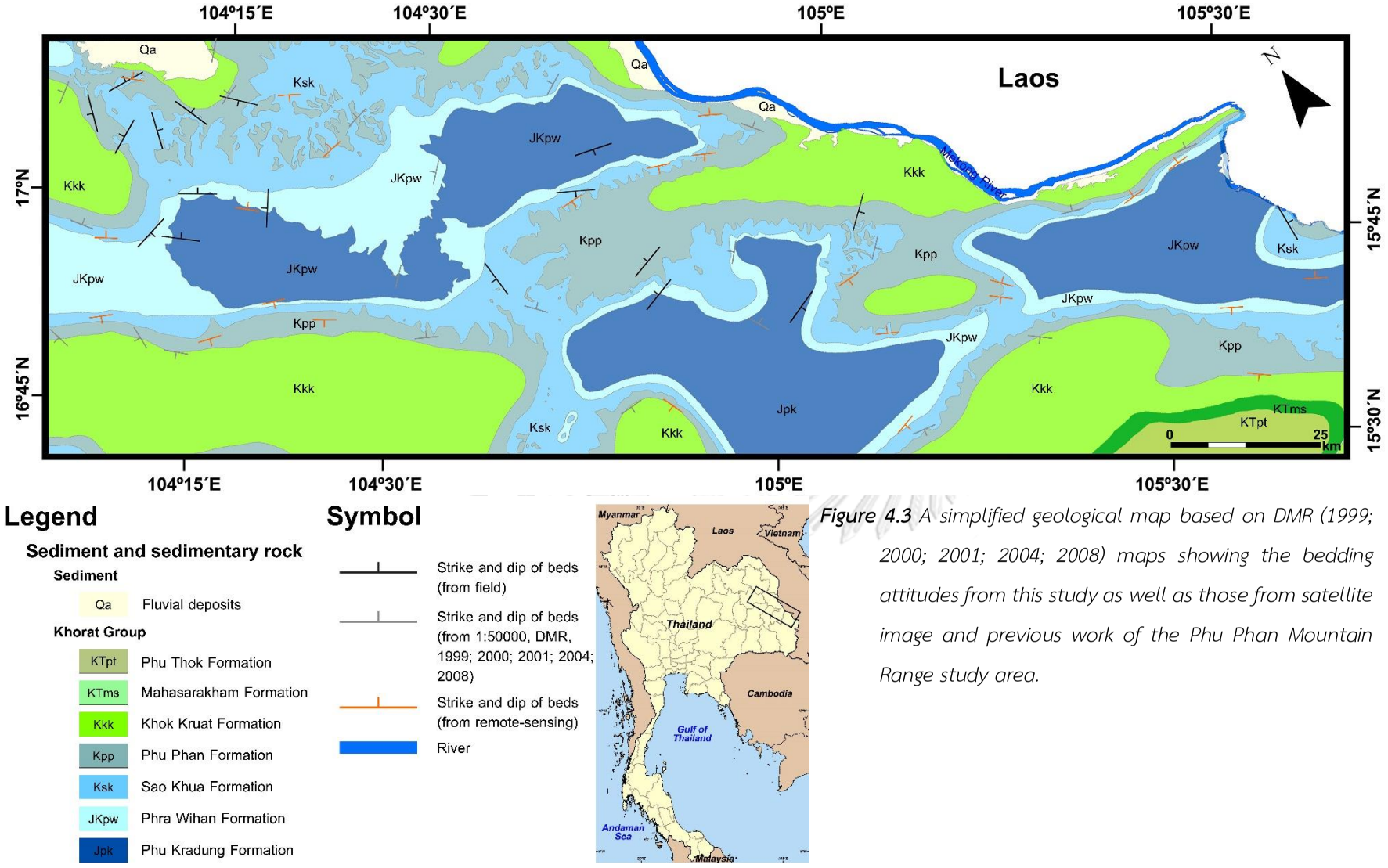

Figure 4.3 A simplified geological map based on DMR (1999; 2000; 2001; 2004; 2008) maps showing the bedding attitudes from this study as well as those from satellite image and previous work of the Phu Phan Mountain Range study area.

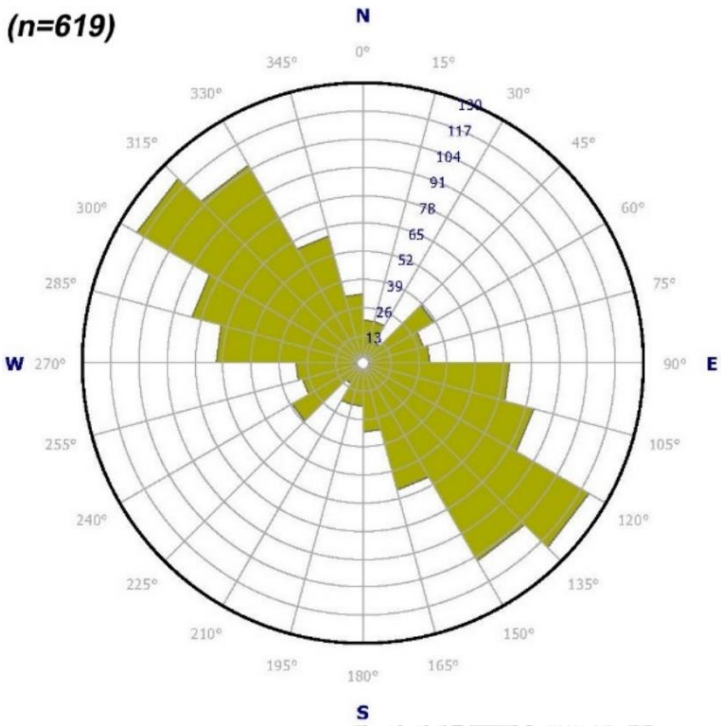

Figure 4.4 *A rose diagram showing strikes of beds in Phu Phan Mountain area are NW-SE. (n is number of bed)*

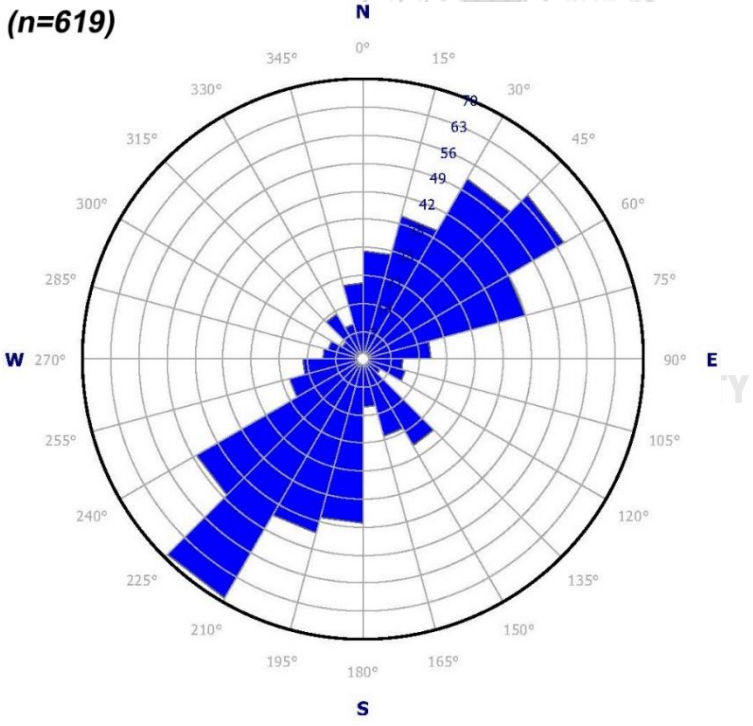

Figure 4.5 *A rose diagram showing dip direction of beds in Phu Phan Mountain area are NE-SW. (n is number of bed)*

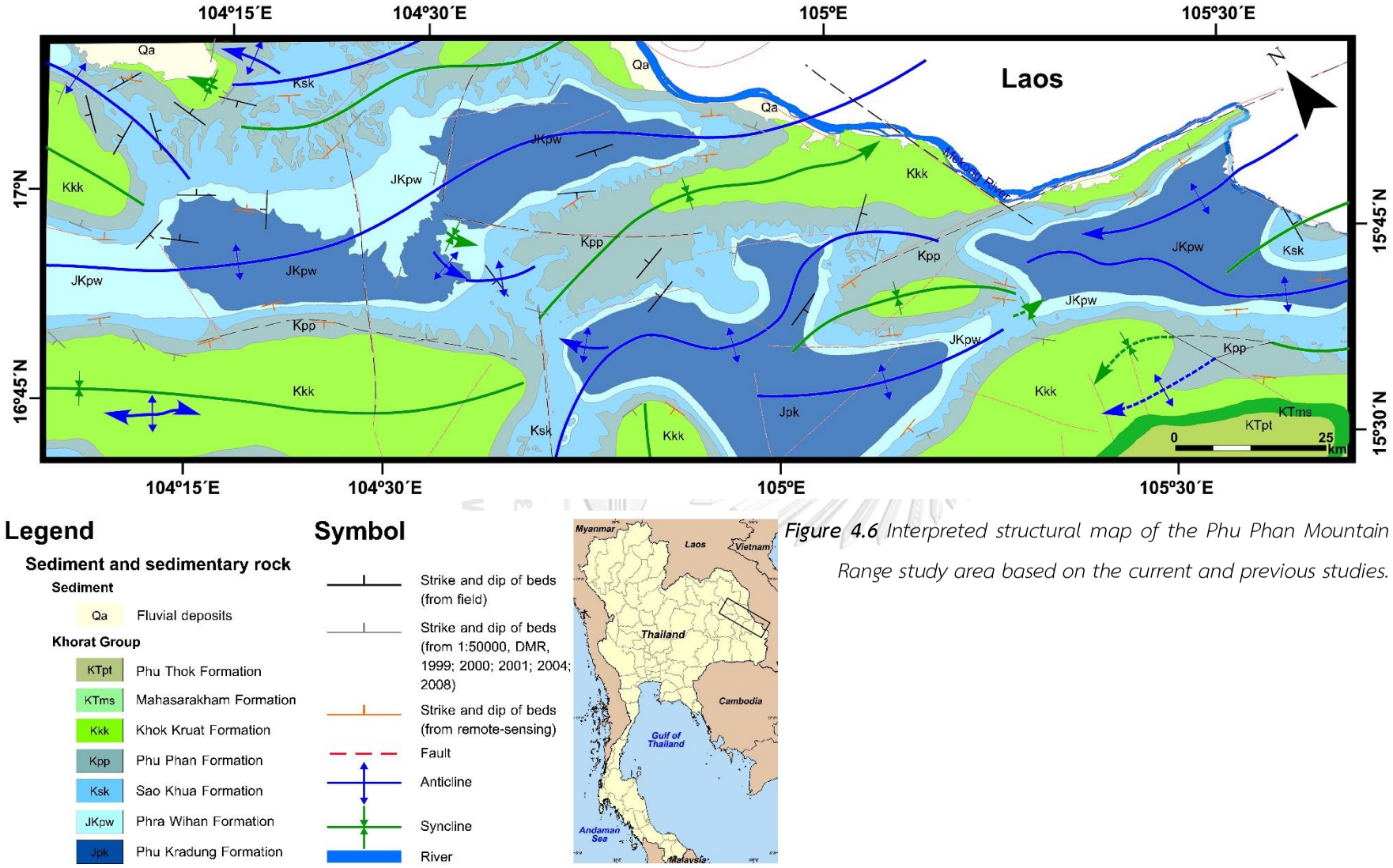

Figure 4.6 *Interpreted structural map of the Phu Phan Mountain Range study area based on the current and previous studies.*

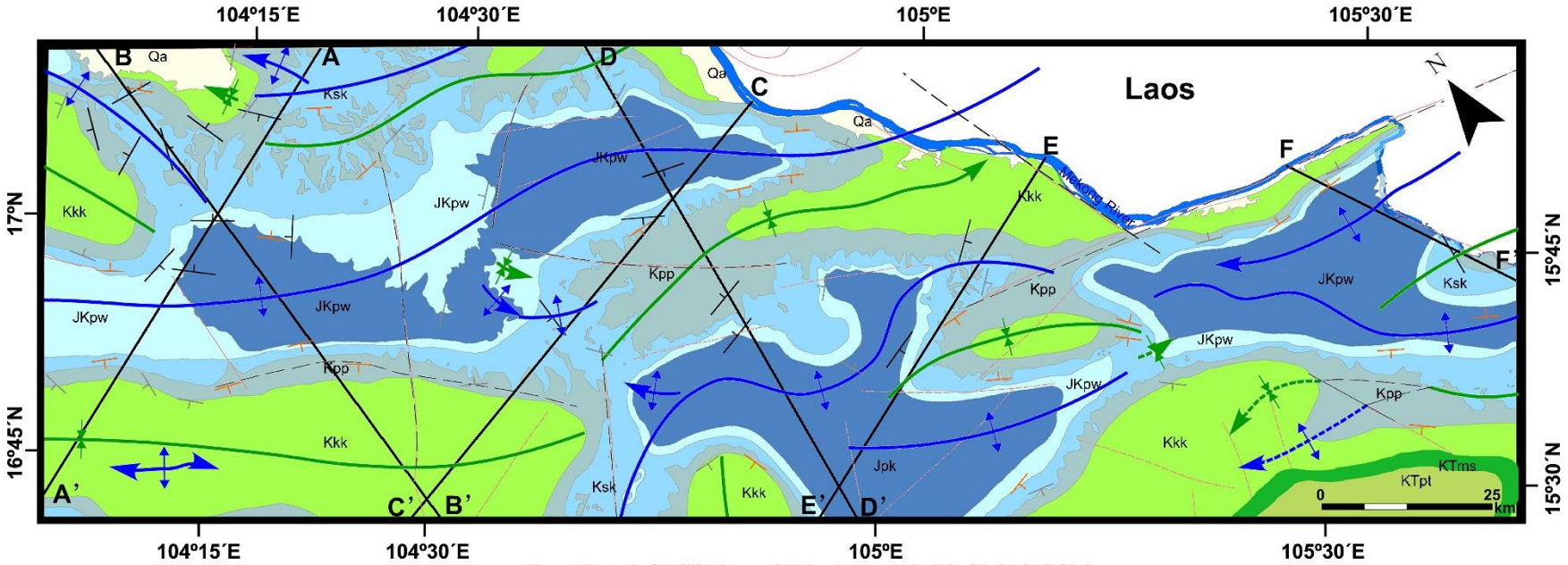

Legend

Sediment and sedimentary rock

Sediment

- Qa — Fluvial deposits

Khorat Group

- KTpt — Phu Thok Formation
- KTms — Mahasarakham Formation
- Kkk — Khok Kruat Formation
- Kpp — Phu Phan Formation
- Ksk — Sao Khua Formation
- JKpw — Phra Wihan Formation
- Jpk — Phu Kradung Formation

Symbol

- Strike and dip of beds (from field)
- Strike and dip of beds (from 1:50000, DMR, 1999; 2000; 2001; 2004; 2008)
- Strike and dip of beds (from remote-sensing)
- Fault
- Anticline
- Syncline
- A — A' Line of section
- River

Figure 4.7 *A simplified geological map based on 1:50,000 map modified from DMR (1999; 2000; 2001; 2004; 2008) showing beddings and structural geology of this study area with cross-section line.*

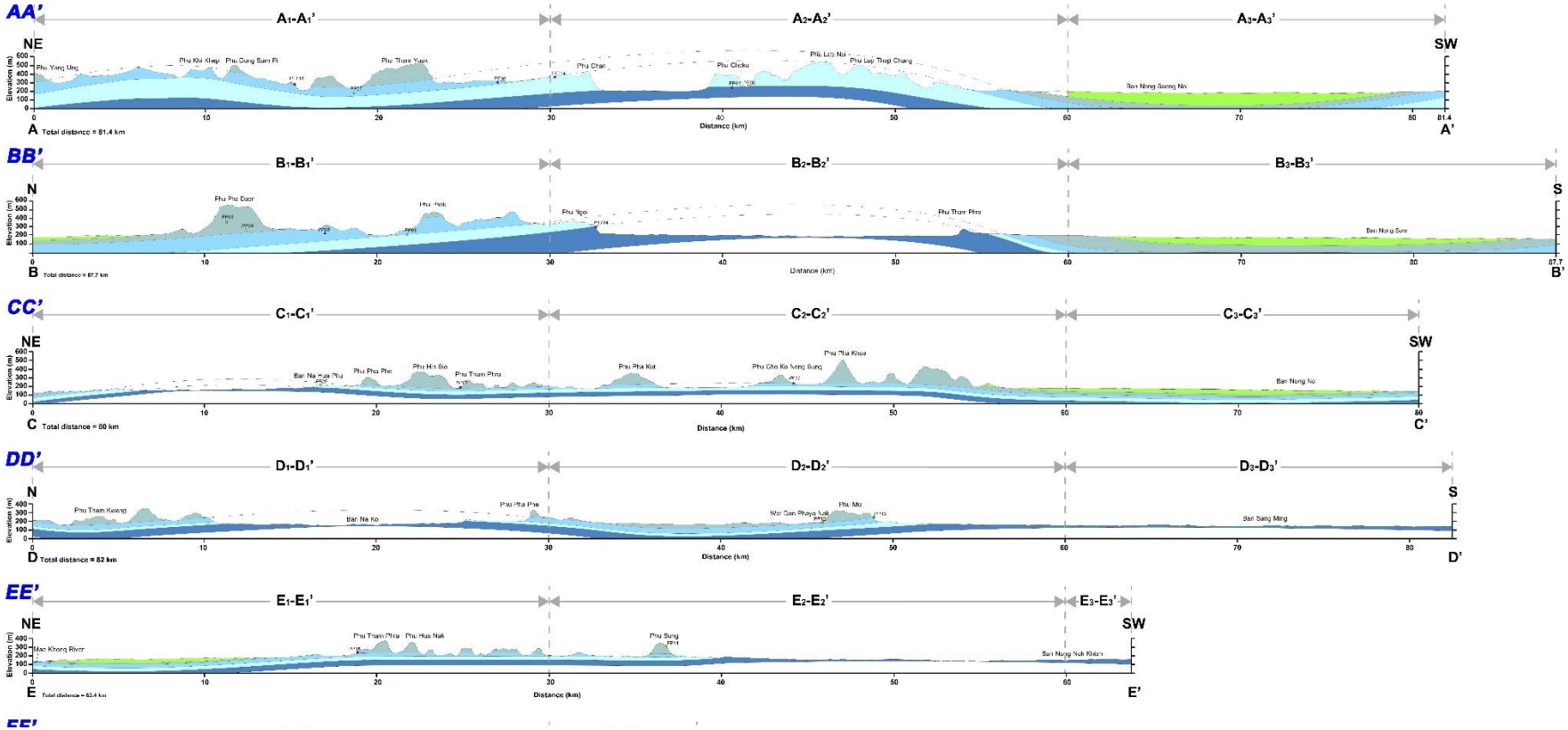

Figure 4 8 *The cross-sections of this study from Figure 4.5. The maximized pictures are in appendix B.*

4.2.1 Phu Kradung Formation

The oldest formation of Khorat Group is the Phu Kradung Formation that can be found in the Phu Phan Mountain Range study area. The Phu Kradung Formation exposed clearly along the highway 2287 (16°07'48"N/104°41'39"E) in Nong Phue District, Kalasin Province (Figure 4.9). The other well exposed rocks are along the highway 2219 km 41+700 at 16°48'18"N/103°57'53"E in Nakhu District, Kalasin Province. The attitudes of beddings are 218/10 NW and 313/02 NE. The bed trending of this formation is NW-SE. The measured thickness varies from 15 - 47 meters. Lithology of the Formation includes red, fine-grained sandstone with well-defined cross-bedding with minority of mudstone.

Figure 4.9 *Natural outcrop of sandstone of the Phu Kradung Formation along the Highway 2287 (16°07'48"N/104°41'39"E), Nong Phue District, Kalasin Province (Mr. Wason Kongpermpool, 172 cm-tall, is to scale). White rectangle is the sampling site.*

4.2.2 Phra Wihan Formation

The Phra Wihan Formation is well exposed at Kham Toei Waterfalls in Na Khu District in Kalasin Province (Figure 4.10). The other good exposures of the Phra Wihan

Formation are at Na Sok municipal District post, local road 2092, 16°30'45"N, 104°35'05"E in Mueang Mukdahan District, Mukdahan Province. In general, bedding attitudes are 290/10 NE and 107/10 SW. The bed trending of this formation is NW-SE. The thickness is about 10 - 30 meters. The sandstone is mainly white medium-grained sandstone with cross-bedding. Mudstone is always alternated with this white sandstone.

Figure 4.10 *Natural outcrop of sandstone of the Phra Wihan Formation in front of the entrance of Kham Toei Waterfall (16°48'48"N/103°57'37"E), Na Khu District, Kalasin Province (Ms. Chonnipha Fakseangsa, 150 cm-tall, is to scale). White rectangle is the sampling site.*

4.2.3 Sao Khua Formation

The Sao Khua Formation is well exposed at Phu Phan Buddha Nimit temple (16°58'53"N/103°59'29"E), Phu Phan District, Sakhon Nakhon Province (Figure 4.11). The other good outcrop is at Wat Phuttha Kiri (16°27'08"N/104°20'21"E), Nong Sung District in Mukdahan Province. Bedding attitudes strike from 127 to 276 and dip angle from 2 to 18 in SW to N. The bed trending of this formation is NW-SE. The thickness varies from 5 to 30. meters. Lithology of the formation is characterized by reddish brown fine-grain sandstone with few cross-bedding shale and mudstone.

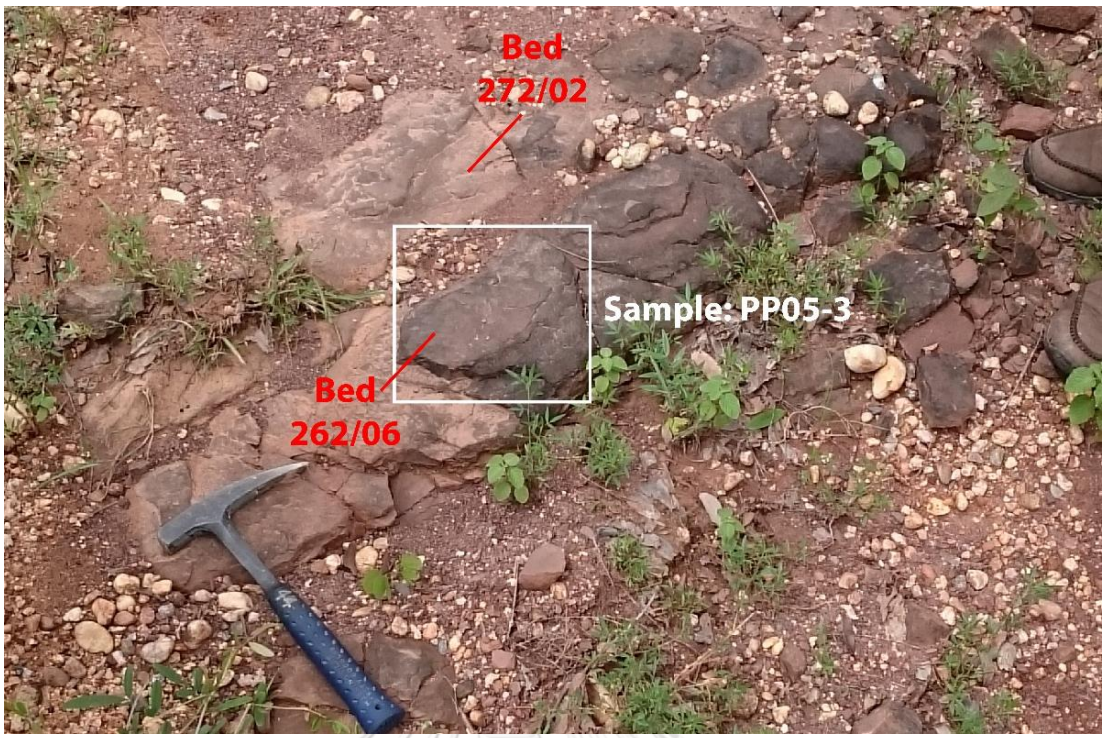

Figure 4.11 *Natural outcrop of sandstone of the Sao Khua Formation in front of the entrance of Phu Phan Buddha Nimit Temple (16°58'53"N/103°59'29"E), Phu Phan District, Sakhon Nakhon Province (Geological hammer, 32.5 cm-long, is to scale). White rectangle is sampling site.*

4.2.4 Phu Phan Formation

Rocks of the Phu Phan Formation are well exposed along the highway 2358 (16°11'41"N/104°51'35"E), Tao Ngoi District, Sakhon Nakhon Province (Figure 4.12), Few good exposures are at Local road 4001 km 11 (16°49'55"N/104°03'51"E) in Na Khu District, Kalasin Province. The bed trending attitude of this formation are 20 to 342 Strikes and 3 to 22 dip angles in SW to NE. The thickness is from 6 to 30 meters. Whitish gray to grayish yellow fine to medium-grained sandstones are quite dominate with some cross-beddings, Mudstone is locally found in association.

Figure 4.12 *Natural outcrop of sandstone of the Phu Phan Formation along Highway 2358 (16°11'41"N/104°51'35"E), Tao Ngoi District, Sakhon Nakhon Province (Right person-Mr. Sitichok Kumrangwat, 180 cm-tall, is to scale). White border square is sampling site.*

4.2.5 Khok Kruat Formation

The youngest formation of Khorat Group is the Khok Kruat Formation. The formation is well exposed only in the south where no good road is available in the Phu Phan Mountain Range study area. However, based on the geological map by Department of Mineral Resource (2008), Khok Kruat Formation has been found in Pathum Ratchawongsa District in Amnat Charoen Province and Kut Khaopun District in Ubon Ratchathani Province. The average strike of bed is in the NW-SE direction. The thickness varies from 4 to 33. meters. The main rocks of the Khok Kruat Formation are reddish brown to brown fine-grained sandstones with some cross-beddings are also reworked by DMR (2008).

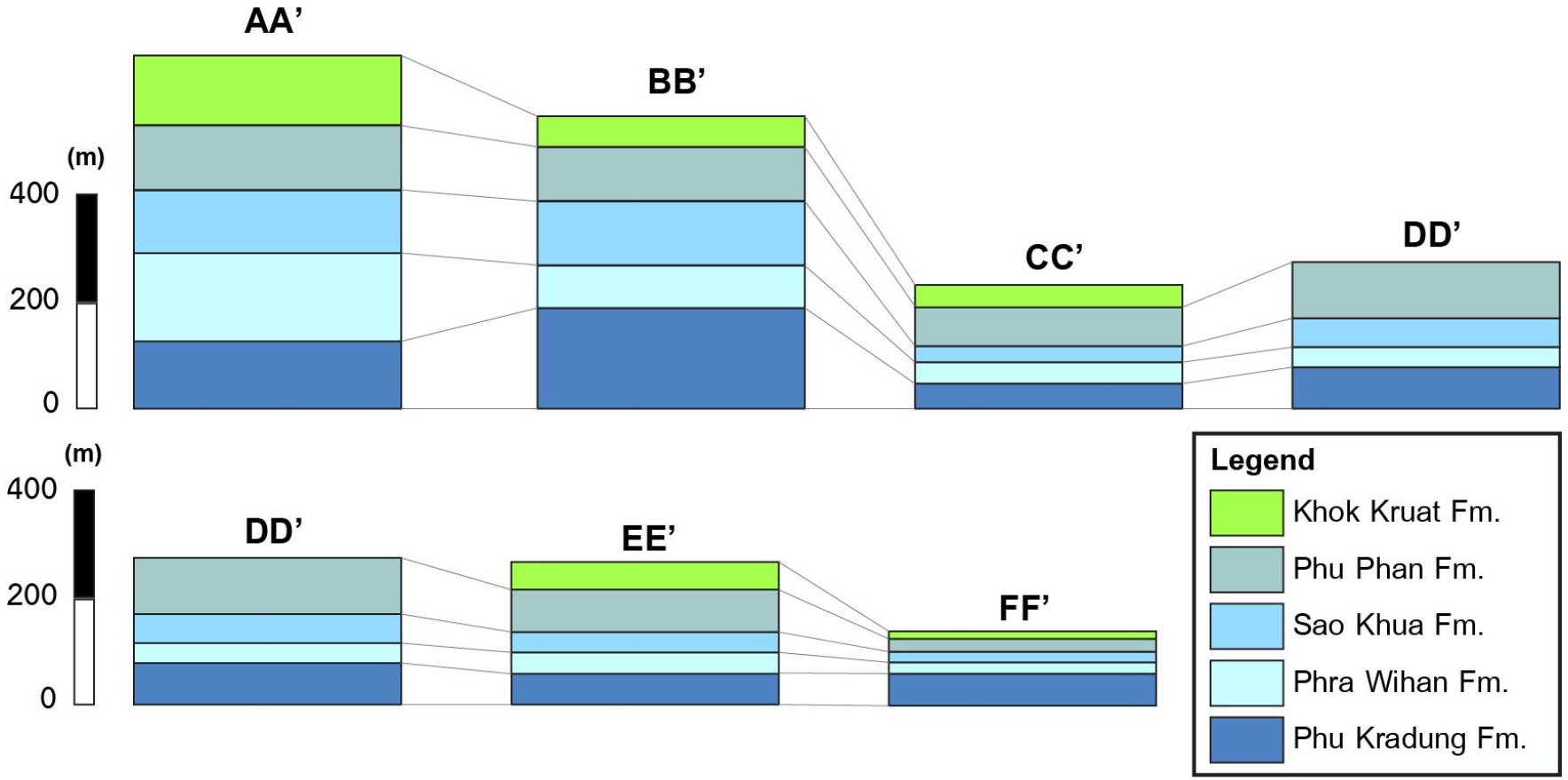

Figure 4.13 *Lithostratigraphy columns of the Phu Phan Mountain Range study area based upon individual cross sections appeared in Figure 4.6.*

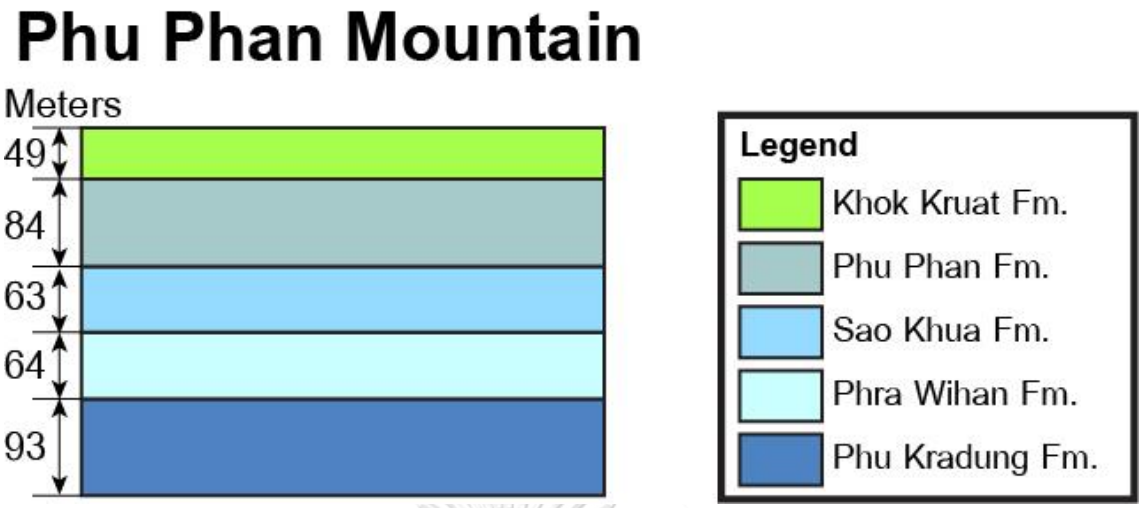

Figure 4.14 *Composite lithostratigraphic column showing thickness of individual formations found in the Phu Phan Mountain Range study area.*

4.3 Paleocurrent patterns

From the detailed surveys of 18 site visits, cross bed can be found in 13 sites which is from Phra Wihan Formation 1 site, Sao Khua Formation 3 sites, and Phu Phan Formation 9 sites. Attitude of cross bed from each outcrop is shown in Table 4.2. The details are as follows.

4.3.1 Phra Wihan Formation

Only one cross bedding was encountered. The direction of each studied site is shown in Figure 4.16. A rose diagram displays the direction of flow is to northwestward (Figure 4.19 top-left).

4.3.2 Sao Khua Formation

There are approximately 13 data of cross beddings from 3 outcrops in the Phu Phan Range area. The directions of individual sites are illustrated in Figure 4.17. A rose diagram displays that the direction of current is mainly from NE to SW and some from NW to SE direction (Figure 4.19 top-right).

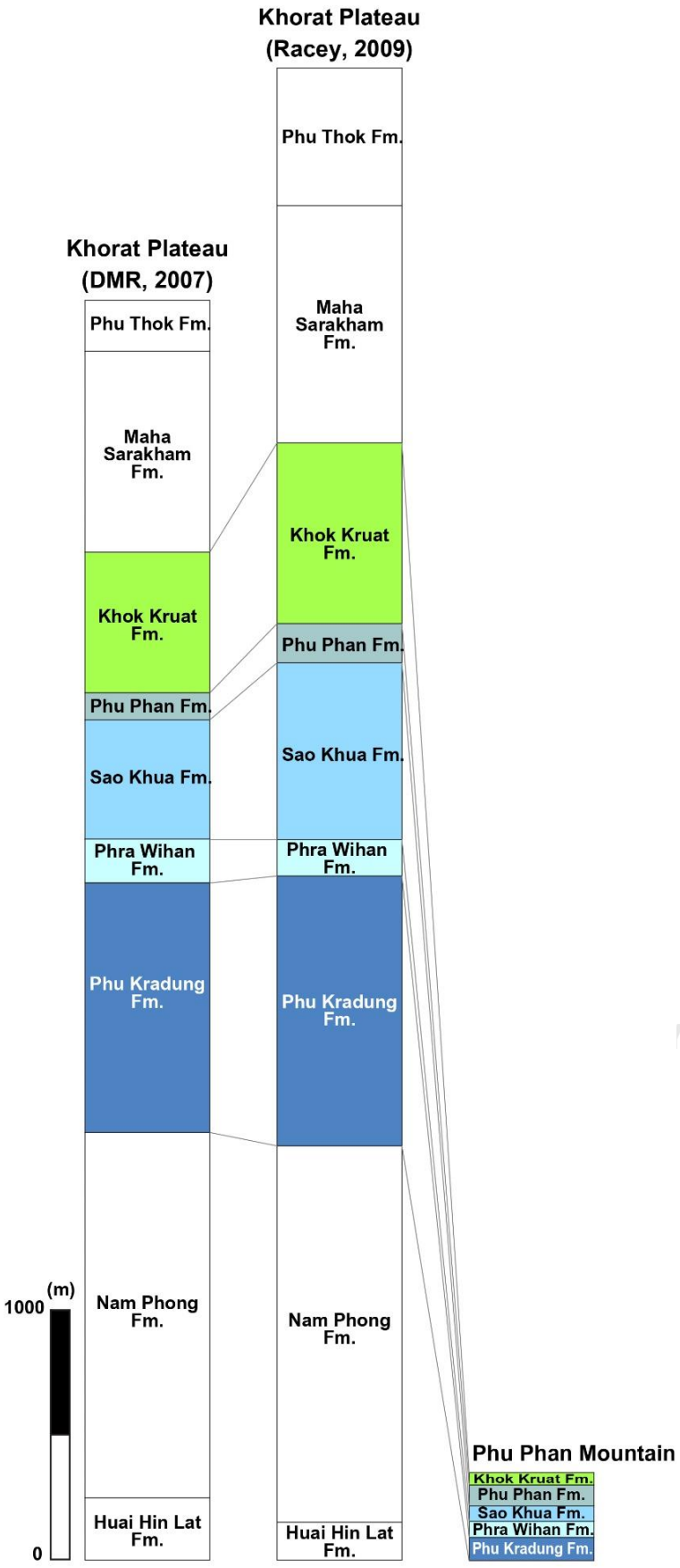

Figure 4.15 *Lithostratigraphic columns of the Khorat Group based on the works of DMR (2007) and Racey (2009) and Phu Phan Mountain Range from this study.*

4.3.3 Phu Phan Formation

There are 77 data of cross beddings from 9 outcrops in the study area. The direction of each studied site is shown in Figure 4.18. A rose diagram displays the two current directions – one is from NE to SW direction and the other NNE to SSW direction. Because the fold structure of the Phu Phan Mountain Range study area is broad fold, so paleocurrent direction is not much affected by tectonic deformation. Therefore, in conclusion, the regional flow pathway is from NE to SW direction. (Figure 4.19 bottom-left).

Table 4.2 Attitude of cross bedding in this study

Site	Strike/Dip	Site	Strike/Dip	Site	Strike/Dip	Site	Strike/Dip
PP02	007/28	**PP07**	131/32	**PP11**	234/14	PP15	076/30
PP03	155/05		093/18		170/21		047/14
	172/14		145/28	**PP12**	179/16		165/34
	052/14		068/27		140/12		272/29
	073/07		038/25		204/16		172/15
	328/15		019/14		168/14		091/17
	062/18		101/28		146/05		113/31
PP04	253/24		077/17		112/16		102/31
	240/29		027/20	**PP13**	264/11		151/23
	158/25		112/22		154/15	**PP16**	106/18
PP05	148/20		955/21		181/07		154/24
	159/22		115/08		253/19		098/29
	183/30	**PP08**	288/10		208/07		106/18
	162/27		285/08		128/27		114/18
	148/20		224/12		138/25		104/08
PP07	122/33		125/25	**PP14**	107/26		098/17
	027/06	**PP10**	142/06		293/17		111/19
	142/23		189/12		077/08		049/11
	165/24		202/19		153/18		113/17
	076/26		249/23		151/16	**PTT14**	070/10
	098/15		337/25		178/16	**PTT15**	258/10
	146/28		262/09		239/13		
	080/20		303/05		152/19		
	082/19		236/10		007/39		

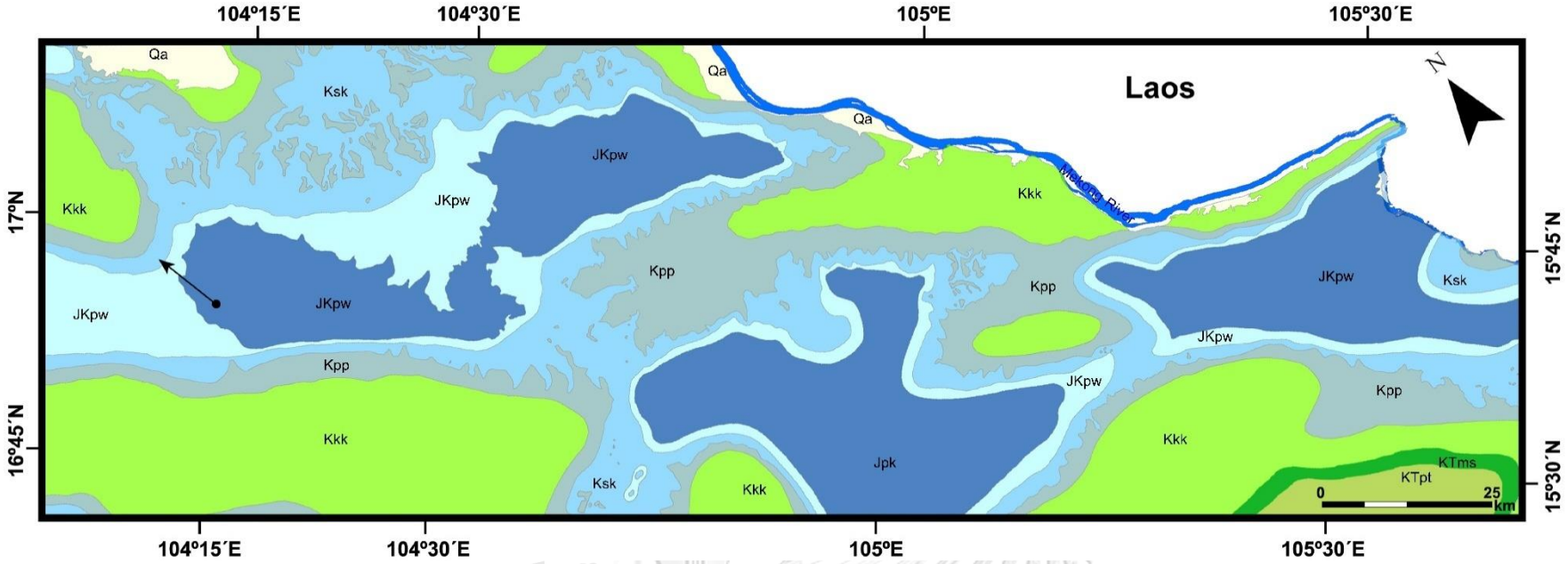

Legend

Sediment and sedimentary rock

Sediment

Qa	Fluvial deposits

Khorat Group

KTpt	Phu Thok Formation
KTms	Mahasarakham Formation
Kkk	Khok Kruat Formation
Kpp	Phu Phan Formation
Ksk	Sao Khua Formation
JKpw	Phra Wihan Formation
Jpk	Phu Kradung Formation

Symbol

Flow direction

River

Figure 4.16 *A simplified geological map based on 1:50,000 map modified from DMR (1999; 2000; 2001; 2004; 2008) showing the direction of cross-bed from exposures of the Phra Wihan Formation in this study area.*

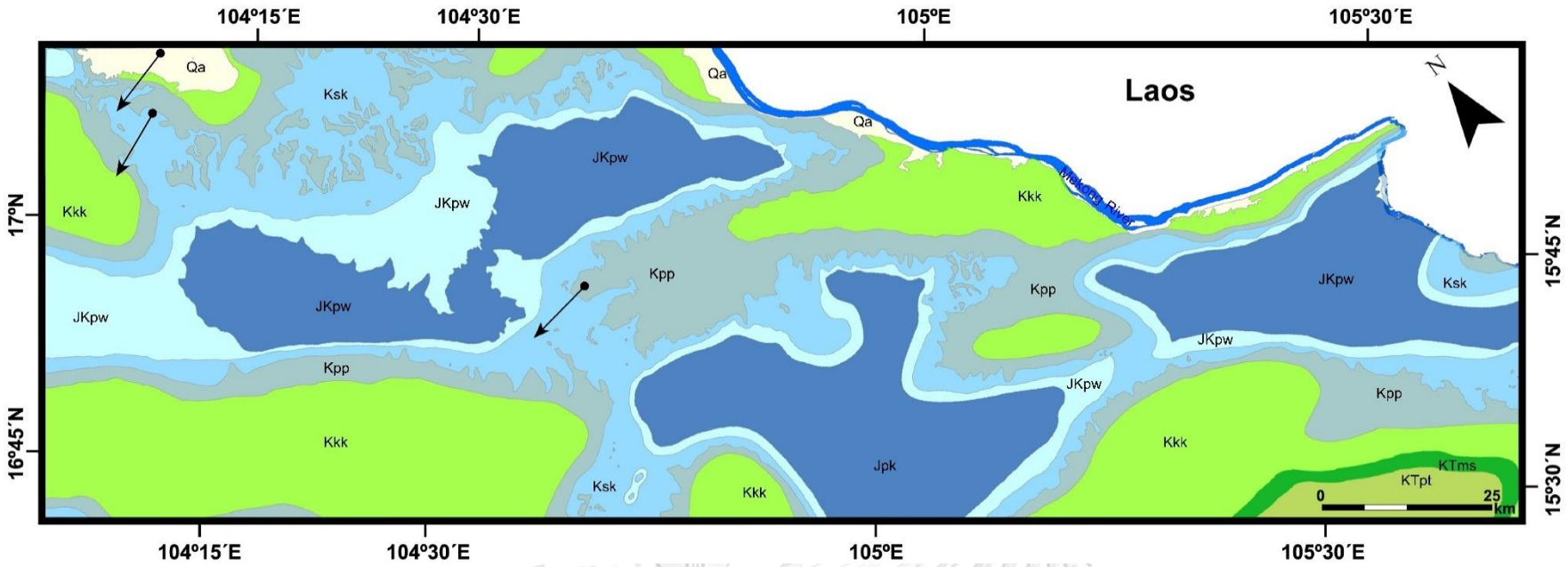

Legend

Sediment and sedimentary rock

Sediment

- Qa — Fluvial deposits

Khorat Group

- KTpt — Phu Thok Formation
- KTms — Mahasarakham Formation
- Kkk — Khok Kruat Formation
- Kpp — Phu Phan Formation
- Ksk — Sao Khua Formation
- JKpw — Phra Wihan Formation
- Jpk — Phu Kradung Formation

Symbol

- Flow direction
- River

Figure 4.17 A simplified geological map based on 1:50,000 map modified from DMR (1999; 2000; 2001; 2004; 2008) showing the direction of cross-bed from exposures of the Sao Khua Formation in this study area.

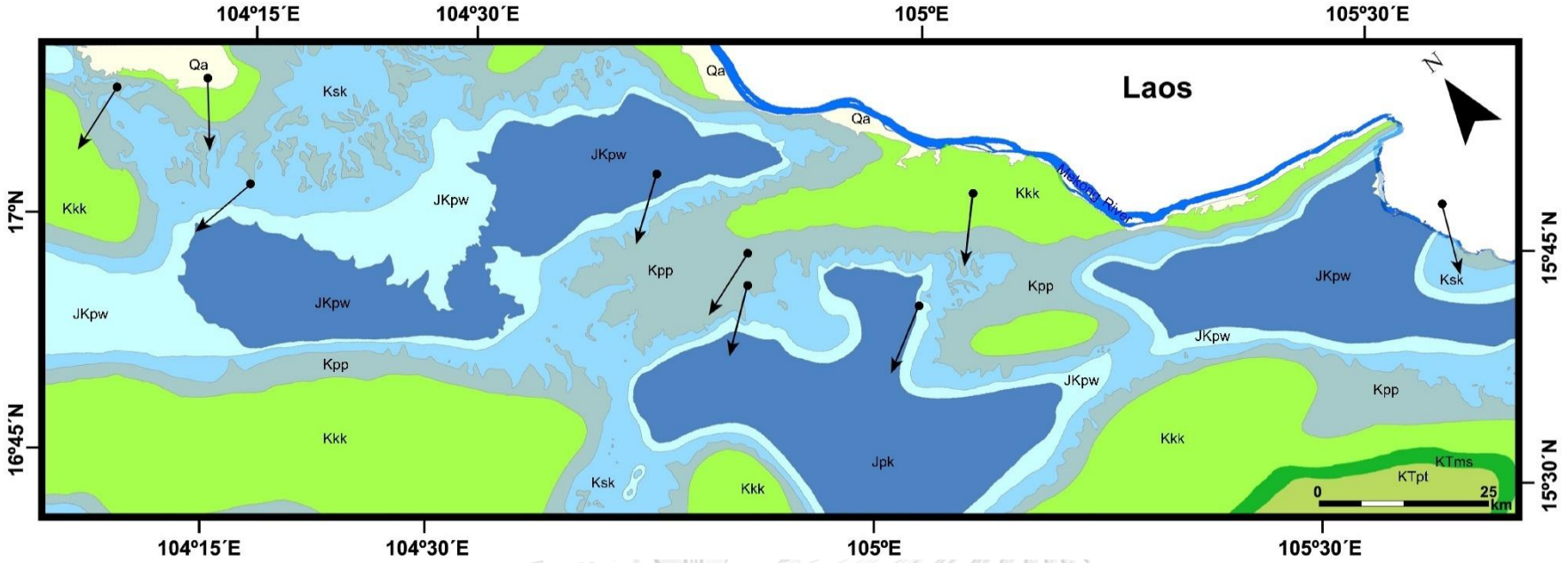

Legend

Sediment and sedimentary rock

Sediment

- Qa — Fluvial deposits

Khorat Group

- KTpt — Phu Thok Formation
- KTms — Mahasarakham Formation
- Kkk — Khok Kruat Formation
- Kpp — Phu Phan Formation
- Ksk — Sao Khua Formation
- JKpw — Phra Wihan Formation
- Jpk — Phu Kradung Formation

Symbol

- Flow direction
- River

Figure 4.18 A simplified geological map based on 1:50, 000 map modified from DMR (1999; 2000; 2001; 2004; 2008) showing the direction of cross-bed from exposures of the Phu Phan Formation in this study area.

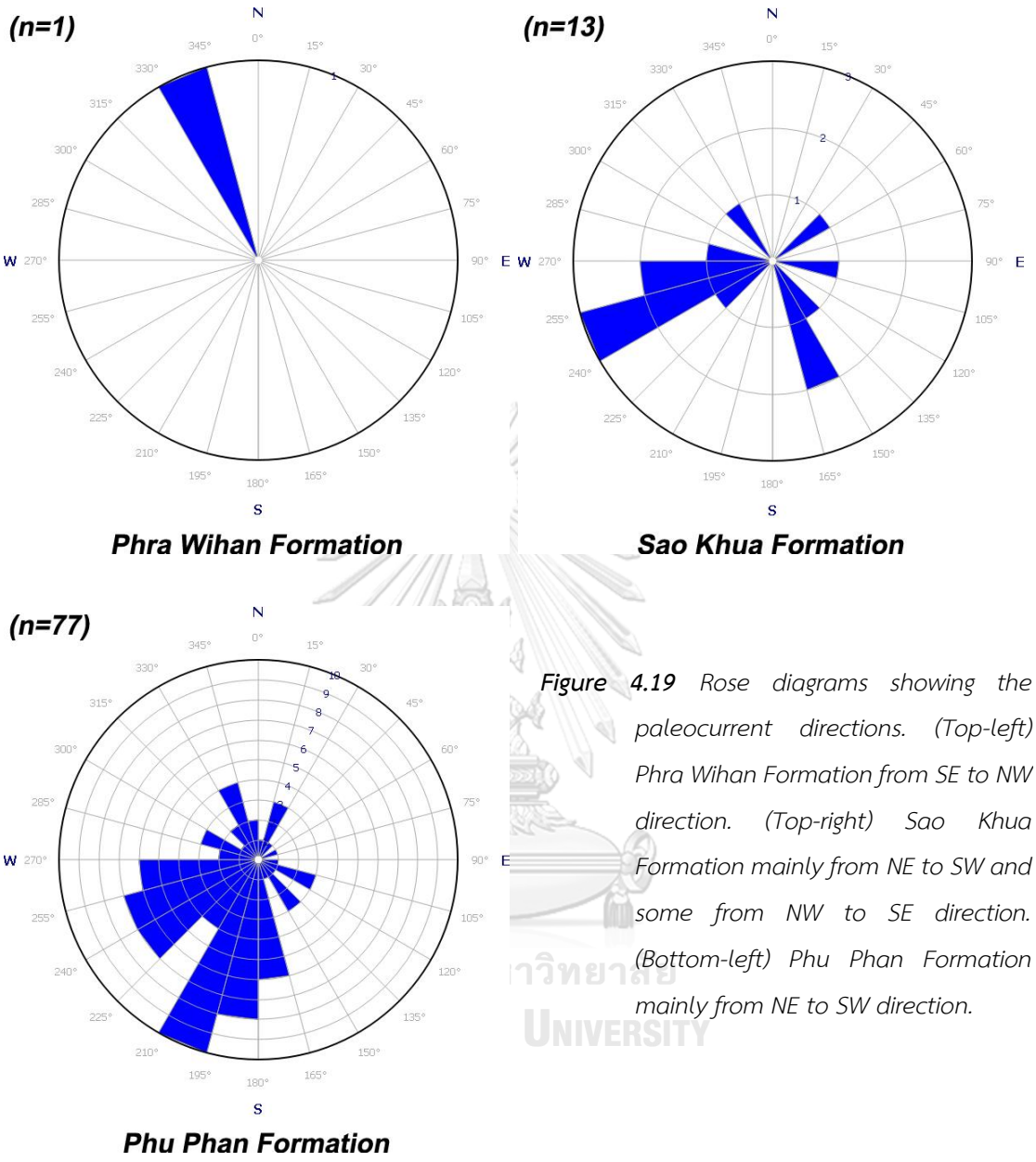

Figure 4.19 *Rose diagrams showing the paleocurrent directions. (Top-left) Phra Wihan Formation from SE to NW direction. (Top-right) Sao Khua Formation mainly from NE to SW and some from NW to SE direction. (Bottom-left) Phu Phan Formation mainly from NE to SW direction.*

4.4 Petrographic analysis

4.4.1 Sample location

The sampling sites are displayed on Figure 4.20 and grid reference with some of description in table 4.3. In addition to their location relative to the Phu Phan Mountain, fieldwork sited were also selected based on their rock type, elevation and folded structure (Figure 4.6).

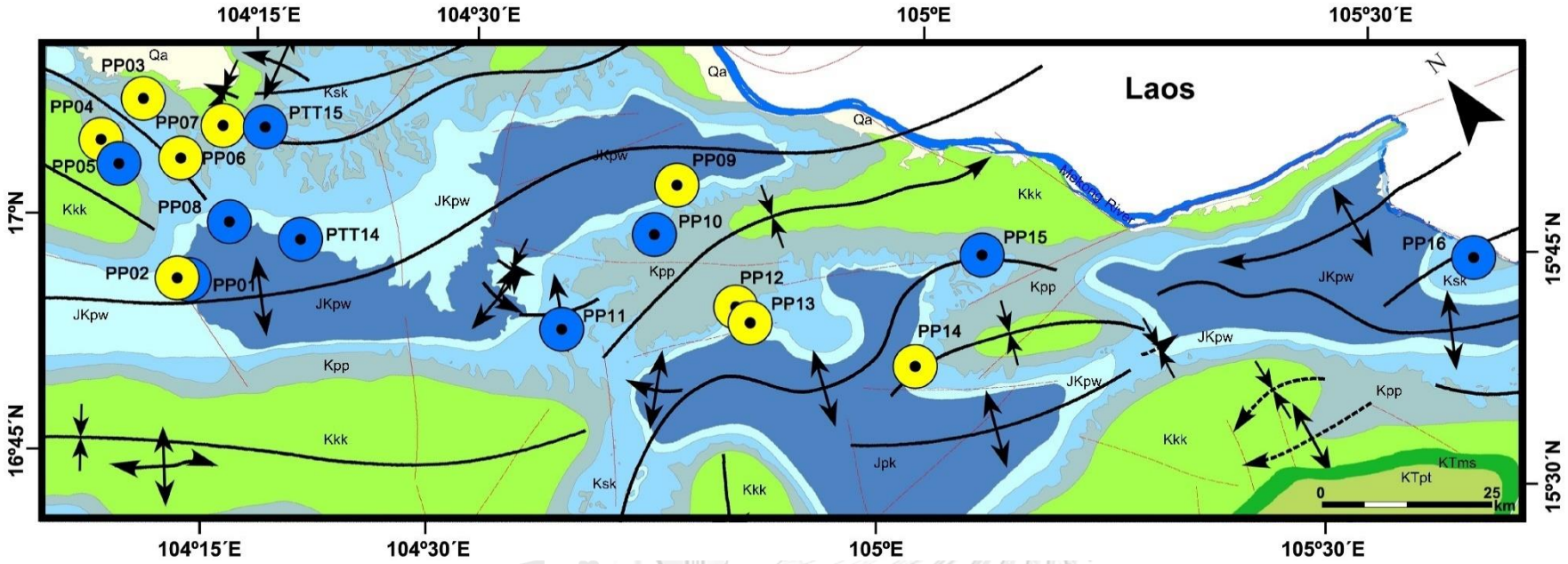

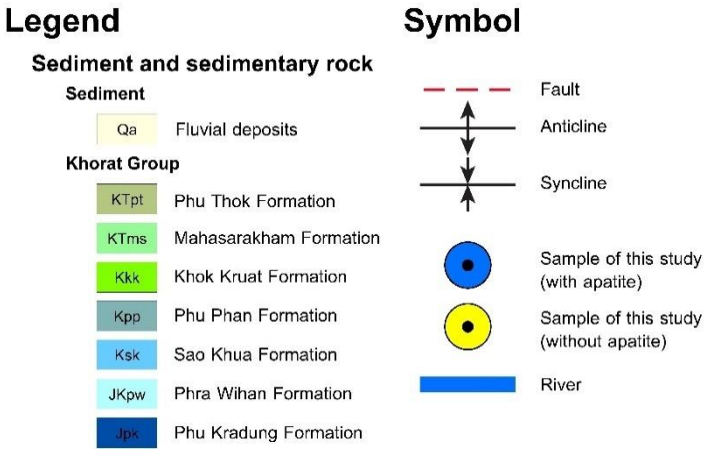

Figure 4.20 *Geological map based on 1:50,000 map modified from DMR (1999; 2000; 2001; 2004; 2008) showing sample locations of this study area (purple circle is a sample containing apatite grains and yellow circle is a sample without apatite grains).*

Table 4.3 Sample locations of sandstones

Sample	Latitude	Longitude	Site visit	Elevation*[1] (m)	Formation*[3]	Stratigraphic age*[2]
PP01	16°48'18"N	103°57'53"E	Highway 2219 km 41+700	239	Phu Kradung	Jurassic
PP02	16°48'48"N	103°57'37"E	Entrance of Kham Toei Waterfall	312	Phra Wihan	Jurassic-Cretaceous
PP03	17°01'52"N	104°04'20"E	Wat Tham Pha Daen	373	Sao Khua	Cretaceous
PP04-1	17°01'17"N	103°59'31"E	Huai Yai Waterfall	255	Phu Phan	Cretaceous
PP04-2	17°01'17"N	103°59'31"E	Huai Yai Waterfall	255	Phu Phan	Cretaceous
PP05-1	16°58'53"N	103°59'29"E	Phu Phan Buddha Nimit temple	246	Sao Khua	Cretaceous
PP05-2	16°58'53"N	103°59'29"E	Phu Phan Buddha Nimit temple	246	Sao Khua	Cretaceous
PP05-3	16°58'53"N	103°59'29"E	Phu Phan Buddha Nimit temple	246	Sao Khua	Cretaceous
PP06	16°56'17"N	104°03'49"E	Ban Na Phang Reservoir	203	Sao Khua	Cretaceous
PP07	16°56'19"N	104°08'14"E	Phaya Tao Ngoi Cave	195	Phu Phan	Cretaceous
PP08	16°49'55"N	104°03'51"E	Local road 4001 km 11	270	Phu Phan	Cretaceous
PP09	16°30'45"N	104°35'05"E	Local road 2092, Na Sok municipal District Post	215	Phra Wihan	Jurassic-Cretaceous
PP10	16°28'42"N	104°31'09"E	Wat Tham Pha Mong	191	Phu Phan	Cretaceous
PP11	16°27'08"N	104°20'21"E	Wat Phuttha Kiri	263	Sao Khua	Cretaceous
PP12	16°20'13"N	104°32'51"E	Wat Dan Phaya Nak	178	Phu Phan	Cretaceous
PP13	16°18'31"N	104°33'00"E	Phu Moo Forest Park	371	Phu Phan	Cretaceous
PP14	16°07'48"N	104°41'39"E	Wat Phu Sung	334	Phu Phan	Cretaceous
PP15	16°11'41"N	104°51'35"E	Entrance of Phu Tham Phra temple	217	Phu Phan	Cretaceous
PP16	15°47'53"N	105°23'33"E	Sam Phan Bok	120	Phu Phan	Cretaceous
PTT14	16°45'39"N	104°7'46"E	Highway 2287	380	Phu Kradung	Jurassic
PTT15	16°54'12"N	104°10'56"E	Highway 2358	282	Phu Phan	Cretaceous

*[1] Elevation based on GPS (Garmin) which accurate from an elevation pin at Phu Mu Forest Park, Mukdahan Province, Thailand (Figure 4.41); *[2] Stratigraphic age based on Department of Mineral Resources (2014); *[3] Based on geological map scale 1:50,000 of Department of Mineral Resource (1999; 2000; 2001; 2004; 2008)

Figure 4.21 *Elevation pin situating at Phu Mu Forest Park, Mukdahan province showing an elevation of 409 meters and is located at latitude 16°18'31"N – longtitude 104°33'00"E.*

4.4.2 Petrographic description

Lithology in the Phu Phan Mountain Range study area was described based on mesoscopic and microscopic analysis. A total of 21 selected sandstone samples were collected from Phu Kradung, Phra Wihan, Sao Khua and Khoh Kruat Formations which they are generally slightly weathered and show various colours. Most of the collected sandstones are very fine- to medium- grained. The microscopic observation using polarized light microscope reveal that types of sandstone samples are feldspathic litharenite, sublitharenite and litharenite (Pettijohn, 1975). The studied sandstones were also performed for model analysis. In details of petrographic description and mineral grain counting is in table 4.4).

4.4.2.1 Phu Kradung Formation

a. Macroscopic description

Only 2 sandstone samples of this formation were collected (PP01 and PTT14). The rocks have greenish grey and red color (Figure 4.22) and show a clastic texture. The grain size of them are very fine grain which are made up mostly of quartz (colorless), small amount of feldspar (white) and lithic fragments with less opaque minerals.

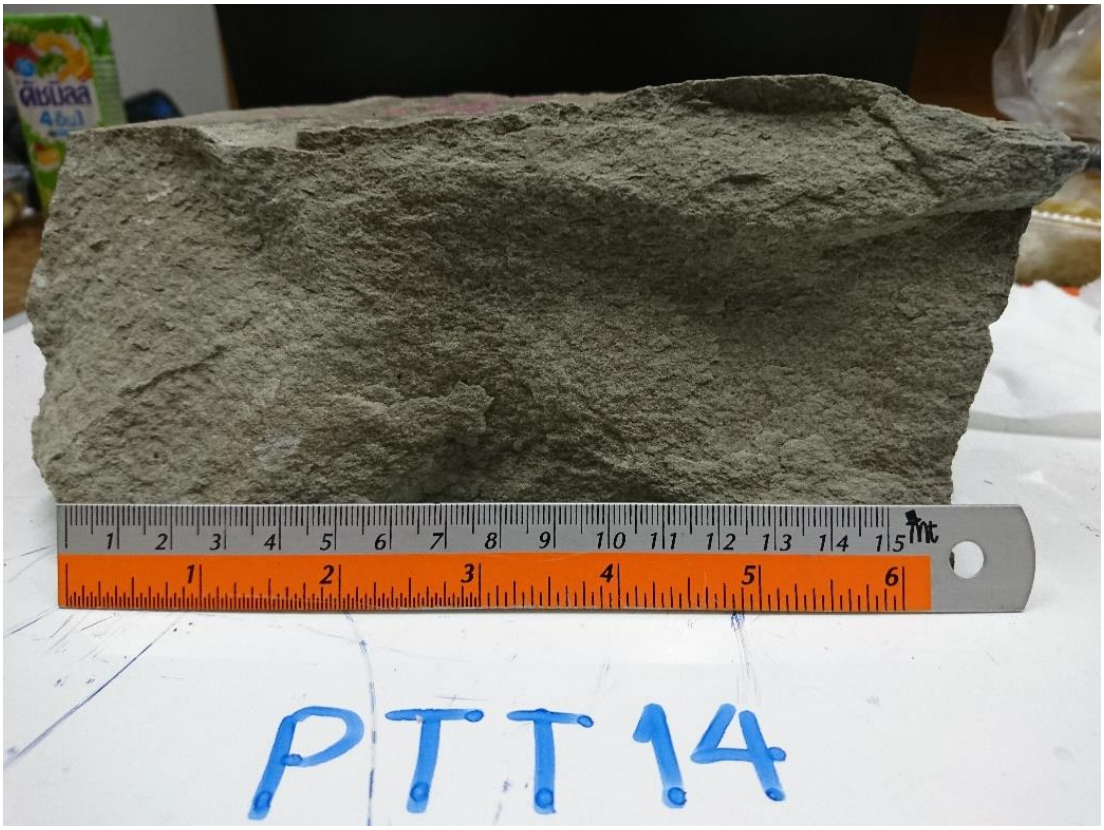

Figure 4.22 *A handspecimen of Red very fine-grained sandstone with faint lamination of the Phu Kradung Formation (sample no. PTT14).*

b. Microscopic description

The rocks are composed mainly of quartz (including monocrystalline quartz and polycrystalline quartz). Quartz component varies from 69 to 77 modal%. Feldspar is present in smaller amount with 11 – 15 modal%. Modal % of lithic fragments is from 12 to 16. Detailed description of modal analysis is shown in table 4.2. Therefore,

sandstones of the Phu Kradung Formation are classified as feldspathic litharenite (PP01) and sublitharenite (PTT14) (Pettijohn, 1975) (see Figure 4.24). The rock sample are also included of muscovite, biotite, apatite and zircon (Figure 4.23). The size of mineral is up to 0.05 to 0.2 mm with well sorted. The grains show a low sphericity and angular shape. The cement of the rocks is siliceous.

4.4.2.2 Phra Wihan Formation

a. Macroscopic description

Only 2 sandstone samples of this formation were collected (PP02 and PP09). The rocks are whitish grey (Figure 4.25) and show a distinct clastic texture. The grain sizes are medium grain which are made up mostly of quartz (colorless), small amount of feldspar (white) and lithic fragments with less opaque minerals.

b. Microscopic description

Petrographically, the rocks are composed mainly of quartz (including monocrystalline quartz and polycrystalline quartz) (69 - 70 modal %), with small amount of feldspar (2 - 3 modal %) and lithic fragment (28 modal %) Detailed description of Phra Wihan sandstone is shown in table 4.2. Figure 4.47 shows that the studies sandstones are litharenite (Pettijohn, 1975). The accessories minerals are muscovite, biotite, chlorite and zircon (Figure 4.26). The grain sizes of sandstone vary from 0.2 to 0.6 mm. The sorting of sandstones is good to moderately good. The grains show low sphericity and angular shape. Cementing materials of the sandstones are siliceous.

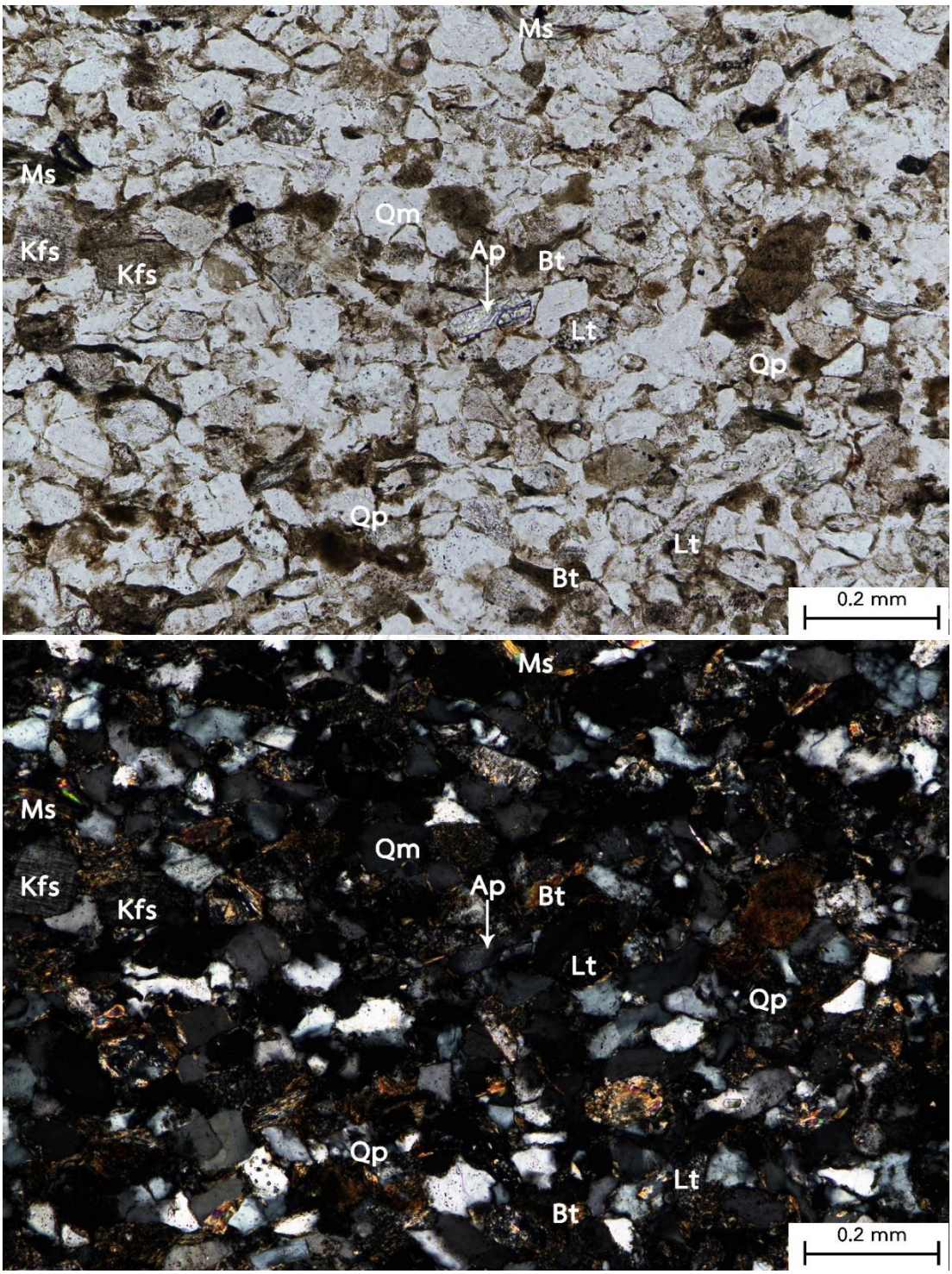

Figure 4.23 *Photomicrographs of feldspathic litharenite (sample no. PTT14) from the Phu Kradung Formation at Phu Phan Mountain Range showing well defined clastic texture and grains of quartz, alkaline feldspar, lithic fragments, muscovite, biotite, and apatite. (top) Ordinary light and (bottom) Cross polar. (Qm = monocrystalline quartz, Qp = polycrystalline quartz, Kfs = alkaline feldspar, Lt = lithic fragment, Ms = muscovite, Bt = biotite, and Ap = apatite)*

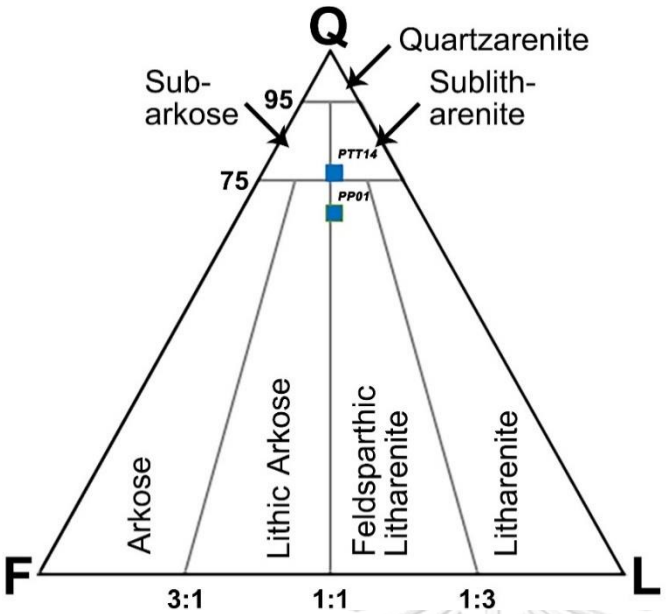

Figure 4 24 *Quartz-Feldspar-Lithic (QFL) ternary diagram for the Phu Phan Mountain Range sandstones of the Phu Kradung Formation (diagram after Pettijohn, 1975)*

Figure 4.25 *A handspecimen of Whitish grey, medium-grained sandstone with well lamination of the Phra Wihan Formation (sample no. PP02).*

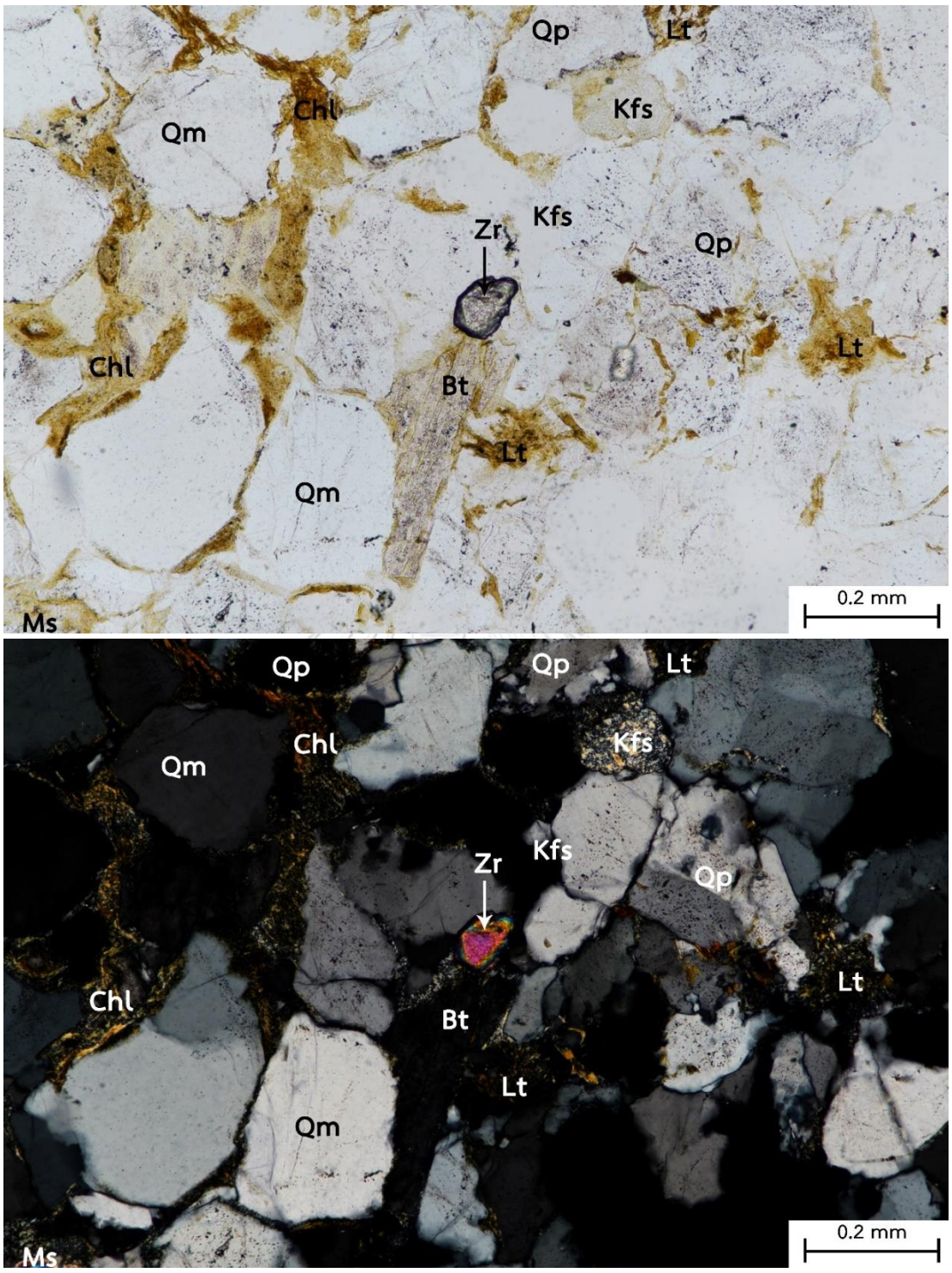

Figure 4.26 *Photomicrographs of litharenite (sample no. PP02) from the Phra Wihan Formation at Phu Phan Mountain Range showing well defined clastic texture and grains of quartz, alkaline feldspar, lithic fragments, muscovite, biotite, chlorite, and zircon. (top) Ordinary light and (bottom) Cross polar. (Qm = monocrystalline quartz, Qp = polycrystalline quartz, Kfs = alkaline feldspar, Lt = lithic fragment, Ms = muscovite, Bt = biotite, Chl = chlorite, and Zr = zircon)*

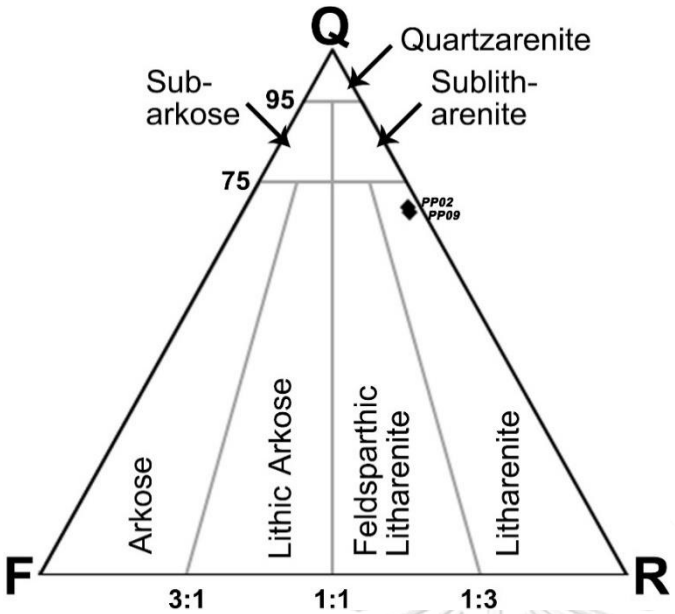

Figure 4.27 *Quartz-Feldspar-Lithic (QFL) ternary diagram for the Phu Phan Mountain Range sandstones of the Phra Wihan Formation, (diagram after Pettijohn, 1975).*

4.4.2.3 Sao Khua Formation

a. Macroscopic description

There are 6 sandstone samples belonging to the Sao Khua Formation (PP03, PP05-1, PP05-2, PP05-3, PP06, and PP11). The studies rocks are reddish grey sandstone (Figure 4.28) and show a clastic texture. The sandstones are fine– medium- grained are made up mostly of quartz (colorless), small amount of feldspar (white), lithic fragments, and mica.

b. Microscopic description

Under microscope, the studied sandstones are composed largely of quartz (both monocrystalline and polycrystalline) with the modal composition of 67 – 78%. Subordinate amounts are feldspar (1 modal %) and lithic fragments (21 - 34 modal %) Table 4.2 displays detailed decription of the studied samples. Based on Pettijohn (1975)'s classification, the studies rocks are litharenite (PP03, PP05-1, PP05-2, PP05-3, and PP06) and sublitharenite (PP11) (see Figure 4.30). Accessory minerals are muscovite, biotite, chlorite, calcite, and zircon. Only sample PP05-2, PP05-3, and PP11 contain appreciable amount of apatite (Figure 4.29). The grain sizes of sandstone vary from 0.05 to 0.6 mm. The studied sandstones have well to moderately well-sorted

Figure 4.28 *A handspecimen of Reddish grey, fine-grained sandstone with faint lamination of the Sao Khua Formation (sample no. PP05-3),*

and moderate sphericity clast. Some clasts have angular shape. Only sample PP11 shows the clasts with high sphericity and subangular shape. Almost cementing materials of the studied sandstones are siliceous, but one sample (PP11) has calcareous cement.

4.4.2.4 Phu Phan Formation

a. Macroscopic description

There are 11 sandstone samples of the Phu Phan Formation that were studied (PP04-1, PP04-2, PP07, PP08, PP10, PP12, PP13, PP14, PP15, PP16 and PTT15). The sandstones are whitish grey and reddish brown (Figure 4.31) and show clastic texture. Their grain sizes are generally fine to medium grained. Clasts are made up mostly of quartz (colorless) with small amount of feldspar (white), lithic fragments, and mica.

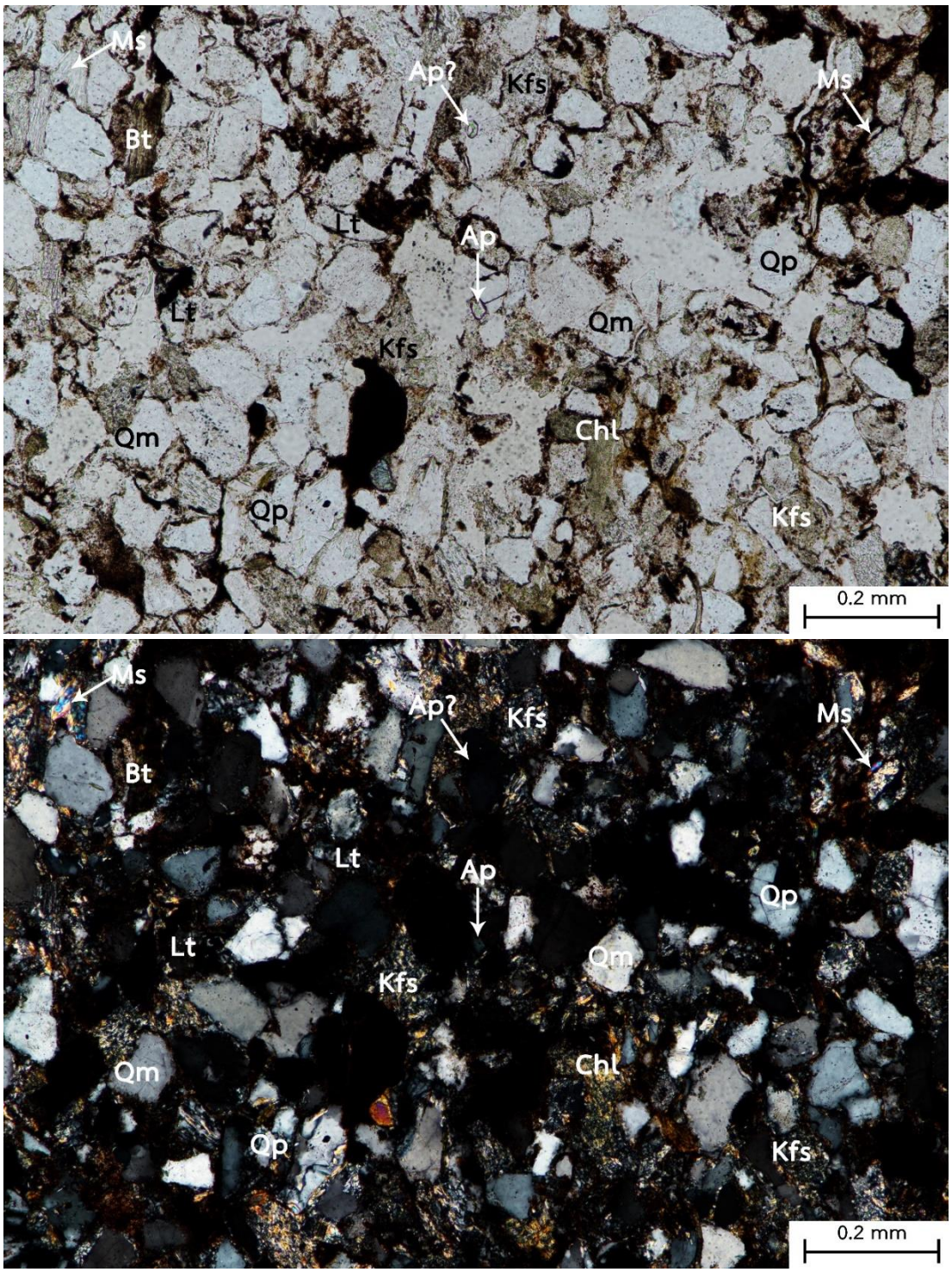

Figure 4.29 *Photomicrographs of litharenite (sample no. PP05-3) from the Sao Khua Formation at Phu Phan Mountain Range showing well defined clastic texture and grains of quartz, alkaline feldspar, lithic fragments, muscovite, biotite, chlorite, and apatite. (top) Ordinary light and (bottom) Cross polar. (Qm = monocrystalline quartz, Qp = polycrystalline quartz, Kfs = alkaline feldspar, Lt = lithic fragment, Ms = muscovite, Bt = biotite, Chl = chlorite, and Ap = apatite)*

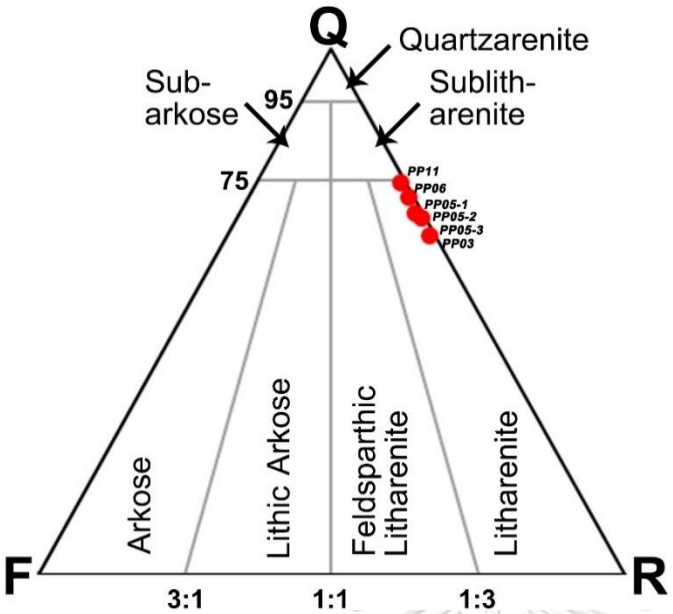

Figure 4.30 *Quartz-Feldspar-Lithic (QFL) ternary diagram for the Phu Phan Mountain Range sandstones of the Sao Khua Formation (diagram after Pettijohn, 1975).*

Figure 4.31 *A handspecimen of Reddish brown fine-grained sandstone of the Phu Phan Formation (sample no. PTT15).*

b. Microscopic description

The rocks are composed mainly of quartz (including monocrystalline quartz and polycrystalline quartz) (62 - 88 modal %), with small amount of feldspar (0 - 13 modal %) and lithic fragments (9 - 32 modal %) Detailed data are shown in table 4.2. Based on Pettijohn (1975), the rocks are classified as litharenite (PP10, PP12, PP13, PP14, and PP15) and sublitharenite (PP04-1, PP04-2, PP07, PP16, and PTT15) (see Figure 4.33). The other mineral constituents are muscovite, biotite, calcite, amphibole? and zircon (Figure 4.32). Only sample nos. PP10, PP15, PP16, and PTT15 contain appropriate amount of apatite. The size of clast ranges from 0.05 to 0.8 mm. The studied sandstones have with well to moderate well sorted clasts. The clasts have low sphericity and angular shape. Only two samples (PP15 and PP16) have clasts with high sphericity and subangular shape. Almost studied samples have siliceous cement, and only one sample (PTT15) is calcareous cement.

4.5 Apatite fission track ages

Overall 21 samples were processed for AFT dating. However, there are 11 samples that did not yield any apatite grains during mineral separation process. Among these, 4 samples which contain apatite were not analyzed due to the samples contain less amount of apatite grains, so the detail data are not here in included. Therefore, AFT dating analysis was undertaken on 6 samples. Table 4.2 displays that all samples analyzed contain appreciable amount of zircon, suggesting that the host rocks are felsic igneous rock.

4.5.1 Phu Kradung Formation

Two samples of the Phu Phan Mountain Range study are selected for apatite fission track dating, they are sample nos. PTT14 and PP01. Figure 4.34 shows an apatite grain with fission tracks in the sandstone (sample PTT14). The age dispersion value for sample PTT14 is 7.9% with $P(\chi)^2$ of about 6.2%, suggesting a single population of apatite grain ages. The apatite grains yield the AFT age derived from 36 apatite crystals analysed; i.e., pooled FT age estimation *ca.* 72.5±4.4 Ma and central FT age calculation

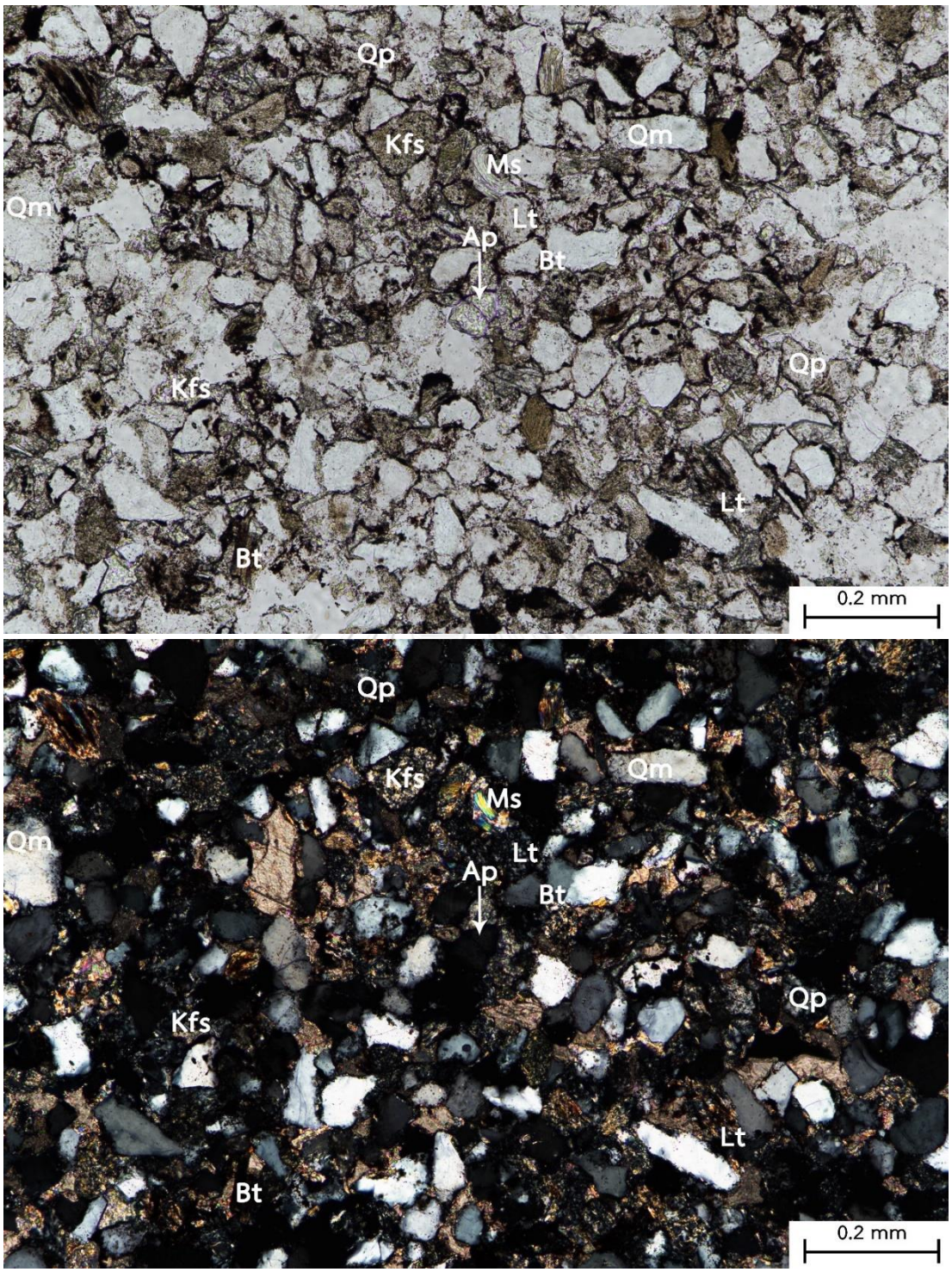

Figure 4.32 *Photomicrographs of sublitharenite (sample no. PTT15) from the Phu Phan at Phu Phan Mountain Range showing well defined clastic texture and grains of quartz, alkaline feldspar, lithic fragments, muscovite, biotite, and apatite. (top) Ordinary light and (bottom) Cross polar. (Qm = monocrystalline quartz, Qp = polycrystalline quartz, Kfs = alkaline feldspar, Lt = lithic fragment, Ms = muscovite, Bt = biotite, and Ap = apatite)*

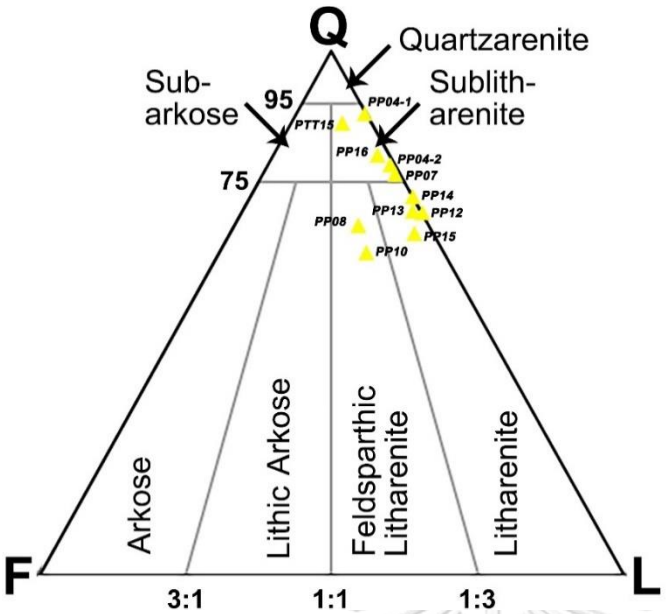

Figure 4.33 *Quartz-Feldspar-Lithic (QFL) ternary diagram for the Phu Phan Mountain Range sandstones of the Phu Phan Formation (diagram after Pettijohn, 1975).*

to be *ca.* 77.6±4.7 Ma, (see Figure 4.35 Top-left). Moreover, sample no. PP01 is 0.094 of the χ^2 test with the age dispersion of 15%, verified that the pooled FT age and central FT age calculation to be 65.4±3.8 Ma and 72.8±7.1 Ma, respectively, obtained from 14 apatite grains (see Figure 4.35 bottom-left).

According to Department of Mineral Resources (2014), the depositional age of Phu Kradung Formation is about 163.5 to 145 Ma. So, all of the AFT age data suggest that central age of the samples is younger than the depositional age.

Number of tracks in apatite vary from 0 to 87 within the areas of 426 to 1,704 μm^2 (PTT14) and from 6 to 68 within the areas of 2,247 to 7,693 μm^2 (PP01). Mean track length distribution given by sample PTT14 is about 12.84±0.7 μm (15 confined tracks) (see Figure 4.35 top-right) with attached standard deviation of 2.71 μm Therefore, it is not sure if the result show either, implying bimodal or mixed model. Confined tracks are not found in sample no. PP01 during the course of analysis. U-Ca ratios of apatite of sample no. PTT14 and PP01 divided by that of external standard (NIST SRM610) fall within the range of 0.0008 to 0.0715 and 0.002 to 0.0240, respectively. Besides, the error is in the range of 0.0002 to 0.0003 (sample no. PTT14) and 0.00001 to 0.00035 (sample no. PP01) (see more detail in Tables 4.5 and 4.6).

Table 4.4. Mineral compositions of the clastic sedimentary rocks in the Phu Phan Mountain Range.

Sample	Rock type	Grain size (mm)	Sorting	Spheri-city	Round-ness	Cement	Mineral grain counting								Other mineral			Rock name *(Pettijohn, 1975)*
							Qt	F	Lt	T	Qt (%)	F (%)	Lt (%)	T (%)	Ap	Zr	Etc.	
PP01	Sed.	0.1 – 0.2	Well	Low	Angular	Siliceous	374	82	87	543	68.88	15.10	16.02	100	✔	✔	muscovite, biotite	Feldspathic litharenite
PP02	Sed.	0.2 – 0.4	Well	Low	Angular	Siliceous	219	7	87	313	69.97	2.24	27.80	100	✘	✔	muscovite, biotite?, chlorite	Litharenite
PP03	Sed.	0.2 – 0.6	Well	Low	Angular	Siliceous	245	4	130	379	64.64	1.06	34.30	100	✘	✔	muscovite	Litharenite
PP04–1	Sed.	0.1 – 0.6	Well	Low	Angular	Siliceous	403	1	53	457	88.18	0.22	11.60	100	✘	✔	–	Sublith–arenite
PP04–2	Sed.	0.2 – 0.8	Well	Low	Angular	Siliceous	220	2	58	280	78.57	0.71	20.71	100	✘	✔	muscovite, biotite, amphibole	Sublith–arenite
PP05–1	Sed.	0.1 – 0.3	M. well	Low	Angular	Siliceous	707	10	266	983	71.92	1.02	27.06	100	✘	✔	Muscovite, Chlorite?	Litharenite
PP05–2	Sed.	0.1 – 0.6	M. well	Low	Angular	Siliceous	467	9	201	677	68.98	1.33	29.69	100	✔	✔	Muscovite, Biotite, Calcite	Litharenite
PP05–3	Sed.	0.1 – 0.2	Well	Low	Angular	Siliceous	617	8	283	908	67.95	0.88	31.17	100	✔	✔	Muscovite, Biotite, Chlorite	Litharenite
PP06	Sed.	0.05 – 0.2	Well	Low	Subangular	Siliceous	487	6	158	651	74.81	0.92	24.27	100	✘	✔	Muscovite, Chlorite	Litharenite
PP07	Sed.	0.1 – 0.4	Well	Low	Subangular	Siliceous	292	3	86	381	76.64	0.79	22.57	100	✘	✔	Muscovite	Sublith–arenite

*Qt = all quartz grains (monocrystalline and polycrystalline); F = feldspar grains; Lt = unstable (volcanic, sedimentary) lithic (rock) (Dickinson, 1985); Ap = apatite; Zr = zircon, ss = sandstone; *[1] = sample for apatite fission track dating; ✓ = Mineral contained in sample. ✘ = Mineral didn't contain in sample.

Table 4.4 (cont.)

Sample	Rock type	Grain size (mm)	Sorting	Spheri–city	Round–ness	Cement	Mineral grain counting								Other mineral			Rock name (*Pettijohn, 1975*)
							Qt	F	Lt	T	Qt (%)	F (%)	Lt (%)	T (%)	Ap	Zr	Etc.	
PP08	Sed.	0.1 – 0.2	Well	Low	Angular	Siliceous	304	55	95	454	66.96	12.11	20.93	100	✔	✔	muscovite	Litharenite
PP09	Sed.	0.1 – 0.6	M. well	Low	Angular	Siliceous	245	9	101	355	69.01	2.54	28.45	100	✘	✔	muscovite	Litharenite
PP10	Sed.	0.1 – 0.4	Well	Low	Angular	Siliceous	228	49	92	369	61.79	13.28	24.93	100	✔	✔	muscovite, biotite	Litharenite
PP11	Sed.	0.1 – 0.5	Well	High	Subangular	Cal-careous	312	2	85	399	78.20	0.50	21.30	100	✔	✔	calcite, opaque mineral	Sublith–arenite
PP12	Sed.	0.1 – 0.6	M. well	Low	Angular	Siliceous	343	0	153	496	69.15	0.00	30.85	100	✘	✔	muscovite, calcite, amphibole, opaque mineral	Litharenite
PP13	Sed.	0.1 – 0.7	Well	Low	Angular	Siliceous	209	4	87	300	69.67	1.33	29.00	100	✘	✔	–	Litharenite
PP14	Sed.	0.2 – 0.8	M. well	Low	Angular	Siliceous	516	0	196	712	72.47	0.00	27.53	100	✘	✔	–	Litharenite
PP15	Sed.	0.1 – 0.5	Well	High	Angular	Siliceous	205	10	99	314	65.29	3.18	31.53	100	✔	✔	–	Litharenite
PP16	Sed.	0.2 – 0.8	Well	High	Subangular	Siliceous	374	9	83	466	80.26	1.93	17.81	100	✔	✔	Calcite	Sublith–arenite
PTT14	Sed.	0.05 – 0.1	Well	Low	Angular	Siliceous	636	93	101	830	76.63	11.2	12.17	100	✔	✔	Muscovite, Biotite, Chlorite	Sublith–arenite
PTT15	Sed.	0.05 – 0.2	M. well	Low	Angular	Cal-careous	918	54	91	1063	86.36	5.08	8.56	100	✔	✔	Muscovite, Biotite	Sublith–arenite

*Qt = all quartz grains (monocrystalline and polycrystalline); F = feldspar grains; Lt = unstable (volcanic, sedimentary) lithic (rock) (Dickinson, 1985); Ap = apatite; Zr = zircon; ss = sandstone; *[1] = sample for apatite fission track dating; ✓ = Mineral contained in sample. ✘ = Mineral didn't contain in sample.

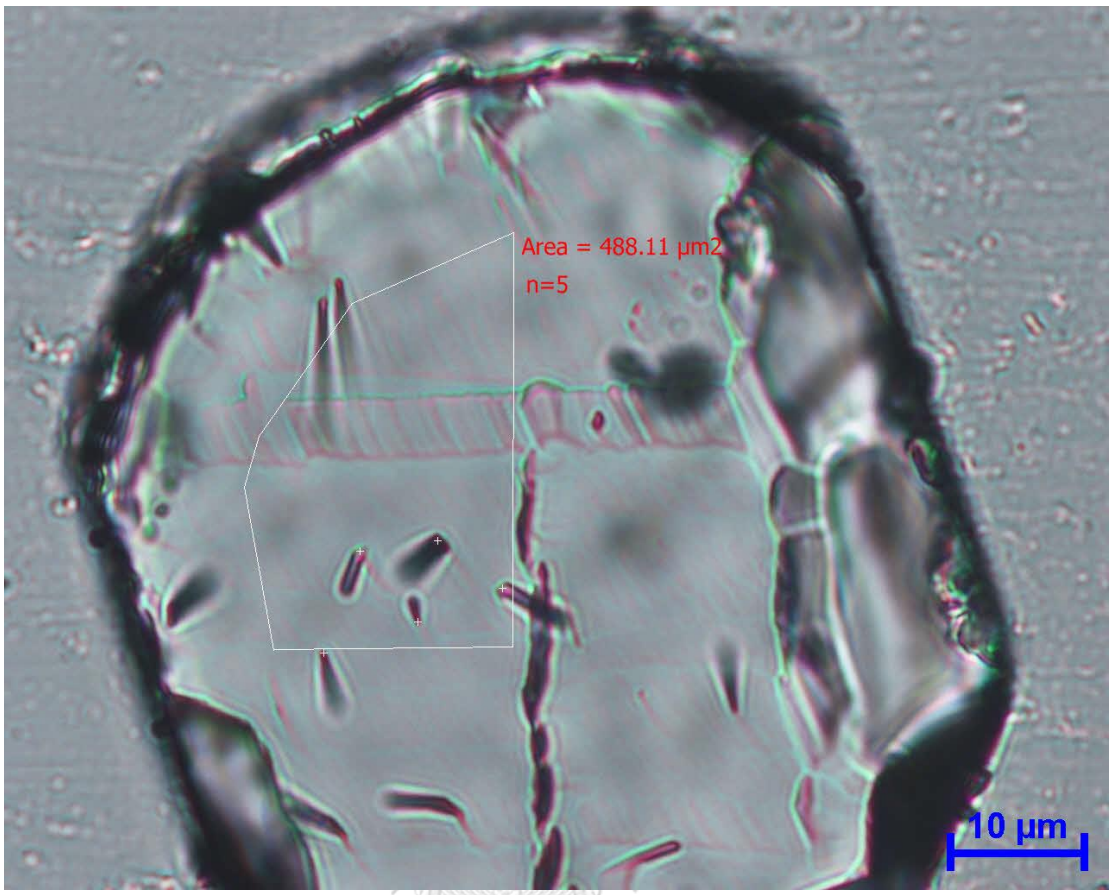

Figure 4.34 *An apatite grain with fission tracks from sandstone (sample no. PTT14) belonging to the Phu Kradung Formation, Phu Phan Mountain Range.*

4.5.2 Phu Phan Formation

Four samples have been selected from the Phu Phan Formation including sample nos. PP10, PP15, PP16, and PTT15. Figure 4.36 illustrates an apatite grain with fission tracks from sandstone (sample PP16).

AFT age obtained from 13 apatite grains sandstone (no. PP10) shows value of P(χ^2) less than 1 and age dispersion of 29%. The result of analysis gives the pooled age of 56.1±2.9 Ma and central age of 62.6±6 Ma. It is likely that the central age is little older than the pooled age *ca.* 10% (or 6 Ma). Based on the radial plot of single grain age shown in (Figure 4.37 left), two age groups can be visualized; i.e., the older is about 91.3±8.9 Ma (n=5) and the younger group is about 49.7±3 Ma (n=8).

Table 4.5 LA-ICP-MS data and fission-track dating sample PP01, belonging to the Phu Kradung Formation, Phu Phan Mountain Range.

PP01 grain ID	spot ID	LA-ICP-MS data				FT dating									
		Ap		NIST610		Ap/NIST610	SE	U	Average	SE	ρ_s	Ns	A	T	σ
		$^{238}U/^{43}Ca$	SE (%)	$^{238}U/^{43}Ca$	SE (%)	($^{238}U/^{43}Ca$)	(%)	(μg/g)	Ap/NIST610	(%)	($10^6/cm^2$)		(μm^2)	(Ma)	(Ma)
2	a	0.0108	1.7716	4.2708	0.9937	0.0025	2.03	5.5266	0.0025	0.79	0.2390	12	5020.58	88.3	25.6
	b	0.0105	2.2366	4.2609	0.9876	0.0025	2.44	5.4047							
3	a	0.0149	1.7451	4.2509	0.9814	0.0035	2.00	7.6877	0.0034	3.25	0.2546	14	5498.04	70.0	18.9
	b	0.0136	1.8341	4.2409	0.9752	0.0032	2.08	7.0127							
6	a	0.0143	1.4326	4.2417	0.9103	0.0034	1.70	7.4052	0.0036	5.14	0.3991	11	2756.02	100.8	30.9
	b	0.0166	1.7645	4.2471	0.8809	0.0039	1.97	8.5668							
11	a	0.0111	3.0172	4.2525	0.8515	0.0026	3.14	5.7019	0.0026	0.59	0.1661	6	3,612	59.4	24.3
	b	0.0109	2.2413	4.2579	0.8221	0.0026	2.39	5.6070							
13	a	0.0579	1.1555	4.2633	0.7927	0.0136	1.40	29.7520	0.0122	7.88	0.9697	46	4743.85	73.2	12.4
	b	0.0463	1.4053	4.2669	2.9495	0.0109	3.27	23.7861							
15	a	0.0695	1.3064	4.2650	5.1358	0.0163	5.30	35.7169	0.0157	2.07	0.9449	42	4444.8	55.5	8.7
	b	0.0647	1.5951	4.2631	7.3221	0.0152	7.49	33.2413							
21	a	0.0108	1.9013	4.2594	11.6946	0.0025	11.85	5.5491	0.0024	2.96	0.2671	6	2246.73	101.1	41.5
	b	0.0099	2.0685	4.2576	13.8809	0.0023	14.03	5.1029							
22	a	0.0477	1.1859	4.2431	11.7126	0.0113	11.77	24.6443	0.0155	20.00	1.0507	68	6472.15	62.8	14.8
	b	0.0975	1.0560	4.2368	9.5353	0.0230	9.59	50.4121							
	c	0.0512	1.8100	4.2306	7.3581	0.0121	7.58	26.5210							
26	a	0.0137	1.4977	4.2243	5.1808	0.0032	5.39	7.0781	0.0032	0.71	0.2514	16	6365.4	73.0	18.3
	b	0.0133	1.5901	4.2180	3.0036	0.0031	3.40	6.8816							
	c	0.0133	1.6707	4.2113	0.8125	0.0032	1.86	6.9160							
32	a	0.0174	1.4908	4.3102	0.7993	0.0040	1.69	8.8652	0.0047	9.90	0.2551	6	2351.69	50.1	21.1
	b	0.0233	1.2195	4.3441	0.8224	0.0054	1.47	11.7509							
34	a	0.0518	1.3938	4.3781	0.8455	0.0118	1.63	25.9298	0.0111	4.60	1.1630	33	2837.46	96.4	17.5
	b	0.0458	1.8424	4.4120	0.8686	0.0104	2.04	22.7603							
37	a	0.0561	1.8903	4.4211	3.2741	0.0127	3.78	27.8027	0.0130	1.73	0.7311	32	4377.07	51.9	9.3
	b	0.0586	1.4625	4.3963	5.6564	0.0133	5.84	29.1944							
44	a	0.1047	1.3490	4.3714	8.0388	0.0240	8.15	52.4760	0.0216	7.66	1.1018	36	3267.38	47.1	8.7
	b	0.0838	1.1103	4.3466	10.4212	0.0193	10.48	42.2179							
49	a	0.0157	1.6942	4.3668	4.5031	0.0036	4.81	7.8968	0.0035	1.27	0.3510	27	7692.51	92.0	17.9
	b	0.0152	1.3124	4.3784	2.7227	0.0035	3.02	7.6039							
	c	0.0153	1.5710	4.4097	0.9272	0.0035	1.82	7.6033							
						Weighted mean								70.7	5.6
						Pooled mean			0.0081	0.38	0.5755	355	61,686.09	65.4	3.8

Note: Pooled AFT age is calculated with ζ_{MS}= 0.928±0.022

The other sandstone samples are those of nos. PP15, PP16, and PTT15, shows χ^2 test of 0.0000053 (PP15), 0.061 (PP16), and 0.072 (PTT15) with contributed age dispersion of about 26%, 1.7%, and 15%, respectively. Nevertheless, sandstone sample no. PTT15 may be possible is likely to be composed of 2 age components but the two young plots are obscure because number of tracks counted is small. The samples yield the AFT age from pooled age calculation to be 48.5±2 Ma (PP15), 45.5±1.6 Ma (PP16),

Table 4.6 LA-ICP-MS data and fission-track dating sample PTT14, belonging to the Phu Kradung Formation, Phu Phan Mountain Range.

PTT14 grain ID	spot ID	LA-ICP-MS data				FT dating									
		Ap		NIST610		Ap/NIST610	SE	U	Average	SE	ρ_s	Ns	A	T	σ
		$^{238}U/^{43}Ca$	SE (%)	$^{238}U/^{43}Ca$	SE (%)	($^{238}U/^{43}Ca$)	(%)	(μg/g)	Ap/NIST610	(%)	($10^6/cm^2$)		(μm^2)	(Ma)	(Ma)
1-2	a	0.0318	2.9556	4.4878	0.9928	0.0071	3.12	15.5441	0.0071	3.12	0.0000	0	532.53	0.0	0.0
1-4	a	0.2126	2.3320	4.5127	1.0237	0.0471	2.55	103.177	0.0471	2.55	1.8627	14	751.6	36.6	9.9
1-11	a	0.1946	2.3725	4.5376	1.0547	0.0429	2.60	93.9602	0.0429	2.60	3.4878	20	573.43	75.0	17.0
1-12	a	0.0053	2.9255	4.5625	1.0857	0.0012	3.12	2.56157	0.0012	3.12	0.0000	0	889.22	0.0	0.0
1-13	a	0.0901	3.4519	4.5874	1.1166	0.0196	3.63	43.0125	0.0196	3.63	1.8146	23	1267.53	85.2	18.1
1-14	a	0.1398	2.5676	4.5908	1.1573	0.0305	2.82	66.72	0.0305	2.82	3.8686	21	542.83	116.8	25.8
1-16	a	0.0160	2.5623	4.5694	1.1669	0.0035	2.82	7.65245	0.0035	2.82	0.0000	0	717.26	0.0	0.0
1-17	a	0.0129	2.7300	4.5479	1.1766	0.0028	2.97	6.2017	0.0029	1.38	0.2935	5	1703.63	93.6	42.0
	b	0.0133	2.4991	4.5264	1.1863	0.0029	2.77	6.44773							
1-21	a	0.0105	2.2752	4.5049	1.1959	0.0023	2.57	5.10596	0.0023	2.57	0.2697	2	741.49	106.5	75.4
1-22	a	0.0699	3.1529	4.4835	1.2056	0.0156	3.38	34.1298	0.0156	3.38	1.5325	13	848.27	90.6	25.4
1-23	a	0.0163	2.3075	4.4533	1.1798	0.0037	2.59	7.99527	0.0037	2.59	0.3190	4	1253.99	80.6	40.4
1-27	a	0.0484	2.5002	4.4445	1.1443	0.0109	2.75	23.8392	0.0112	2.01	0.5074	11	2168.01	41.9	12.7
	b	0.0511	2.7197	4.4402	1.1266	0.0115	2.94	25.231							
1-31	a	0.0240	2.2107	4.4358	1.1088	0.0054	2.47	11.8462	0.0059	5.63	0.5319	6	1128.11	83.5	34.4
	b	0.0281	2.3698	4.4304	1.0569	0.0063	2.59	13.8967							
1-41	a	0.0034	3.1194	4.4273	0.9544	0.0008	3.26	1.66101	0.0008	3.26	0.0000	0	833.8	0.0	0.0
1-48	a	0.0582	2.0957	4.4262	0.9202	0.0131	2.29	28.7864	0.0131	2.29	0.8932	5	559.81	62.8	28.1
1-52	a	0.0121	2.2137	4.3849	0.9475	0.0028	2.41	6.04077	0.0028	2.41	0.0384	1	2605.8	12.9	12.9
1-55	a	0.0382	2.1094	4.3653	0.9953	0.0088	2.33	19.1814	0.0088	2.33	0.9336	6	642.68	98.2	40.2
3-42	a	0.0079	2.0338	3.9213	0.9451	0.0020	2.24	4.39337	0.0020	2.24	0.2996	2	667.52	137.2	97.1
3-61	a	0.0038	2.3023	3.9423	0.8981	0.0010	2.47	2.13848	0.0010	2.47	0.1496	2	1336.73	140.7	99.6
4-14	a	0.0453	1.5711	3.9432	0.8719	0.0115	1.80	25.191	0.0115	1.80	1.0244	5	488.11	82.1	36.8
4-21	a	0.0151	1.7791	3.9401	0.8666	0.0038	1.98	8.40908	0.0038	1.98	0.2498	2	800.5	60.1	42.5
4-31	a	0.0242	1.5868	3.9371	0.8613	0.0061	1.81	13.4506	0.0061	1.81	0.4737	5	1055.61	71.2	31.9
4-62	a	0.0447	1.7219	3.9340	0.8561	0.0114	1.92	24.8666	0.0114	1.92	1.6124	9	558.16	130.5	43.7
5-5	a	0.2805	1.7894	3.9245	0.8668	0.0715	1.99	156.572	0.0715	1.99	6.1147	87	1422.79	78.9	8.8
5-7	a	0.0578	1.8777	3.9180	0.8828	0.0148	2.07	32.3154	0.0148	2.07	1.1079	11	992.89	69.3	21.0
5-8	a	0.0242	2.3255	3.9116	0.8987	0.0062	2.49	13.5342	0.0062	2.49	0.5946	6	1009.06	88.7	36.3
5-16	a	0.0910	2.1651	3.9052	0.9147	0.0233	2.35	51.0527	0.0233	2.35	2.5498	21	823.61	100.7	22.2
5-19	a	0.0494	2.1275	3.8923	0.9467	0.0127	2.33	27.794	0.0127	2.33	0.8601	6	697.58	62.6	25.6
5-20	a	0.0222	2.1640	3.8858	0.9626	0.0057	2.37	12.5069	0.0057	2.37	0.3651	2	547.82	59.1	41.8
5-22	a	0.0090	2.3047	3.8800	0.9438	0.0023	2.49	5.07992	0.0023	2.49	0.0000	0	425.95	0.0	0.0
5-28	a	0.0052	2.2905	3.8804	0.9264	0.0013	2.47	2.94591	0.0013	2.47	0.0000	0	550.83	0.0	0.0
5-31	a	0.0051	3.1294	3.8807	0.9089	0.0013	3.26	2.86974	0.0013	3.26	0.2225	1	449.53	155.7	155.8
5-36	a	0.0133	2.2195	3.8811	0.8915	0.0034	2.39	7.50827	0.0034	2.39	0.4486	4	891.63	120.3	60.3
5-41	a	0.0386	2.1023	3.8814	0.8741	0.0099	2.28	21.7606	0.0094	3.71	0.6060	9	1485.19	59.3	19.9
	b	0.0348	2.0418	3.8866	0.8662	0.0089	2.22	19.5926							
5-45	a	0.0174	2.6790	3.8914	0.8757	0.0045	2.82	9.76778	0.0045	2.82	0.3584	6	1674.2	74.2	30.4
5-53	a	0.0786	2.4222	3.8963	0.8853	0.0202	2.58	44.2135	0.0202	2.58	1.2742	9	706.32	58.3	19.5
								Weighted mean						79.9	7.1
								Pooled mean	0.0118	0.61	0.9259	318	34,344.02	72.6	4.4

Note: Pooled AFT age is calculated with ζ_{MS}= 0.928±0.022

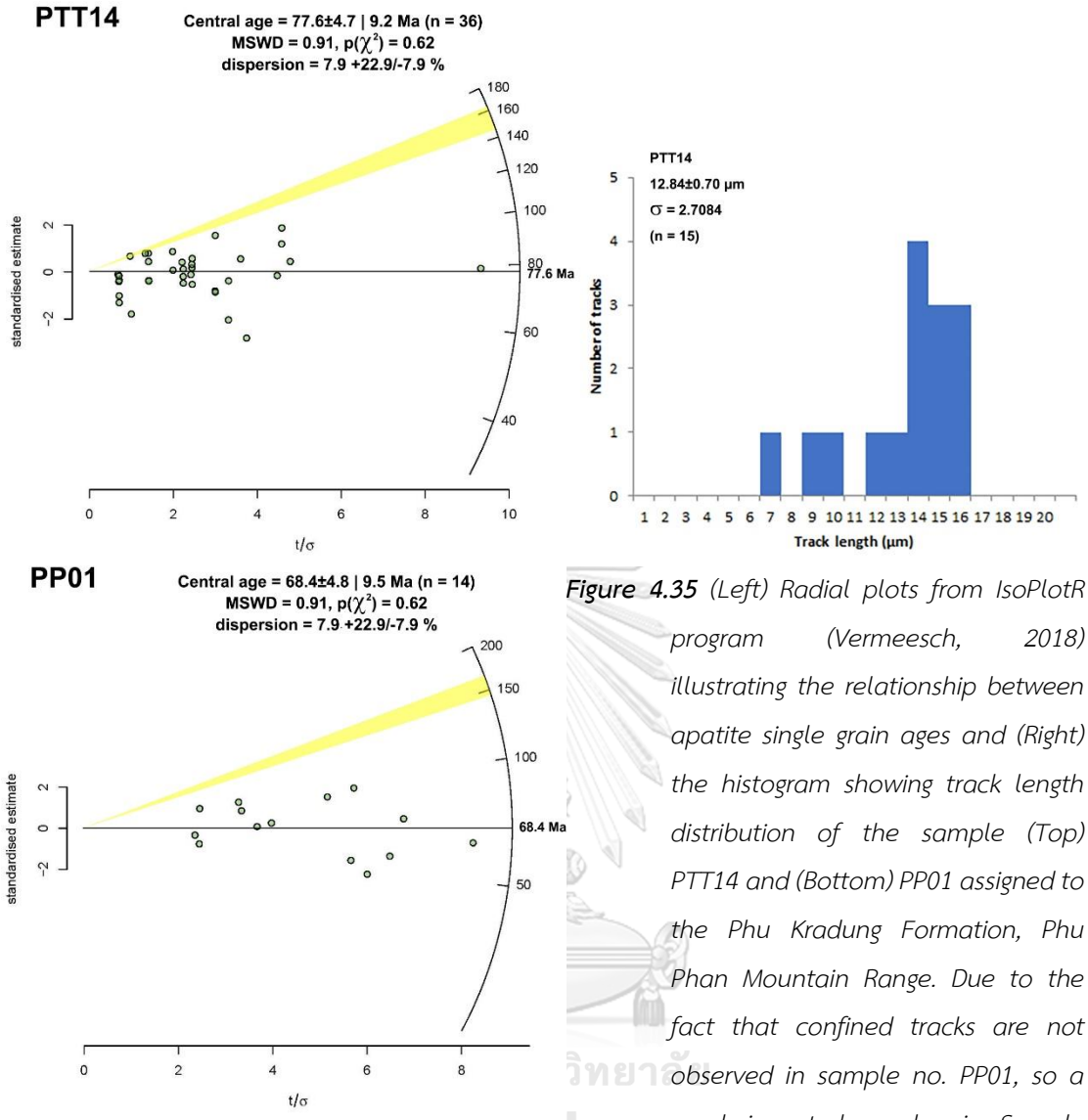

Figure 4.35 (Left) Radial plots from IsoPlotR program (Vermeesch, 2018) illustrating the relationship between apatite single grain ages and (Right) the histogram showing track length distribution of the sample (Top) PTT14 and (Bottom) PP01 assigned to the Phu Kradung Formation, Phu Phan Mountain Range. Due to the fact that confined tracks are not observed in sample no. PP01, so a graph in not shown herein. Sample no. PTT14 contain apatite with the track length 12.84±0.7 and the S.D. of 2.7084.

and 55.1±4.3 Ma (PTT15) and central age to be 50.2±3.6 Ma for sample PP15, 45.8±1.3Ma for sample PP16, 60.8±6.7 Ma for sample PTT15. Their results were analyzed from 25 (PP15), 7 (PP16), and 5 (PTT15) apatite crystals (Figure 4.37 and 4.38).

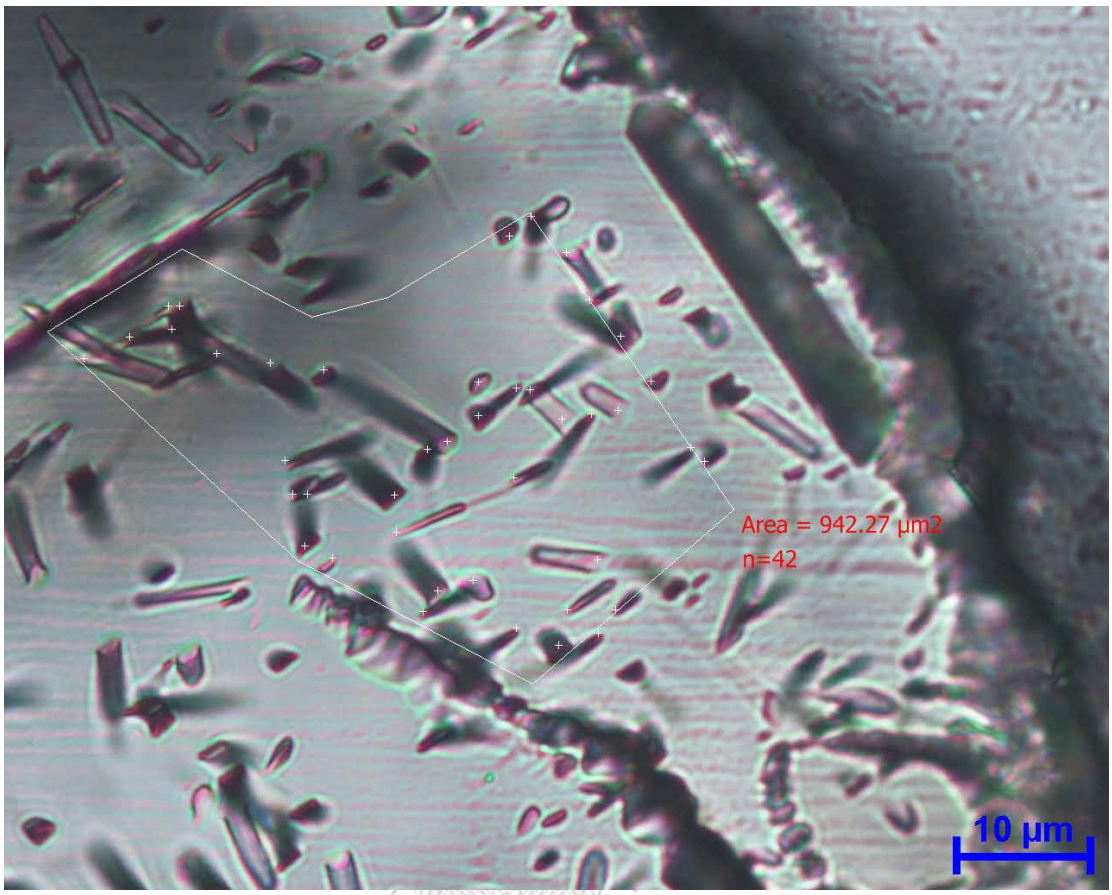

Figure 4.36 *An apatite grain with fission tracks from sandstone (sample no. PP16) belonging to the Phu Phan Formation, Phu Phan Mountain Range.*

According to Department of Mineral Resources (2014), the depositional age of Phu Phan Formation is about 145 to 100 Ma. So, all of the AFT age data suggest that central age of the samples is younger than the depositional age.

Number of tracks from the analyzed samples show wide range of variation. There are about 7 – 88 tracks in apatite grains of sample no. PP10, about 0 – 165 tracks for sample no. PP15, 1 – 492 tracks for sample no. PP16, and 8 – 101 tracks for sample PTT15 within an area of 3,685 to 18,212 μm^2, 2,000 to 22,700 μm^2, 3,600 to 22,109 μm^2, and 574 to 6,314 μm^2, respectively. Confined track lengths are relatively low in sample no. PP16 (n=2) with a mean of 10.11±0.13 µm (see Figure 4.38 top-right) and standard deviation of about 0.18. The result is not clearly to be in any model. The other samples have not found confined track in the measurement.

U/Ca ratio of this apatite of sample nos. PP10, PP15, PP16, and PTT15 divided by U/Ca of external standard (NIST SRM610) falls within 0.002 to 0.023, 0.0014 to 0.0353, 0.0011 to 0.0704, and 0.009 to 0.0311, respectively. Furthermore, the error of ratio U/Ca of apatite standard divided by error of U/Ca of external standard (NIST SRM610) for sample nos. PP10, PP15, PP16, and PTT15 fall within the ranges of 0.00019 to 0.00027, 0.00014 to 0.00034, 0.00022 to 0.00026, and 0.00014 to 0.00025, respectively (see more detail in Tables 4.7, 4.8, 4.9, and 4.10).

Table 4.7 The LA-ICP-MS data and fission-track dating from sample PP10, belonging to the Phu Phan Formation, Phu Phan Mountain Range.

PP10 grain ID	spot ID	LA-ICP-MS data				FT dating									
		Ap		NIST610		Ap/NIST610	SE	U	Average	SE	ρ_s	Ns	A	T	σ
		$^{238}U/^{43}Ca$	SE (%)	$^{238}U/^{43}Ca$	SE (%)	($^{238}U/^{43}Ca$)	(%)	(μg/g)	Ap/NIST610	(%)	($10^6/cm^2$)		(μm^2)	(Ma)	(Ma)
1	a	0.0961	1.8214	4.4294	0.9122	0.0217	2.04	47.5392	0.0232	4.68	1.4256	88	6172.91	56.7	6.7
	b	0.1102	1.6029	4.4491	0.8972	0.0248	1.84	54.2726							
4	a	0.0064	1.8006	4.4688	0.8822	0.0014	2.01	3.1578	0.0104	60.95	0.8994	51	5670.66	79.5	49.7
	b	0.0872	2.3831	4.4885	0.8671	0.0194	2.54	42.5760							
5	a	0.0529	2.3010	4.5081	0.8521	0.0117	2.45	25.7180	0.0123	3.23	0.5778	41	7096.05	43.4	7.0
	b	0.0575	1.8814	4.4701	0.8375	0.0129	2.06	28.1800							
6	a	0.0216	2.3890	4.4412	0.8376	0.0049	2.53	10.6366	0.0033	19.83	0.1884	21	11144.7	53.2	15.7
	B	0.0116	2.6665	4.4124	0.8378	0.0026	2.80	5.7544							
	c	0.0103	2.4088	4.3835	0.8380	0.0023	2.55	5.1249							
7	a	0.0215	1.9822	4.3546	0.8382	0.0049	2.15	10.8027	0.0052	3.06	0.5362	22	4102.76	95.8	20.8
	b	0.0233	1.8965	4.3380	0.8525	0.0054	2.08	11.7796							
8	a	0.0073	1.9920	4.3503	0.8667	0.0017	2.17	3.6532	0.0017	2.17	0.1092	7	6409.16	60.5	22.9
9	a	0.0729	1.5501	4.3748	0.8950	0.0167	1.79	36.5091	0.0166	7.81	0.8209	68	8283.33	45.6	6.7
	b	0.0608	1.7757	4.3871	0.9091	0.0139	1.99	30.3689							
	c	0.0852	1.7507	4.3993	0.9233	0.0194	1.98	42.4401							
14	a	0.0071	1.9432	4.4099	0.9546	0.0016	2.17	3.5302	0.0016	2.76	0.1555	25	16080.18	89.6	18.2
	b	0.0066	2.4294	4.4091	0.9631	0.0015	2.61	3.2850							
	c	0.0074	1.8379	4.4083	0.9717	0.0017	2.08	3.6923							
15	a	0.0303	2.0258	4.4074	0.9802	0.0069	2.25	15.0683	0.0033	43.47	0.1471	25	16993.03	40.7	19.5
	b	0.0055	2.3068	4.4066	0.9888	0.0013	2.51	2.7520							
	c	0.0083	2.1082	4.3867	1.0145	0.0019	2.34	4.1310							
18	a	0.0220	2.0231	4.3676	1.0316	0.0050	2.27	11.0113	0.0042	7.64	0.2361	43	18211.88	51.5	8.9
	b	0.0169	1.9215	4.3485	1.0488	0.0039	2.19	8.5141							
	c	0.0164	2.3191	4.3294	1.0659	0.0038	2.55	8.3095							
19	a	0.0127	2.9369	4.3103	1.0831	0.0030	3.13	6.4646	0.0030	3.13	0.4614	17	3684.63	143.5	35.2
20	a	0.0129	1.8877	4.2912	1.1002	0.0030	2.18	6.6035	0.0028	4.58	0.2936	19	6470.83	95.5	22.5
	b	0.0114	3.3798	4.3051	1.1378	0.0026	3.57	5.7994							
24	a	0.0783	2.2330	4.3160	1.1446	0.0181	2.51	39.7454	0.0155	11.23	0.8265	79	9558.13	49.3	7.9
	b	0.0488	1.9448	4.3270	1.1514	0.0113	2.26	24.6982							
	c	0.0740	2.4631	4.3380	1.1582	0.0171	2.72	37.3601							
						Weighted mean								58.2	3.6
						Pooled mean			0.0070	1.26	0.4221	506	119,878.25	56.1	2.9

Note: Pooled AFT age is calculated with ζ_{MS}= 0.928±0.022

Table 4.8 The LA-ICP-MS data and fission-track dating from sample PP15, belonging to the Phu Phan Formation, Phu Phan Mountain Range.

PP15 grain ID	spot ID	LA-ICP-MS data				FT dating									
		Ap		NIST610		Ap/NIST610	SE	U	Average	SE	ρ_s	Ns	A	T	σ
		$^{238}U/^{43}Ca$	SE (%)	$^{238}U/^{43}Ca$	SE (%)	($^{238}U/^{43}Ca$)	(%)	(μg/g)	Ap/NIST610	(%)	($10^6/cm^2$)		(μm^2)	(Ma)	(Ma)
1	a	0.1597	1.6324	3.9087	0.7799	0.0409	1.81	89.5152	0.0413	0.78	2.1719	139	6400	48.6	4.3
	b	0.1631	2.0512	3.9036	0.7747	0.0418	2.19	91.5233							
2	a	0.0073	1.9886	3.8984	0.7695	0.0019	2.13	4.0801	0.0018	2.05	0.1771	17	9600	90.2	22.0
	b	0.0068	1.8743	3.8933	0.7643	0.0018	2.02	3.8496							
3	a	0.0094	1.7799	3.8881	0.7591	0.0024	1.93	5.2711	0.0024	1.93	0.2464	17	6900	94.3	23.1
5	a	0.1372	1.5430	3.8854	0.7879	0.0353	1.73	77.3653	0.0353	1.73	1.8400	92	5000	48.2	5.2
6	a	0.0279	1.8849	3.8879	0.8219	0.0072	2.06	15.7094	0.0072	2.06	0.7500	21	2800	96.3	21.2
13	a	0.0020	3.1237	3.8953	0.9241	0.0005	3.26	1.1115	0.0005	4.06	0.0364	2	5500	69.9	49.6
	b	0.0018	3.3115	3.8978	0.9581	0.0005	3.45	0.9908							
15	a	0.1130	1.1661	3.9353	0.9137	0.0287	1.48	62.9001	0.0277	2.59	1.0811	80	7400	36.1	4.2
	b	0.1052	1.4361	3.9423	0.8981	0.0267	1.69	58.4570							
16	a	0.0101	1.4305	3.9463	0.8771	0.0026	1.68	5.6108	0.0018	16.70	0.0984	6	6100	49.6	21.9
	b	0.0064	1.6784	3.9432	0.8719	0.0016	1.89	3.5397							
	c	0.0052	1.9306	3.9401	0.8666	0.0013	2.12	2.8889							
19	a	0.0327	1.8183	3.9371	0.8613	0.0083	2.01	18.1735	0.0083	2.01	0.3500	14	4000	39.0	10.5
20	a	0.0911	1.7256	3.9340	0.8561	0.0232	1.93	50.7216	0.0232	1.93	1.4500	29	2000	57.9	10.9
22	a	0.0550	1.4109	3.9116	0.8987	0.0141	1.67	30.8222	0.0141	1.67	0.6207	54	8700	40.8	5.7
23	a	0.0029	2.8260	3.8346	1.0455	0.0008	3.01	1.6510	0.0008	3.01	0.0000	0	6600	0.0	0.0
25	a	0.0371	1.6142	3.8923	0.9467	0.0095	1.87	20.8814	0.0051	62.63	0.1023	9	8800	18.7	13.3
	b	0.0022	3.0045	3.8797	0.9612	0.0006	3.15	1.2655							
29	a	0.0543	1.5456	3.8804	0.9264	0.0140	1.80	30.6533	0.0140	1.80	0.5797	40	6900	38.3	6.2
30	a	0.0559	1.5744	3.8807	0.9089	0.0144	1.82	31.5649	0.0144	1.82	0.7778	28	3600	49.9	9.5
31	a	0.0205	1.5835	3.8811	0.8915	0.0053	1.82	11.5842	0.0060	8.58	0.5385	14	2600	82.5	23.2
	b	0.0262	1.8030	3.8814	0.8741	0.0067	2.00	14.7847							
33	a	0.0950	1.8144	3.8914	0.8757	0.0244	2.01	53.4590	0.0260	4.39	1.6500	66	4000	58.6	7.8
	b	0.1077	1.7559	3.8963	0.8853	0.0276	1.97	60.5342							
34	a	0.0278	2.1370	3.8255	1.0610	0.0073	2.39	15.9362	0.0049	35.33	0.1795	7	3900	34.2	17.7
	b	0.0093	2.0440	3.8301	1.0533	0.0024	2.30	5.3181							
37	a	0.0101	2.1381	3.8392	1.0378	0.0026	2.38	5.7719	0.0026	2.38	0.0000	0	2300	0.0	0.0
44	a	0.0041	2.5947	3.9358	0.9295	0.0010	2.76	2.2542	0.0014	18.31	0.0667	8	12000	44.4	17.7
	b	0.0069	2.5388	3.9634	0.9011	0.0017	2.69	3.8293							
46	a	0.0232	1.6515	3.9911	0.8727	0.0058	1.87	12.7291	0.0056	2.34	0.3947	45	11400	64.8	9.9
	b	0.0219	1.8291	4.0204	0.8549	0.0054	2.02	11.9127							
47	a	0.0576	2.3443	4.0221	0.8655	0.0143	2.50	31.3855	0.0112	12.02	0.7225	164	22700	59.8	8.7
	b	0.0417	2.3517	4.0238	0.8760	0.0104	2.51	22.6814							
	c	0.0355	2.4727	4.0256	0.8866	0.0088	2.63	19.2977							
48	a	0.0852	1.9352	4.0290	0.9077	0.0211	2.14	46.2995	0.0211	2.14	0.7442	32	4300	32.6	5.9
49	a	0.0266	2.1901	4.0307	0.9182	0.0066	2.37	14.4315	0.0066	2.37	0.3400	17	5000	47.7	11.7
								Weighted mean						50.1	2.2
								Pooled mean	0.0108	0.48	0.5685	901	158,500	48.5	2.0

Note: Pooled AFT age is calculated with ζ_{MS}= 0.928±0.022

Table 4.9 The LA-ICP-MS data and fission-track dating from sample PP16, belonging to the Phu Phan Formation, Phu Phan Mountain Range.

PP16 grain ID	spot ID	LA-ICP-MS data				FT dating									
		Ap		NIST610		Ap/NIST610	SE	U	Average	SE	ρ_s	Ns	A	T	σ
		$^{238}U/^{43}Ca$	SE (%)	$^{238}U/^{43}Ca$	SE (%)	($^{238}U/^{43}Ca$)	(%)	(μg/g)	Ap/NIST610	(%)	(10^6/cm^2)		(μm^2)	(Ma)	(Ma)
2	a	0.0172	1.9967	3.9059	0.9043	0.0044	2.19	9.6385	0.0046	2.37	0.3342	42	12569.19	67.8	10.7
	b	0.0184	1.9540	3.9108	0.9138	0.0047	2.16	10.3070							
3	a	0.0461	2.1451	3.9191	0.9190	0.0118	2.33	25.7939	0.0114	2.62	0.7161	32	4468.88	58.3	10.5
	b	0.0429	2.5148	3.9225	0.9147	0.0109	2.68	23.9529							
4	a	0.0967	2.1239	3.9259	0.9104	0.0246	2.31	53.9702	0.0296	11.92	1.6172	154	9522.35	50.4	7.4
	b	0.1361	2.0698	3.9294	0.9061	0.0346	2.26	75.8477							
10	a	0.0042	2.4507	3.9328	0.9017	0.0011	2.61	2.3158	0.0011	0.75	0.0278	1	3599.53	24.1	24.1
	b	0.0043	2.2734	3.9363	0.8974	0.0011	2.44	2.3653							
15	a	0.2715	2.0098	3.9351	0.8974	0.0690	2.20	151.1035	0.0704	0.88	3.2423	350	10,795	42.6	2.5
	b	0.2812	2.1991	3.9304	0.9017	0.0716	2.38	156.7307							
	c	0.2778	1.9719	3.9258	0.9060	0.0708	2.17	154.9790							
17	a	0.2150	2.0723	3.9212	0.9103	0.0548	2.26	120.0850	0.0575	1.92	2.7460	492	17917.06	44.1	2.4
	b	0.2306	2.1238	3.9165	0.9146	0.0589	2.31	128.9447							
	c	0.2304	2.1377	3.9119	0.9189	0.0589	2.33	128.9837							
25	a	0.1237	2.2162	3.9219	0.9230	0.0315	2.40	69.0716	0.0287	2.31	1.4338	317	22109.32	46.1	3.0
	b	0.1140	1.8490	3.9292	0.9229	0.0290	2.07	63.5308							
	c	0.1083	2.2213	3.9365	0.9228	0.0275	2.41	60.2535							
	d	0.1096	2.2315	3.9438	0.9226	0.0278	2.41	60.8515							
	e	0.1102	1.8956	3.9511	0.9225	0.0279	2.11	61.0673							
							Weighted mean							45.9	1.5
							Pooled mean		0.0348	0.51	1.7140	1,388	80,981.03	45.5	1.6

Note: Pooled AFT age is calculated with ζ_{MS}= 0.928±0.022

Table 4.10 The LA-ICP-MS data and fission-track dating from sample PTT15, belonging to the Phu Phan Formation, Phu Phan Mountain Range.

PTT15 grain ID	spot ID	LA-ICP-MS data				FT dating									
		Ap		NIST610		Ap/NIST610	SE	U	Average	SE	ρ_s	Ns	A	T	σ
		$^{238}U/^{43}Ca$	SE (%)	$^{238}U/^{43}Ca$	SE (%)	($^{238}U/^{43}Ca$)	(%)	(μg/g)	Ap/NIST610	(%)	(10^6/cm^2)		(μm^2)	(Ma)	(Ma)
1-15	a	0.1423	1.7211	3.9653	0.9263	0.0359	1.95	78.6303	0.0311	10.79	1.5995	101	6314.64	47.5	7.1
p	b	0.1048	2.0339	3.9721	0.9302	0.0264	2.24	57.8183							
2-26	a	0.0777	1.3205	3.9925	0.9420	0.0195	1.62	42.6489	0.0195	1.62	1.9160	11	574.12	90.7	27.5
2-28	a	0.0360	2.3864	3.9857	0.9381	0.0090	2.56	19.8038	0.0090	2.56	0.8510	8	940.08	86.8	30.8
3-1	a	0.0936	1.4075	3.9964	0.8865	0.0234	1.66	51.2865	0.0212	7.21	1.5843	42	2651.00	68.8	11.8
	b	0.0759	1.6280	3.9784	0.8653	0.0191	1.84	41.7945							
5-26	a	0.0805	1.3640	4.0432	1.0003	0.0199	1.69	43.6058	0.0199	1.69	1.2247	24	1959.61	56.8	11.7
							Weighted mean							61.7	5.6
							Pooled mean		0.0251	1.05	1.4952	186	12,439.45	55.1	4.3

Note: Pooled AFT age is calculated with ζ_{MS}= 0.928±0.022

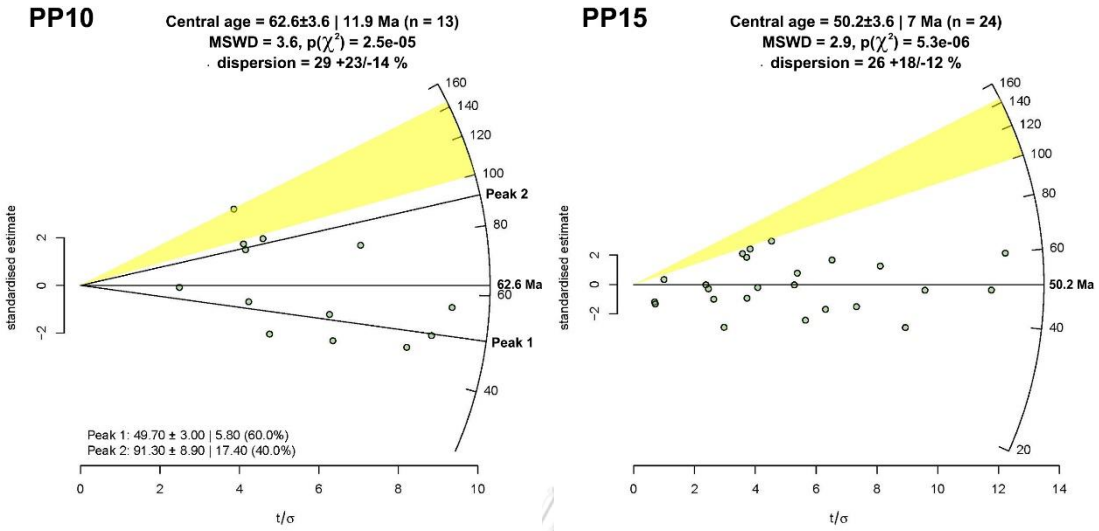

Figure 4.37 *Radial plots from IsoPlotR program (Vermeesch, 2018) displaying the relationship between apatite single grain ages (Left) PP10 and (Right) PP15 assigned to the Phu Phan Formation, Phu Phan Mountain Range. It is noted that no confined tracks are found in both samples.*

4.5.3 Summary of the AFT ages

Six samples out of the selected 21 sandstone samples of the Phu Phan Range study area. The central ages are always older than the pooled age with the difference in ages of about 10%. Due to the fact that P(χ^2) of the analyzed samples (nos. PP01, PP01, PTT14, and PTT15) are more than 5%, both central and pooled ages can be applied. In the case of sample nos. PP10 and PP15, P(χ^2) is lower than 5%, suggesting that only the central age data is accepted. As shown in Figures 4.39 and 4.40, two AFT age groups are obtained for both pooled and central age data, one group is about 57.2 Ma and the other is about 61.6 Ma

It is inferred from the current result that the sandstone of bearing-apatite always yields the pooled age younger than central age. Moreover, the pooled AFT age is invalid because in general, detrital samples in sedimentary basins can derive from multiple source areas as noted by Galbraith (2005). The results show a wide spread of AFT ages in a radial plot and have various apatite chemistry which control annealing behavior (Galbraith, 2005). Therefore, the central AFT age is more suitable for the interpretation of thermal overprint on rocks in this area. In case of the sample PP10,

has 2 age components, indicates that the sample might be incompletely reset. Therefore, younger age component is preferred for the current interpretation.

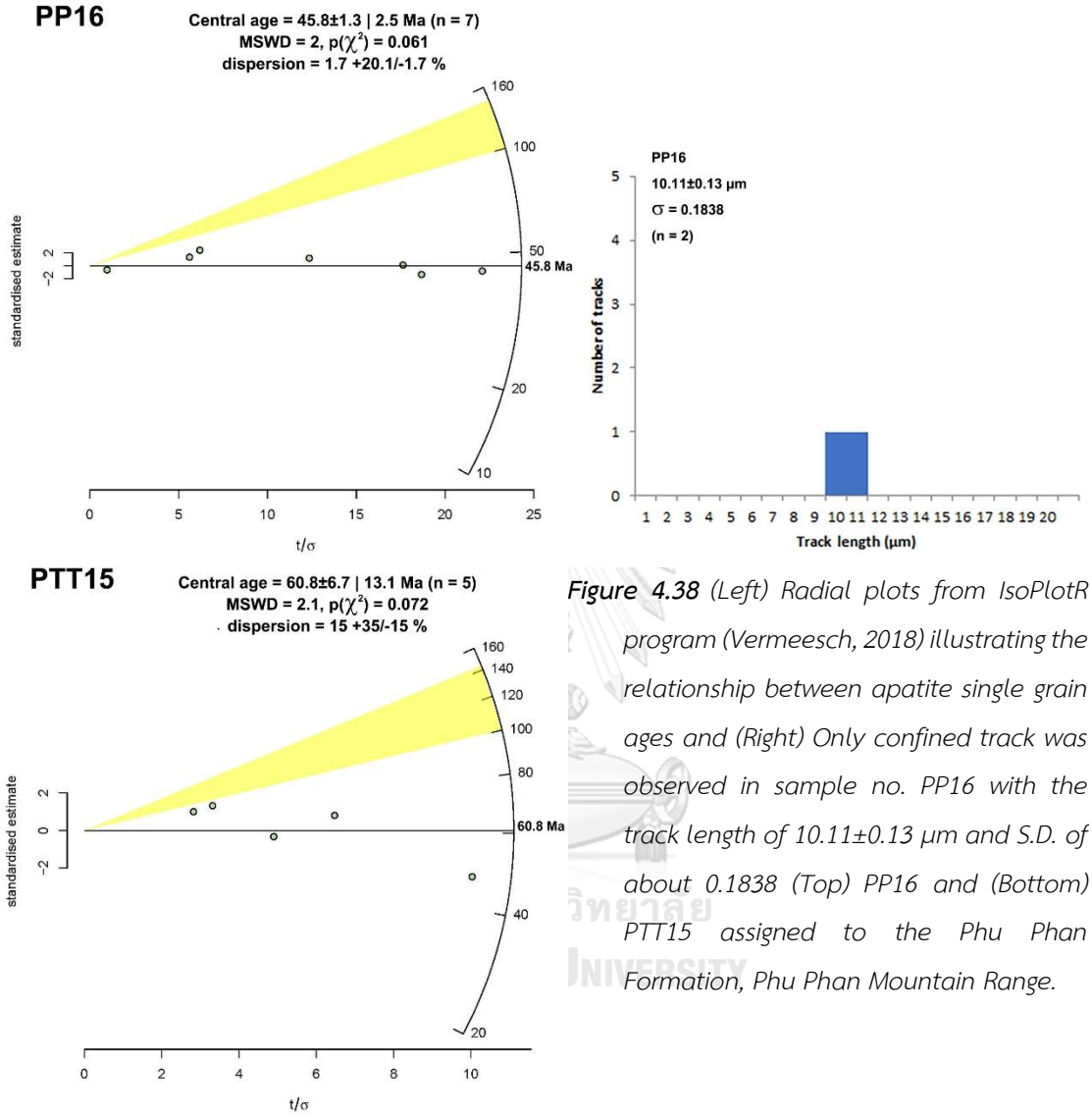

Figure 4.38 *(Left) Radial plots from IsoPlotR program (Vermeesch, 2018) illustrating the relationship between apatite single grain ages and (Right) Only confined track was observed in sample no. PP16 with the track length of 10.11±0.13 µm and S.D. of about 0.1838 (Top) PP16 and (Bottom) PTT15 assigned to the Phu Phan Formation, Phu Phan Mountain Range.*

Table 4.9 illustrates AFT ages from samples no. PP01, PTT14, PP10, PP15, PP16, and PTT15 with pooled FT age as 45.5±1.6 to 72.5±4.4 Ma (1**σ**). The central FT radial plots (Vermeesch, 2018) fall within the range of 45.8±1.3 to 77.6±4.7 Ma (see Figure 4.36, 4.37 and 4.38). Sample locations and AFT age data from the pooled age plot and the central age (except sample PP10 will use the younger age) plot is displayed on a geological map based on 1:50,000 map modified from DMR (1999; 2000; 2001; 2004; 2008) in Figure 4.39 and 4.40, respectively.

In case of grouping of the pooled and central AFT age, the results unveil the 2 AFT age ranges are 45 - 56 Ma and 65 - 73 Ma for pooled AFT age grouping (Figure 4.41) and 45 - 50 Ma and 60 - 77 Ma for central AFT age grouping (Figure 4.42).

Table 4.9 Summary of obtained AFT dating results from samples of the Khorat Group in Phu Phan Mountain Range.

Sample No.	P(χ^2)	Disp (%)	Fission track age (Ma)		Number of Grains	P1±1σ (Ma)	P2±1σ (Ma)	MTL±SD (μm)	nl
			P. age (Ma)	C. age (Ma)					
Phu Phan Fm.									
PP10	0.000025	29	56.1±2.9	62.6±6	13	49.7±3	91.3±8.9	-	-
PP15	0.0000053	26	48.5±2	50.2±3.6	25	-	-	-	-
PP16	0.061	1.7	45.5±1.6	45.8±1.3	7	-	-	10.11±0.18	2
PTT15	0.072	15	55.1±4.3	60.8±6.7	5	-	-	-	-
Phu Kradung Fm.									
PP01	0.094	15	65.4±3.8	72.8±7.1	14	-	-	-	-
PTT14	0.62	7.9	72.5±4.4	77.6±4.7	36	-	-	12.84±2.7	15

Note:

- **P. age** (Pooled AFT age): calculated from an equation (Hasebe et al., 2013).
- **C. age** (Central AFT age): calculated from radial plot with IsoPlotR program (Vermeesch, 2018).
- FT pooled age are calculated with ζ_{MS}= 0.928±0.022 (Hasebe et al., 2013)
- FT central age are calculated with ζ = 1.8560±0.044 by using an equation from Vermeesch (2017).
- Laser spot diameter size = 20 μm
- **Disp** gives the percentage of single-grain age dispersion
- **P(χ^2)**= is the chi-squared probability that the dated grains belong to a single statistical population (samples fail this test if P(χ^2) < 0.05).
- **nl** is the number of measured confined tracks.
- **MTL** is the average confined track length in μm with **σ** standard deviation
- **P1** and **P2** is used for while the AFT data shows a bimodality of single-grain ages, the data set was decomposed into 2 age polulations that were statistically derived using IsoPlotR program (Vermeesch, 2018).

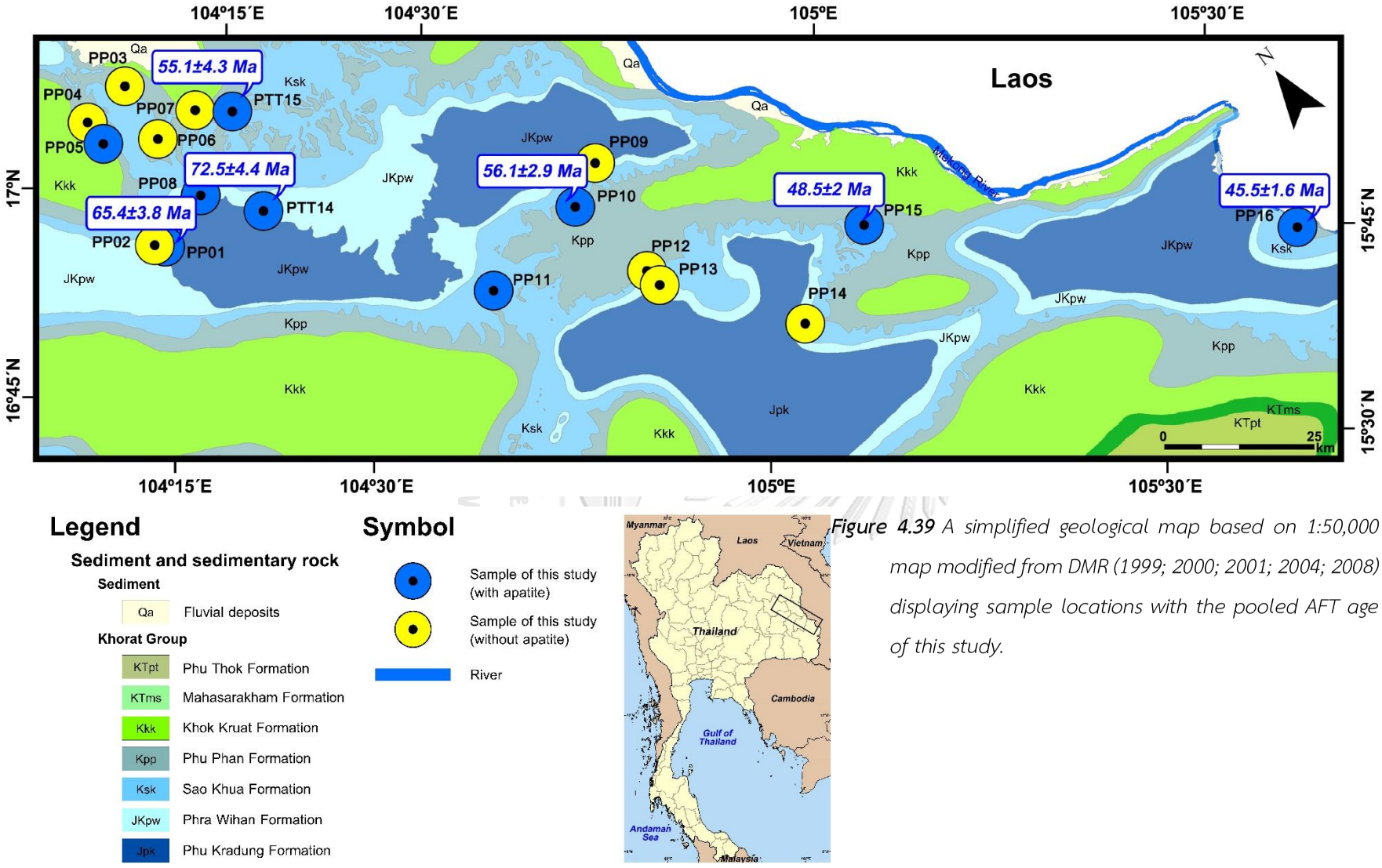

Figure 4.39 A simplified geological map based on 1:50,000 map modified from DMR (1999; 2000; 2001; 2004; 2008) displaying sample locations with the pooled AFT age of this study.

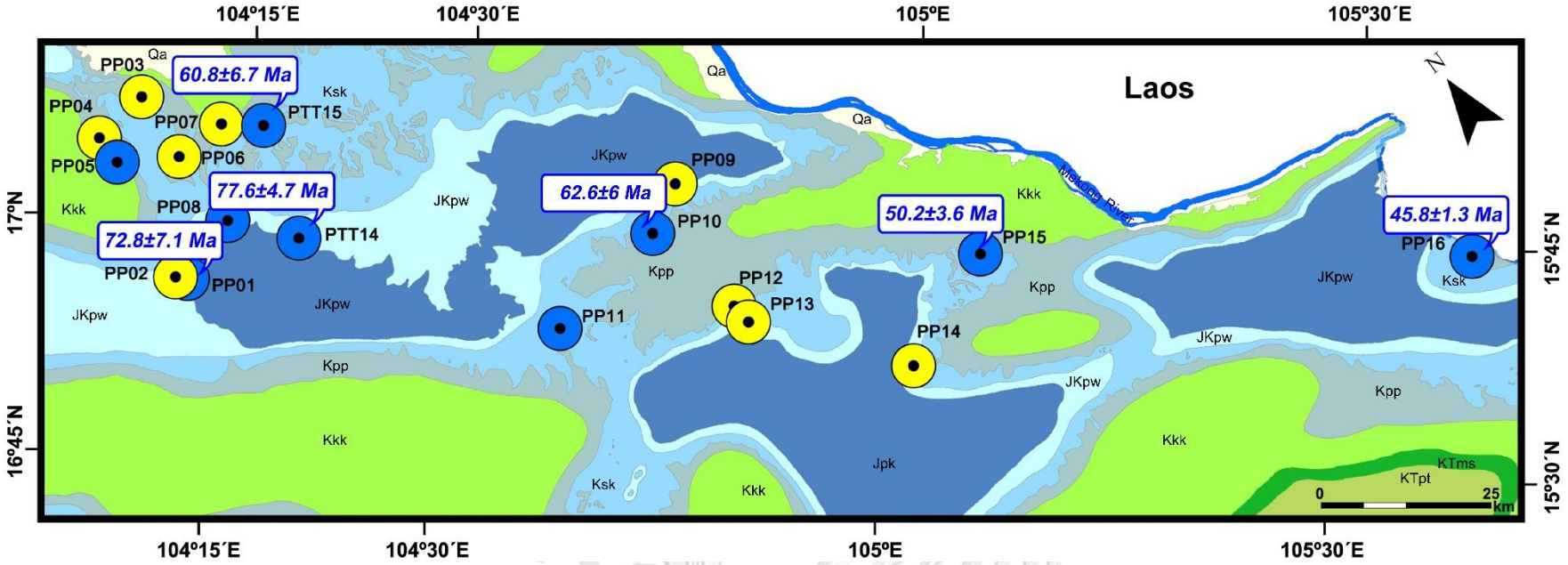

Figure 4.40 *A simplified geological map based on 1:50,000 map modified from DMR (1999; 2000; 2001; 2004; 2008) displaying sample locations with the central AFT age of this study.*

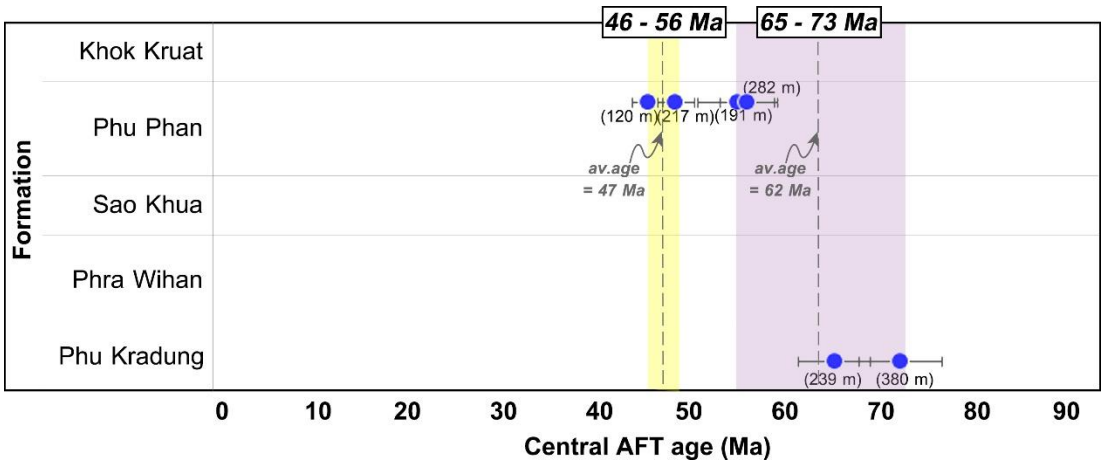

Figure 4.41 *Two pooled AFT age groups of the sandstones of the Khorat Group in the Phu Phan Mountain Range from this study.*

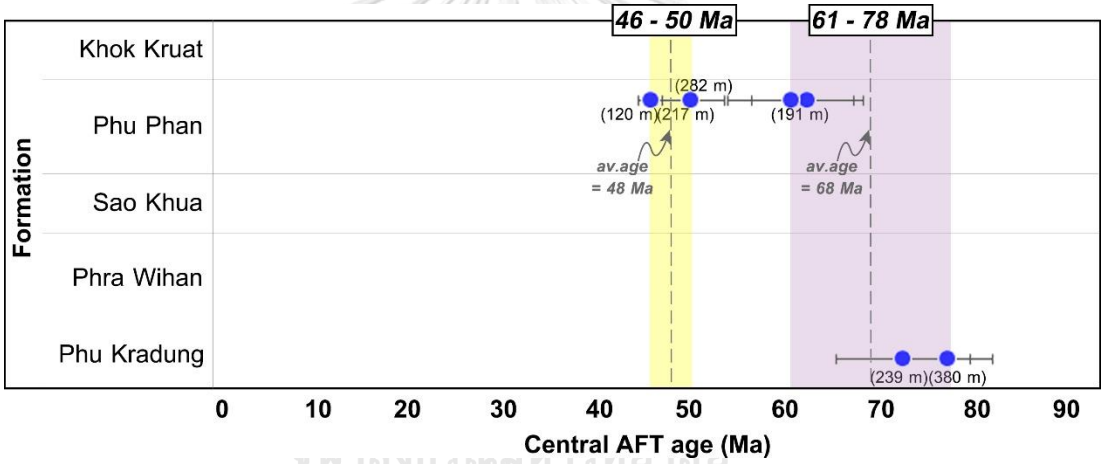

Figure 4.42 *Two central AFT age groups of the sandstones of the Khorat Group in the Phu Phan Mountain Range from this study.*

Chapter 5 Discussion

Based upon the results of field, petrographic, and geochronological investigation, 3 topics are herein discuss, namely provenance, AFT age grouping and uplift rates, and tectonic implication.

5.1 Provenance

Ternary diagram of sedimentary rock mineral composition (Pettijohn, 1975) reveals that sandstones of the Khorat Group (Phu Kradung to Phu Phan Formation) sandstone of this study are mostly litharenite, sublitharenite and some of feldspathic litharenite, all of which have high percentages of quartz and lithic fragments, but less feldspar. The mineral compositions of the Phu Phan Range sandstones are harmonized with those of Racey (2009) as shown in Figure 5.1

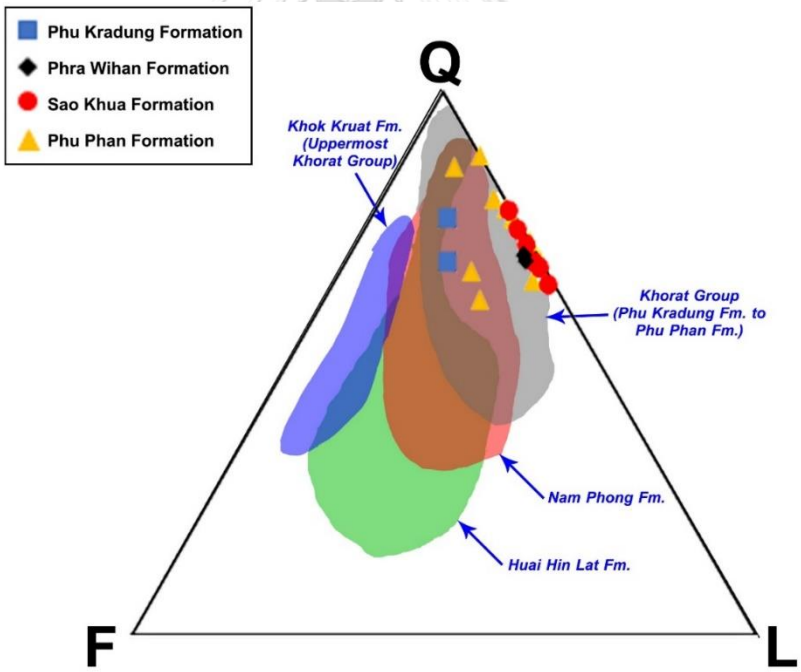

Figure 5.1 *Quartz-Feldspar-Lithic (QFL) ternary diagram (after Pettijohn, 1975) showing the Phu Phan Mountain Range sandstone samples of this study conform to the results of Racey (2009) in gray area.*

Figure 5.2 shows the relationship between detrital mode of sandstone and different generic types of provenance terrane. The detrital minerals of the Phu Phan Range sandstone samples are plotted in ternary diagram (after Dickinson, 1985) and all of them are related to the recycled orogens.

As a whole, the current study indicates that the Phu Phan Range sandstones are lithic- (<10%) and feldspathic- (<5%) poor and dominated by quartz fragments (>85%) based on the Gazzi-Dickinson method of point counting. The ternary plots of Q-F-L strongly show a continental block provenance (Figure 5.2) for the Khorat Basin suggesting a deeply eroded continental basement provenance.

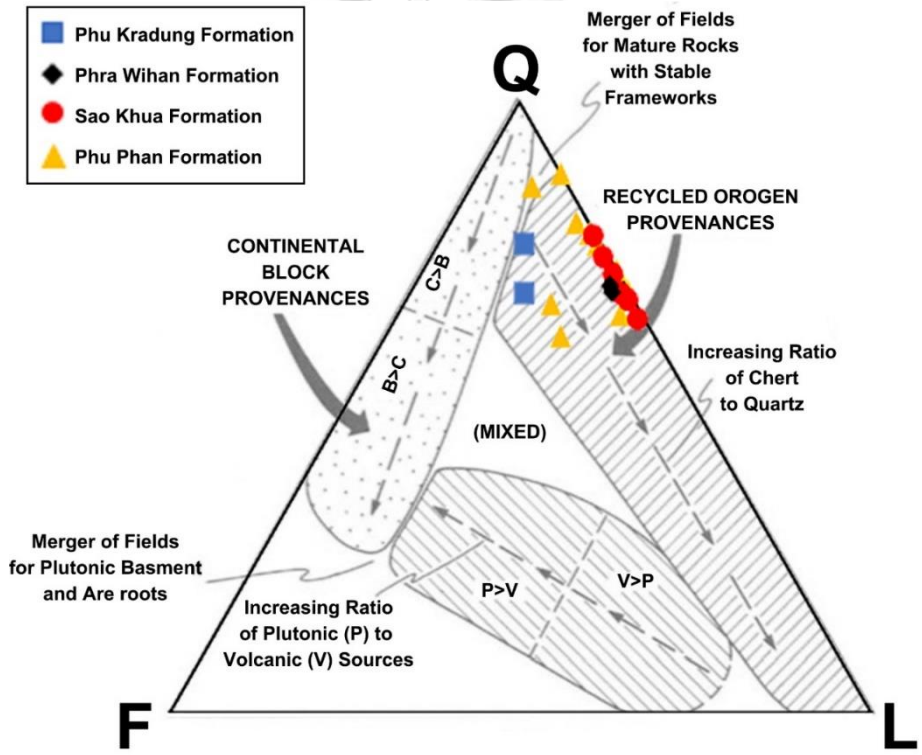

Figure 5.2 *Ternary diagram of relationship between detrital mineral composition of the Khorat Group sandstone in Phu Phan Mountain and types of provenance (after Dickinson, 1985). The sandstone samples of this study are related to "recycled orogen provenances".*

The Khorat Plateau is largely bounded by two tectonic belts, i.e., Loei Fold Belt in the west and the south and Troung Son Fold Belt in the east (Figure 5.3). Results of the paleocurrent patterns report by Racey (2009), Horiuchi et al. (2012), and Chenrai (2012) reveals that the sedimentary source of sandstones belonging to Phu Kradung,

Phra Wihan, Sao Khua and Phu Phan Formations sandstone was derived from the NNE to SSW direction and from ENE to WSW direction. As mentioned above, Trung Son Belt is located to the east and the north. Therefore, it is considered that most reliable source for the sandstone of the Phu Phan Range area is the Troung Son Belt (Figures 5.4, 5.5, 5.6, 5.7, and 5.8). The cross bed of the Khok Kruat Formation, on the other hand show different flow direction; i.e., from east to west direction. It also considered that sediments were transported from the more uplifted and eroded region in the north until denudation is ceased and afterward the uplifted and eroded area is to the west and sedimentation developed to become the Khok Kruat Formation.

5.2 AFT-age grouping

Table 5.1 shows the AFT age dating results of Racey et al. (1997) and Upton (1999) for the sandstones of the Phra Wihan and Phu Phan Formations in Phu Phan Mountain Range area have range of central AFT age is from 54.7±6.9 Ma to 37.4±4.1 Ma. The sample locations and their age results included this study central AFT age are show in Figure 5.9. Moreover, the AFT age results of the Western edge of Khorat Plateau from Carter et al. (1995), Racey et al. (1997), and Upton (1999) is shown Table 5.2. Figure 5.11 illustrates total AFT age data of the whole Khorat Plateau.

From the AFT age results on the Phu Phan Range from this study and previous studies, the total average AFT age is 53 Ma with the total standard deviation of 11.8. However, the AFT ages of sandstones from the Phu Phan Range fall into 3 groups by using statistic (1σ) are 78 - 60 Ma, 55 - 42 Ma, and 37 Ma (Figure 5.10). Meanwhile, the AFT age results on the whole Khorat Plateau from Carter et al. (1995), Racey et al. (1997), Upton (1999), and this study (Figure 5.11) contribute 50 Ma of total average AFT age 10.8 of total standard deviation. The AFT age grouping can unite into 3 periods that are range from 84 - 60 Ma, 55 - 45 Ma, and 37 - 31 Ma (Figure 5.12).

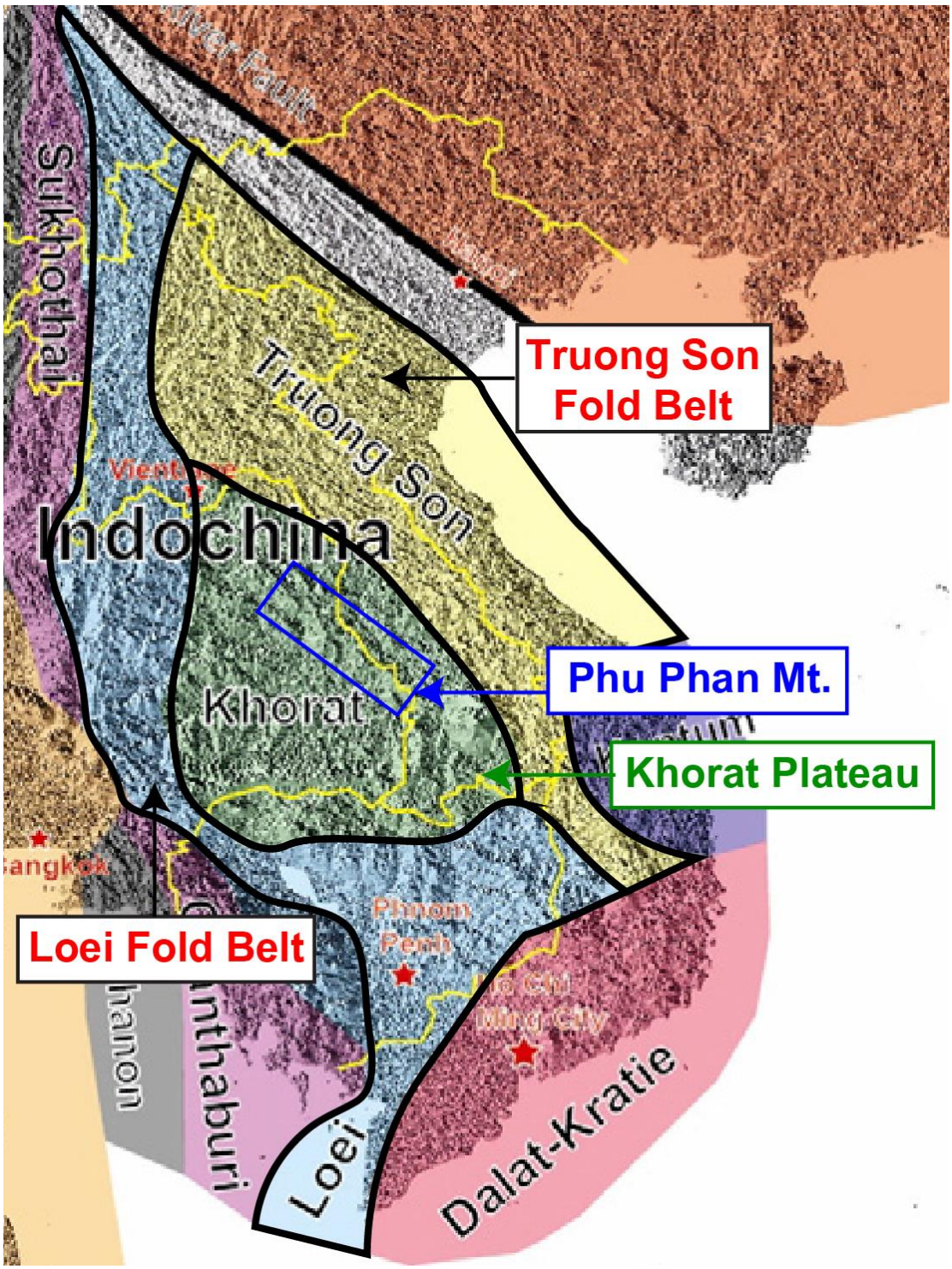

Figure 5.3 *Map illustrating the Khorat Plateau located on the Indochina tectonic block is bounded by two major tectonic belts which are Loei Belt in the west and the south and Troung Son Belt in the north and the east (modified from Khin Zaw et al., 2014).*

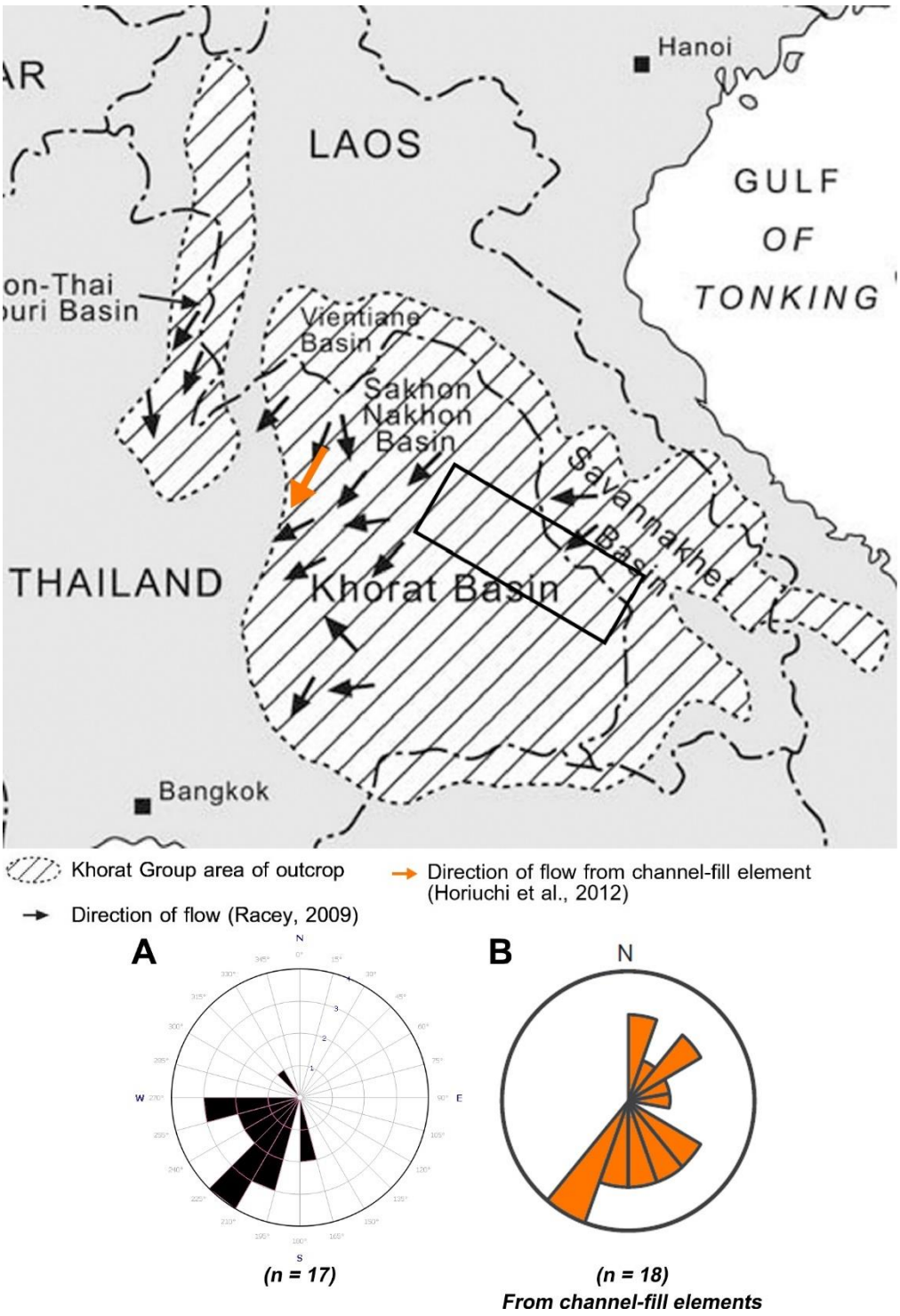

Figure 5.4 *(Top) Map showing the direction of paleocurrent for Phu Kradung Formation flowing mostly from the E to W and some of N to S, NE to SW and SE to NW (modified from Racey, 2009). Black rectangular is PPR study area. (Bottom) Rose diagram shows comparing of paleocurrent flow directions (A) mostly NE to SW (Racey, 2009) and (B) mainly from NE to SW from channel-fill elements data (Horiuchi et al., 2012).*

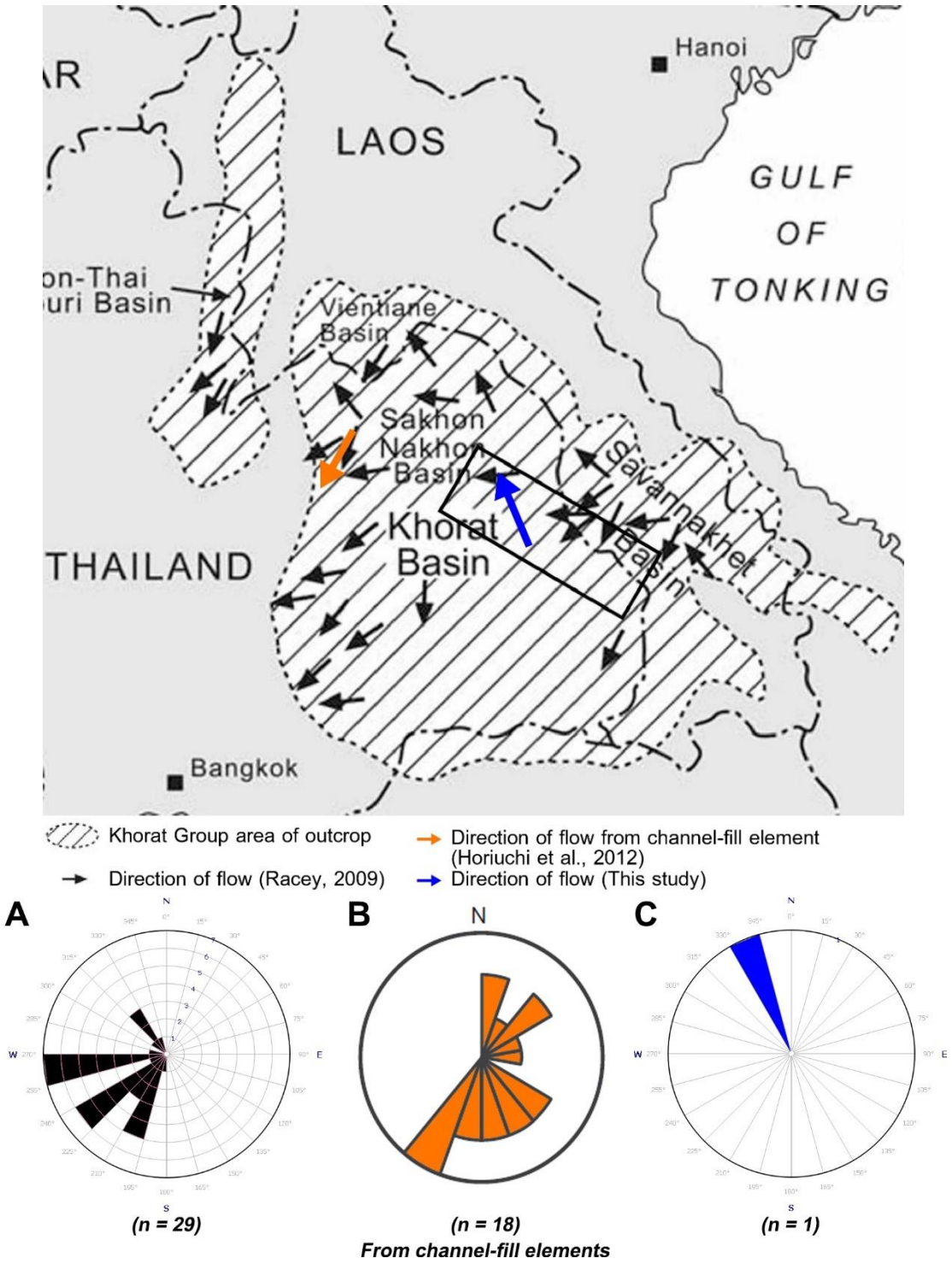

Figure 5.5 *(Top) Map showing the direction of paleocurrent for Phra Wihan Formation flowing mostly from the E to W and NE to SW and some of N to S and SE to NW (modified from Racey, 2009). Black rectangular is PPR study area. (Bottom) Rose diagram shows comparing of paleocurrent flow directions (A) mostly from E to W and NE to SW (Racey, 2009) (B) mainly from NE to SW from channel-fill elements data (Horiuchi et al., 2012) and (C) result of this study to the NW.*

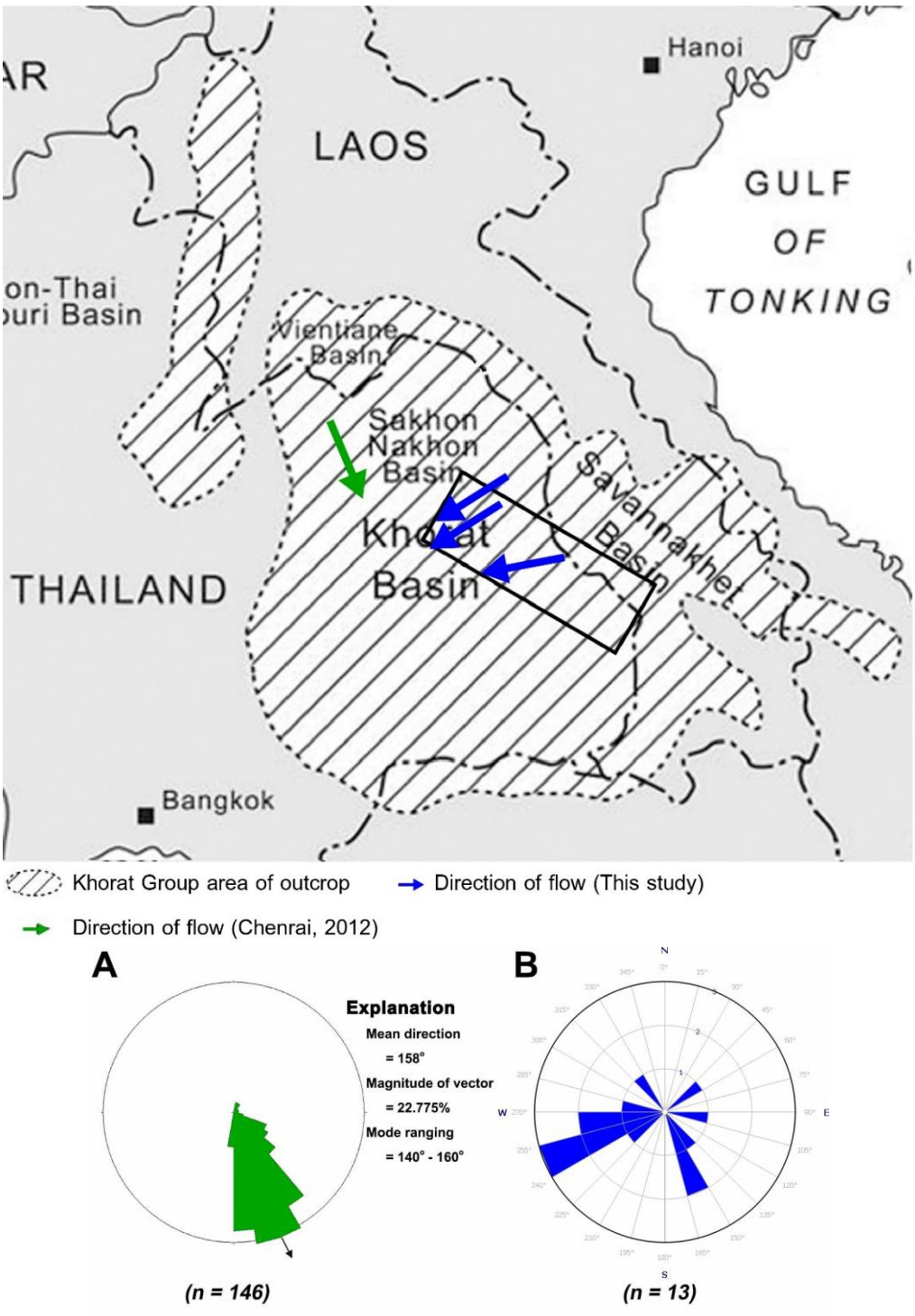

Figure 5.6 *(Top) Map showing the direction of paleocurrent for Sao Khua Formation flowing from the NE to SW and NW to SE (modified from Racey, 2009). Black rectangular is PPR study area. (Bottom) Rose diagram shows comparing of paleocurrent flow directions (A) from the NW to SE direction (Chenrai, 2012) and (B) for this study, the major paleocurrent of the Sao Khua sandstones is mostly from ENE to WSW direction and the other direction is from NNW to SSE direction.*

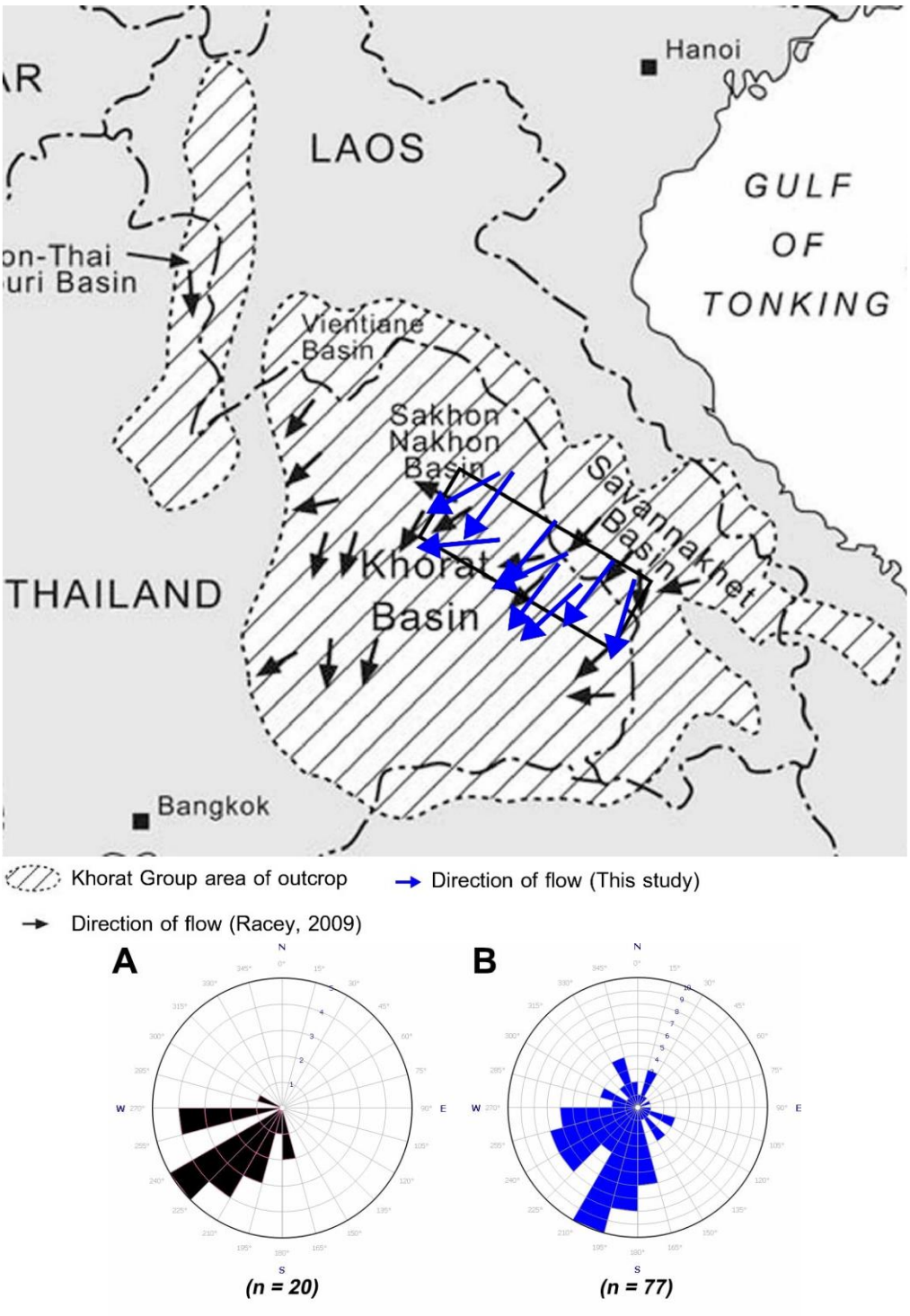

Figure 5.7 *(Top) Map showing the direction of paleocurrent for Phu Phan Formation flowing mostly from the NE to SW and some of N to S (modified from Racey, 2009). Black rectangular is PPR study area. (Bottom) Rose diagram shows comparing of paleocurrent flow directions (A) from NE to SW and E to W (Racey, 2009) and (B) paleocurrent result of this study to the SW.*

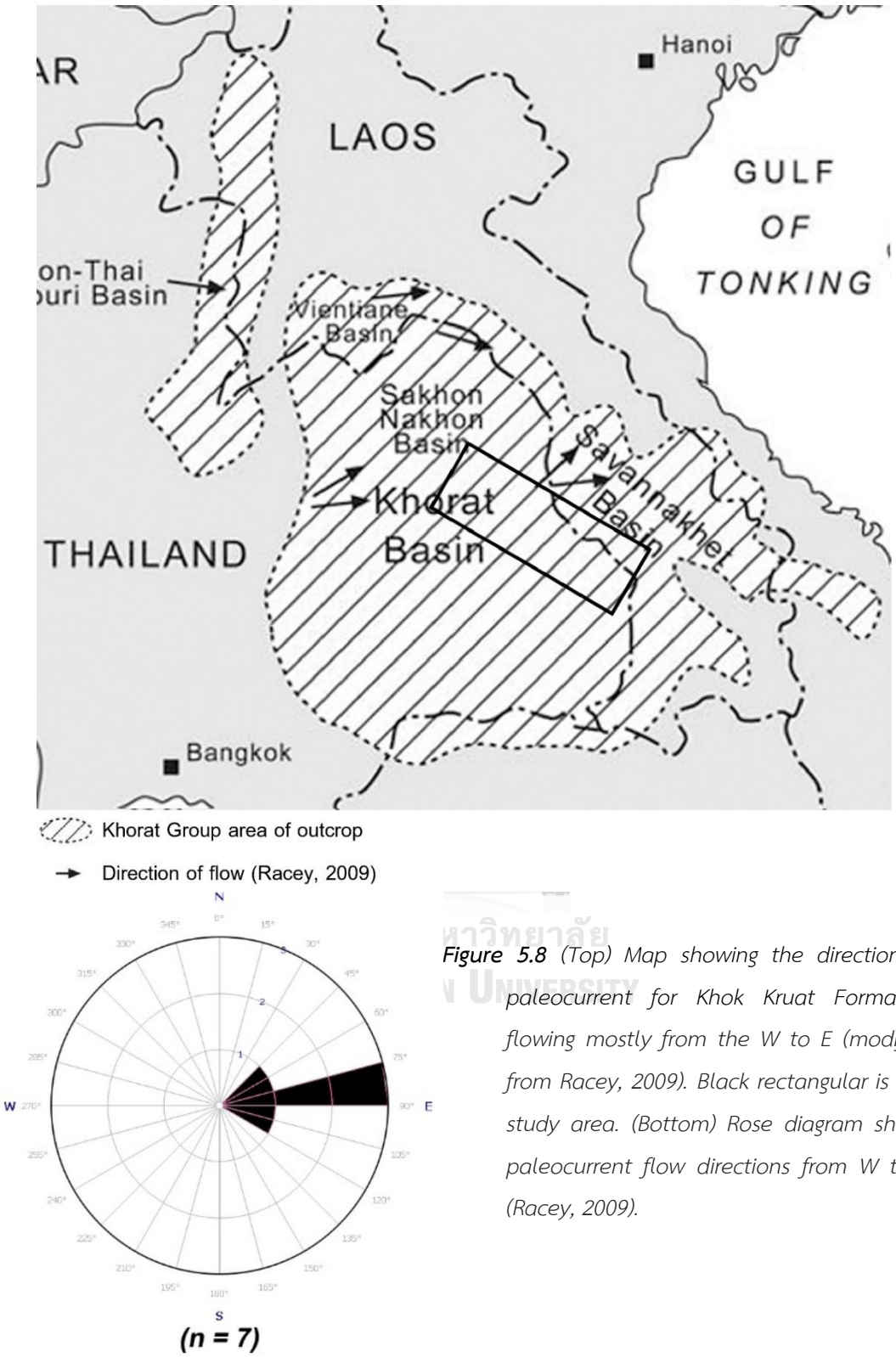

Figure 5.8 *(Top) Map showing the direction of paleocurrent for Khok Kruat Formation flowing mostly from the W to E (modified from Racey, 2009). Black rectangular is PPR study area. (Bottom) Rose diagram shows paleocurrent flow directions from W to E (Racey, 2009).*

Table 5.1 Apatite fission track analytical results of sandstones for the Phu Phan Mountain Range, Khorat Plateau, northeastern Thailand.

Sample No. *(elevation)*	Location	Age Dispersion		Fission track age (Ma)		Number of Grains	References
		χ^2	%	P. age	C. age		
Phu Phan Fm.							
GC-394-7	17°4'30"N			-	42.5±4.1	20	Racey
(320 m)	103°59'6"E						et al. (1997)
GC-394-2	17°12'9"N			-	37.4±4.1	20	Racey
(284 m)	103°54'18"E						et al. (1997)
GC-394-3	17°12'53"N			-	46.6±3.7	21	Racey
(390 m)	103°54'16"E						et al. (1997)
GC-394-8	17°6'16"N			-	50.2±4.8	20	Racey
(235 m)	103°31'12"E						et al. (1997)
Phra Wihan Fm.							
THI9559	16°47'31"N	<1	33	-	51±5	20	Upton (1999)
(288 m)	103°57'30"E						
GC-394-6	17°12'9"N			-	54.7±6.9	8	Racey
(348 m)	103°57'5"E						et al. (1997)

N.B.: P. age = Pooled AFT age; C. age = Central AFT age

Table 5.2 Apatite fission track analytical results from previous studies for the western edge of the Khorat Plateau, northeastern Thailand.

Sample No. *(elevation)*	Location	Age Dispersion		Fission track age (Ma)		Number of Grains	Reference
		χ^2	%	P. age	C. age		
Khok Kruat Fm.							
THI9034	15°32'17"N	<1	37	-	40±5	15	Upton (1999)
(232 m)	101°40'1"E						
THI9035	15°31'46"N	<1	34	-	70±8	20	Upton (1999)
(211 m)	101°43'57"E						
THI97147	17°27'18"N	9	22	-	41±4	19	Upton (1999)
(995 m)	100°55'9"E						
Phu Phan Fm.							
THI9032	15°40'18"N	<1	31	-	44±4	20	Upton (1999)
(306 m)	101°30'47"E						
THI9033	15°40'11"N	<1	32	-	53±6	20	Upton (1999)
(282 m)	101°33'35"E						
Sao Khua Fm.							
THI9014	15°21'29"N	<1	31	-	41±4	18	Upton (1999)
(208 m)	101°23'16"E						
THI9020	15°10'9"N	<1	45	-	84±8	30	Upton (1999)
(278 m)	101°25'56"E						

Table 5.2 (cont.)

Sample No. *(elevation)*	Location	Age Dispersion		Fission track age		Number of Grains	Reference
		χ^2	%	P. age	C. age		
Sao Khua Fm.							
THI97144 *(443 m)*	18°8'36"N 101°6'31"E	82	6	-	37±4	20	Upton (1999)
Phra Wihan Fm.							
THI9011 *(410 m)*	15°41'13"N 101°23'15"E	<1	22	-	42±3	24	Upton (1999)
THI9012 *(689 m)*	15°40'38"N 101°24'48"E	<1	38	-	58±4	35	Upton (1999)
THI9431 *(159 m)*	14°9'42"N 101°55'17"E	2	17	-	50±4	15	Upton (1999)
THI9434 *(535 m)*	14°28'12"N 101°55'39"E	4	16	-	40±2	20	Upton (1999)
THI9438 *(300 m)*	14°49'6"N 101°32'9"E	0	28	-	47±5	10	Upton (1999)
THI9439 *(300 m)*	14°47'29"N 101°30'58"E	0	28	-	49±4	20	Upton (1999)
T90/12 *(281 m)*	15°49'35"N 101°35'53"E	<1	38	-	58±5	35	Carter et al. (1995)
T90/17 *(242 m)*	15°4'18"N 101°24'22"E	<1	36	-	50±5	20	Carter et al. (1995)
T90/33 *(210 m)*	15°49'39"N 101°51'37"E	<1	32	-	53±6	20	Carter et al. (1995)
Phu Kradung Fm.							
THI9008	No data	4	19	-	50±3	28	Upton (1999)
THI9017 *(233 m)*	15°9'44"N 101°24'12"E	<1	36	-	50±5	20	Upton (1999)
THI9432 *(95 m)*	14°16'34"N 101°53'41"E	4	22	-	39±3	20	Upton (1999)
THI9556 *(647 m)*	16°43'10"N 101°38'25"E	6	22	-	49±6	14	Upton (1999)
THI97153 *(229 m)*	17°13'33"N 102°25'33"E	<1	21	-	47±3	28	Upton (1999)
GC-394-1 *(298 m)*	16°39'16" 101°43'51"			-	46.7±8.3	22	Racey et al. (1997)
Nam Phong Fm.							
THI97150 *(877 m)*	16°43'36"N 101°34'46"E	32	0	-	48±3	32	Upton (1999)
THI97151 *(487 m)*	16°43'46"N 101°24'3"E	22	<1	-	47±4	22	Upton (1999)

Table 5.2 (cont.)

Sample No. *(elevation)*	Location	Age Dispersion		Fission track age		Number of Grains	Reference
		χ^2	%	P. age	C. age		
Huai Hin Lat Fm.							
THI97160 *(287 m)*	16°39'28"N 101°44'13"E			-	43±3	20	Upton (1999)
Triassic granite							
THI9430 *(53 m)*	13°46'5"N 101°30'36"E	92	0	-	31±3	15	Upton (1999)
THI97156 *(219 m)*	17°54'18"N 101°43'18"E	36	7	-	54±3	20	Upton (1999)

5.3 Rate of exhumation

In the AFT age (Ma) versus sample elevation (m) plot (Figure 5.13 and 5.14) shows a trend with increasing AFT ages with elevation.

Figure 5.13 illustrates rate of uplift on the Phu Phan Range by AFT age versus elevation of sample point plot from the results of Racey et al. (1997), Upton (1999), and this study. The graph depicts a positive-trending linear that give rise to almost consistent uplift rate, viz 0.0192 mm/yr, 0.0112 mm/yr, and 0.0113 mm/yr. It can be stated that on average, the rate of uplift is about 0.01 mm/year. The maximum uplift rate of the PPR study area is 0.019.

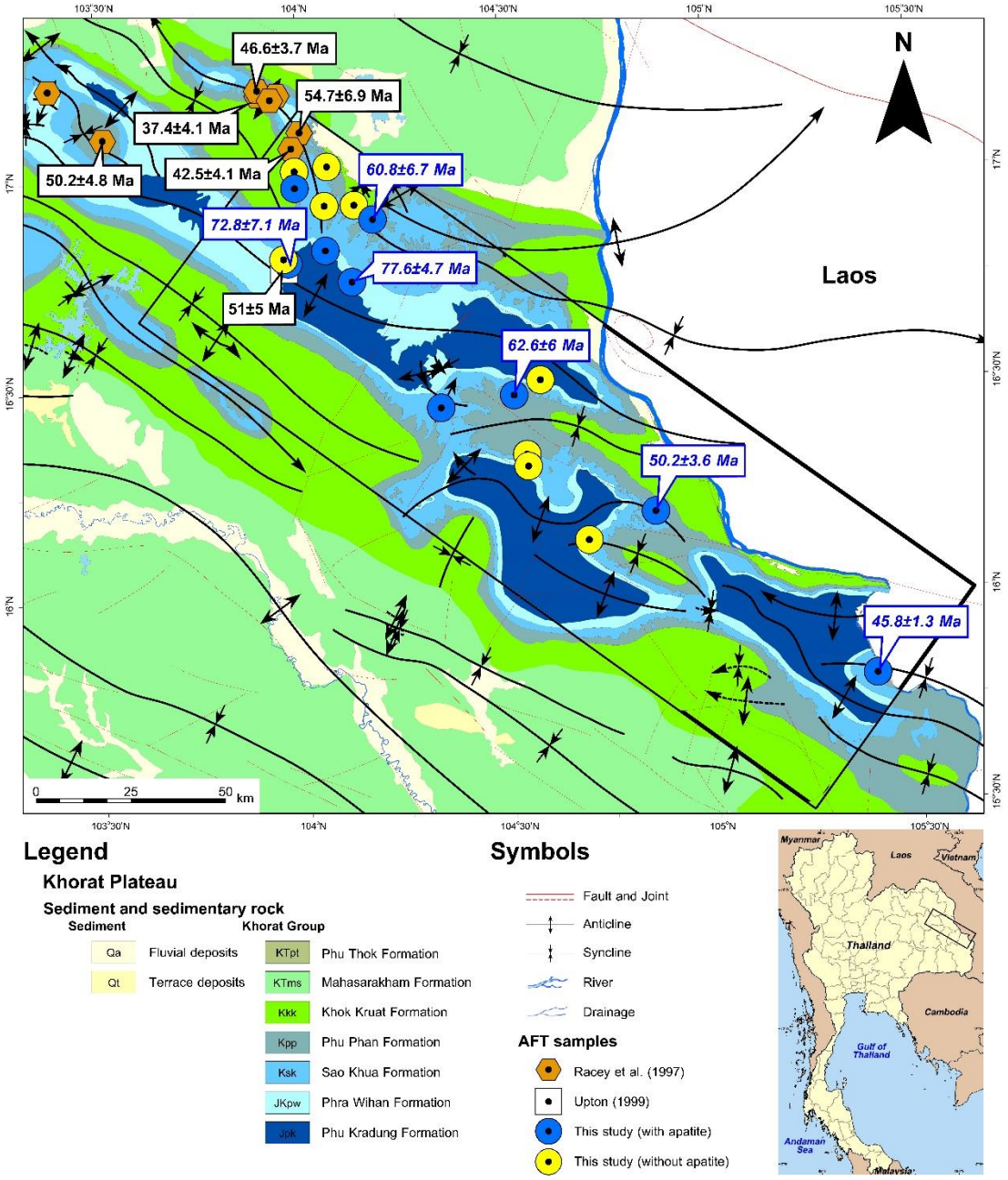

Figure 5.9 *Geological map showing series of broad deformation structure with the major NW-SE trend based on DMR (1999; 2000; 2001; 2004; 2008) with sample locations with AFT age results by Racey et al. (1997), Upton (1999), and this study.*

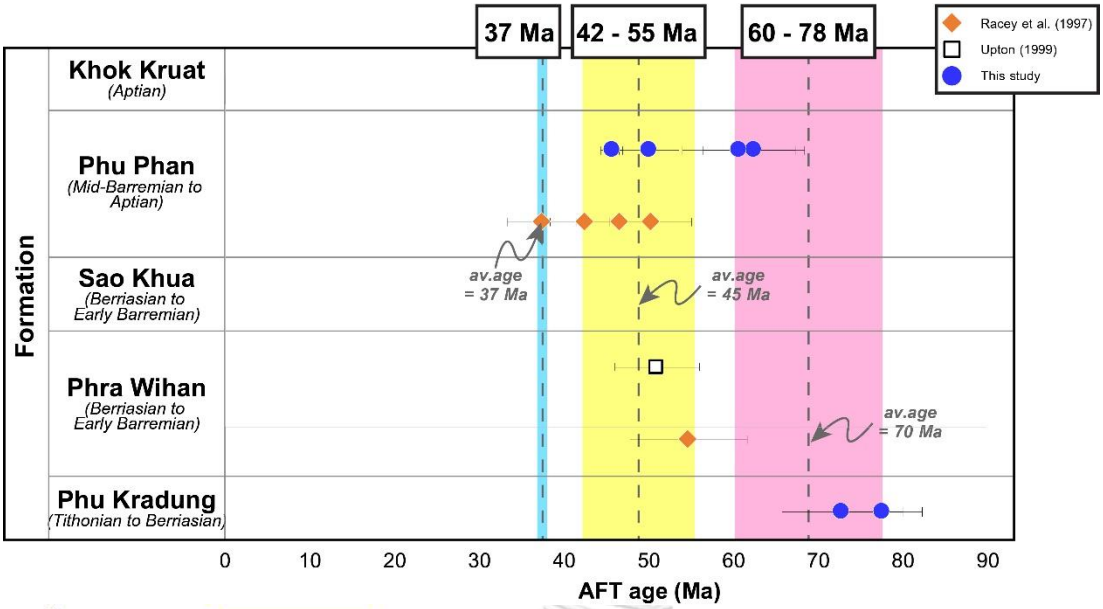

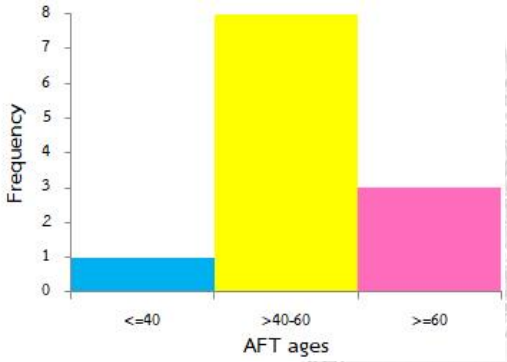

Total average age = 53.3

Total S.D. = 11.8

Figure 5.10 *(top) Three AFT age groups of the sandstones of the Khorat Group in the Phu Phan Mountain Range from previous study (Racey et al., 1997; Upton, 1999) included this study. Dash line showing average ages deduced from age-grouping of the result. (bottom-left) A histogram shows the number of AFT age on the Khorat Plateau in each age range with total average age = 53.3 and total S.D. = 11.8.*

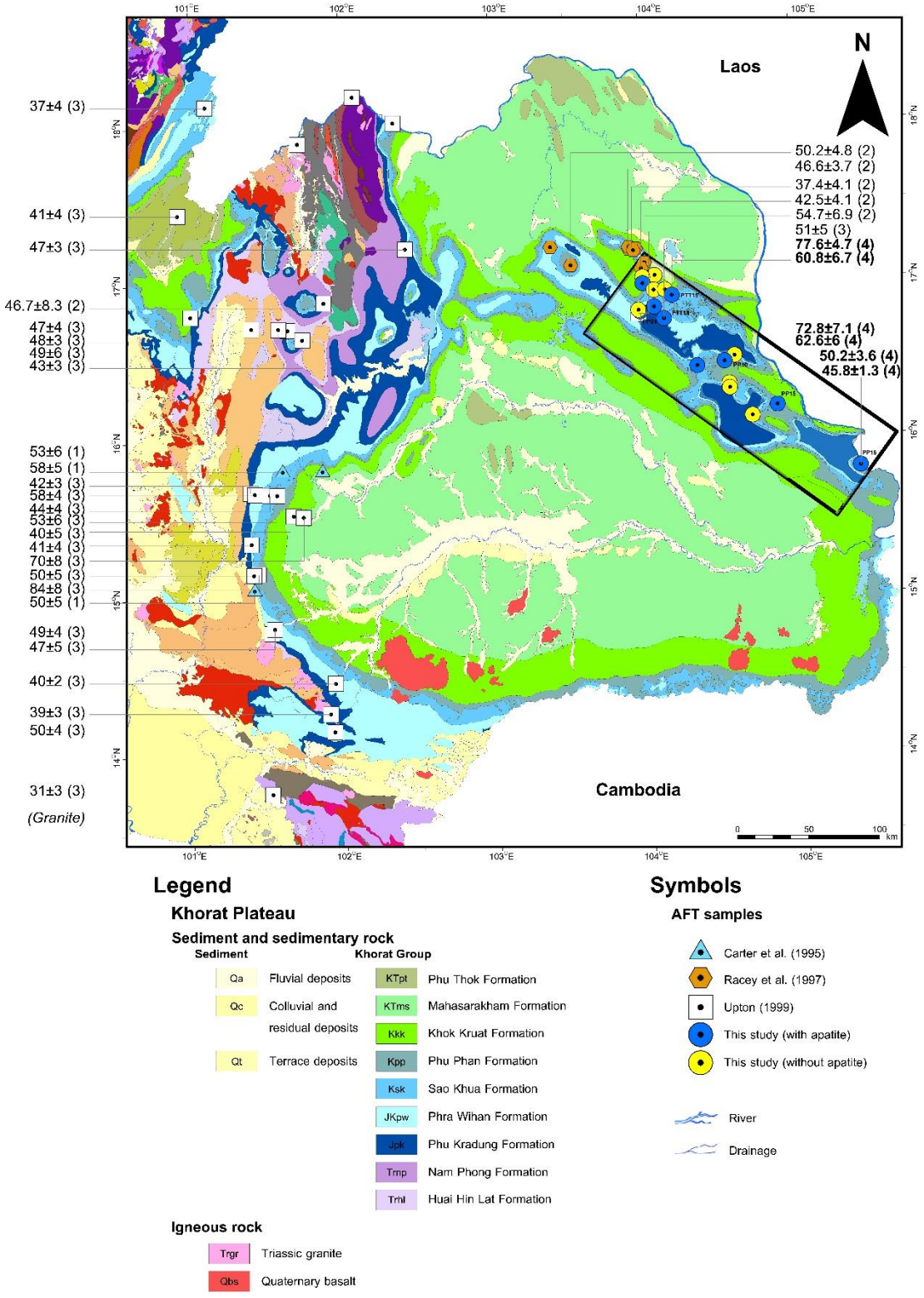

Figure 5.11 *Geological map of the NE Thailand based on 1:50,000 map modified from DMR (1999; 2000; 2001; 2004; 2008) of Phu Phan Mountain area and 1:250,000 map modified from DMR (2007) displaying sample locations with central AFT age results from Carter et al. (1995), Racey et al. (1997), Upton (1999), and this study.*

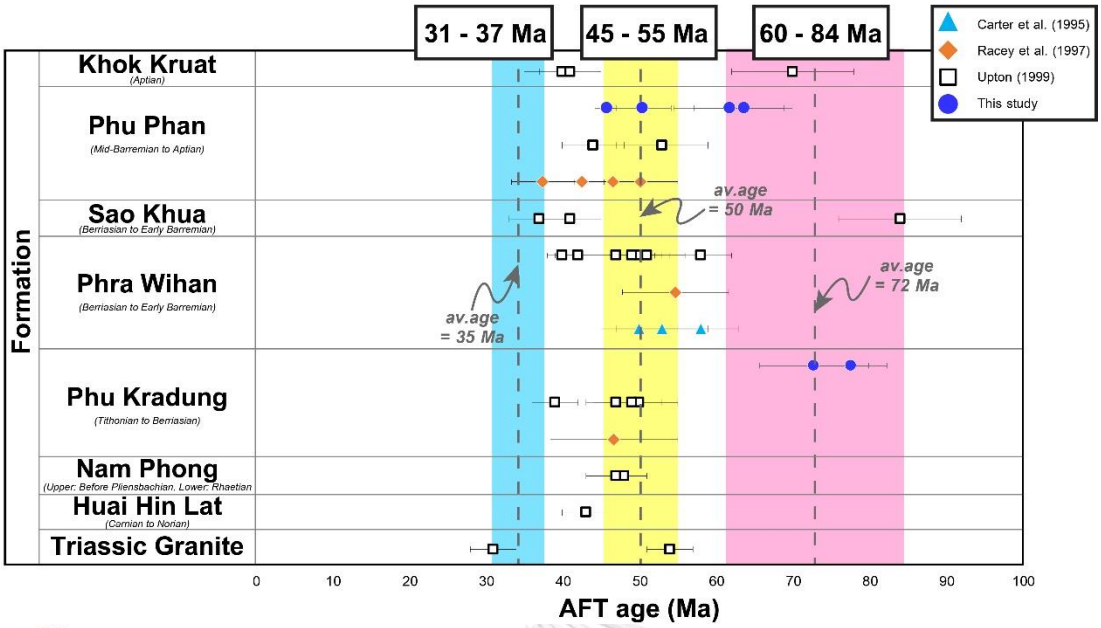

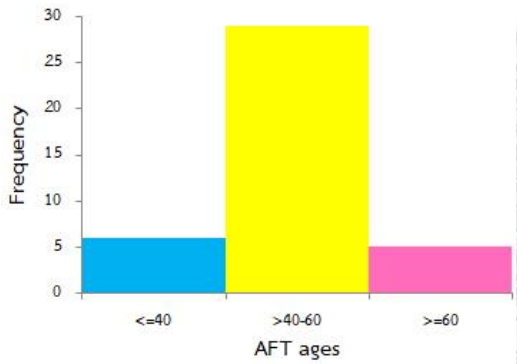

Total average age = 50

Total S.D. = 10.8

Figure 5.12 *(top) Three AFT age groups of the sandstones of the Khorat Group in the whole Khorat Plateau as defined from previous studies (Carter et al., 1995; Racey et al., 1997; Upton, 1999) and this study. Dash line shows average ages deduced from age grouping of the result. (bottom-left) A histogram shows the number of AFT age on the Khorat Plateau in each age range with total average age = 50 and total S.D. = 10.8.*

After combination of the rate of uplift of the Phu Phan Mountain Range and the western edge of the Khorat Plateau, the rate of uplift of whole Khorat region can be constrained.

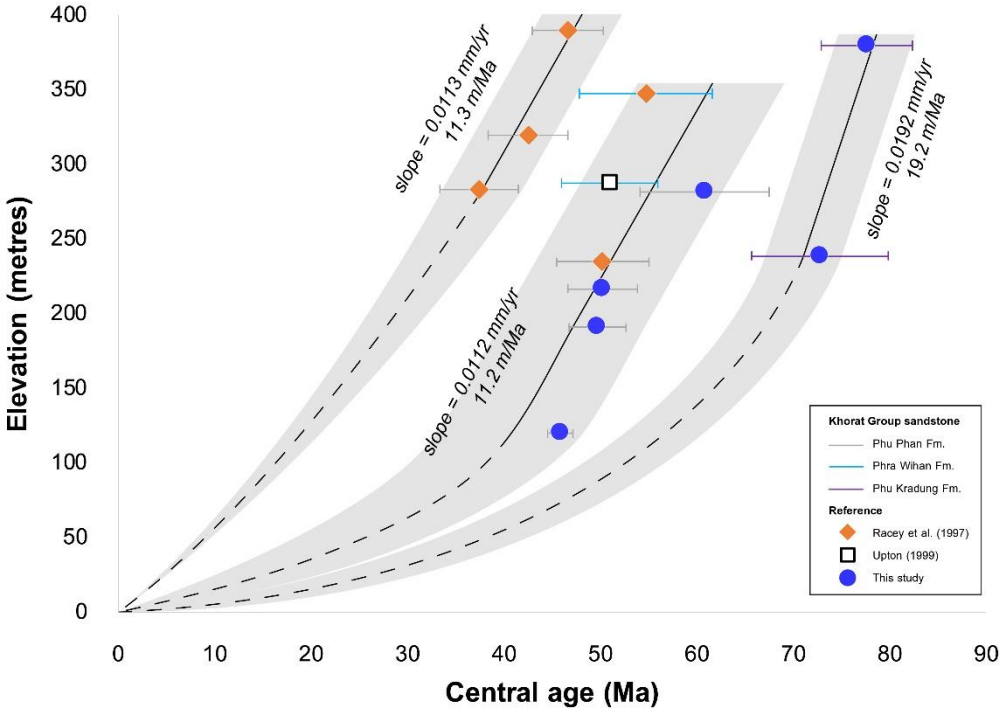

Figure 5.13 *Apatite fission track age versus elevation plots for the Phu Phan Mountain Range from previous studies (Racey et al., 1997; Upton, 1999) and this study.*

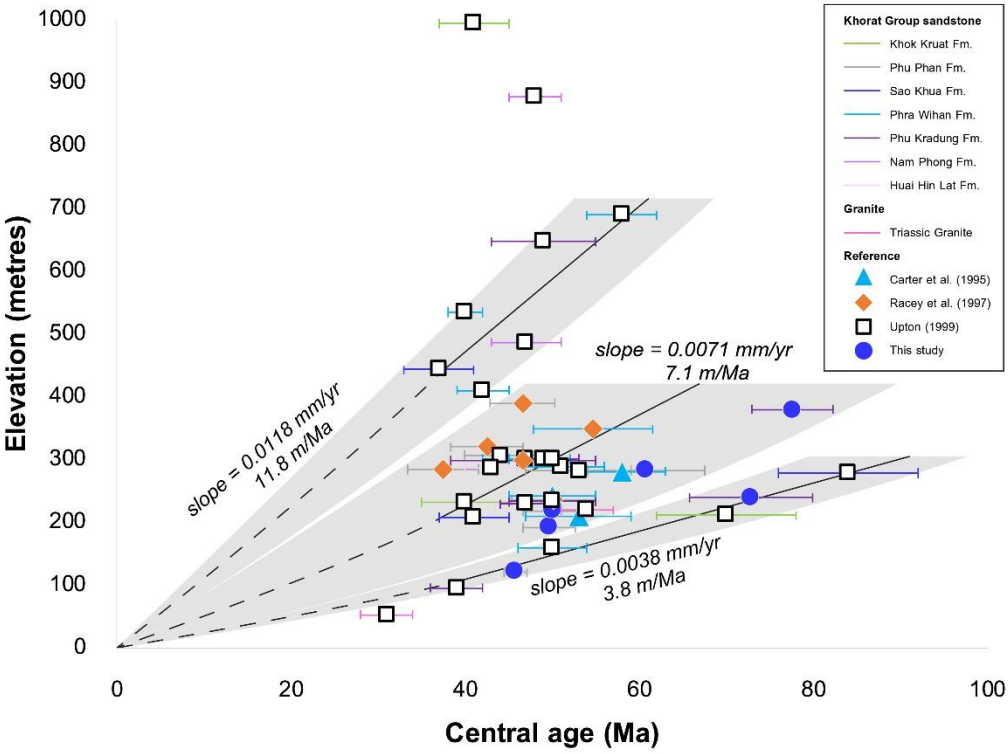

Figure 5.14 *Apatite fission track age versus elevation plots for western edge of the Khorat Plateau from the previous studies (Carter et al., 1995; Racey et al., 1997; Upton, 1999) and this study.*

5.4 Comparison of AFT ages of Phu Phan Mountain Range and geological events in Thailand and associated regions.

Based up on the previous and the current geochronological studies (Figure 5.15), tectonic episodes of the Phu Phan Mountain Range and neighboring regions can be delineated as explained below.

1. The first episode is the 78-60 Ma (Late Cretaceous to Early Paleogene) episode which is limited within the Cretaceous-Paleogene Boundary (KPB) may have been caused by the interaction of between Indochina and the surrounding plates, viz. one from the west and the other to the south. A broad structural style of the Phu Phan Range study area has the axial plane in the NW-SE trend, suggesting the maximum stress axis in the rough NE-SW direction. The maximum stress is split into 2 directional forces in the approximate N-S and E-W direction. It is quite likely that such two-tectonic stress are mainly due to the interaction of the Western Burma block to Indochina (Charusiri et al., 1993; Hutchison, 1989; Morley et al., 2004; Upton, 1999) in the west and the northwest subduction of Paleo-South China Sea Plate (Sun, 2016). The structural deformation as evident by the broad foldings occurred postdating major tectonic disturbance.
2. The second episode is the 55-42 Ma (Eocene) episode which corresponds to the period of India-Asia collision (Searle and Morley, 2011). It initiates foldings, thrustings, uplift and erosion (exhumation) of the Khorat Plateau (Upton, 1999 and this study) and Dextral strike-slip fault of Khlong Marui Fault (Kanjanapayont et al., 2012; Watkinson et al., 2011). Moreover, the granite suite in Phuket area were also unroofed (Putthapiban, 1984).
3. The lastest episode is about 37 Ma (Oligocene) episode which is equivalent of the N-S trending, rifting of the Central Plain and Gulf of Thailand. The effect of rifting may have the principle stress axis in the E-W direction. It has the minor fault over the anticlinal structure of Phu Phan Mountain Range related to extension tectonic which affect from India-Eurasia collision (Aitchison et al., 2007; Hall et al., 2008) and initiate sinistral strike-slip movement of Three

Pagoda Fault (Barley et al., 2003; Lacassin et al., 1997; Nantasin et al., 2012; Upton, 1999) and Mae Ping Fault (Barley et al., 2003; Lacassin et al., 1997; Morley et al., 2007; Upton, 1999).

4. About 23 Ma, the Three Pagoda fault and Mae Ping fault changed to Dextral strike-slip movement (Huchon et al., 1994; Lacassin et al., 1997; Morley et al., 2004; Upton, 1999) and initiation of an inversion of the Ranong and the Khlong Marui fault (Nachtergaele et al., 2017; Watkinson et al., 2011; Watkinson et al., 2008).

5.5 Tectonic implication of the Phu Phan Mountain Range and adjoining Khorat region

Figure 5.16 is a cooling age data complied from the previous and current studies. These age data are not only from the Khorat Plateau of the Indochina block, but also from the other region of the Sibumasu and associated block. It is seen clearly that age data fall within four age groups similar to that of the Phu Phan Range study area, implying that these age group can be also applied tectonically to the whole country.

The first group is the 84 - 60 Ma episode (or event) which correspond to the interaction of Indochina terrane with the proto-South China Sea plate in the east. In the Phu Phan Range study area, the strata of Mesozoic red beds (Figure 5.17A) of the Khorat Basin have been structurally deformed by tectonic compression, as a result to the broad foldings and faultings (thrusting) the plateau region (Figure 5.17B). Such Mesozoic strata can be thermally divided into 3 successive zones (Figure 5.17A) the completely reset ages in the lowermost zone, the partially annealing zone (PAZ) of fission track, and the uppermost zone where the ages are no reset. It is considered that all sandstone samples from the current study have been taken from this zone (Figure 5.17A). Such tectonic compression acting upon the Khorat Basin can give rise to initiation of the broad anticlinal structure of the Phu Phan Range area. Some fault movements have been ascribed to form in the WNW-ESE direction of this stage. Two large sedimentary basins may have been formed, namely the Sakon (-Udon) Basin and

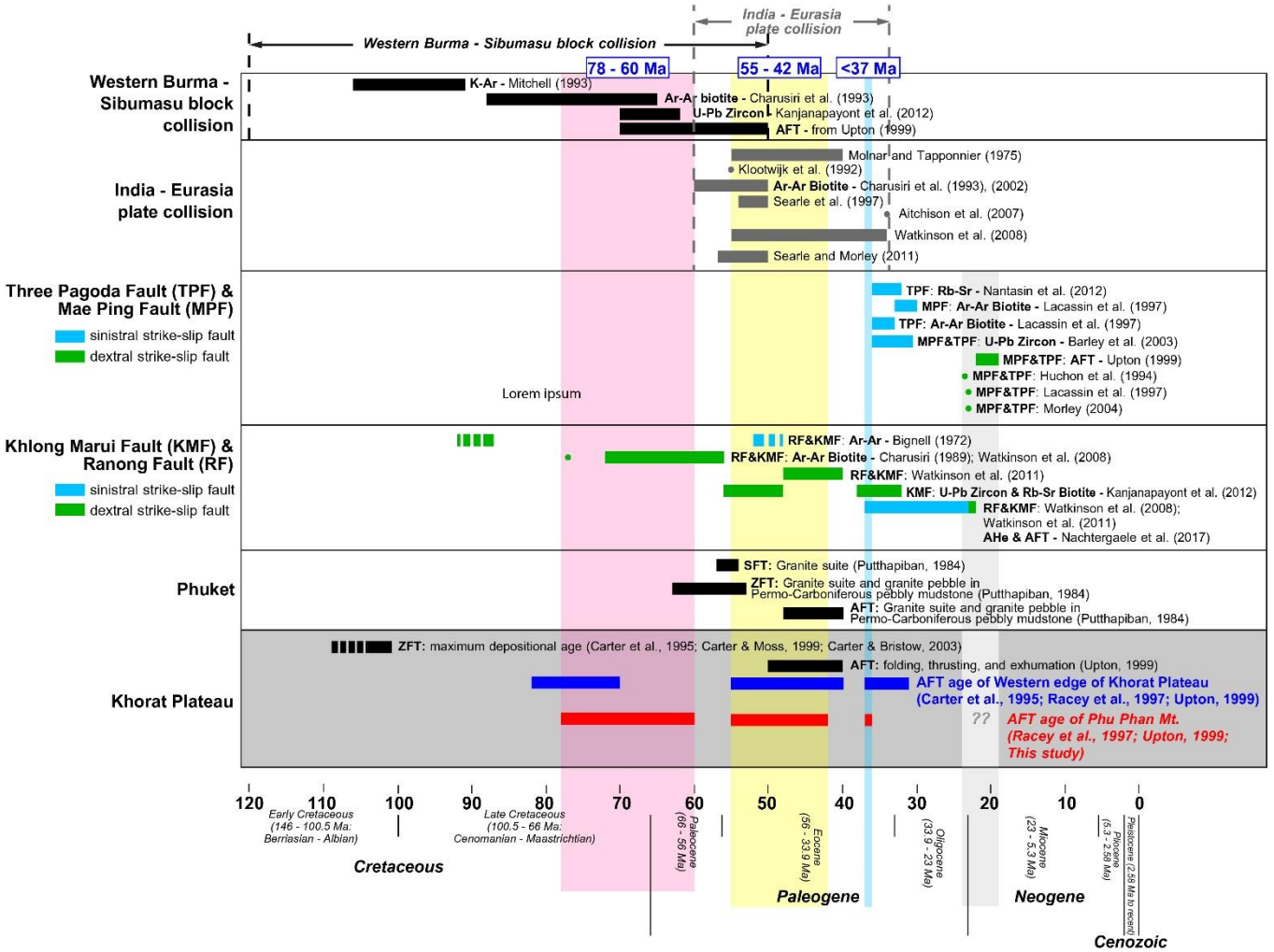

Figure 5.15 *Geological events in Thailand in comparison with the AFT ages ranges obtain from previous studies and this study in the Phu Phan Mountain Range during Late Cretaceous to Neogene.*

Khorat (-Ubon) basin along both sides of the anticlinal structures. It is also considered that such bulging feature may have caused the uplift at are of about 11.2 m/Ma.

The second group is the 55 – 45 Ma episode (or Eocene event) which is coeval with the timing of the India-Asia continental collision (Hu et al., 2016). This episode is subdivided into 2 successive events; the first event with the PPR and adjoining region and the second event is for outside region. The first event includes the regional and large-scale tectonic event involves initiation of the clockwise rotation of Indochina terrane and perhaps mild tectonic uplift within the Khorat Basin occurred at this stage (Figure 5.17C1). The entire Khorat region including the Phu Phan Range study area may have been gradually uplift at the rate of about 19.2 m/Ma. The second event is about 45 - 40 Ma which is equivalent to the continuing clockwise rotation of SE Asia (Indochina terrane). Continuing exhumation with the uplifting rate of 11.3 m/Ma occurred in the Khorat and neighbouring regions. Several fault movements occurred widespread in Thailand such as western edge of the Khorat Plateau, eastern peninsular Thailand. It is also inferred that the onset of rifting in northern and central Thailand as well as that of the Gulf of Thailand may have occurred and formed rift basin at this stage. In the PPR study area, continuing uplift with erosion and exposures of Phu Kradung Formation may have developed.

The third group is 37 – 31 Ma episode (Late Eocene to Early Oligocene event) which corresponds to continuing uplifting with some minor faultings of the Khorat Plateau (Figure 5.17D) and the major development of the N-S trending rift basins in the Gulf of Thailand and central to northern Thailand. Such basin formation requires the maximum stress in the east-west direction. Initiation of sinistral strike-slip movement of Three Pagoda Fault (Barley et al., 2003; Lacassin et al., 1997; Nantasin et al., 2012; Upton, 1999) and Mae Ping Fault (Barley et al., 2003; Lacassin et al., 1997; Morley et al., 2007; Upton, 1999) of the Sibumasu may have occurred at stage.

The last and final tectonic episode is 23 - 19 Ma episode (or early to middle Miocene event) which has not been affected the PPR and adjoining region. corresponding to the uplift disturbance exhumation in the Shan-Thai (Sibumasu block) and ongoing subsidence associated with inversion within Tertiary basin. Movements along the Three pagoda and Mae Ping Faults may have happened at this stage.

However, changing direction of fault movement may have formed. So, , the Three Pagoda fault and Mae Ping fault changed to Dextral strike-slip movement (Huchon et al., 1994; Lacassin et al., 1997; Morley et al., 2004; Upton, 1999) and initiation of an inversion of the Ranong and the Khlong Marui fault (Nachtergaele et al., 2017; Watkinson et al., 2011; Watkinson et al., 2008).

Several AFT age data are clear in the western peninsular Thailand (or Andaman sea side) as well as the western region of Thailand (high mountainous area) (Nachtergaele et al., 2017). It is considered that uplift or exhumation may have been more developed in Indochina prior to that of the Shan-Thai (or Sibumasu). This is the reason of both age data have not been reported from this episode in the PPR study area.

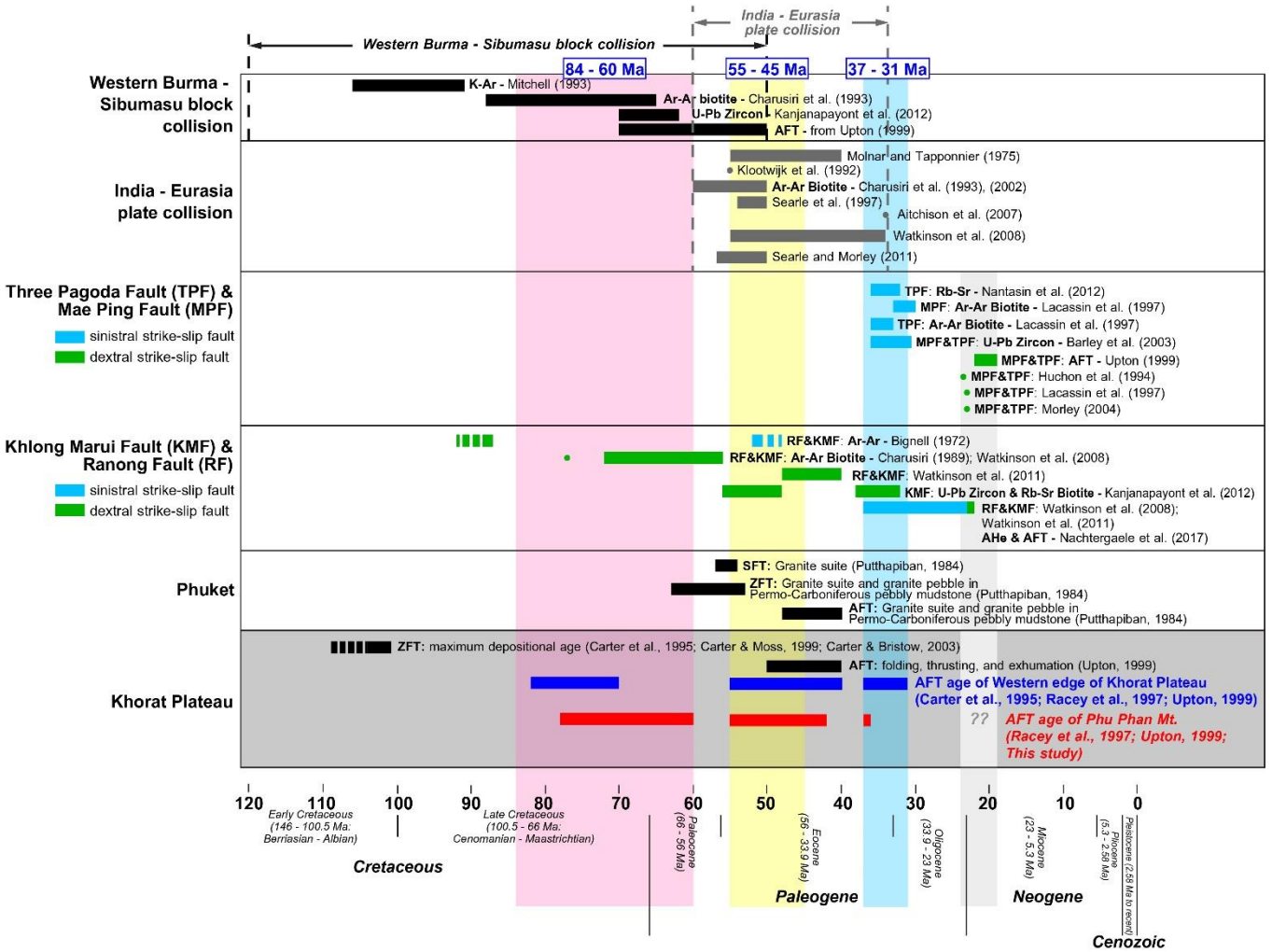

Figure 5.16 *Geological events in Thailand in comparison with the AFT ages ranges obtain from previous studies and this study in the whole Khorat Plateau during Late Cretaceous to Neogene.*

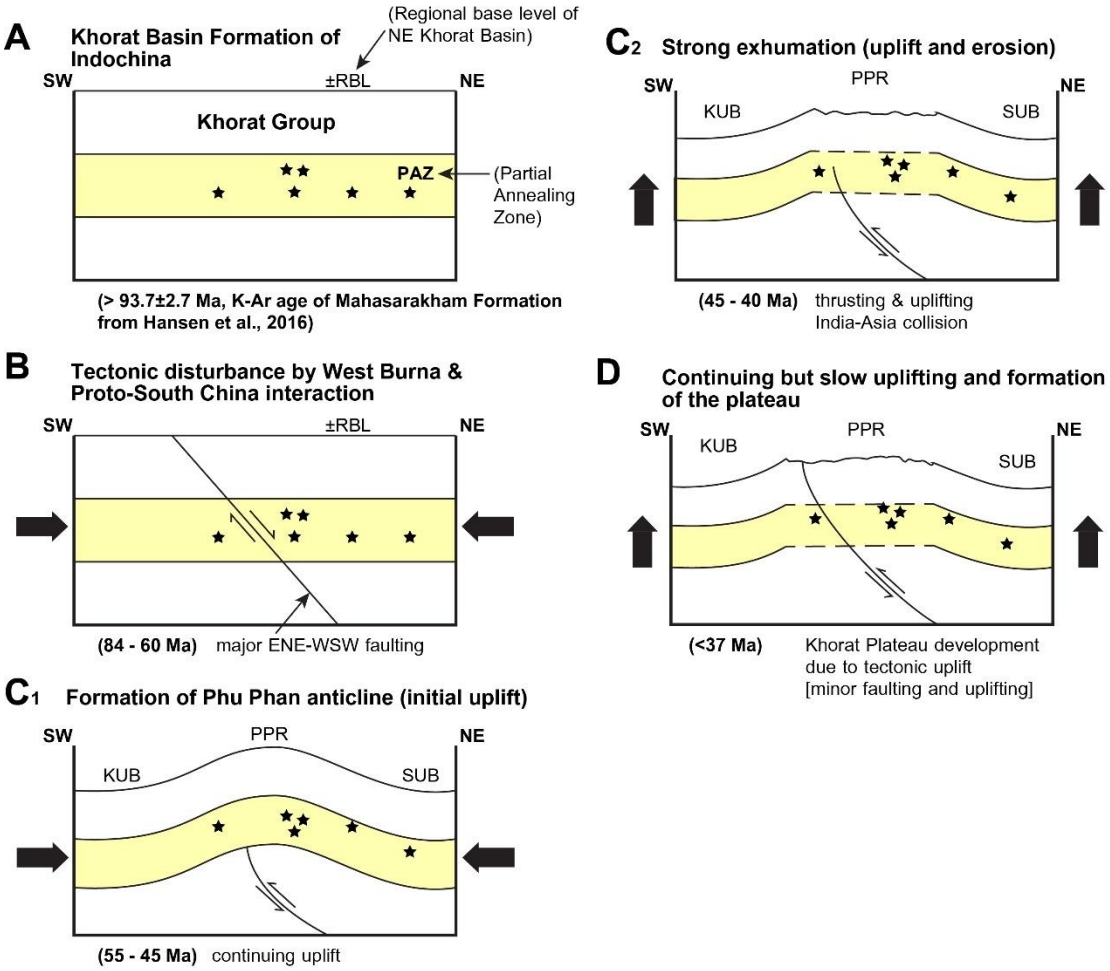

Figure 5.17 *Tectonic evolution of Phu Phan Range and its adjoining Khorat region.*

Chapter 6 Conclusion

Five formations of the Phu Phan Range (PPR) study area are remapped. Petrographic investigation of feldspathic litharenite and litharenite of the PPR sandstones reveals the recycled orogen for their provenance. Loei-Phetchabun Belt to the west and Trong Son Belt to the east have been inferred to represent the source region. Results of the apatite fission track analysis of the studied sandstones in the PPR study area and its adjoining area as well as these of the previous geochronological studies show 3 successive age ranges.

1. The first tectonic episode is that of 78 – 60 Ma (Campanion to Early Paleocene), corresponding to the essential lateral movement in response to the compressive stress within the Khorat region. Folding and faulting of Mesozoic rocks strata in the Khorat Basin, forming the Phu Phan Mountain Range, may have developed at this episode.
2. The second tectonic episode is during 55 – 42 Ma (Eocene), as indicated by foldings, thrustings. Exhumation (uplift and erosion) of the Khorat region including the PPR study area have developed in this episode and became a Khorat Plateau. This episode is regarded as the most essential tectonic episode of the PPR and nearby area.
3. The final tectonic episode is younger than 37 Ma (Oligocene) is marked by the minor movement along the strike-slip fault movement which slightly displaced the Phu Phan anticlinal structure in response to the clock-wise rotation (Charusiri et al., 2006; Maranate and Vella, 1986; McCabe et al., 1988; Richter and Fuller, 1996) of the Indochina block during 40-35 Ma (Late Eocene-Oligocene).

Based on the current AFT and previous geochronological work, tectonic uplift of Phu Phan Mountain Range has occurred since very Late Cretaceous/Early Paleogene times at an average rate of 0.0192 mm/yr. However, during Paleogene, the rate of uplift became lower, between 0.0112 mm/yr and 0.0113 mm/yr.

REFERENCES

Aitchison, J.C., Ali, J.R., and Davis, A.M. 2007. When and where did India and Asia collide? Journal of Geophysical Research: Solid Earth 112.

Bachmann, O., Oberli, F., Dungan, M., Meier, M., Mundil, R., and Fischer, H. 2007. 40 Ar/39 Ar and U–Pb dating of the Fish Canyon magmatic system, San Juan Volcanic field, Colorado: Evidence for an extended crystallization history. Chemical Geology 236: 134-166.

Barbarand, J., Carter, A., Wood, I., and Hurford, T. 2003a. Compositional and structural control of fission-track annealing in apatite. Chemical Geology 198: 107-137.

Barbarand, J., Hurford, T., and Carter, A. 2003b. Variation in apatite fission-track length measurement: implications for thermal history modelling. Chemical Geology 198: 77-106.

Barbarand, J., and Pagel, M. 2001. Importance of the chemistry to characterise apatite fission-track annealing. Comptes Rendus de l'Academie des Sciences. Serie 2a, Sciences de la Terre et des Planetes 259-265.

Barley, M., Pickard, A., Khin Zaw, Rak, P., and Doyle, M. 2003. Jurassic to Miocene magmatism and metamorphism in the Mogok metamorphic belt and the India-Eurasia collision in Myanmar. Tectonics 22.

Bergman, S., and Corrigan, J. 1996. Compositional variation of natural apatites subjected to fission track analysis. 8th Int. in Workshop Fission-Track Dating, Gent. pp.

Bhandari, N., Bhat, S., Lal, D., Rajagopalan, G., Tamhane, A., and Venkatavaradan, V. 1971. Fission fragment tracks in apatite: recordable track lengths. Earth and Planetary Science Letters 13: 191-199.

Bignell, J. 1972. The geochronology of the Malayan granites. PhD, University of Oxford.

Booth, J., and Sattayarak, N. 2011. Subsurface Carboniferous–Cretaceous geology of Northeast Thailand. In Ridd, M.F., Barber, A.J. and Crow, M.J. (ed.), The Geology of Thailand, pp. 185-222.

Brown, R., Gallagher, K., and Duane, M. 1994. A quantitative assessment of the effects of magmatism on the thermal history of the Karoo sedimentary sequence. Journal of African Earth Sciences 18: 227-243.

Carlson, W.D., Donelick, R.A., and Ketcham, R.A. 1999. Variability of apatite fission-track annealing kinetics: I. Experimental results. American mineralogist 84: 1213-1223.

Carter, A., and Bristow, C. 2003. Linking hinterland evolution and continental basin sedimentation by using detrital zircon thermochronology: a study of the Khorat Plateau Basin, eastern Thailand. Basin Research 15: 271-285.

Carter, A., Bristow, C.S., and Hurford, A.J. 1995. The application of fission track analysis to the dating of barren sequences: examples from red beds in Scotland and Thailand. Geological Society, London, Special Publications 89: 57-68.

Carter, A., and Moss, S.J. 1999. Combined detrital-zircon fission-track and U-Pb dating: A new approach to understanding hinterland evolution. Geology 27: 235-238.

Chairangsee, C., Hinze, C., Machareonsap, S., Nakornsri, N., Silpalit, M., and Ainpool-Anunt, S. 1990. Geological map of Thailand 1: 50,000: explanation for the sheets Amphoe Pak Chom. Ban Huai Khop, Ban Na Kho and King Amphoe Nam Som. Geologisches Jahrbuch Reihe B 73: 1-109.

Charusiri, P. 1989. Lithophite metallogenetic epochs of Thailand: A geological and geochronology investigation. PhD Thesis, Queen's University

Charusiri, P. 2002. Geotectonic evolution of Thailand: a new synthesis. J. Geol. Soc. Thai 1: 1-20.

Charusiri, P., Clark, A., Farrar, E., Archibald, D., and Charusiri, B. 1993. Granite belts in Thailand: evidence from the 40Ar/39Ar geochronological and geological syntheses. Journal of Southeast Asian Earth Sciences 8: 127-136.

Charusiri, P., Imsamut, S., Zhuang, Z., Ampaiwan, T., and Xu, X. 2006. Paleomagnetism of the earliest Cretaceous to early late Cretaceous sandstones, Khorat Group, Northeast Thailand: implications for tectonic plate movement of the Indochina block. Gondwana Research 9: 310-325.

Charusiri, P., Sangsomphong, A., Veeravinantanakul, A., and Kumrangwat, S. 2018. Geophysical, Geochronological, Paleontological and Remote-Sensing: Investigations

of the Khorat Plateau, Northeast Thailand. Trans.). In (Ed.),^(Eds.), (ed., Vol. pp.). Thailand: PTT Exploration and Production. (Reprinted from.

Chenrai, P. 2012. Paleocurrent Analysis of the Sao Khua Formation, Khorat Group, Nong Bua Lamphu region, NE Thailand. Arabian Journal for Science and Engineering 37: 115-120.

Chuaviroj, S. 1997. Deformations in Khorat plateau, Thailand. in Proceeding of the International Conference on Stratigraphy and Tectonic Evolution of Southeast Asia and the South Pacific, Bangkok, Thailand. pp. 321-325. 19-24 August 1997.

Crowley, K., Cameron, M., and Schaefer, R. 1991. Experimental studies of annealing of etched fission tracks in fluorapatite. Geochimica et Cosmochimica Acta 55: 1449-1465.

Department of Mineral Resources. 2000a. Geological map of Thailand 1:50,000 F5742 2 Sheet 5742 II Amphoe Somdet Trans.). In (Ed.),^(Eds.), (ed., Vol. pp.). Bangkok: Department of Mineral Resources, Thailand. (Reprinted from.

Department of Mineral Resources. 2000b. Geological map of Thailand 1:50,000 F5743 1 Sheet 5743 I Phanna Nikhom Trans.). In (Ed.),^(Eds.), (ed., Vol. pp.). Bangkok: Department of Mineral Resources, Thailand. (Reprinted from.

Department of Mineral Resources. 2000c. Geological map of Thailand 1:50,000 F5743 2 Sheet 5743 II Amphoe Kut Bak Trans.). In (Ed.),^(Eds.), (ed., Vol. pp.). Bangkok: Department of Mineral Resources, Thailand. (Reprinted from.

Department of Mineral Resources. 2000d. Geological map of Thailand 1:50,000 F5743 3 Sheet 5743 III King Amphoe Nikhom Nam Un Trans.). In (Ed.),^(Eds.), (ed., Vol. pp.). Bangkok: Department of Mineral Resources, Thailand. (Reprinted from.

Department of Mineral Resources. 2000e. Geological map of Thailand 1:50,000 F5841 1 Sheet 5841 I Ban Hong Saeng Trans.). In (Ed.),^(Eds.), (ed., Vol. pp.). Bangkok: Department of Mineral Resources, Thailand. (Reprinted from.

Department of Mineral Resources. 2000f. Geological map of Thailand 1:50,000 F5841 4 Sheet 5841 IV Amphoe Nong Phok Trans.). In (Ed.),^(Eds.), (ed., Vol. pp.). Bangkok: Department of Mineral Resources, Thailand. (Reprinted from.

Department of Mineral Resources. 2000g. Geological map of Thailand 1:50,000 F5842 1 Sheet 5842 I Phu Phan Trans.). In (Ed.),^(Eds.), (ed., Vol. pp.). Bangkok: Department of Mineral Resources, Thailand. (Reprinted from.

Department of Mineral Resources. 2000h. Geological map of Thailand 1:50,000 F5842 2 Sheet 5842 II Amphoe Khamcha-I Trans.). In (Ed.),^(Eds.), (ed., Vol. pp.). Bangkok: Department of Mineral Resources, Thailand. (Reprinted from.

Department of Mineral Resources. 2000i. Geological map of Thailand 1:50,000 F5842 3 Sheet 5842 III Amphoe Kuchinarai Trans.). In (Ed.),^(Eds.), (ed., Vol. pp.). Bangkok: Department of Mineral Resources, Thailand. (Reprinted from.

Department of Mineral Resources. 2000j. Geological map of Thailand 1:50,000 F5842 4 Sheet 5842 IV Amphoe Tao Ngoi Trans.). In (Ed.),^(Eds.), (ed., Vol. pp.). Bangkok: Department of Mineral Resources, Thailand. (Reprinted from.

Department of Mineral Resources. 2000k. Geological map of Thailand 1:50,000 F5941 2 Sheet 5941 II Ban Kham Duai Trans.). In (Ed.),^(Eds.), (ed., Vol. pp.). Bangkok: Department of Mineral Resources, Thailand. (Reprinted from.

Department of Mineral Resources. 2000l. Geological map of Thailand 1:50,000 F5941 3 Sheet 5941 III Amphoe Loeng Nok Tha Trans.). In (Ed.),^(Eds.), (ed., Vol. pp.). Bangkok: Department of Mineral Resources, Thailand. (Reprinted from.

Department of Mineral Resources. 2000 Geological map of Thailand 1:50,000 F5841 2 Sheet 5841 II Amphoe Kut Chum Trans.). In (Ed.),^(Eds.), (ed., Vol. pp.). Bangkok: Department of Mineral Resources, Thailand. (Reprinted from.

Department of Mineral Resources. 2001a. Geological map of Thailand 1:50,000 F5742 1 Sheet 5742 I King Amphoe Phu Phan Trans.). In (Ed.),^(Eds.), (ed., Vol. pp.). Bangkok: Department of Mineral Resources, Thailand. (Reprinted from.

Department of Mineral Resources. 2001b. Geological map of Thailand 1:50,000 F5742 3 Sheet 5742 III Amphoe Sahat Sakhan Trans.). In (Ed.),^(Eds.), (ed., Vol. pp.). Bangkok: Department of Mineral Resources, Thailand. (Reprinted from.

Department of Mineral Resources. 2001c. Geological map of Thailand 1:50,000 F5742 4 Sheet 5742 IV Amphoe Khum Muang Trans.). In (Ed.),^(Eds.), (ed., Vol. pp.). Bangkok: Department of Mineral Resources, Thailand. (Reprinted from.

Department of Mineral Resources. 2007. Geological Map of Thailand 1:250,000 Trans.). In (Ed.),^(Eds.), (ed., Vol. pp.). Bangkok: Department of Mineral Resources, Thailand. (Reprinted from.

Department of Mineral Resources. 2008a. Geological map of Thailand 1:50,000 F5841 3 Sheet 5841 III Ban Nong Fa Trans.). In (Ed.),^(Eds.), (ed., Vol. pp.). Bangkok: Department of Mineral Resources, Thailand. (Reprinted from.

Department of Mineral Resources. 2008b. Geological map of Thailand 1:50,000 F5843 1 Sheet 5843 I Amphoe Kusuman Trans.). In (Ed.),^(Eds.), (ed., Vol. pp.). Bangkok: Department of Mineral Resources, Thailand. (Reprinted from.

Department of Mineral Resources. 2008c. Geological map of Thailand 1:50,000 F5940 1 Sheet 5940 I Amphoe Patum Rachawongsa Trans.). In (Ed.),^(Eds.), (ed., Vol. pp.). Bangkok: Department of Mineral Resources, Thailand. (Reprinted from.

Department of Mineral Resources. 2008d. Geological map of Thailand 1:50,000 F5940 4 Sheet 5940 IV Amphoe Mueang Ammnat Charoen Trans.). In (Ed.),^(Eds.), (ed., Vol. pp.). Bangkok: Department of Mineral Resources, Thailand. (Reprinted from.

Department of Mineral Resources. 2008e. Geological map of Thailand 1:50,000 F5941 1, 6041 4 Sheet 5941 I, 6041 IV Amphoe Don Tan and East of Amphoe Don Tan Trans.). In (Ed.),^(Eds.), (ed., Vol. pp.). Bangkok: Department of Mineral Resources, Thailand. (Reprinted from.

Department of Mineral Resources. 2008f. Geological map of Thailand 1:50,000 F5941 4 Sheet 5941 IV Amphoe Nikham Kham Soi Trans.). In (Ed.),^(Eds.), (ed., Vol. pp.). Bangkok: Department of Mineral Resources, Thailand. (Reprinted from.

Department of Mineral Resources. 2008g. Geological map of Thailand 1:50,000 F5942 3,2 Sheet 5942 III, II Changwat Mukdahan and Ban Chanod Trans.). In (Ed.),^(Eds.), (ed., Vol. pp.). Bangkok: Department of Mineral Resources, Thailand. (Reprinted from.

Department of Mineral Resources. 2008h. Geological map of Thailand 1:50,000 F6040 1 Sheet 6040 I Amphoe Pho Sai Trans.). In (Ed.),^(Eds.), (ed., Vol. pp.). Bangkok: Department of Mineral Resources, Thailand. (Reprinted from.

Department of Mineral Resources. 2008i. Geological map of Thailand 1:50,000 F6040 2 Sheet 6040 II Ban Fa Huan Trans.). In (Ed.),^(Eds.), (ed., Vol. pp.). Bangkok: Department of Mineral Resources, Thailand. (Reprinted from.

Department of Mineral Resources. 2008j. Geological map of Thailand 1:50,000 F6040 3 Sheet 6040 III Amphoe Trakan Phuetphon Trans.). In (Ed.),^(Eds.), (ed., Vol. pp.). Bangkok: Department of Mineral Resources, Thailand. (Reprinted from.

Department of Mineral Resources. 2008k. Geological map of Thailand 1:50,000 F6040 4 Sheet 6040 IV Amphoe Kud Khao Pun Trans.). In (Ed.),^(Eds.), (ed., Vol. pp.). Bangkok: Department of Mineral Resources, Thailand. (Reprinted from.

Department of Mineral Resources. 2008l. Geological map of Thailand 1:50,000 F6041 2 Sheet 6041 II Ban Na Waeng Trans.). In (Ed.),^(Eds.), (ed., Vol. pp.). Bangkok: Department of Mineral Resources, Thailand. (Reprinted from.

Department of Mineral Resources. 2008m. Geological map of Thailand 1:50,000 F6041 3 Sheet 6041 III Amphoe Khemarat Trans.). In (Ed.),^(Eds.), (1 ed., Vol. pp.). Bangkok: Department of Mineral Resources, Thailand. (Reprinted from.

Department of Mineral Resources. 2008n. Geological map of Thailand 1:50,000 F6140 3,4 Sheet 6140 III,IV Ban Na Pho Klang-Ban Pha Chan Trans.). In (Ed.),^(Eds.), (ed., Vol. pp.). Bangkok: Department of Mineral Resources, Thailand. (Reprinted from.

Department of Mineral Resources. 2014. Geology of Thailand. Bangkok, Thailand: Department of Mineral Resources, Ministry of Natural Resources and Environment.

Dickinson, W.R. 1985. Interpreting provenance relations from detrital modes of sandstones. In Provenance of arenites, pp. 333-361. Springer.

Doepke, D. 2017. Modelling the thermal history of onshore Ireland, Britain and its offshore basins using low-temperature thermochronology. Ph.D. Thesis, Trinity College Dublin.

Donelick, R.A. 1991. Crystallographic orientation dependence of mean etchable fission track length in apatite: An empirical model and experimental observations. American Mineralogist;(United States) 76.

Donelick, R.A. 1993. Method of fission track analysis utilizing bulk chemical etching of apatite Trans.). In (Ed.),^(Eds.), (ed., Vol. pp.). Google Patents. (Reprinted from.

Donelick, R.A., and Miller, D.S. 1991. Enhanced TINT fission track densities in low spontaneous track density apatites using 252Cf-derived fission fragment tracks: A model and experimental observations. International Journal of Radiation

Applications and Instrumentation. Part D. Nuclear Tracks and Radiation Measurements 18: 301-307.

Donelick, R.A., O'Sullivan, P.B., and Ketcham, R.A. 2005. Apatite fission-track analysis. Reviews in Mineralogy and Geochemistry 58: 49-94.

Fleischer, R.L., and Price, P.B. 1964. Techniques for geological dating of minerals by chemical etching of fission fragment tracks. Geochimica et Cosmochimica Acta 28: 1705-1714.

Fleischer, R.L., Price, P.B., Walker, R.M., and Walker, R.M. 1975. Nuclear Tracks in Solids: Principles and Applications. Univ of California Press.

Friedlander, G., Kennedy, J.W., and Macias, E.S. 1981. Nuclear and Radiochemistry. John Wiley & Sons.

Galbraith, R. 1981. On statistical models for fission track counts. Journal of the International Association for Mathematical Geology 13: 471-478.

Galbraith, R., and Laslett, G. 1993. Statistical models for mixed fission track ages. Nuclear Tracks and Radiation Measurements 21: 459-470.

Galbraith, R.F. 2005. Statistics for fission track analysis. CRC Press.

Gallagher, K. 2012. Transdimensional inverse thermal history modeling for quantitative thermochronology. Journal of Geophysical Research: Solid Earth 117.

Gallagher, K., Brown, R., and Johnson, C. 1998. Fission track analysis and its applications to geological problems. Annual Review of Earth and Planetary Sciences 26: 519-572.

Gardner, L.S., Haworth, H.F., and Chiangmai, P.N. 1967. Salt Resources of Thailand. Department of Mineral Resources.

Gleadow, A., and Duddy, I. 1981. A natural long-term track annealing experiment for apatite. Nuclear Tracks 5: 169-174.

Gleadow, A., Duddy, I., Green, P.F., and Lovering, J. 1986. Confined fission track lengths in apatite: a diagnostic tool for thermal history analysis. Contributions to Mineralogy and Petrology 94: 405-415.

Gleadow, A.J. 1981. Fission-track dating methods: what are the real alternatives? Nuclear Tracks 5: 3-14.

Gleadow, A.J., Belton, D.X., Kohn, B.P., and Brown, R.W. 2002. Fission track dating of phosphate minerals and the thermochronology of apatite. Reviews in Mineralogy and Geochemistry 48: 579-630.

Glorie, S., Alexandrov, I., Nixon, A., Jepson, G., Gillespie, J., and Jahn, B.-M. 2017. Thermal and exhumation history of Sakhalin Island (Russia) constrained by apatite U-Pb and fission track thermochronology. Journal of Asian Earth Sciences 143: 326-342.

Green, P. 1981. A new look at statistics in fission-track dating. Nuclear Tracks 5: 77-86.

Green, P. 1985. Comparison of zeta calibration baselines for fission-track dating of apatite, zircon and sphene. Chemical Geology: Isotope Geoscience Section 58: 1-22.

Green, P. 1988. The relationship between track shortening and fission track age reduction in apatite: combined influences of inherent instability, annealing anisotropy, length bias and system calibration. Earth and Planetary Science Letters 89: 335-352.

Green, P., Duddy, I., Gleadow, A., Tingate, P., and Laslett, G. 1986. Thermal annealing of fission tracks in apatite: 1. A qualitative description. Chemical Geology: Isotope Geoscience Section 59: 237-253.

Green, P., and Hurford, A. 1984. Thermal neutron dosimetry for fission track dating. Nuclear Tracks and Radiation Measurements (1982) 9: 231-241.

Hall, R., van Hattum, M.W., and Spakman, W. 2008. Impact of India–Asia collision on SE Asia: the record in Borneo. Tectonophysics 451: 366-389.

Hanna, G., Westcott, C., Lemmel, H., Leonard Jr, B., Story, J., and Attree, P. 1969. Revision of values for the 2200 m/s neutron constants for four fissile nuclides Trans.). In (Ed.),^(Eds.), (ed., Vol. pp.). International Atomic Energy Agency. (Reprinted from.

Hansen, B.T., Wemmer, K., Eckhardt, M., Putthapiban, P., and Assavapatchara, S. 2016. Isotope Dating of the Potash and Rock Salt Deposit at Bamnet Narong, NE-Thailand. Open Journal of Geology 6: 875-894.

Hasebe, N., Barbarand, J., Jarvis, K., Carter, A., and Hurford, A.J. 2004. Apatite fission-track chronometry using laser ablation ICP-MS. Chemical Geology 207: 135-145.

Hasebe, N., Tamura, A., and Arai, S. 2013. Zeta equivalent fission - track dating using LA - ICP - MS and examples with simultaneous U—Pb dating. Island Arc 22: 280-291.

Hite, R.J., and Japakasetr, T. 1979. Potash deposits of the Khorat plateau, Thailand and Laos. Economic Geology 74: 448-458.

Horiuchi, Y., Charusiri, P., and Hisada, K.-i. 2012. Identification of an anastomosing river system in the Early Cretaceous Khorat Basin, northeastern Thailand, using stratigraphy and paleosols. Journal of Asian Earth Sciences 61: 62-77.

Hu, X., Garzanti, E., Wang, J., Huang, W., An, W., and Webb, A. 2016. The timing of India-Asia collision onset–Facts, theories, controversies. Earth-Science Reviews 160: 264-299.

Huchon, P., Pichon, X.L., and Rangin, C. 1994. Indochina Peninsula and the collision of India and Eurasia. Geology 22: 27-30.

Hurford, A.J., and Green, P.F. 1982. A users' guide to fission track dating calibration. Earth and Planetary Science Letters 59: 343-354.

Hutchison, C.S. 1989. Geological Evolution of South-east Asia. Clarendon Press Oxford.

Ishida, Y., Morishita, T., Arai, S., and Shirasaka, M. 2004. Simultaneous in-situ multi-element analysis of minerals on thin section using LA-ICP-MS. Science Reports of Kanazawa University 48: 31-42.

Jaffey, A., Flynn, K., Glendenin, L., Bentley, W.t., and Essling, A. 1971. Precision measurement of half-lives and specific activities of U 235 and U 238. Physical Review C 4: 1889.

Kanjanapayont, P., Klötzli, U., Thöni, M., Grasemann, B., and Edwards, M.A. 2012. Rb–Sr, Sm–Nd, and U–Pb geochronology of the rocks within the Khlong Marui shear zone, southern Thailand. Journal of Asian Earth Sciences 56: 263-275.

Ketcham, R.A. 2005. The role of crystallographic angle in characterizing and modeling apatite fission-track length data. Radiation Measurements 39: 595-601.

Ketcham, R.A., Carter, A., Donelick, R.A., Barbarand, J., and Hurford, A.J. 2007a. Improved measurement of fission-track annealing in apatite using c-axis projection. American Mineralogist 92: 789-798.

Ketcham, R.A., Carter, A., Donelick, R.A., Barbarand, J., and Hurford, A.J. 2007b. Improved modeling of fission-track annealing in apatite. American Mineralogist 92: 799-810.

Ketcham, R.A., Donelick, R.A., and Carlson, W.D. 1999. Variability of apatite fission-track annealing kinetics: III. Extrapolation to geological time scales. American Mineralogist 84: 1235-1255.

Khin Zaw, et al. 2014. Tectonics and metallogeny of mainland Southeast Asia—a review and contribution. Gondwana Research 26: 5-30.

Klootwijk, C.T., Gee, J.S., Peirce, J.W., and Smith, G.M. 1992. Neogene evolution of the Himalayan-Tibetan region: constraints from ODP Site 758, northern Ninetyeast Ridge; bearing on climatic change. Palaeogeography, Palaeoclimatology, Palaeoecology 95: 95-110.

Kozar, M., Crandall, G., and Hall, S. 1992. Integrated structural and stratigraphic study of the Khorat Basin, Rat Buri limestone (Permian), Thailand. in National Conf. on Geol. Resources of Thailand: Potential for Future Development, Bangkok. pp. 692-736.

Lacassin, R., et al. 1997. Tertiary diachronic extrusion and deformation of western Indochina: structural and 40Ar/39Ar evidence from NW Thailand. Journal of Geophysical Research: Solid Earth 102: 10013-10037.

Lanphere, M.A., and Baadsgaard, H. 2001. Precise K–Ar, 40Ar/39Ar, Rb–Sr and U/Pb mineral ages from the 27.5 Ma Fish Canyon Tuff reference standard. Chemical Geology 175: 653-671.

Laslett, G., Gleadow, A., and Duddy, I. 1984. The relationship between fission track length and track density in apatite. Nuclear Tracks and Radiation Measurements (1982) 9: 29-38.

Laslett, G., Green, P.F., Duddy, I., and Gleadow, A. 1987. Thermal annealing of fission tracks in apatite 2. A quantitative analysis. Chemical Geology: Isotope Geoscience Section 65: 1-13.

Lederer, C.M., Hollander, J.M., and Perlman, I. 1967. Table of isotopes.

Maranate, S., and Vella, P. 1986. Paleomagnetism of the Khorat Group, Mesozoic, Northeast Thailand. Journal of Southeast Asian Earth Sciences 1: 23-31.

McCabe, R., et al. 1988. Extension tectonics: the Neogene opening of the North–South trending basins of central Thailand. Journal of Geophysical Research: Solid Earth 93: 11899-11910.

Mitchell, A. 1993. Cretaceous–Cenozoic tectonic events in the western Myanmar (Burma)–Assam region. Journal of the Geological Society 150: 1089-1102.

Molnar, P., and Tapponnier, P. 1975. Cenozoic tectonics of Asia: effects of a continental collision. science 189: 419-426.

Morishita, T., Ishida, Y., Arai, S., and Shirasaka, M. 2005. Determination of Multiple Trace Element Compositions in Thin (> 30 μ m) Layers of NIST SRM 614 and 616 Using Laser Ablation - Inductively Coupled Plasma - Mass Spectrometry (LA - ICP - MS). Geostandards and Geoanalytical Research 29: 107-122.

Morley, C., Haranya, C., Phoosongsee, W., Pongwapee, S., Kornsawan, A., and Wonganan, N. 2004. Activation of rift oblique and rift parallel pre-existing fabrics during extension and their effect on deformation style: examples from the rifts of Thailand. Journal of Structural Geology 26: 1803-1829.

Morley, C., Smith, M., Carter, A., Charusiri, P., and Chantraprasert, S. 2007. Evolution of deformation styles at a major restraining bend, constraints from cooling histories, Mae Ping fault zone, western Thailand. Geological Society, London, Special Publications 290: 325-349.

Nachtergaele, S.M., Glorie, S., Charusiri, P., Kanjanapayont, P., and De Grave, J. 2017. Cenozoic exhumation of Thailand: constraints from apatite fission track and apatite (U-Th)/He thermochronology. in 16 Puzzlingout Gondwana. pp. 6. 7 – 21 November 2017. Bangkok, Thailand. (abstract).

Naeser, C. 1967. The use of apatite and sphene for fission track age determinations. Geological Society of America Bulletin 78: 1523-1526.

Nantasin, P., Hauzenberger, C., Liu, X., Krenn, K., Dong, Y., and Thöni, M. 2012. Exhumation of the Thabsila metamorphic complex in the Three Pagodas shear zone, Kanchanaburi Province, western Thailand: Geothermobarometry and Geochronology. in EGU General Assembly Conference Abstracts. pp. 13988.

O'Sullivan, P.B., and Parrish, R.R. 1995. The importance of apatite composition and single-grain ages when interpreting fission track data from plutonic rocks: a case study from the Coast Ranges, British Columbia. Earth and Planetary Science Letters 132: 213-224.

Paul, T.A., and Fitzgerald, P.G. 1992. Transmission electron microscopic investigation of fission tracks in fluorapatite. American Mineralogist 77.

Pettijohn, F.J. 1975. Sedimentary Rocks. 2nd Edition. New York: Harper and Row Publishers.

Putthapiban, P. 1984. Geochemistry, Geochronology and Tin Mineralization of Phuket Granites, Phuket, Thailand. Ph.D. Thesis, Department of Geology, La Trobe University.

Racey, A. 2009. Mesozoic red bed sequences from SE Asia and the significance of the Khorat Group of NE Thailand. Geological Society, London, Special Publications 315: 41-67.

Racey, A., Duddy, L., and Love, M. 1997. Apatite fission track analysis of Mesozoic red beds. in The International Conference on Stratigraphy and Tectonic Evolution of Southeast Asia and the South Pacific. pp. 200-209. Bangkok, Thailand.

Ravenhurst, C., Roden, M., Willett, S., and Miller, D. 1992. Dependence of fission track annealing on apatite crystal chemistry. in Proceeding of the 7th International Workshop Fission-Track Thermochronology, Philadelphia. pp.

Richter, B., and Fuller, M. 1996. Palaeomagnetism of the Sibumasu and Indochina blocks: Implications for the extrusion tectonic model. Geological Society, London, Special Publications 106: 203-224.

Roberts, J., Gold, R., and Armani, R.J. 1968. Spontaneous-fission decay constant of U 238. Physical Review 174: 1482.

Searle, M., Corfield, R.I., Stephenson, B., and McCarron, J. 1997. Structure of the North Indian continental margin in the Ladakh–Zanskar Himalayas: implications for the timing of obduction of the Spontang ophiolite, India–Asia collision and deformation events in the Himalaya. Geological Magazine 134: 297-316.

Searle, M.P., and Morley, C.K. 2011. Tectonic and thermal evolution of Thailand in the regional context of SE Asia. In Ridd, M.F., Barber, A.J. and Crow, M.J. (ed.), The Geology of Thailand, pp. 539-571.

Smith, P.L., and Stokes, R. 1997. Geology and petroleum potential of the Khorat Plateau Basin in the Vientiane area of Lao PDR. Journal of Petroleum Geology 20: 27-49.

Spadavecchia, A., and Hahn, B. 1967. Die Rotation-skammer und einige Anwendungen. Helvetica Physica Acta 40: 1063-1079.

Spiegel, C., Kohn, B., Raza, A., Rainer, T., and Gleadow, A. 2007. The effect of long-term low-temperature exposure on apatite fission track stability: A natural annealing experiment in the deep ocean. Geochimica et Cosmochimica Acta 71: 4512-4537.

Steiger, R.H., and Jäger, E. 1977. Subcommission on geochronology: convention on the use of decay constants in geo-and cosmochronology. Earth and Planetary Science Letters 36: 359-362.

Sun, W. 2016. Initiation and evolution of the South China Sea: an overview. Acta Geochimica 35: 215-225.

Tagami, T., Lal, N., Sorkhabi, B.R., Ito, H., and Nishimura, S. 1988. Fission Track Dating Using External Detector Method: a Laboratory Procedure. Memoirs of the Faculty of Science Kyoto University 53: 14–30.

Upton, D.R. 1999. A regional fission track study of Thailand: implications for thermal history and denudation. Unpublished, Ph.D. Thesis, Birkbeck (University of London).

Vermeesch, P. 2017. Statistics for LA-ICP-MS based fission track dating. Chemical Geology 456: 19-27.

Vermeesch, P. 2018. IsoplotR: a free and open toolbox for geochronology. Geoscience Frontiers (in press).

Wagner, A.G., and Van den Haute, P. 1992. Fission-Track Dating. Dordrecht: Kluwer Academic Publishers.

Wagner, G. 1968. Fission track dating of apatites. Earth and Planetary Science Letters 4: 411-415.

Wagner, G. 1979. Correction and interpretation of fission track ages. In Lectures in Isotope Geology, pp. 170-177. Springer.

Warren, J. 1999. Evaporites: their Evolution and Economics. Wiley-Blackwell.

Watkinson, I., Elders, C., Batt, G., Jourdan, F., Hall, R., and McNaughton, N.J. 2011. The timing of strike ‐ slip shear along the Ranong and Khlong Marui faults, Thailand. Journal of Geophysical Research: Solid Earth 116.

Watkinson, I., Elders, C., and Hall, R. 2008. The kinematic history of the Khlong Marui and Ranong Faults, southern Thailand. Journal of Structural Geology 30: 1554-1571.

Workman, D. 1975. Tectonic evolution of Indochina. Journal of Geological Society of Thailand 1: 3-19.

Yates, F. 1934. Contingency tables involving small numbers and the χ 2 test. Supplement to the Journal of the Royal Statistical Society 1: 217-235.

Young, E., Myers, A., Munson, E.L., and Conklin, N.M. 1969. Mineralogy and geochemistry of fluorapatite from Cerro de Mercado, Durango, Mexico. US Geological Survey Professional Paper 650: 84-93.

APPENDICES

APPENDIX A: Field investigation and sample description

Sample no: PP01

Location: Highway 2219 km 41+700 (Lat: 16°48'18"N Long: 103°57'53"E)

Rock name: Feldspathic litharenite

Type of outcrop: Natural **Outcrop size:** 3x100 m

Rock units: Phu Kradung Formation (Khorat Group)

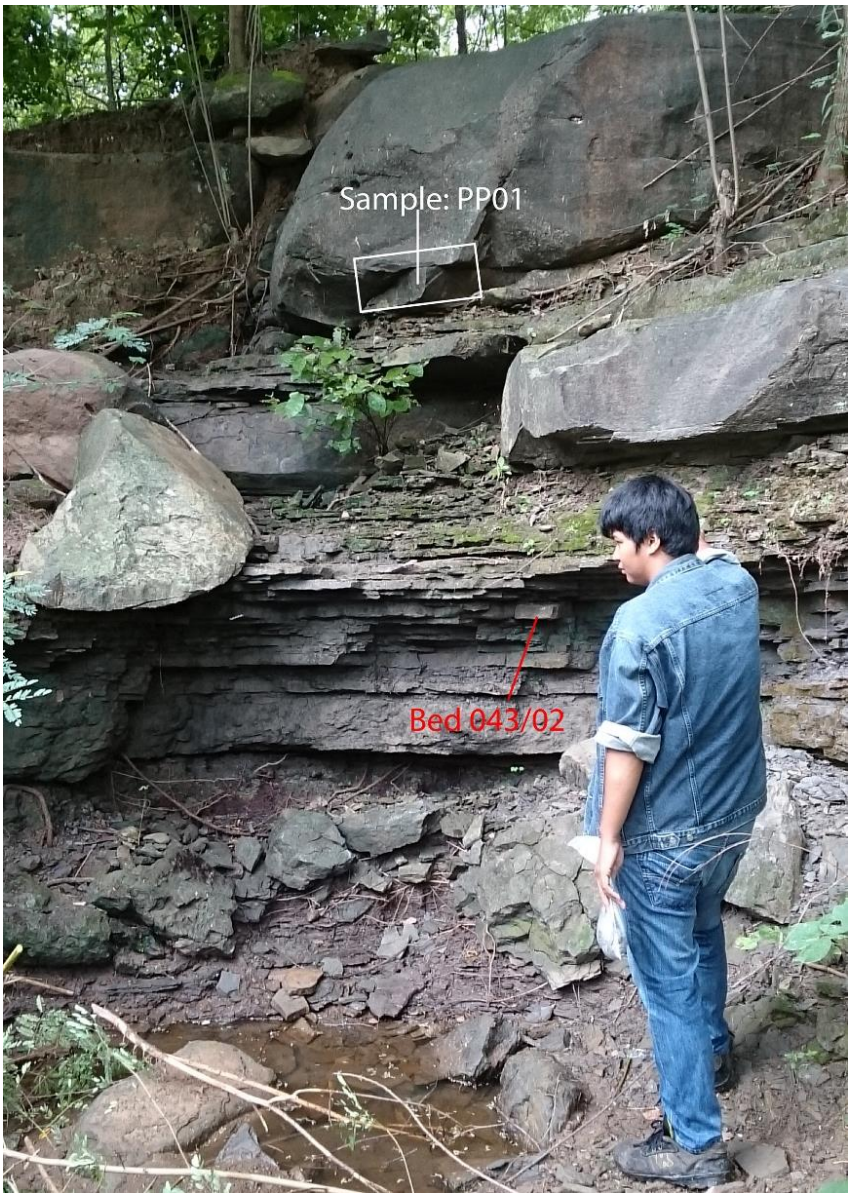

Figure 1 *Natural outcrop of sandstone of the Phu Kradung Formation along the highway 2219 km 41+700, Na Khu District, Kalasin Province (Mr. Sitichok Kumrangwat, 180 cm tall, is to scale). White rectangle is sampling site.*

Macroscopic description

The greenish gray rock sample is very fine-grained sandstone and shows a clastic texture. It is a reddish-brown weathering surfaces. The grains are made up mostly of quartz (colorless), feldspar (white), and less opaque minerals and lithic fragments.

Figure 2 *Greenish-gray very fine-grained sandstone of the Phu Kradung Formation sample no. PP01.*

Microscopic description

The weathered rock sample shows a clastic texture. The rock compositions are composed of largely of quartz (including monocrystalline quartz and polycrystalline quartz) (69 modal %), with small amount of feldspar (15 modal %) and lithic fragment (16 modal %). The rock sample are also included of muscovite, biotite, apatite and zircon. The size of mineral is up to 0.1 to 0.2 mm with well sorted. The grains show a high sphericity and subangular shape. The cement of the rock is siliceous.

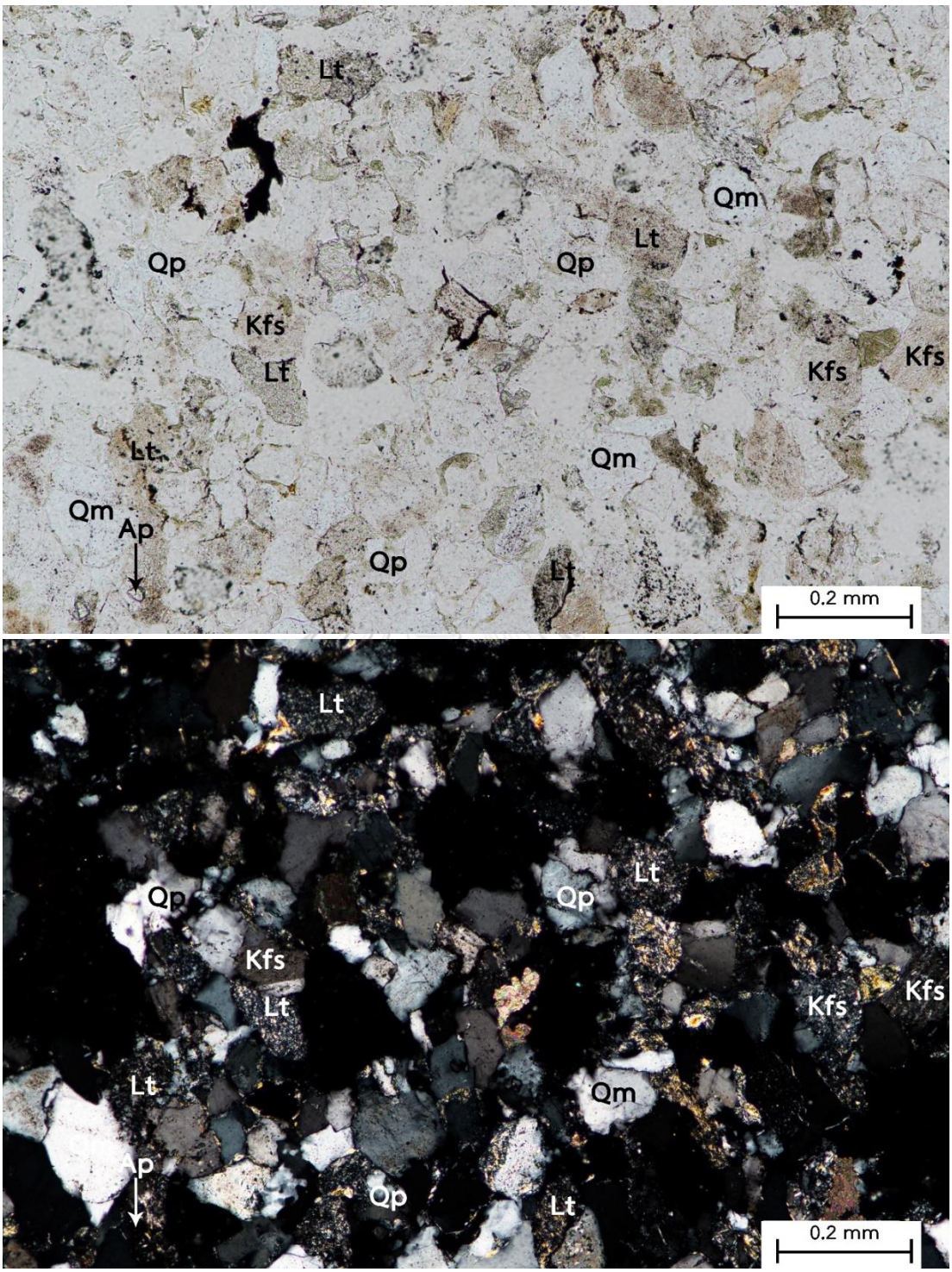

Figure 3 *Photomicrographs of Feldspathic litharenite (sample PP02) from the Phu Phan Formation at Phu Phan Mountain Range showing well defined clastic texture and grains of quartz, alkaline feldspar, lithic fragments, and apatite. (top) Ordinary light (bottom) Cross polar. (Qm = monocrystalline quartz, Qp = polycrystalline quartz, Kfs = alkaline feldspar, Lt = lithic fragment, and Ap = apatite)*

Sample no: PP02

Location: The entrance of Kham Toei Waterfall
(Lat: 16°48'48"N Long: 103°57'37"E)

Rock name: Litharenite

Type of outcrop: Road-cut **Outcrop size:** 3x200 m

Rock units: Phra Wihan Formation (Khorat Group)

Figure 4 *Natural outcrop of sandstone of the Phra Wihan Formation in front of the entrance of Kham Toei Waterfall, Na Khu District, Kalasin Province (Ms. Chonnipha Fakseangsa, 150 cm-tall, is to scale). White rectangle is the sampling site.*

Macroscopic description

The whitish grey rock sample is medium-grained sandstone and shows a clastic texture. It is a reddish-brown weathering surfaces. The grains are made up mostly of quartz (colorless), feldspar (white), and less opaque minerals and lithic fragments.

Figure 5 *Whitish grey, medium-grained sandstone with well lamination of the Phra Wihan Formation (sample no. PP02).*

Microscopic description

The weathered rock sample shows a clastic texture. The rock compositions are composed of largely of quartz (including monocrystalline quartz and polycrystalline quartz) (70 modal %), with small amount of feldspar (2 modal %) and lithic fragment (28 modal %). The rock sample are also included of muscovite, biotite, chlorite and zircon. The size of mineral is up to 0.2 to 0.4 mm with well sorted. The grains show a low sphericity and angular shape. The cement of the rock is siliceous.

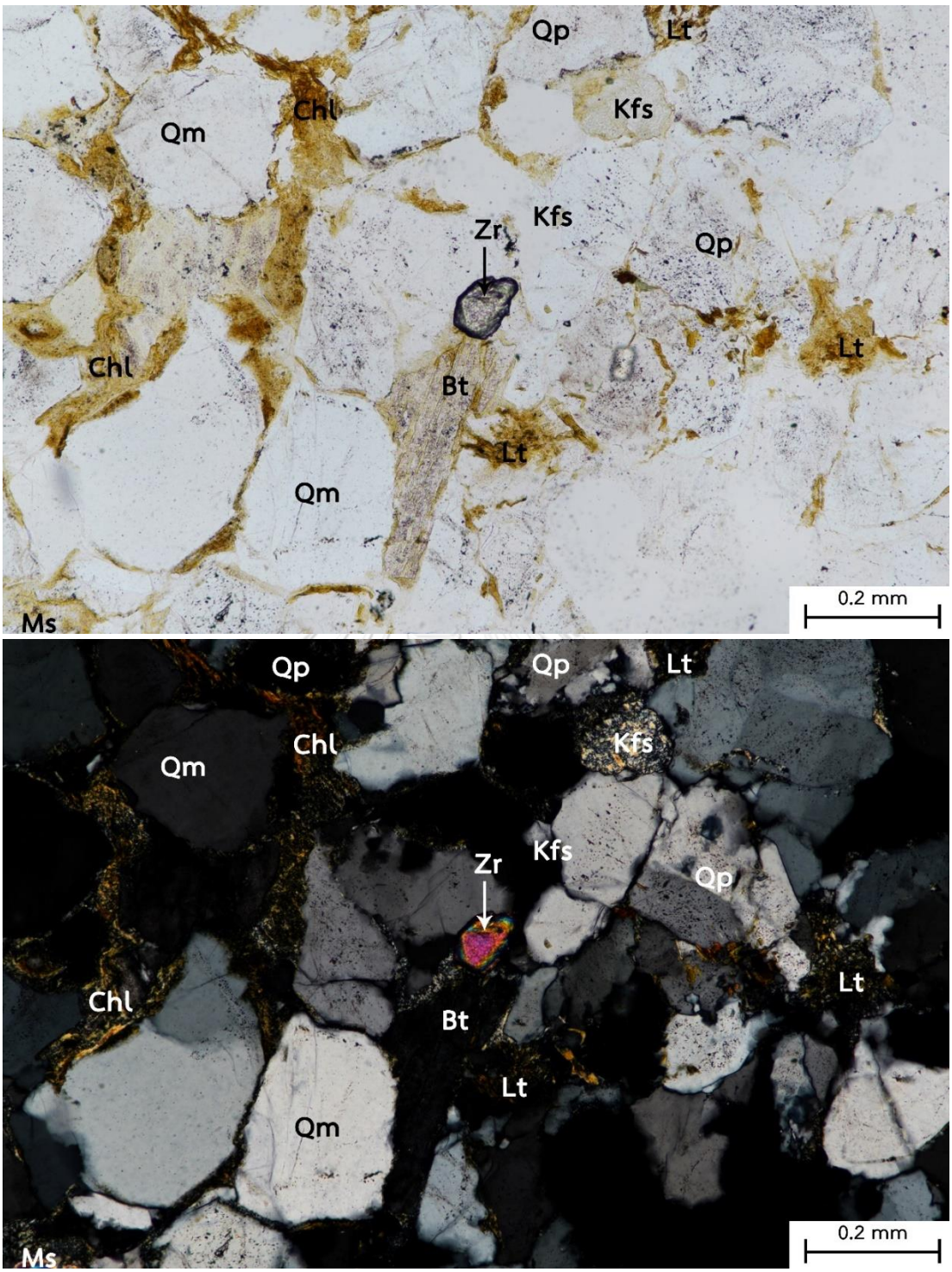

Figure 6 *Photomicrographs of litharenite (sample PP02) from the Phra Wihan Formation at Phu Phan Mountain Range showing well defined clastic texture and grains of quartz, alkaline feldspar, lithic fragments, muscovite, biotite, chlorite, and zircon. (top) Ordinary light and (bottom) Cross polar. (Qm = monocrystalline quartz, Qp = polycrystalline quartz, Kfs = alkaline feldspar, Lt = lithic fragment, Ms = muscovite, Bt = biotite, Chl = chlorite, and Zr = zircon)*

Sample no: PP03

Location: Wat Tham Pha Daen (Lat: 16°48'48"N Long: 103°57'37"E)

Rock name: Litharenite

Type of outcrop: Artificial **Outcrop size:** 4x5 m

Rock units: Sao Khua Formation (Khorat Group)

Figure 7 *Natural outcrop of sandstone of the Sao Khua Formation at Wat Tham Pha Daen, Mueang Sakhon Nakhon District, Sakhon Nakhon Province. (top) The overview of site and (bottom) White rectangle is the sampling site. (Mr. Sitichok Kumrangwat, 180 cm-tall, is to scale).*

Macroscopic description

The brownish grey rock sample is medium-grained sandstone and shows a clastic texture. It is a reddish-brown weathering surfaces. The grains are made up mostly of quartz (colorless), feldspar (white), and less opaque minerals and lithic fragments.

Figure 8 *Reddish-brown, medium-grained sandstone with well lamination of the Sao Khua Formation (sample no. PP03).*

Microscopic description

The weathered rock sample shows a clastic texture. The rock compositions are composed of largely of quartz (including monocrystalline quartz and polycrystalline quartz) (65 modal %), with small amount of feldspar (1 modal %) and lithic fragment (34 modal %). The rock sample are also included of muscovite and zircon. The size of mineral is up to 0.2 to 0.6 mm with well sorted. The grains show a low sphericity and angular shape. The cement of the rock is siliceous.

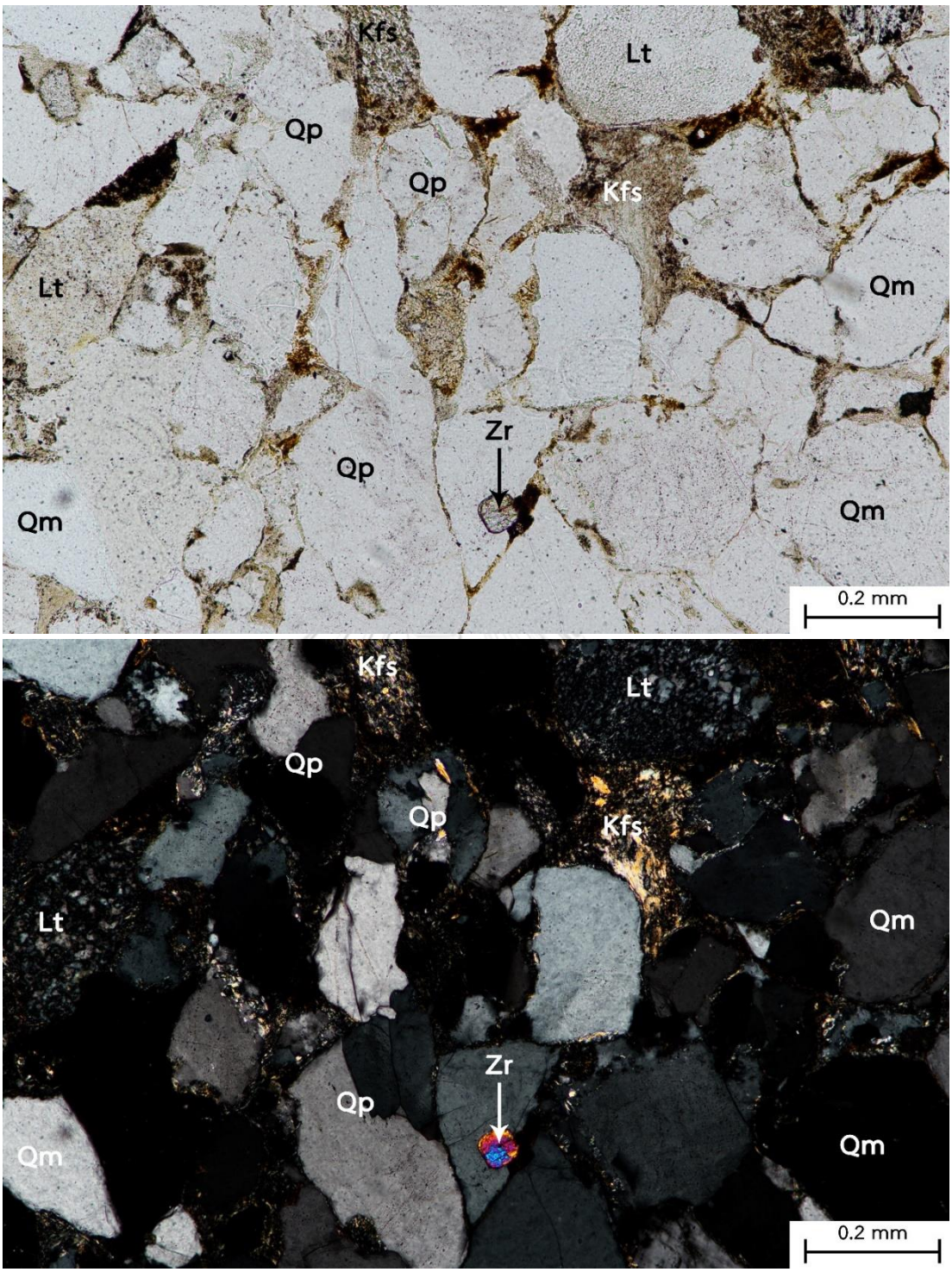

Figure 9 *Photomicrographs of litharenite (sample PP03) from the Sao Khua Formation at Phu Phan Mountain Range showing well defined clastic texture and grains of quartz, alkaline feldspar, lithic fragments, and zircon. (top) Ordinary light and (bottom) Cross polar. (Qm = monocrystalline quartz, Qp = polycrystalline quartz, Kfs = alkaline feldspar, Lt = lithic fragment, and Zr = zircon)*

Sample no: PP04

Location: Huai Yai Waterfall (Lat: 17°01'17"N Long: 103°59'31"E)

Rock name: Sublitharenite (PP04-1, PP04-2)

Type of outcrop: Natural **Outcrop size:** 1x50 m

Rock units: Phu Phan Formation (Khorat Group)

Figure 10 *(a) Natural outcrop of sandstone of the Phu Phan Formation at Huai Yai Waterfall, Phu Phan District, Sakhon Nakhon Province (Geological Hammer, 32.5 cm-long, is to scale). (b) The cross beddings (248/25 and 330/09) were found on the top of outcrop.*

Figure 11 *White rectangle is the sampling site of sample no. (a) PP04-1 at the lowest section and (b) PP04-2 at the top of this outcrop.*

Macroscopic description (PP04-1)

The whitish grey rock sample is medium-grained sandstone and shows a clastic texture. It is a dark brown weathering surfaces. The grains are made up mostly of quartz (colorless), feldspar (white), and less opaque minerals and lithic fragments.

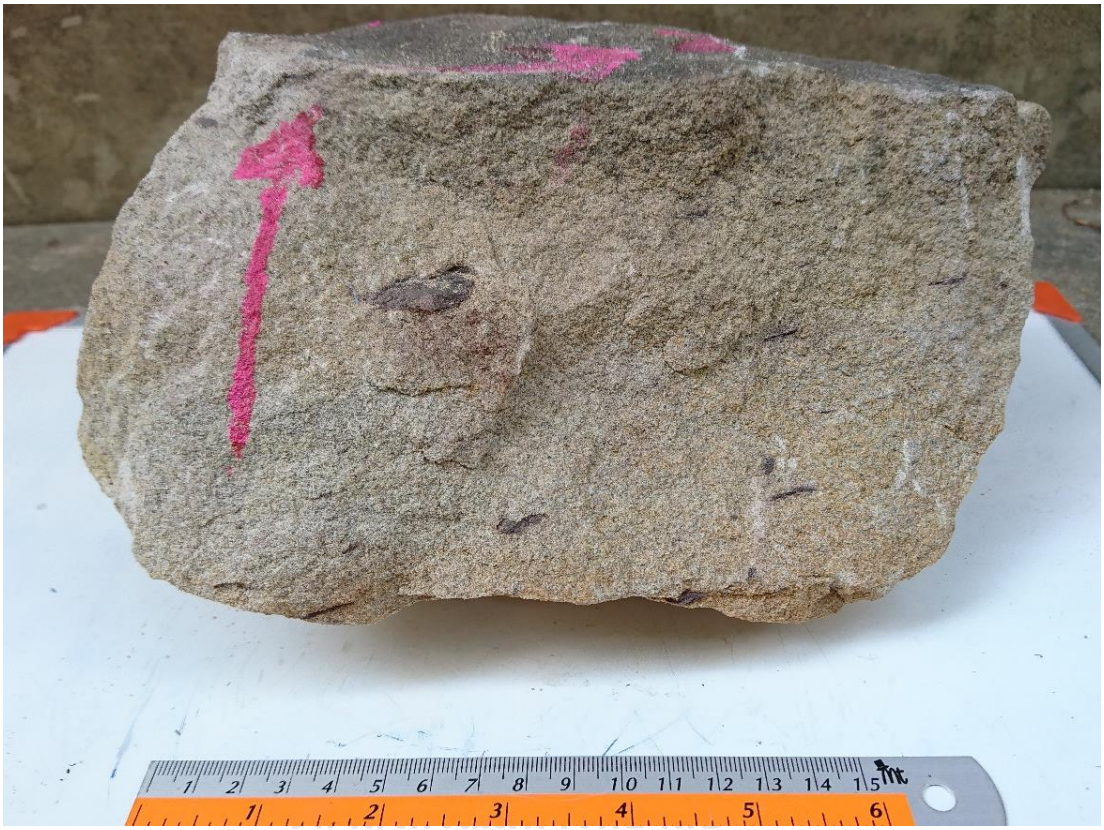

Figure 12 *Whitish grey, medium-grained sandstone of the Phu Phan Formation (sample no. PP04-1).*

Microscopic description (PP04-1)

The weathered rock sample shows a clastic texture. The rock compositions are composed of largely of quartz (including monocrystalline quartz and polycrystalline quartz) (88 modal %), with small amount of feldspar (<1 modal %) and lithic fragment (12 modal %). The rock sample are also included of zircon. The size of mineral is up to 0.1 to 0.6 mm with well sorted. The grains show a low sphericity and angular shape. The cement of the rock is siliceous.

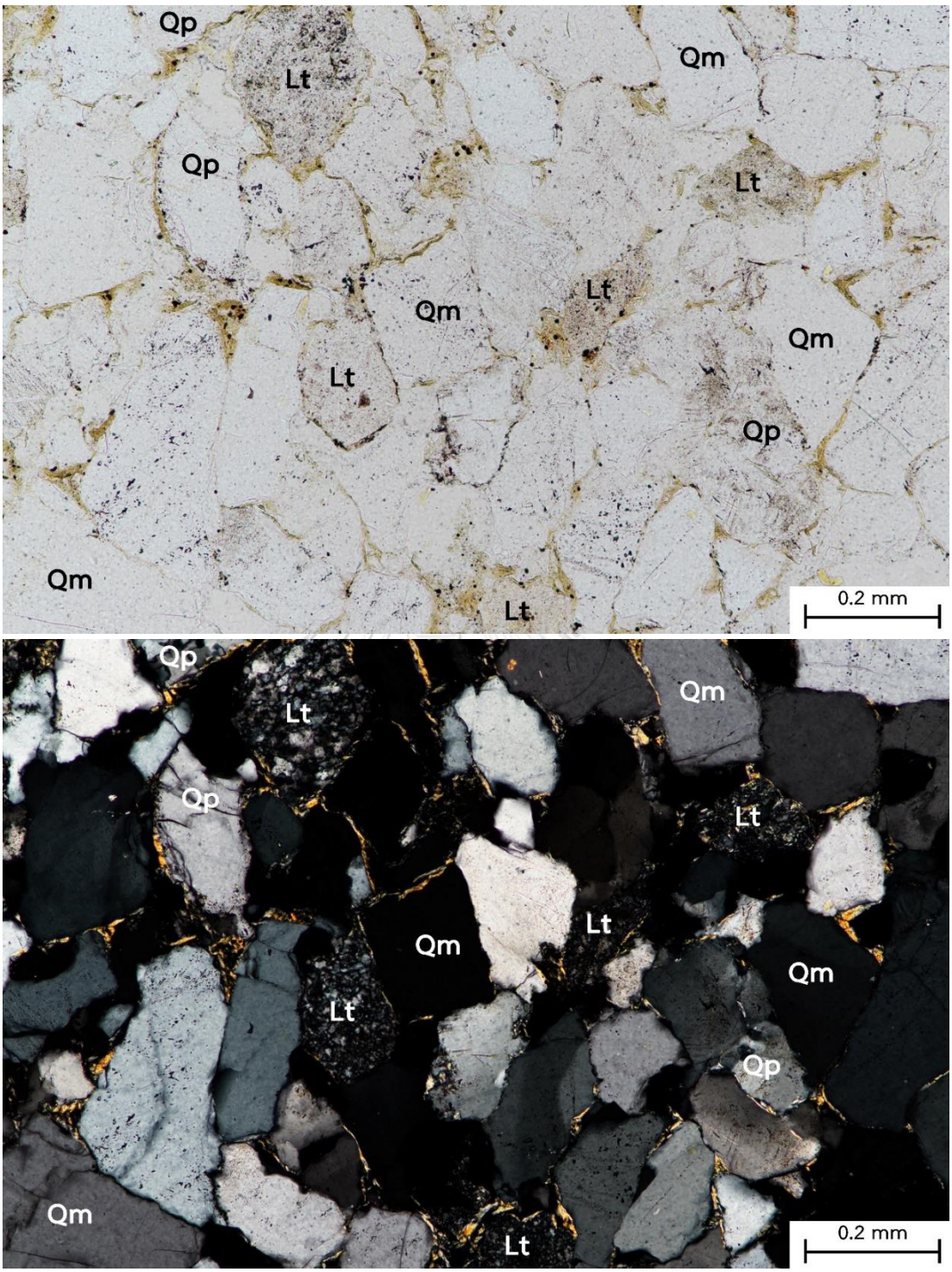

Figure 13 *Photomicrographs of sublitharenite (sample PP04-1) from the Phu Phan Formation at the Phu Phan Mountain Range showing well defined clastic texture and grain of quartz and lithic fragments. (top) Ordinary light (bottom) (Qm = monocrystalline quartz, Qp = polycrystalline quartz, and Lt = lithic fragment)*

Macroscopic description (PP04-2)

The whitish grey rock sample is medium-grained sandstone and shows a clastic texture. It is a dark brown weathering surfaces. The grains are made up mostly of quartz (colorless), feldspar (white), and less opaque minerals and lithic fragments.

Figure 14 *Whitish grey, medium-grained sandstone of the Phu Phan Formation (sample no. PP04-2).*

Microscopic description (PP04-2)

The weathered rock sample shows a clastic texture. The rock compositions are composed of largely of quartz (including monocrystalline quartz and polycrystalline quartz) (79 modal %), with small amount of feldspar (<1 modal %) and lithic fragment (21 modal %). The rock sample are also included of muscovite, biotite, amphibole and zircon. The size of mineral is up to 0.2 to 0.8 mm with well sorted. The grains show a low sphericity and angular shape. The cement of the rock is siliceous.

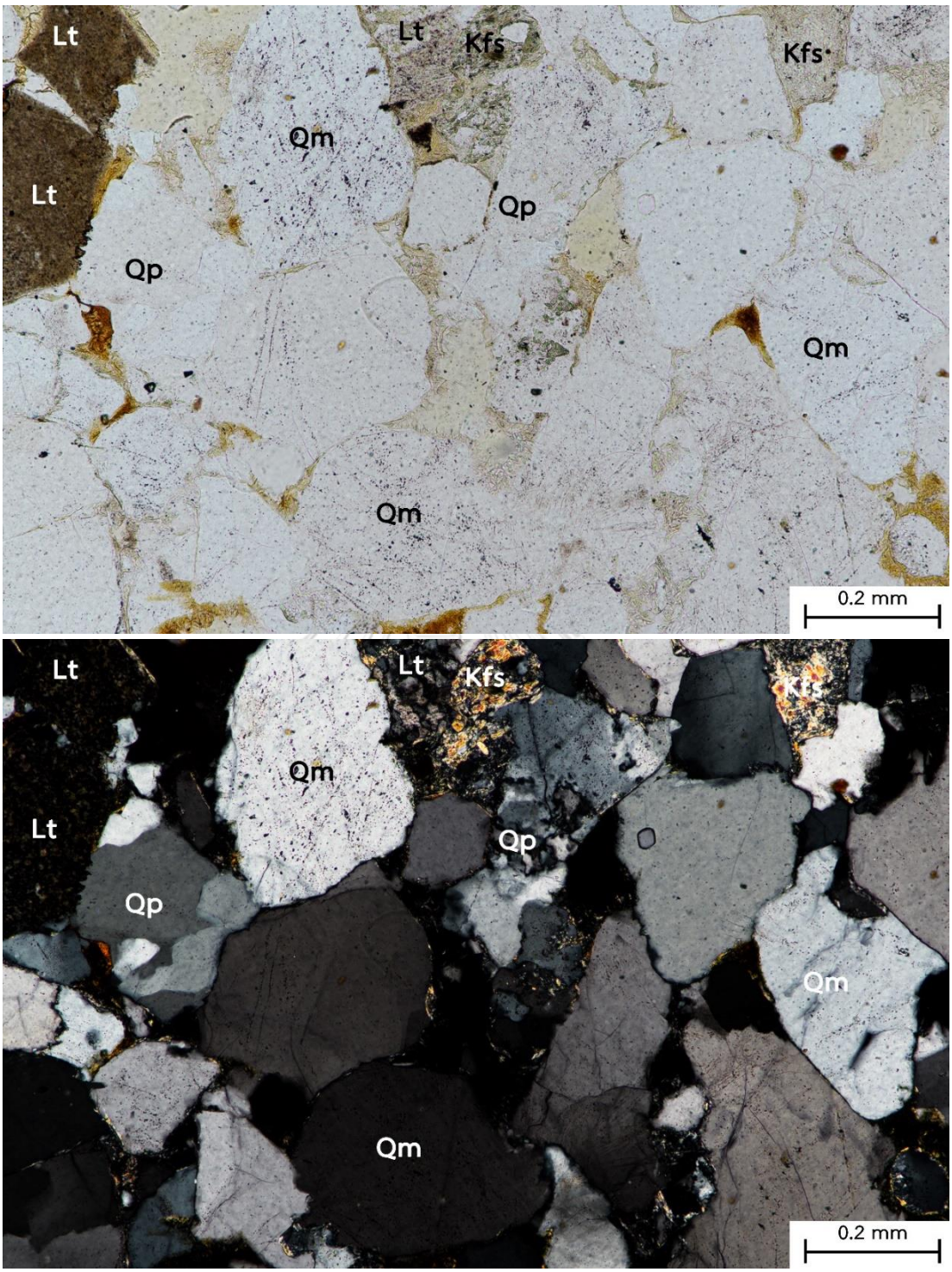

Figure 15 *Photomicrographs of sublitharenite (sample PP04-2) from the Phu Phan Formation at the Phu Phan Mountain Range showing well defined clastic texture and grain of quartz, alkaline feldspar, lithic fragments. (top) Ordinary light (bottom) Cross polar. (Qm = monocrystalline quartz, Qp = polycrystalline quartz, Kfs = alkaline feldspar, and Lt = lithic fragment)*

Sample no: PP05

Location: Phu Phan Buddha Nimit temple (Lat: 16°58'53"N Long: 103°59'29"E)

Rock name: Litharenite (PP05-1, PP05-2, PP05-3)

Type of outcrop: Road-cut **Outcrop size:** 3x100 m

Rock units: Sao Khua Formation (Khorat Group)

Figure 16 *Natural outcrop of sandstone of the Sao Khua Formation in front of the entrance of Phu Phan Buddha Nimit temple, Phu Phan District, Sakhon Nakhon Province (Geological hammer, 32.5 cm-long, is to scale). White rectangle is sampling site. (a) Lowest bed (Sample PP05-1) (b) Second bed (sample PP05-2) and*

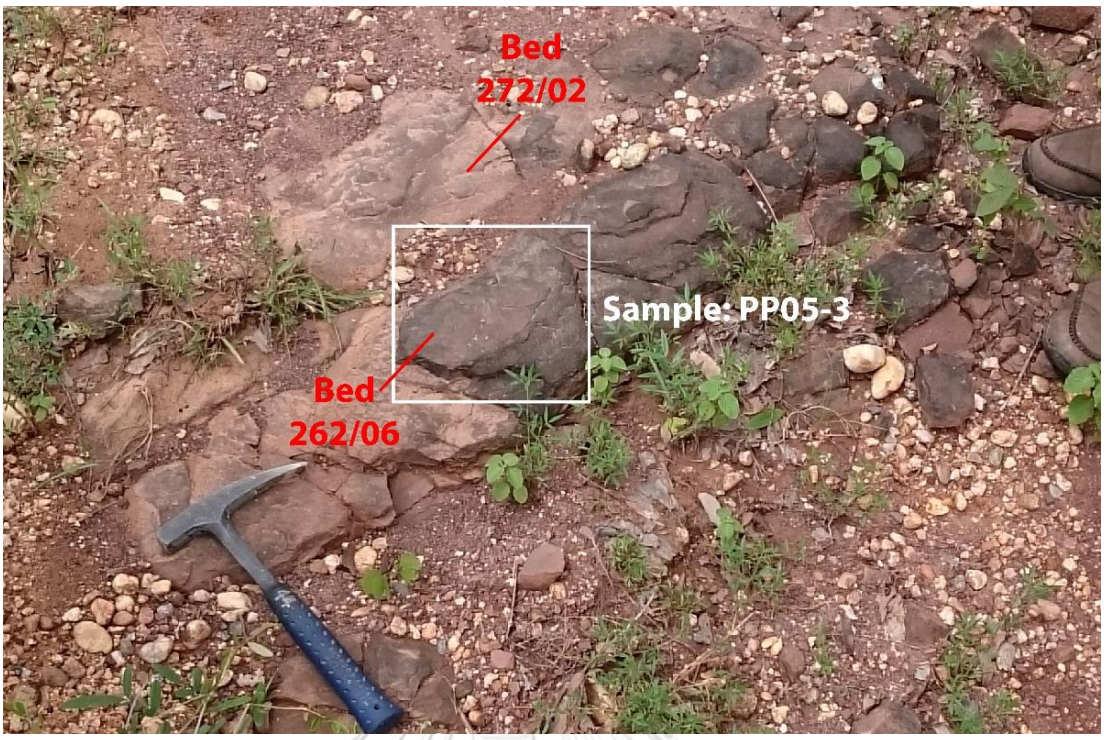

Figure 16 cont. *(c) Top bed of this site (sample PP05-3).*

Macroscopic description (PP05-1)

The reddish grey rock sample is fine-grained sandstone and shows a clastic texture. It is a reddish-brown weathering surfaces. The grains are made up mostly of quartz (colorless), feldspar (white), and less opaque minerals and lithic fragments.

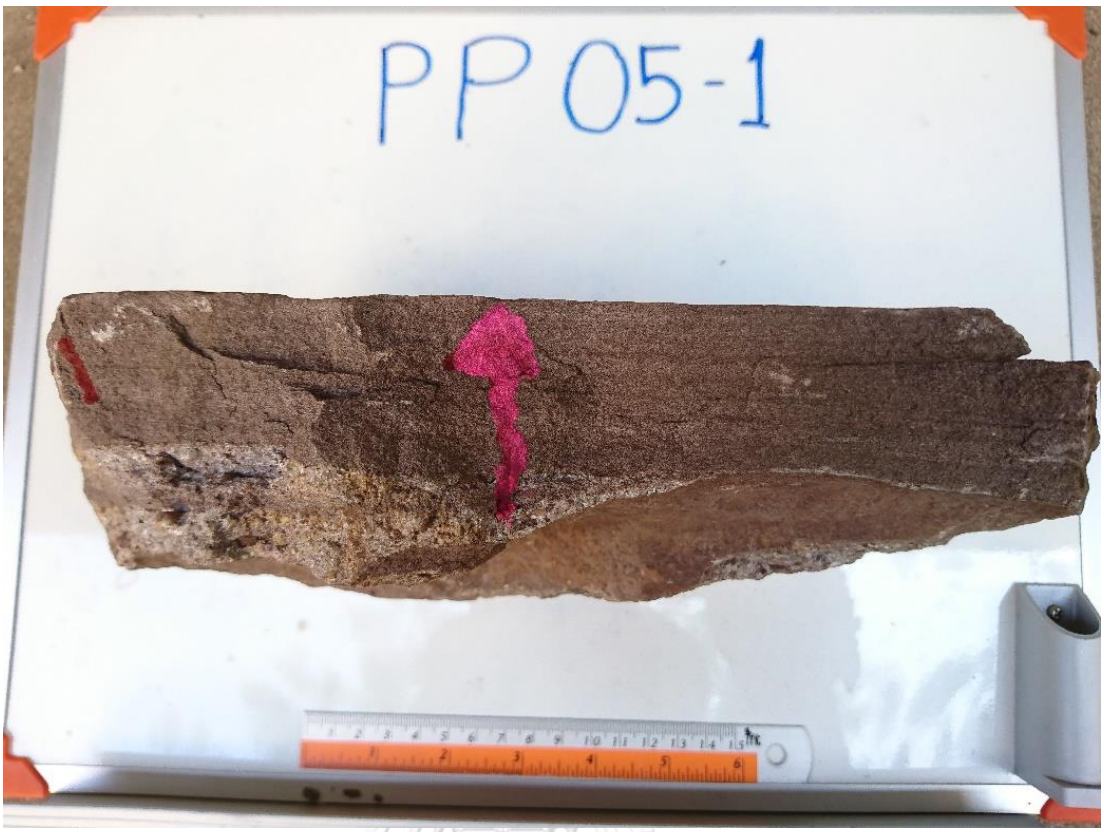

Figure 17 *Reddish grey, fine-grained sandstone of the Sao Khua Formation (sample no. PP05-1).*

Microscopic description (PP05-1)

The weathered rock sample shows a clastic texture. The rock compositions are composed of largely of quartz (including monocrystalline quartz and polycrystalline quartz) (72 modal %), with small amount of feldspar (1 modal %) and lithic fragment (27 modal %). The rock sample are also included of muscovite, chlorite, opaque mineral, and zircon. The size of mineral is up to 0.1 to 0.3 mm with moderated well sorted. The grains show a low sphericity and angular shape. The cement of the rock is siliceous.

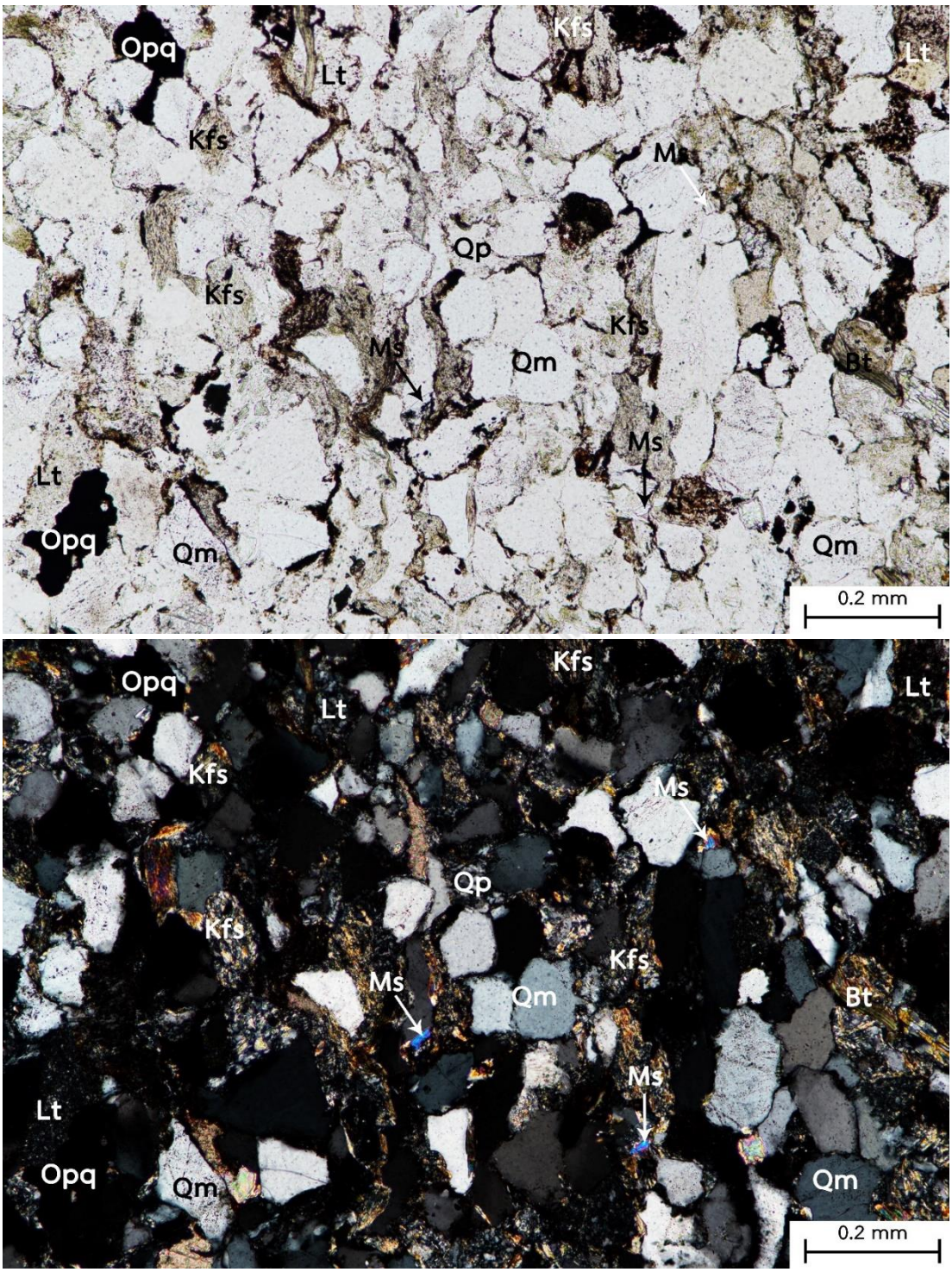

Figure 18 *Photomicrographs of litharenite (sample PP05-1) from the Sao Khua Formation at the Phu Phan Mountain Range showing well defined clastic texture and grain of quartz, alkaline feldspar, lithic fragments, muscovite, biotite, and opaque mineral. (top) Ordinary light (bottom) Cross polar. (Qm = monocrystalline quartz, Qp = polycrystalline quartz, Kfs = alkaline feldspar, Lt = lithic fragment, Ms = muscovite, Bt = biotite, and Opq = opaque mineral)*

Macroscopic description (PP05-2)

The reddish grey rock sample is fine-grained sandstone and shows a clastic texture. It is a reddish-brown weathering surfaces. The grains are made up mostly of quartz (colorless), feldspar (white), and less opaque minerals and lithic fragments.

Figure 19 *Reddish grey, fine-grained sandstone with faint lamination of the Sao Khua Formation (sample no. PP05-2).*

Microscopic description (PP05-2)

The weathered rock sample shows a clastic texture. The rock compositions are composed of largely of quartz (including monocrystalline quartz and polycrystalline quartz) (69 modal %), with small amount of feldspar (1 modal %) and lithic fragment (30 modal %). The rock sample are also included of muscovite, biotite, calcite, apatite and zircon. The size of mineral is up to 0.1 to 0.6 mm with moderate well sorted. The grains show a low sphericity and angular shape. The cement of the rock is siliceous.

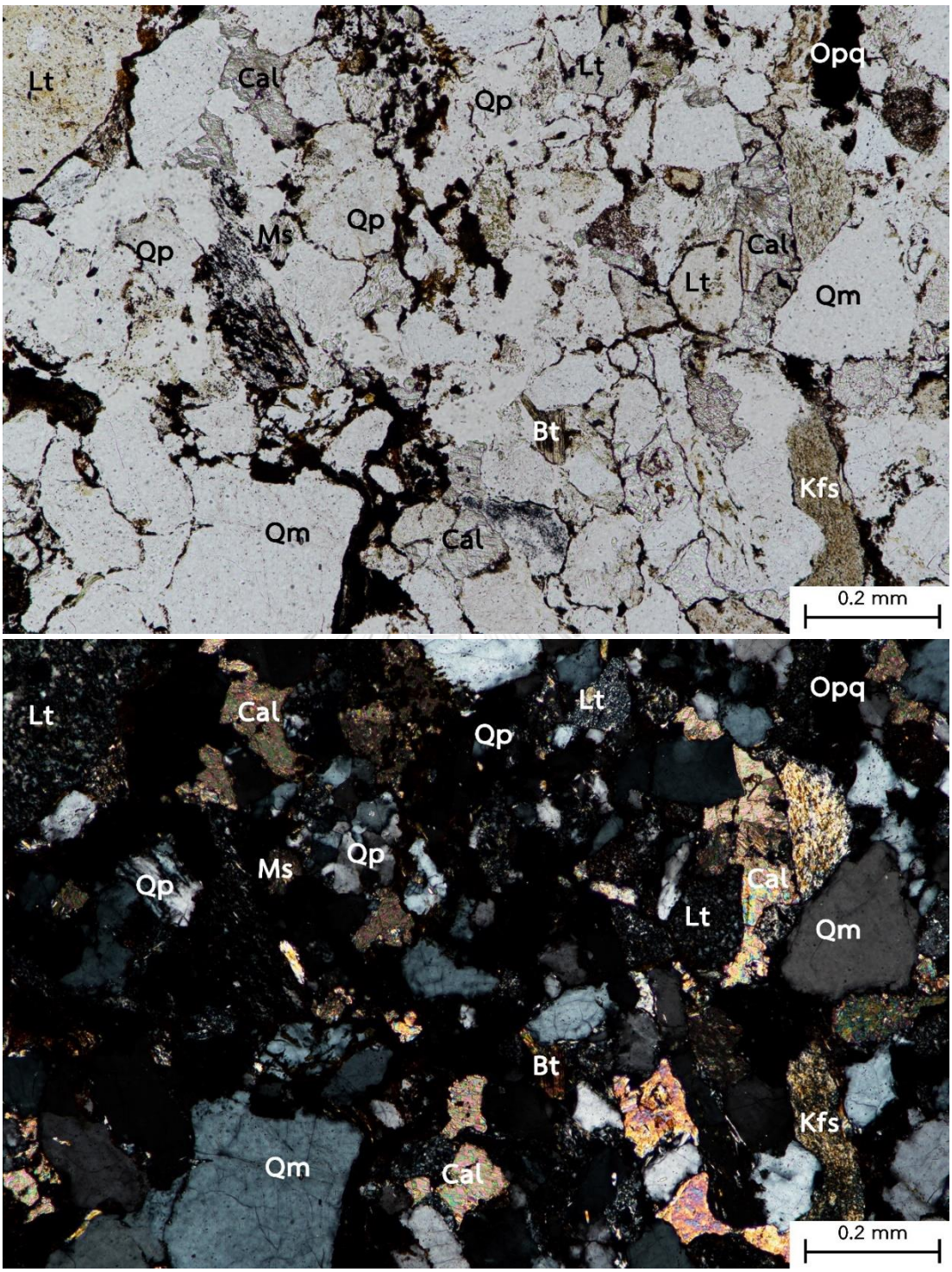

Figure 20 *Photomicrographs of litharenite (sample PP05-2) from the Sao Khua Formation at the Phu Phan Mountain Range showing well defined clastic texture and grain of quartz, alkaline feldspar, lithic fragments, muscovite, biotite, and calcite. (top) Ordinary light (bottom) Cross polar. (Qm = monocrystalline quartz, Qp = polycrystalline quartz, Kfs = alkaline feldspar, Lt = lithic fragment, Ms = muscovite, Bt = biotite, and cal = calcite)*

Macroscopic description (PP05-3)

The reddish grey rock sample is fine-grained sandstone and shows a clastic texture. It is a reddish-brown weathering surfaces. The grains are made up mostly of quartz (colorless), feldspar (white), and less opaque minerals and lithic fragments.

Figure 21 *Reddish grey, fine-grained sandstone with faint lamination of the Sao Khua Formation (sample no. PP05-3),*

Microscopic description (PP05-3)

The weathered rock sample shows a clastic texture. The rock compositions are composed of largely of quartz (including monocrystalline quartz and polycrystalline quartz) (68 modal %), with small amount of feldspar (~1 modal %) and lithic fragment (31 modal %). The rock sample are also included of muscovite, biotite, chlorite and zircon. The size of mineral is up to 0.1 to 0.2 mm with moderate well sorted. The grains show a low sphericity and angular shape. The cement of the rock is siliceous.

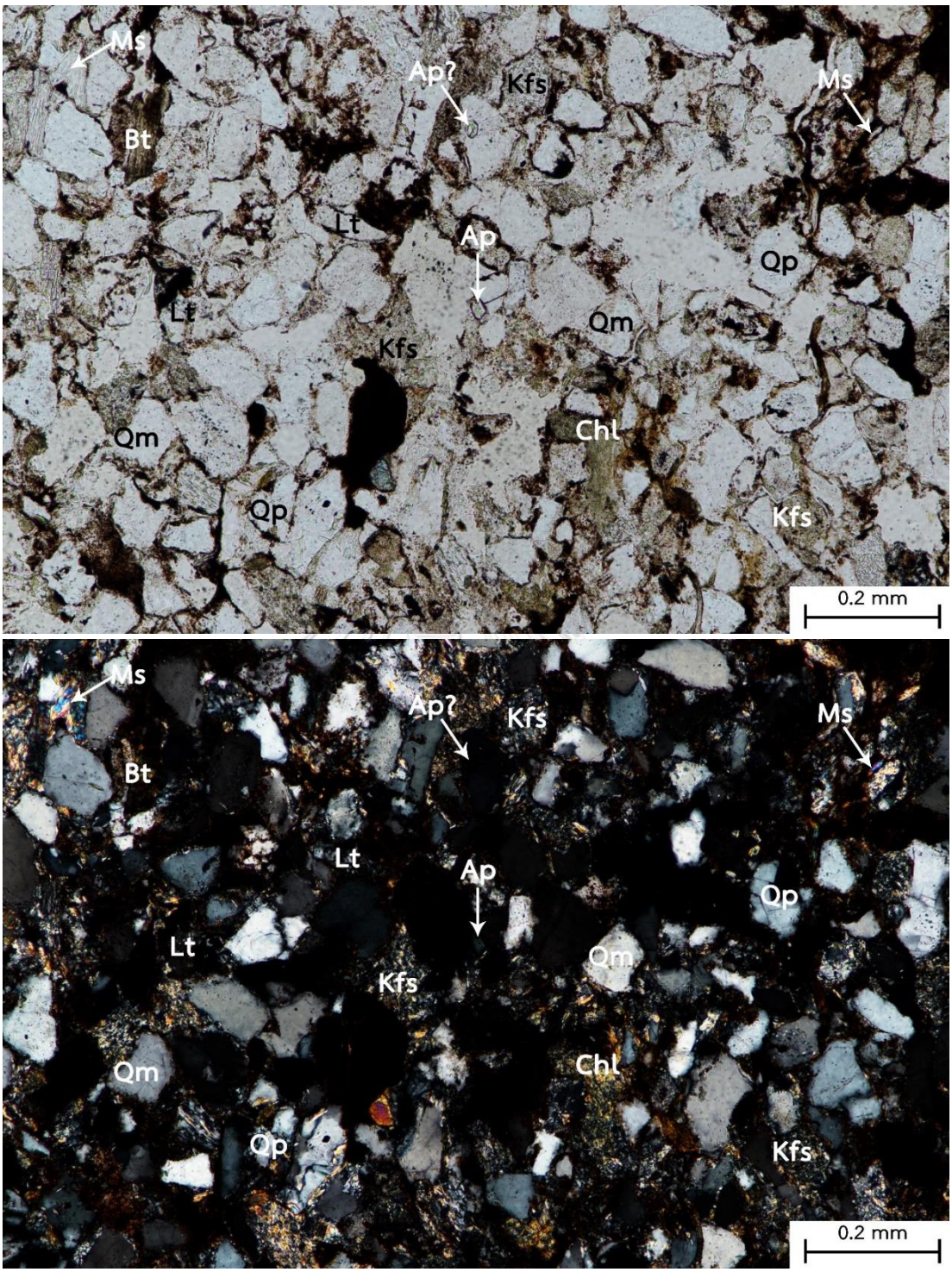

Figure 7.22 *Photomicrographs of litharenite (sample PP05-3) from the Sao Khua Formation at Phu Phan Mountain Range showing well defined clastic texture and grains of quartz, alkaline feldspar, lithic fragments, muscovite, biotite, chlorite, and apatite. (top) Ordinary light and (bottom) Cross polar. (Qm = monocrystalline quartz, Qp = polycrystalline quartz, Kfs = alkaline feldspar, Lt = lithic fragment, Ms = muscovite, Bt = biotite, Chl = chlorite, and Ap = apatite)*

Sample no: PP06

Location: Ban Na Phang Reservoir (Lat: 16°56'17"N Long: 104°03'49"E)

Rock name: Litharenite

Type of outcrop: Natural **Outcrop size:** 0.5x100 m

Rock units: Sao Khua Formation (Khorat Group)

Figure 23 *Natural outcrop of sandstone of the Sao Khua Formation at Ban Na Phang Reservoir, Phu Phan District, Sakhon Nakhon Province (Mr. Norarat Boonkanpai, 175 cm-tall, is to scale). White rectangle is the sampling site.*

Macroscopic description

The reddish grey rock sample is fine-grained sandstone and shows a clastic texture. It is a reddish-brown weathering surfaces. The grains are made up mostly of quartz (colorless), feldspar (white), and less opaque minerals and lithic fragments.

Figure 24 *Reddish grey, fine-grained sandstone with faint lamination of the Sao Khua Formation (sample no. PP06).*

Microscopic description

The weathered rock sample shows a clastic texture. The rock compositions are composed of largely of quartz (including monocrystalline quartz and polycrystalline quartz) (75 modal %), with small amount of feldspar (1 modal %) and lithic fragment (24 modal %). The rock sample are also included of muscovite, chlorite and zircon. The size of mineral is up to 0.05 to 0.2 mm with well sorted. The grains show a low sphericity and subangular shape. The cement of the rock is siliceous.

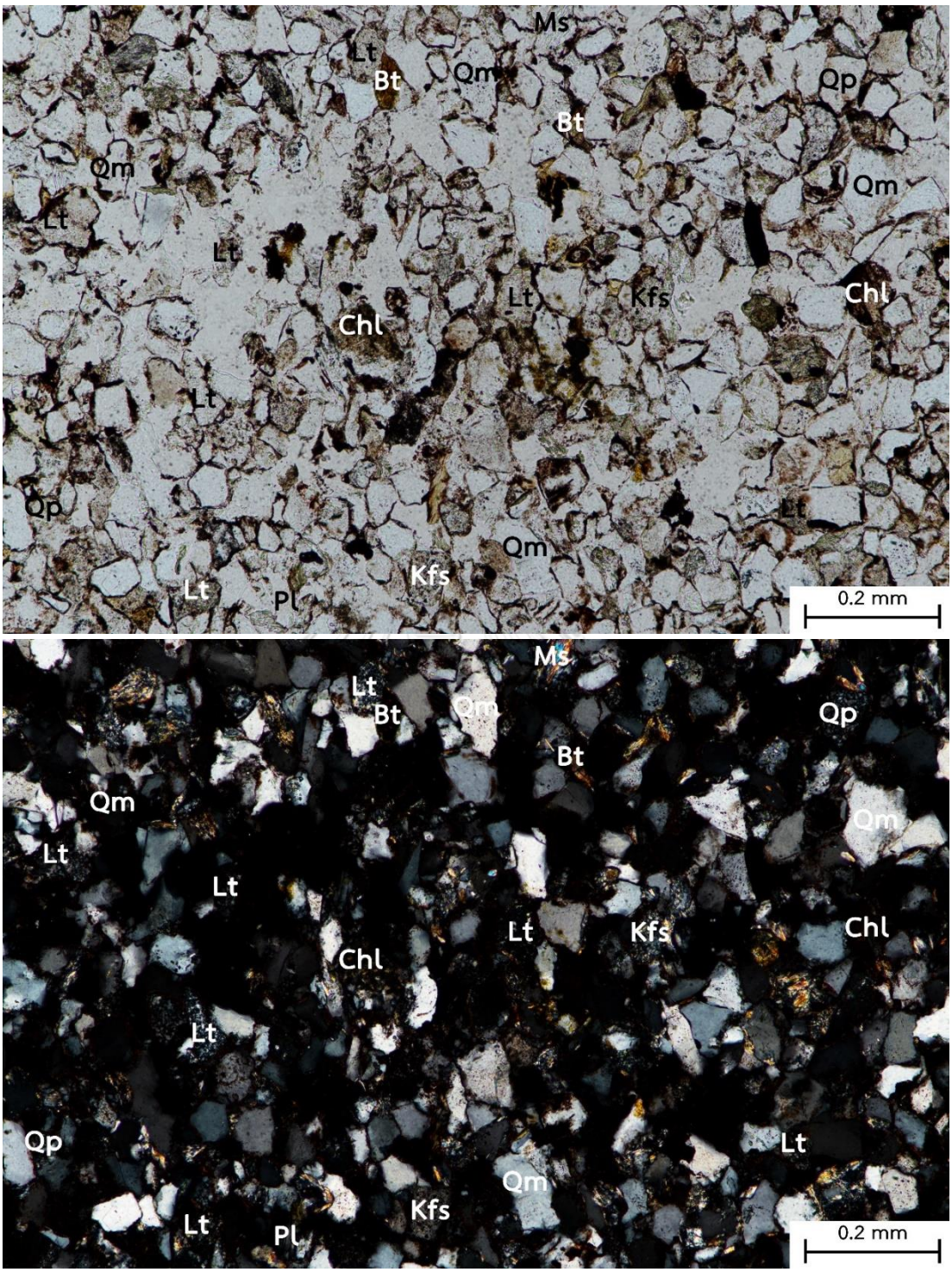

Figure 25 *Photomicrographs of litharenite (sample PP06) from the Sao Khua Formation at the Phu Phan Mountain Range showing well defined clastic texture and grain of quartz, alkaline feldspar, lithic fragments, muscovite, biotite, and chlorite. (top) Ordinary light (bottom) Cross polar. (Qm = monocrystalline quartz, Qp = polycrystalline quartz, Kfs = alkaline feldspar, Lt = lithic fragment, Ms = muscovite, Bt = biotite, and Chl =chlorite)*

Sample no: PP07

Location: Phaya Tao Ngoi Cave (Lat: 16°56'19"N Long: 104°08'14"E)

Rock name: Sublitharenite

Type of outcrop: Natural **Outcrop size:** 6x100 m

Rock units: Phu Phan Formation (Khorat Group)

Figure 26 *Natural outcrop of sandstone of the Phu Phan Formation at Phaya Tao Ngoi Cave, Tao Ngoi District, Kalasin Province (Mr. Sitichok Kumrangwat, 180 cm-tall, is to scale). White rectangle is the sampling site.*

Macroscopic description

The whitish orange rock sample is medium-grained sandstone and shows a clastic texture. It is a brownish orange weathering surfaces. The grains are made up mostly of quartz (colorless), feldspar (white), and less opaque minerals and lithic fragments.

Figure 27 *Whitish orange, medium grained sandstone of the Phu Phan Formation (sample no. PP07).*

Microscopic description

The weathered rock sample shows a clastic texture. The rock compositions are composed of largely of quartz (including monocrystalline quartz and polycrystalline quartz) (77 modal %), with small amount of feldspar (~1 modal %) and lithic fragment (23 modal %). The rock sample are also included of muscovite, chlorite and zircon. The size of mineral is up to 0.1 to 0.4 mm with well sorted. The grains show a low sphericity and subangular shape. The cement of the rock is siliceous.

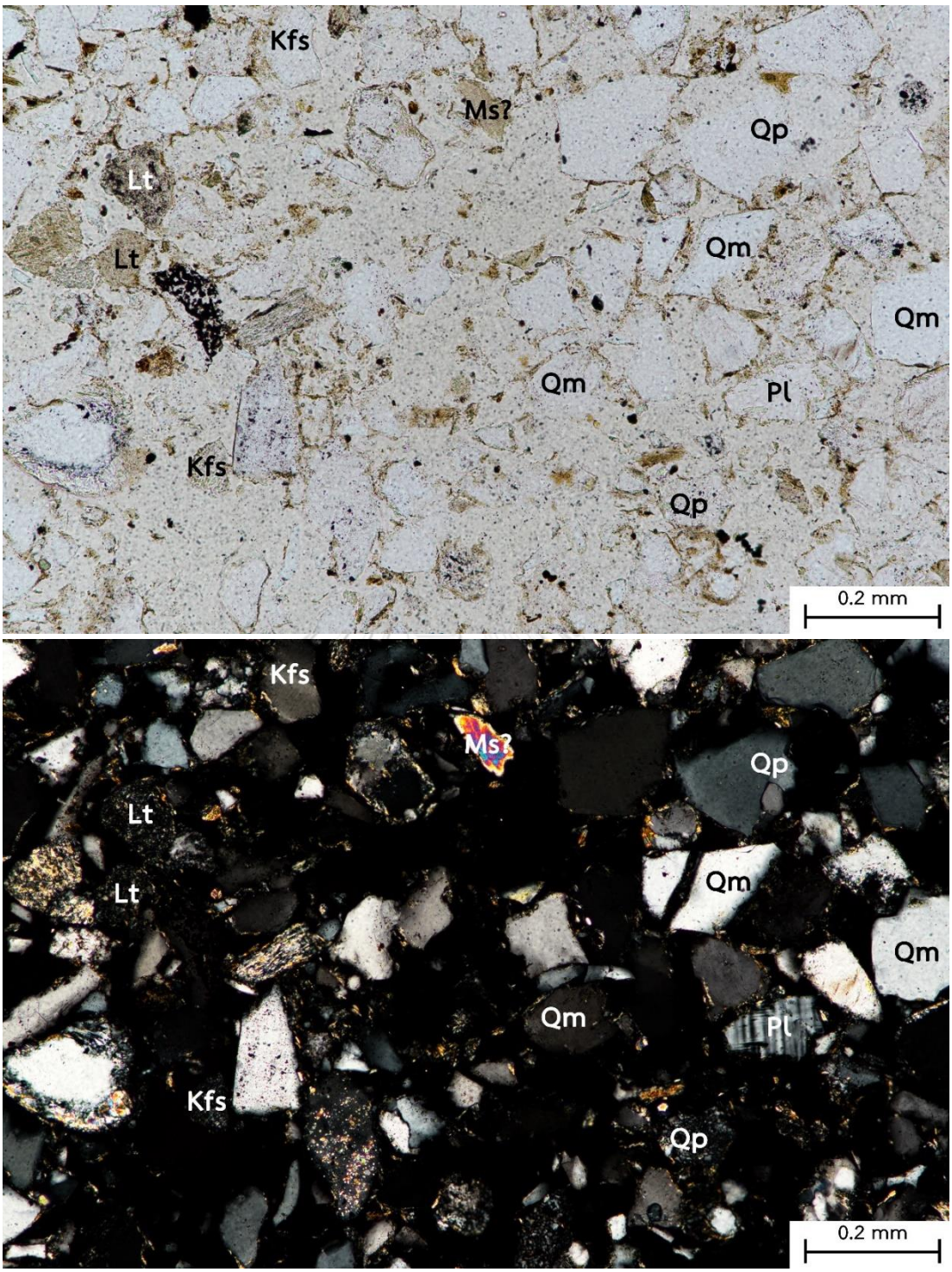

Figure 28 *Photomicrographs of sublitharenite (sample PP07) from the Phu Phan Formation at the Phu Phan Mountain Range showing well defined clastic texture and grain of quartz, alkaline feldspar, plagioclase, lithic fragments, and muscovite. (top) Ordinary light (bottom) Cross polar. (Qm = monocrystalline quartz, Qp = polycrystalline quartz, Kfs = alkaline feldspar, Pl = Plagioclase, Lt = lithic fragment, and Ms? = muscovite?)*

Sample no: PP08

Location: Local road 4001 km 11 (Lat: 16°49'55"N Long: 104°03'51"E)

Rock name: Litharenite

Type of outcrop: Road-cut **Outcrop size:** 8x100 m

Rock units: Phu Phan Formation (Khorat Group)

Figure 29 *Natural outcrop of sandstone of the Phu Phan Formation along the local road 4001 km 11 Na Khu District, Kalasin Province (Mr. Sitichok Kumrangwat, 180-cm tall, is to scale). White rectangle is the sampling site.*

Macroscopic description

The whitish grey rock sample is fine-grained sandstone and shows a clastic texture. It is a reddish-brown weathering surfaces. The grains are made up mostly of quartz (colorless), feldspar (white), and less opaque minerals and lithic fragments.

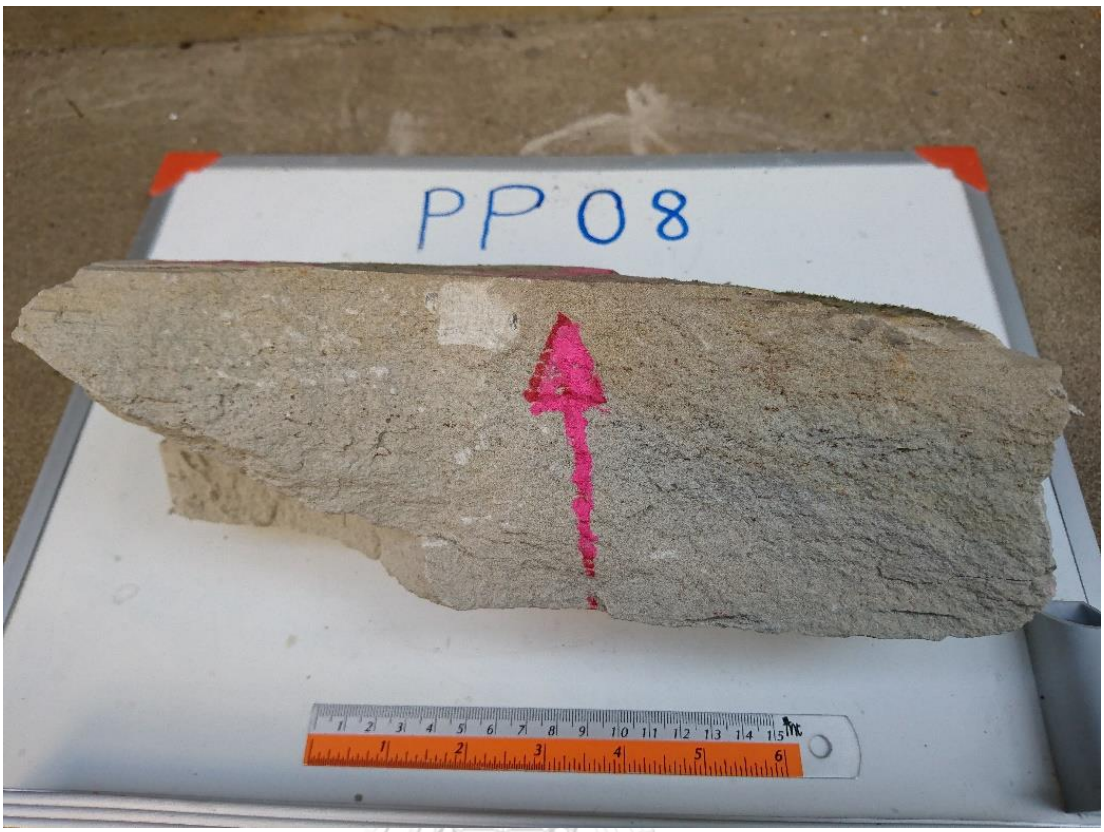

Figure 30 *Whitish grey, fine-grained sandstone with faint lamination of the Phu Phan Formation (sample no. PP08).*

Microscopic description

The weathered rock sample shows a clastic texture. The rock compositions are composed of largely of quartz (including monocrystalline quartz and polycrystalline quartz) (67 modal %), with small amount of feldspar (12 modal %) and lithic fragment (21 modal %). The rock sample are also included of muscovite, apatite, and zircon. The size of mineral is up to 0.1 to 0.2 mm with well sorted. The grains show a high sphericity and subangular shape. The cement of the rock is siliceous.

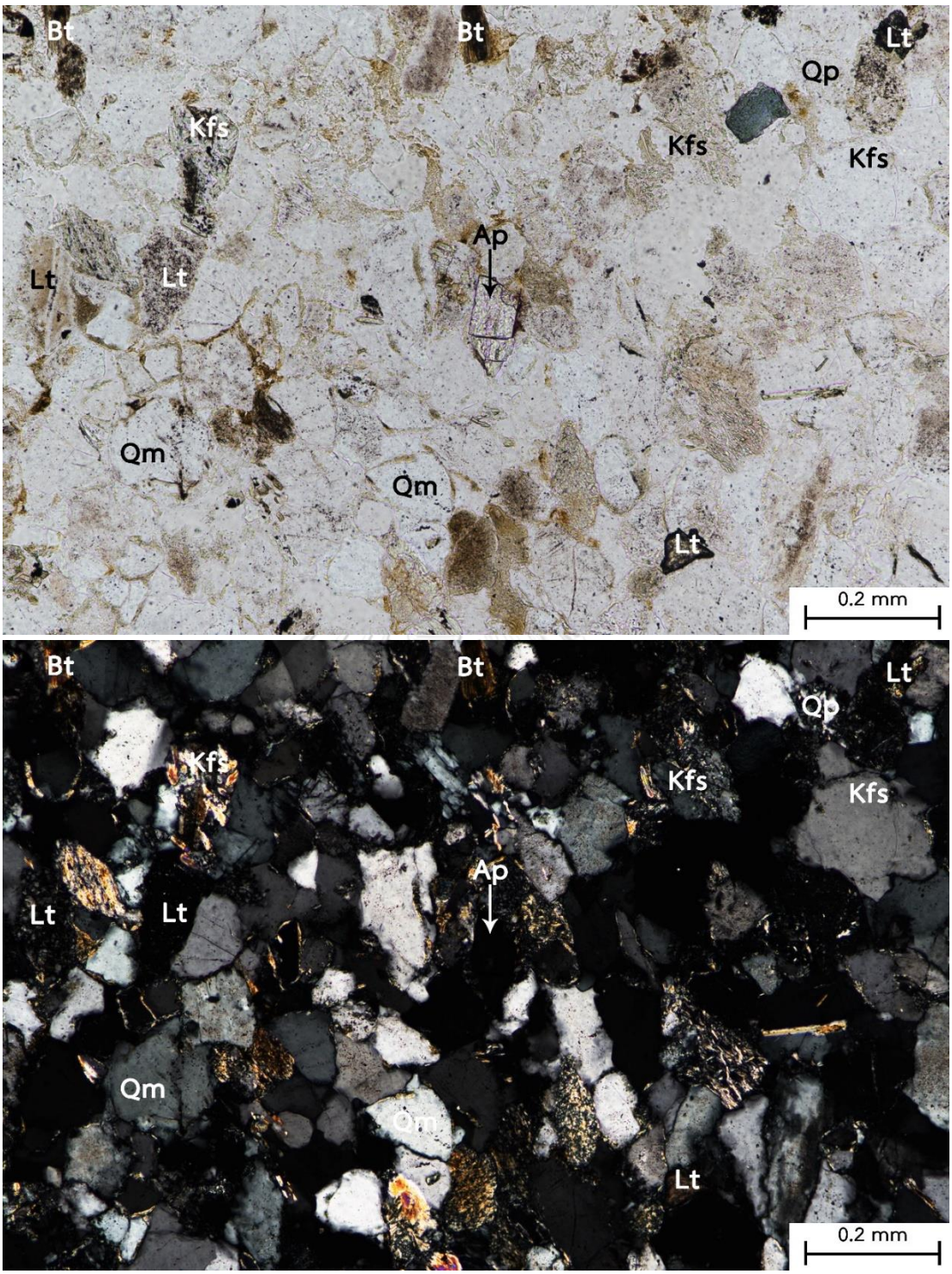

Figure 31 *Photomicrographs of litharenite (sample PP08) from the Phu Phan Formation at the Phu Phan Mountain Range showing well defined clastic texture and grain of quartz, alkaline feldspar, lithic fragments, biotite, and apatite. (top) Ordinary light (bottom) Cross polar. (Qm = monocrystalline quartz, Qp = polycrystalline quartz, Kfs = alkaline feldspar, Lt = lithic fragment, Bt = biotite, and Ap = apatite)*

Sample no: PP09

Location: Local road 2092, Na Sok municipal District Post (Lat: 16°30'45"N Long: 104°35'05"E)

Rock name: Litharenite

Type of outcrop: Road-cut **Outcrop size:** 5x100 m

Rock units: Phra Wihan Formation (Khorat Group)

Figure 32 *Natural outcrop of sandstone of the Phra Wihan Formation along the Local road 2092 (nealby Na Sok municipal District Post), Mueang Mukdahan District, Mukdahan Province (Geological hammer, 32.5 cm-long, is to scale). White rectangle is the sampling site.*

Macroscopic description

The whitish grey rock sample is medium-grained sandstone and shows a clastic texture. It is a reddish-brown weathering surfaces. The grains are made up mostly of quartz (colorless), feldspar (white), and less opaque minerals and lithic fragments.

Figure 33 *Whitish grey, medium grained sandstone of the Phra Wihan Formation (sample no. PP09).*

Microscopic description

The weathered rock sample shows a clastic texture. The rock compositions are composed of largely of quartz (including monocrystalline quartz and polycrystalline quartz) (69 modal %), with small amount of feldspar (3 modal %) and lithic fragment (28 modal %). The rock sample are also included of muscovite and zircon. The size of mineral is up to 0.1 to 0.6 mm with moderate well sorted. The grains show a low sphericity and angular shape. The cement of the rock is siliceous.

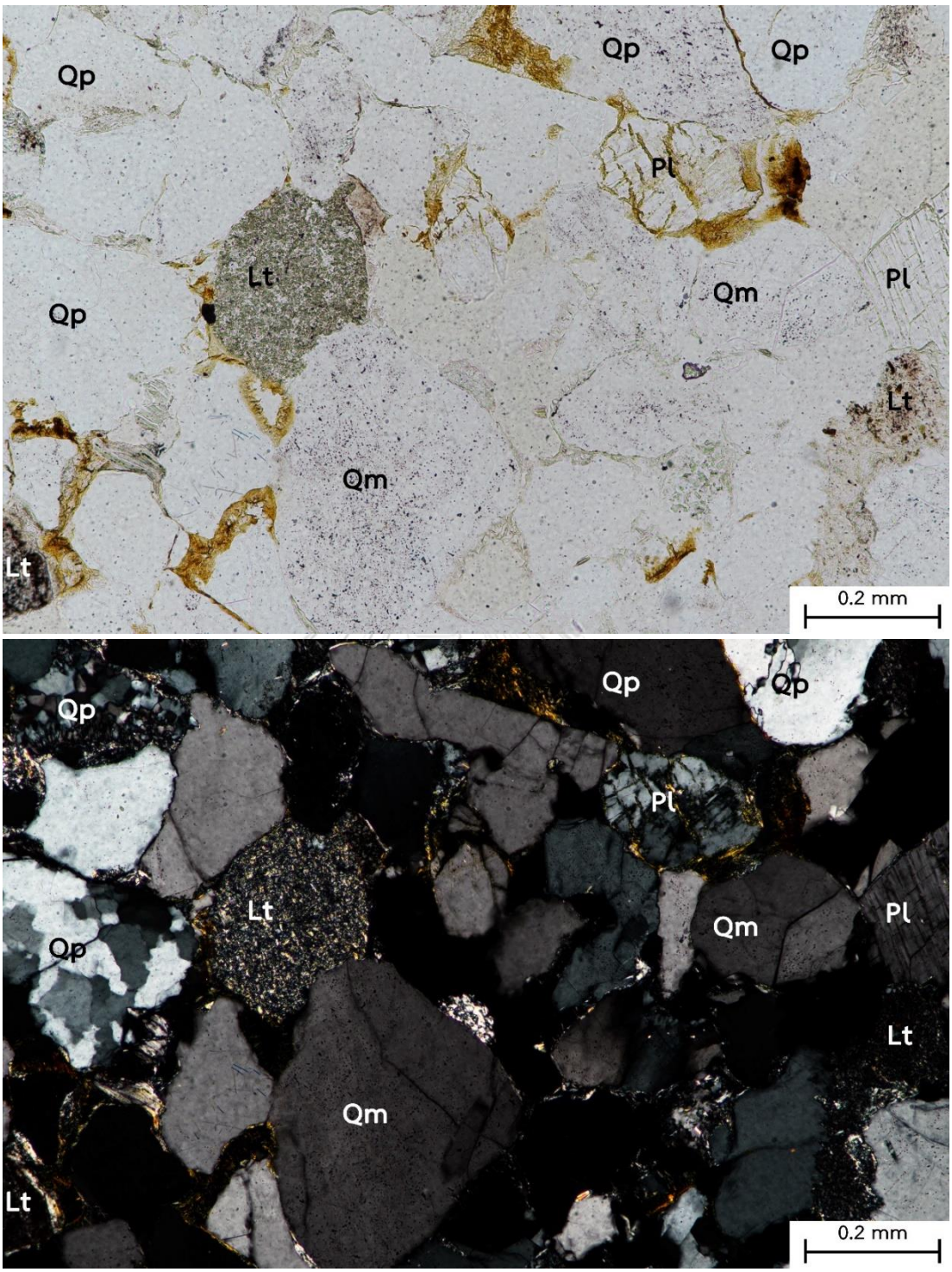

Figure 34 *Photomicrographs of litharenite (sample PP09) from the Phra Wihan Formation at the Phu Phan Mountain Range showing well defined clastic texture and grain of quartz, plagioclase, and lithic fragments. (top) Ordinary light (bottom) Cross polar. (Qm = monocrystalline quartz, Qp = polycrystalline quartz, Pl = Plagioclase, and Lt = lithic fragment)*

Sample no: PP10

Location: Wat Tham Pha Mong (Lat: 16°28'42"N Long: 104°31'09"E)

Rock name: Litharenite

Type of outcrop: Natural **Outcrop size:** 5x250 m

Rock units: Phu Phan Formation (Khorat Group)

Figure 35 *Natural outcrop of sandstone of the Phu Phan Formation at Wat Tham Pha Mong, Mueang Mukdahan District, Mukdahan Province (Orange sledge hammer, 32.5 cm-long, is to scale). White rectangle is the sampling site.*

Macroscopic description

The brownish white rock sample is medium-grained sandstone and shows a clastic texture. It is a reddish-brown weathering surfaces. The grains are made up mostly of quartz (colorless), feldspar (white), and less opaque minerals and lithic fragments.

Figure 36 *Brownish white, medium-grained sandstone of the Phu Phan Formation (sample no. PP10).*

Microscopic description

The weathered rock sample shows a clastic texture. The rock compositions are composed of largely of quartz (including monocrystalline quartz and polycrystalline quartz) (62 modal %), with small amount of feldspar (13 modal %) and lithic fragment (25 modal %). The rock sample are also included of muscovite, biotite, apatite and zircon. The size of mineral is up to 0.1 to 0.4 mm with well sorted. The grains show a low sphericity and angular shape. The cement of the rock is siliceous.

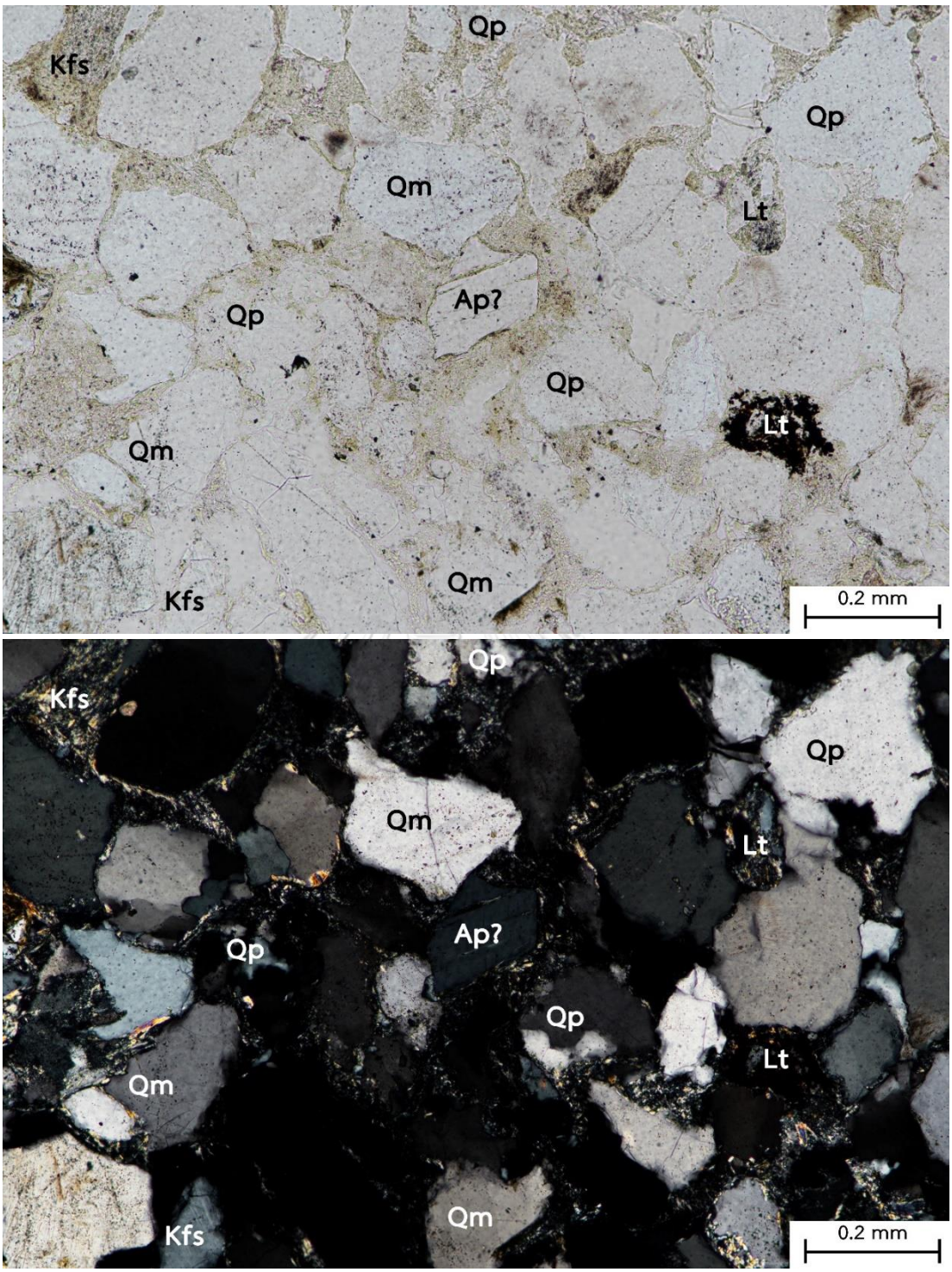

Figure 37 *Photomicrographs of litharenite (sample PP10) from the Phu Phan Formation at the Phu Phan Mountain Range showing well defined clastic texture and grain of quartz, alkaline feldspar, lithic fragments, and apatite. (top) Ordinary light (bottom) Cross polar. (Qm = monocrystalline quartz, Qp = polycrystalline quartz, Kfs = alkaline feldspar, Lt = lithic fragment, and Ap? = apatite?)*

Sample no: PP11

Location: Wat Phuttha Kiri (Lat: 16°27'08"N Long: 104°20'21"E)

Rock name: Sublitharenite

Type of outcrop: Road-cut **Outcrop size:** 1x250 m

Rock units: Sao Khua Formation (Khorat Group)

Figure 38 *Natural outcrop of sandstone of the Sao Khua Formation in front of Wat Phuttha Kiri, Nong Sung District, Mukdahan Province (Geological hammer, 32.5 cm-long, is to scale). White rectangle is the sampling site.*

Macroscopic description

The reddish grey rock sample is medium-grained sandstone and shows a clastic texture. It is a reddish-brown weathering surfaces. The grains are made up mostly of quartz (colorless), feldspar (white), and less opaque minerals and lithic fragments.

Figure 39 *Reddish grey, medium-grained sandstone of the Sao Khua Formation (sample no. PP11).*

Microscopic description

The weathered rock sample shows a clastic texture. The rock compositions are composed of largely of quartz (including monocrystalline quartz and polycrystalline quartz) (78 modal %), with small amount of feldspar (<1 modal %) and lithic fragment (21 modal %). The rock sample are also included of calcite, opaque mineral, apatite, and zircon. The size of mineral is up to 0.1 to 0.5 mm with well sorted. The grains show a high sphericity and subangular shape. The cement of the rock is calcareous.

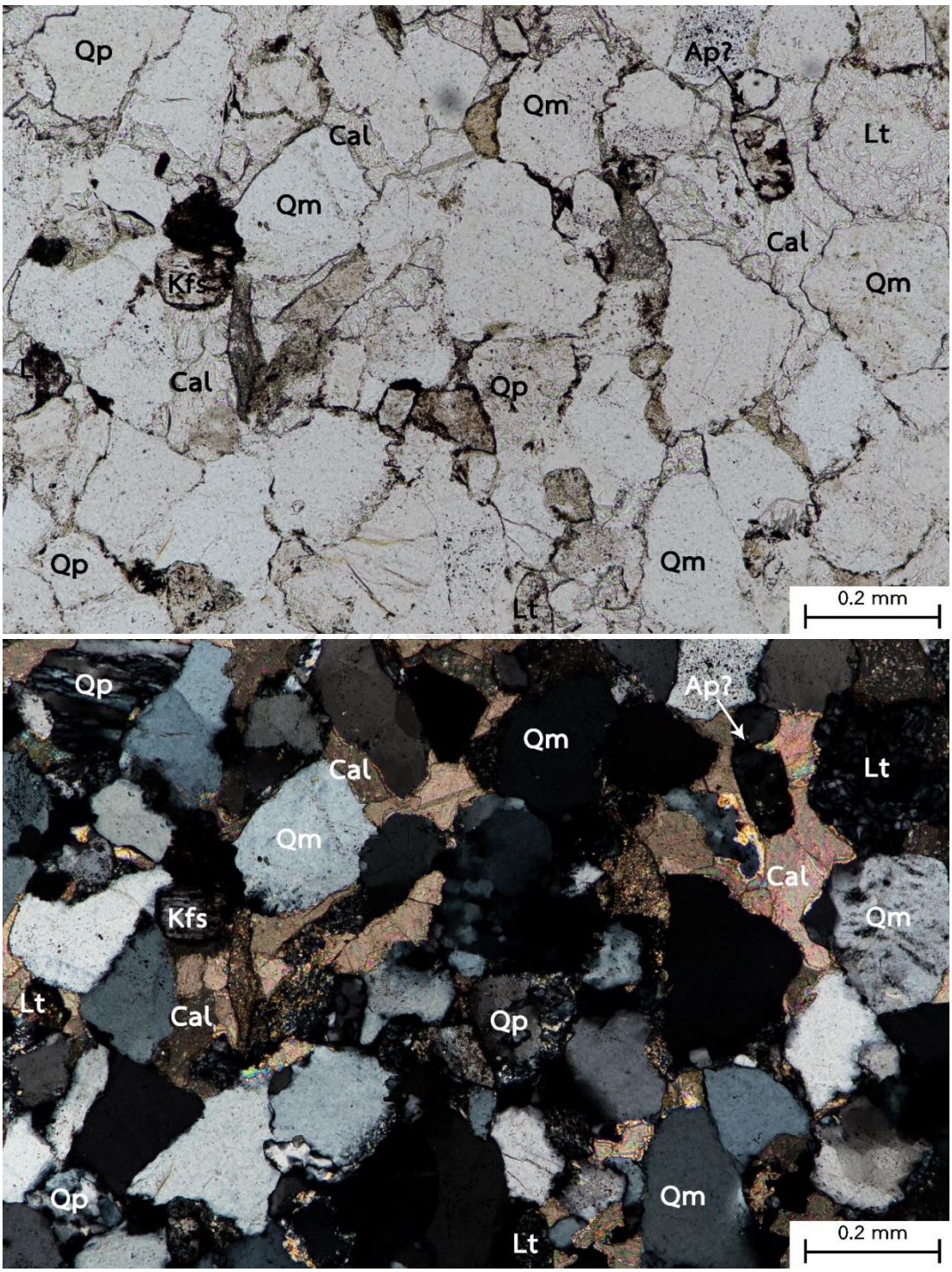

Figure 40 *Photomicrographs of sublitharenite (sample PP11) from the Sao Khua Formation at the Phu Phan Mountain Range showing well defined clastic texture and grain of quartz, alkaline feldspar, lithic fragments, calcite, and apatite. (top) Ordinary light (bottom) Cross polar. (Qm = monocrystalline quartz, Qp = polycrystalline quartz, Kfs = alkaline feldspar, Lt = lithic fragment, Cal = calcite, and Ap? = apatite?)*

Sample no: PP12

Location: Wat Dan Phaya Nak (Lat: 16°20'13"N Long: 104°32'51"E)

Rock name: Litharenite

Type of outcrop: Natural **Outcrop size:** 5x100 m

Rock units: Phu Phan Formation (Khorat Group)

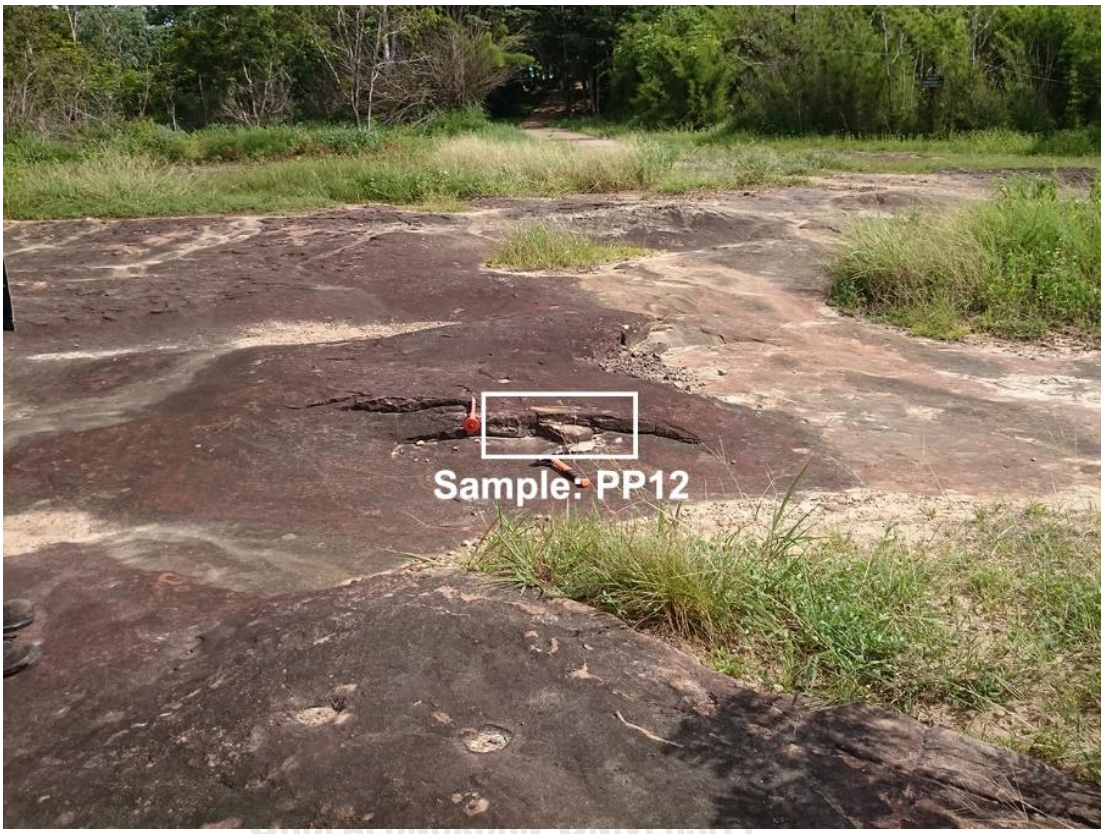

Figure 41 *Natural outcrop of sandstone of the Phu Phan Formation at Wat Dan Phaya Nak, Nikhom Kham Soi District, Mukdahan Province (Orange sledge hammer, 32.5 cm-long, is to scale). White rectangle is the sampling site.*

Macroscopic description

The reddish white rock sample is fine-grained sandstone and shows a clastic texture. It is a reddish-brown weathering surfaces. The grains are made up mostly of quartz (colorless) and opaque minerals and lithic fragments.

Figure 42 *Reddish white, fine-grained sandstone of the Phu Phan Formation (sample no. PP12).*

Microscopic description

The weathered rock sample shows a clastic texture. The rock compositions are composed of largely of quartz (including monocrystalline quartz and polycrystalline quartz) (69 modal %), with small amount of feldspar (<1 modal %) and lithic fragment (31 modal %). The rock sample are also included of muscovite, calcite, amphibole?, opaque mineral, and zircon. The size of mineral is up to 0.1 to 0.6 mm with moderate well sorted. The grains show a low sphericity and angular shape. The cement of the rock is siliceous.

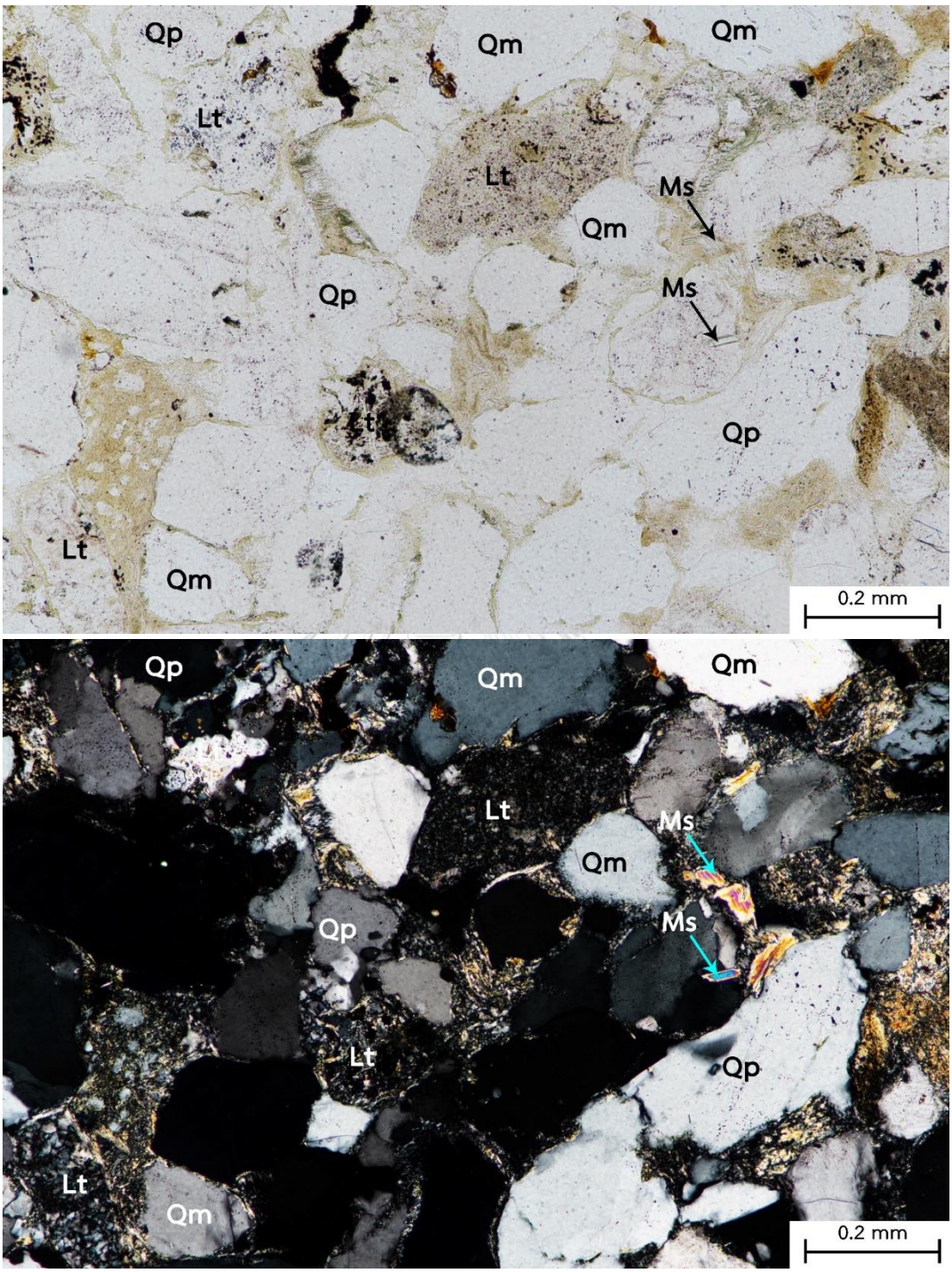

Figure 43 *Photomicrographs of litharenite (sample PP12) from the Phu Phan Formation at the Phu Phan Mountain Range showing well defined clastic texture and grain of quartz, alkaline feldspar, lithic fragments, and muscovite. (top) Ordinary light (bottom) Cross polar. (Qm = monocrystalline quartz, Qp = polycrystalline quartz, Kfs = alkaline feldspar, Lt = lithic fragment, and Ms = muscovite)*

Sample no: PP13

Location: Phu Moo Forest Park (Lat: 16°18'31"N Long: 104°33'00"E)

Rock name: Litharenite

Type of outcrop: Natural **Outcrop size:** 20x50 m

Rock units: Phu Phan Formation (Khorat Group)

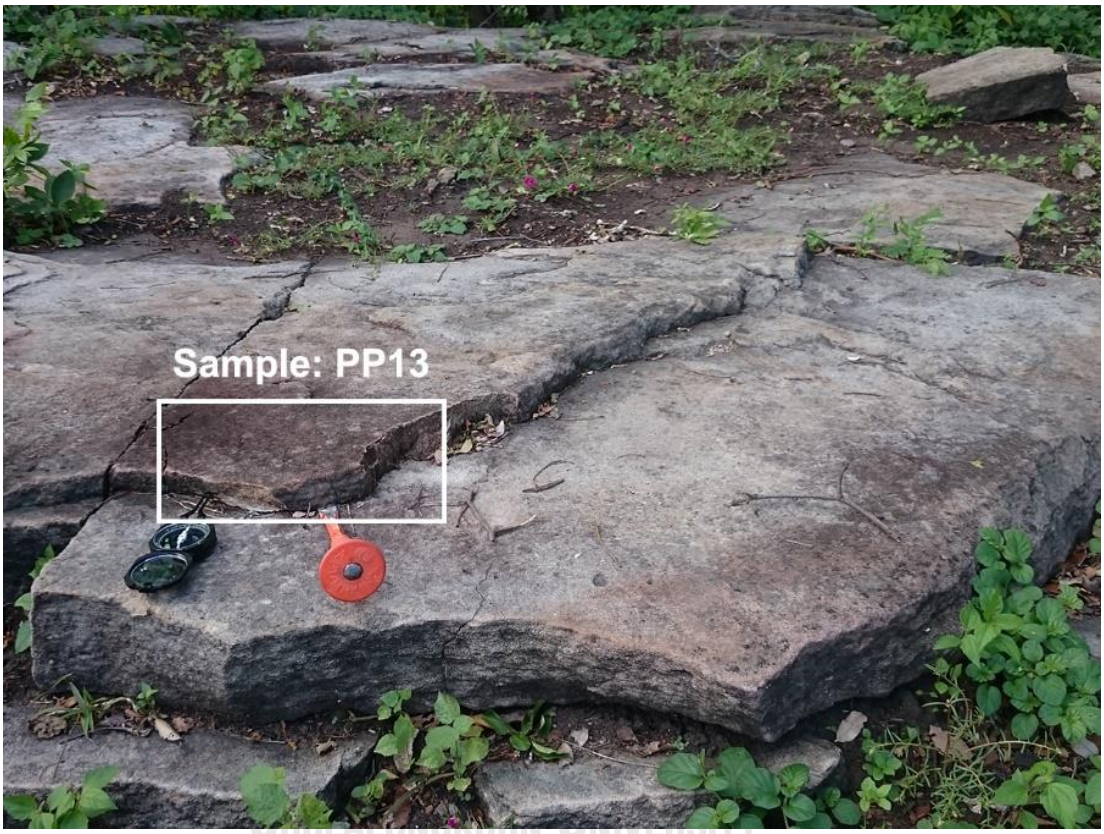

Figure 44 *Natural outcrop of sandstone of the Phu Phan Formation at Phu Moo Forest Park, Nikhom Kham Soi District, Mukdahan Province (Orange wedge, 30 cm-long, is to scale). White rectangle is the sampling site.*

\

Macroscopic description

The pale brown rock sample is medium-grained sandstone and shows a clastic texture. It is a reddish-brown weathering surfaces. The grains are made up mostly of quartz (colorless), feldspar (white), and less opaque minerals and lithic fragments.

Figure 45 *Pale brown, medium-grained sandstone of the Phu Phan Formation (sample no. PP13).*

Microscopic description

The weathered rock sample shows a clastic texture. The rock compositions are composed of largely of quartz (including monocrystalline quartz and polycrystalline quartz) (70 modal %), with small amount of feldspar (1 modal %) and lithic fragment (29 modal %). The rock sample are also included of zircon. The size of mineral is up to 0.1 to 0.7 mm with well sorted. The grains show a low sphericity and angular shape. The cement of the rock is siliceous.

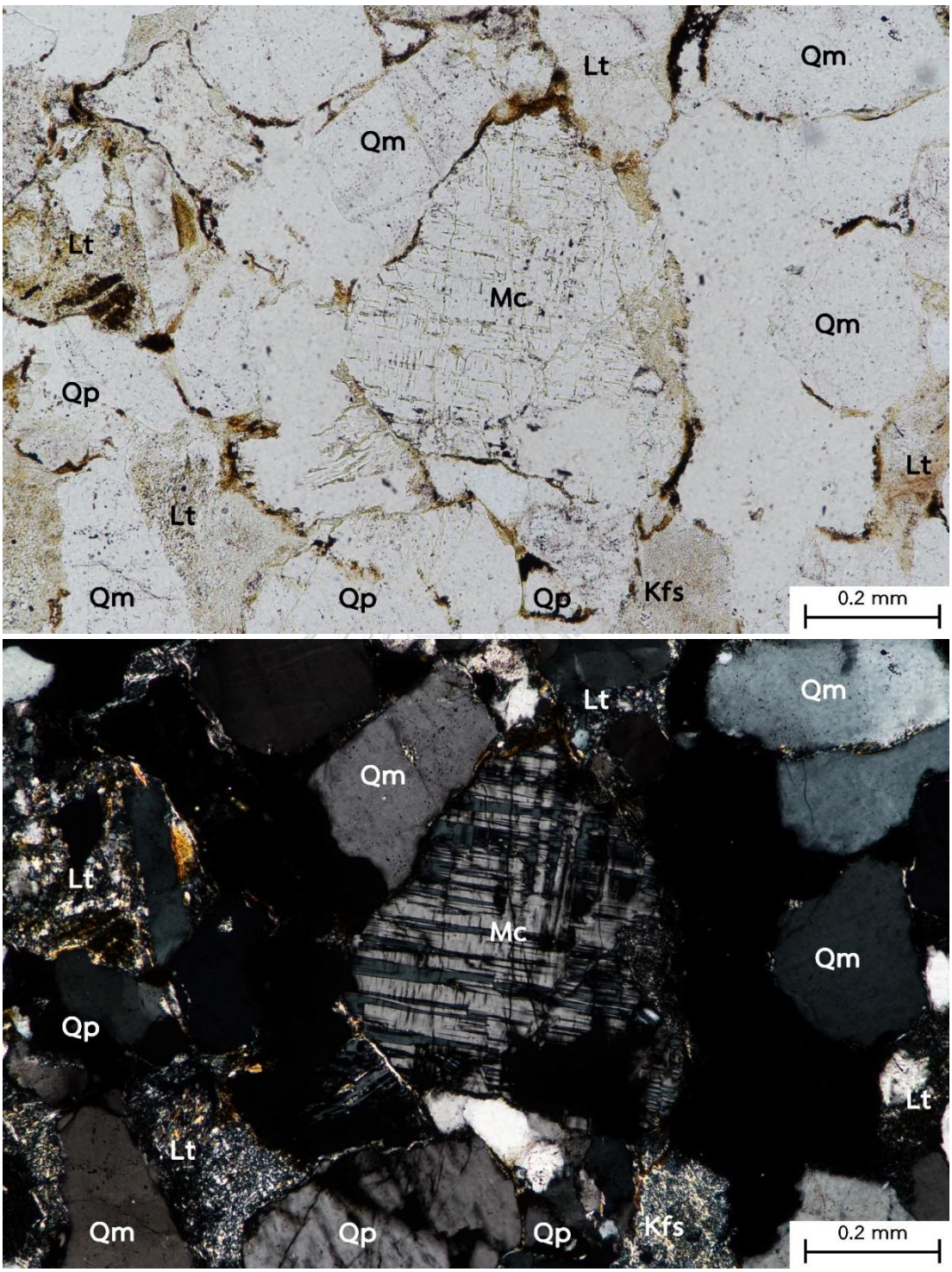

Figure 46 *Photomicrographs of litharenite (sample PP13) from the Phu Phan Formation at the Phu Phan Mountain Range showing well defined clastic texture and grain of quartz, alkaline feldspar and microcline, and lithic fragments. (top) Ordinary light (bottom) Cross polar. (Qm = monocrystalline quartz, Qp = polycrystalline quartz, Kfs = alkaline feldspar, Lt = lithic fragment, Mc = microcline)*

Sample no: PP14

Location: Wat Phu Sung (Lat: 16°07'48"N Long: 104°41'39"E)

Rock name: Litharenite

Type of outcrop: Natural **Outcrop size:** 10x50 m

Rock units: Phu Phan Formation (Khorat Group)

Figure 47 *Natural outcrop of sandstone of the Phu Phan Formation at Wat Phu Sung, Loeng Nok Tha District, Yasothon Province (Orange sledge Hammer, 32.5 cm-long, is to scale). White rectangle is the sampling site.*

Macroscopic description

The white rock sample is medium-grained sandstone and shows a clastic texture. It is a reddish-brown weathering surfaces. The grains are made up mostly of quartz (colorless), feldspar (white), and less opaque minerals and lithic fragments.

Figure 48 *White, medium-grained sandstone of the Phu Phan Formation (sample no. PP14).*

Microscopic description

The weathered rock sample shows a clastic texture. The rock compositions are composed of largely of quartz (including monocrystalline quartz and polycrystalline quartz) (72 modal %), with small amount of feldspar (<1 modal %) and lithic fragment (28 modal %). The rock sample are also included of zircon. The size of mineral is up to 0.2 to 0.8 mm with moderate well sorted. The grains show a low sphericity and angular shape. The cement of the rock is siliceous.

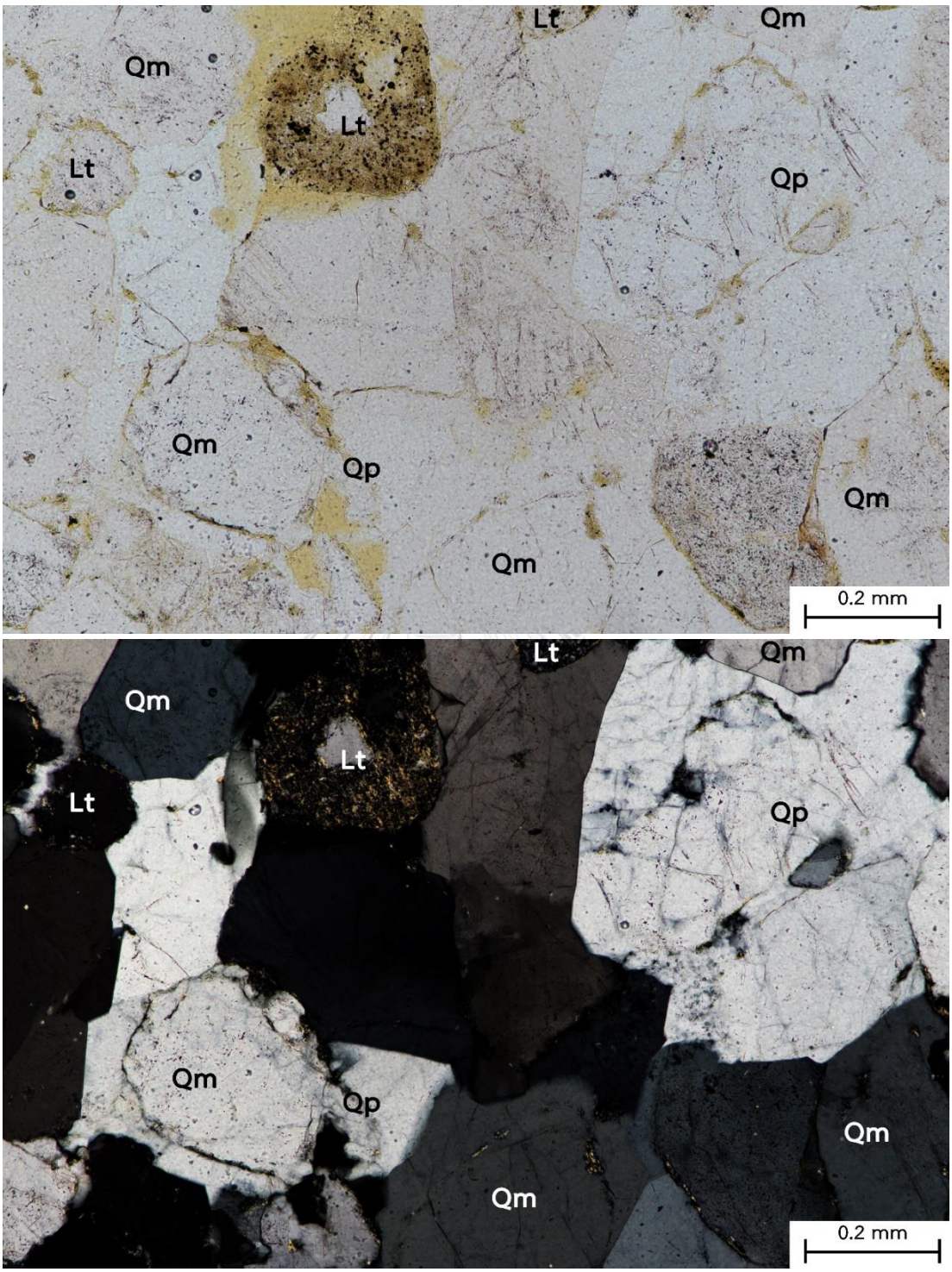

Figure 49 *Photomicrographs of litharenite (sample PP14) from the Phu Phan Formation at the Phu Phan Mountain Range showing well defined clastic texture and grain of quartz and lithic fragments. (top) Ordinary light (bottom) Cross polar. (Qm = monocrystalline quartz, Qp = polycrystalline quartz, Lt = lithic fragment)*

Sample no: PP15

Location: Entrance of Phu Tham Phra temple (Lat: 16°11'41"N Long: 104°51'35"E)

Rock name: Litharenite

Type of outcrop: Natural **Outcrop size:** 5x100 m

Rock units: Phu Phan Formation (Khorat Group)

Figure 50 *Natural outcrop of sandstone of Phu Phan Formation at the entrance of Phu Tham Phra temple, Chanuman District, Amnat Charoen Province (Mr. Sitichok Kumrangwat, 180 cm-tall, is to scale). White rectangle is the sampling site.*

Macroscopic description

The white rock sample is medium-grain sandstone and shows a clastic texture. It is a reddish-brown weathering surfaces. The grains are made up mostly of quartz (colorless), feldspar (white), and less opaque minerals and lithic fragments.

Figure 51 *White, medium-grained sandstone of the Phu Phan Formation (sample no. PP15).*

Microscopic description

The weathered rock sample shows a clastic texture. The rock compositions are composed of largely of quartz (including monocrystalline quartz and polycrystalline quartz) (65 modal %), with small amount of feldspar (3 modal %) and lithic fragment (32 modal %). The rock sample are also included of apatite and zircon. The size of mineral is up to 0.1 to 0.5 mm with well sorted. The grains show a high sphericity and angular shape. The cement of the rock is siliceous.

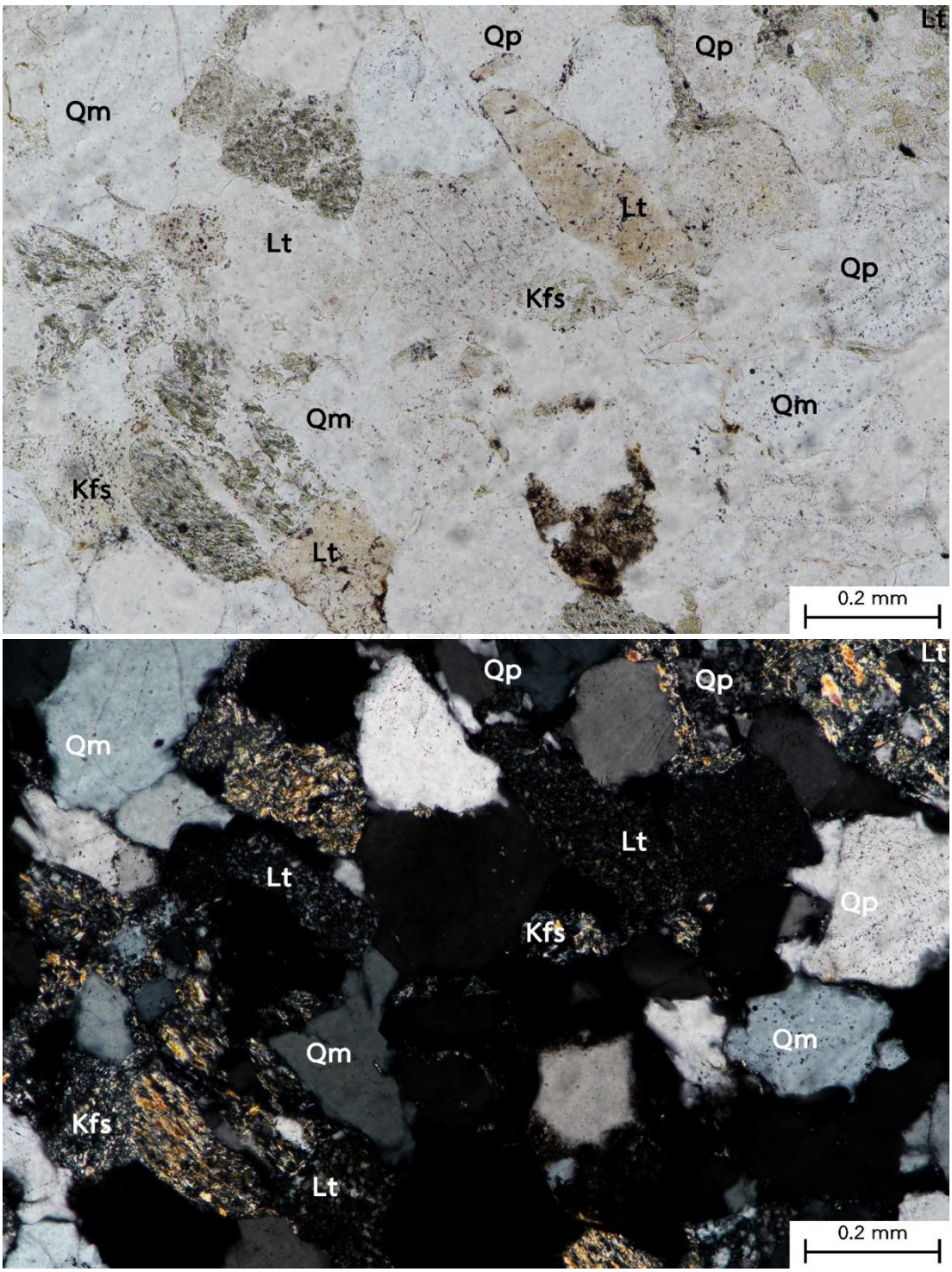

Figure 52 *Photomicrographs of litharenite (sample PP15) from the Phu Phan Formation at the Phu Phan Mountain Range showing well defined clastic texture and grain of quartz, alkaline feldspar, and lithic fragments. (top) Ordinary light (bottom) Cross polar. (Qm = monocrystalline quartz, Qp = polycrystalline quartz, Kfs = alkaline feldspar, and Lt = lithic fragment)*

Sample no: PP16

Location: Sam Phan Bok (Lat: 15°47'53"N Long: 105°23'33"E)

Rock name: Sublitharenite

Type of outcrop: Natural **Outcrop size:** 5x100 m

Rock units: Phu Phan Formation (Khorat Group)

Figure 53 *Natural outcrop of sandstone of the Phu Phan Formation at Sam Phan Bok, Pho Sai District, Ubon Ratchathani (Mr. Sitichok Kumrangwat, 180 cm-tall, is to scale). White rectangle is the sampling site.*

Macroscopic description

The whitish grey rock sample is medium to coarse-grained sandstone and shows a clastic texture. It is a reddish-brown weathering surfaces. The grains are made up mostly of quartz (colorless), feldspar (white), and less opaque minerals and lithic fragments.

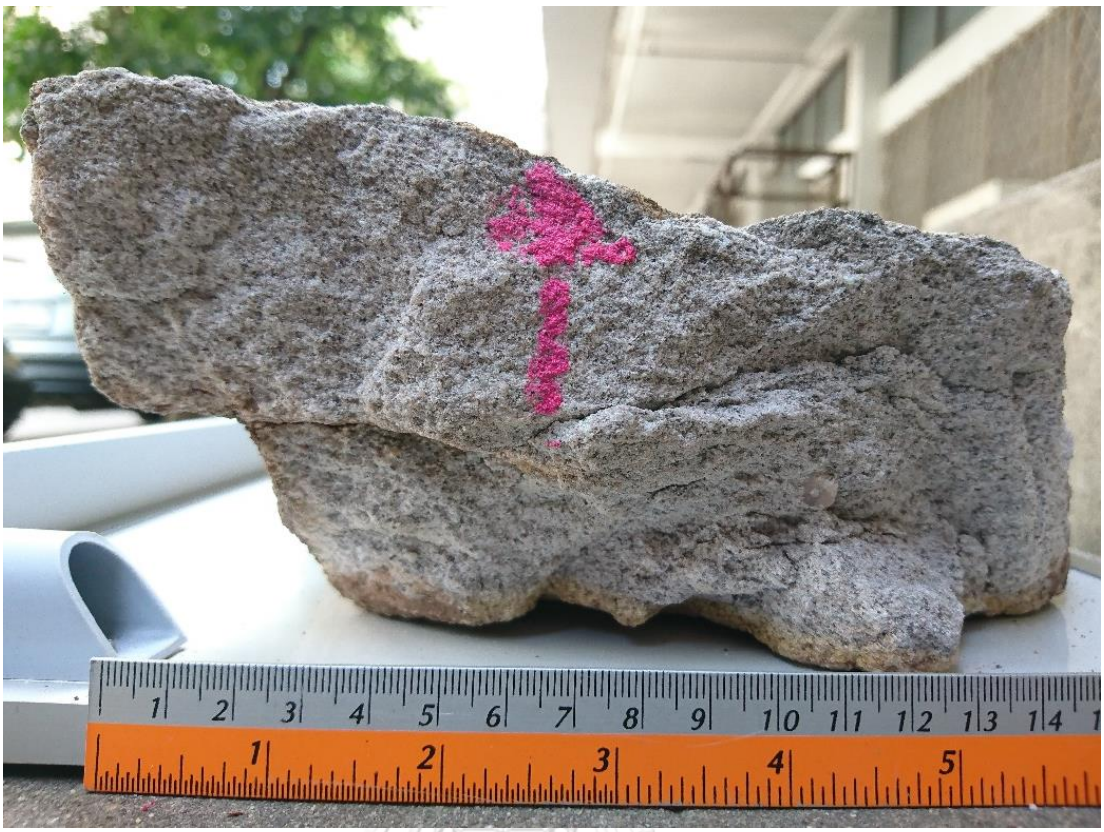

Figure 54 *Whitish grey medium to coarse grained sandstone of the Phu Phan Formation (sample no. PP16).*

Microscopic description

The weathered rock sample shows a clastic texture. The rock compositions are composed of largely of quartz (including monocrystalline quartz and polycrystalline quartz) (80 modal %), with small amount of feldspar (2 modal %) and lithic fragment (18 modal %). The rock sample are also included of calcite, apatite, and zircon. The size of mineral is up to 0.2 to 0.8 mm with well sorted. The grains show a high sphericity and subangular shape. The cement of the rock is siliceous.

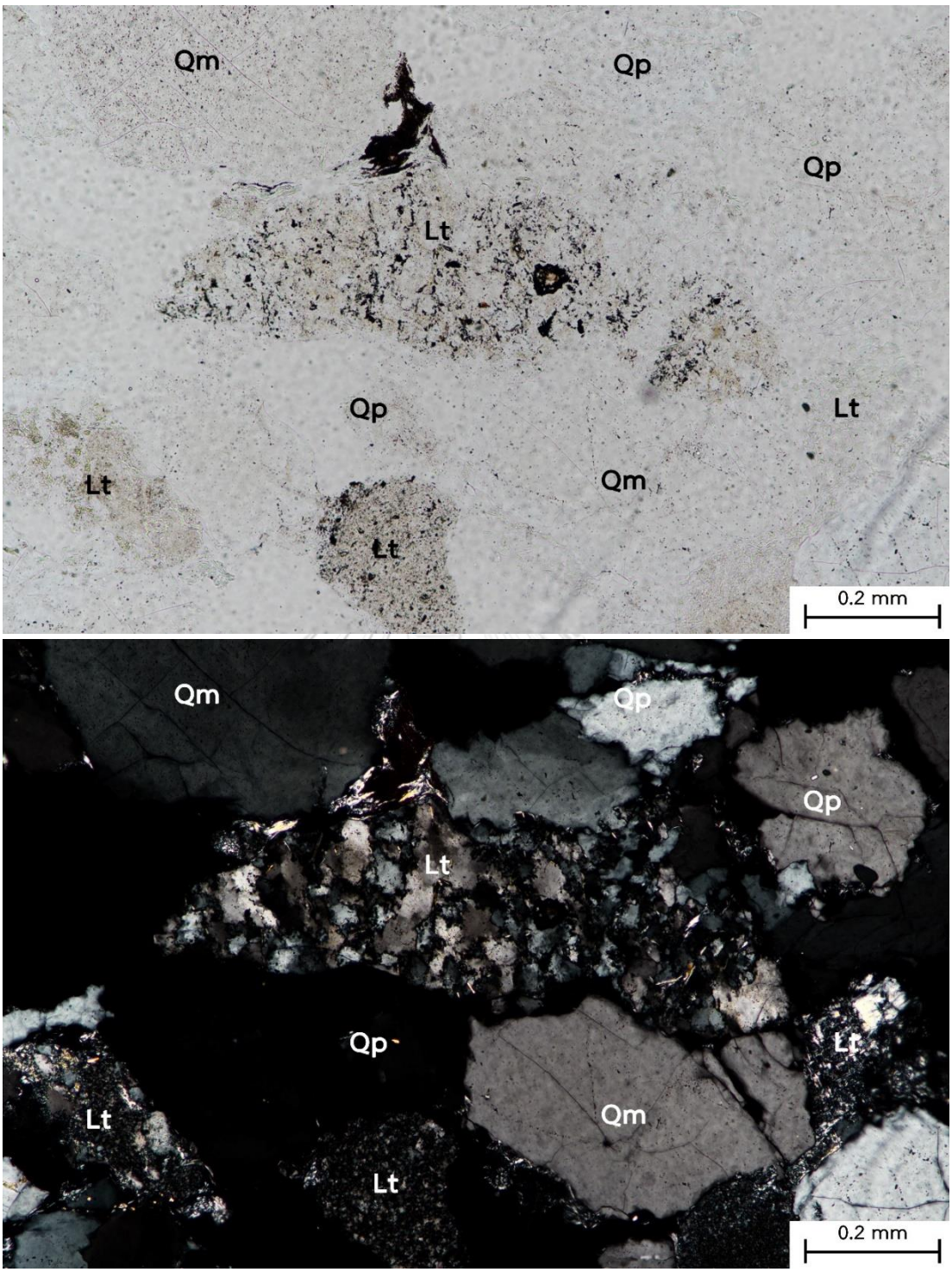

Figure 55 *Photomicrographs of litharenite (sample PP16) from the Phu Phan Formation at the Phu Phan Mountain Range showing well defined clastic texture and grain of quartz and lithic fragments. (top) Ordinary light (bottom) Cross polar. (Qm = monocrystalline quartz, Qp = polycrystalline quartz, and Lt = lithic fragment)*

Sample no: PTT14

Location: Highway 2287 (Lat: 16°45'39”N Long: 104°7'46"E)

Rock name: Feldspathic litharenite

Type of outcrop: Natural **Outcrop size:** 5x200 m

Rock units: Phu Kradung Formation (Khorat Group)

Figure 56 *Natural outcrop of sandstone of the Phu Kradung Formation along the Highway 2287, Nong Phue District, Kalasin Province (Mr. Wason Kongpermpool, 172 cm-tall, is to scale). White rectangle is the sampling site.*

Macroscopic description

The red rock sample is very fine-grain and shows a clastic texture. It is a reddish-brown weathering surfaces. The grains are made up mostly of quartz (colorless), feldspar (white), and less opaque minerals and lithic fragments.

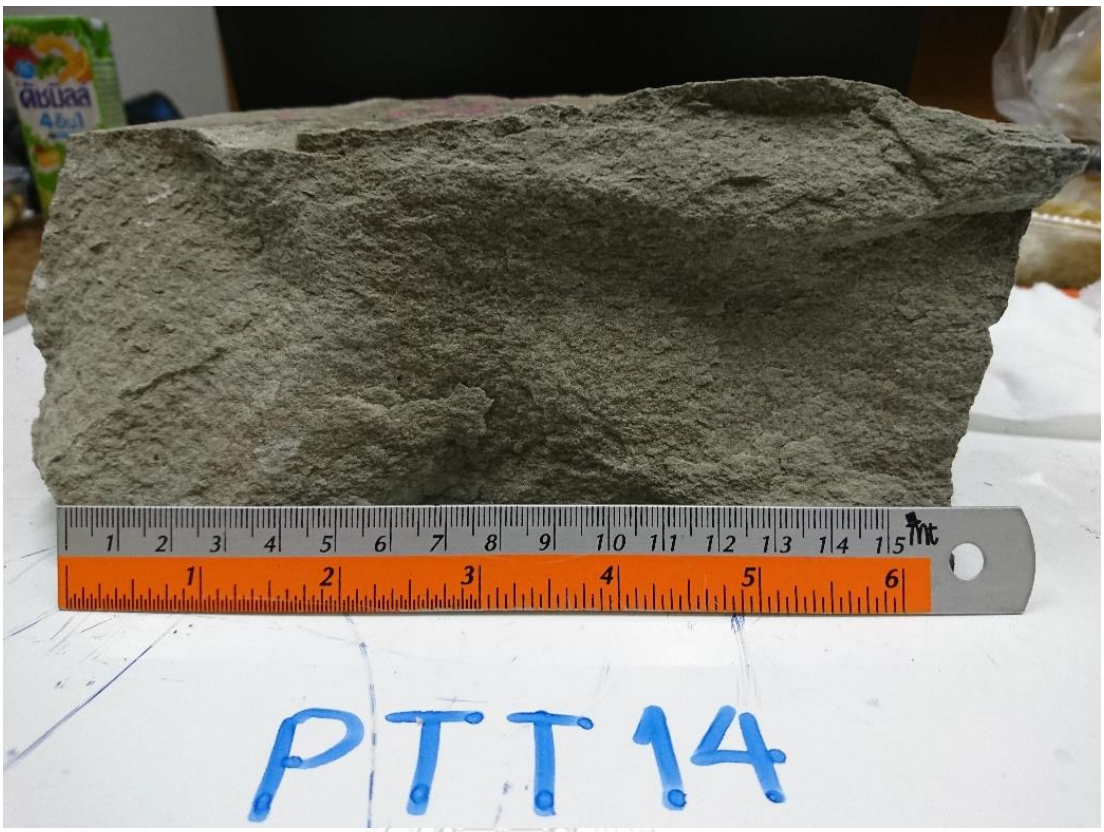

Figure 57 *Red very fine-grained sandstone with faint lamination of the Phu Kradung Formation (sample no. PTT14).*

Microscopic description

The weathered rock sample shows a clastic texture. The rock compositions are composed of largely of quartz (including monocrystalline quartz and polycrystalline quartz) (77 modal %), with small amount of feldspar (11 modal %) and lithic fragment (12 modal %). The rock sample are also included of muscovite, biotite, and apatite. The size of mineral is up to 0.05 to 0.1 mm with well sorted. The grains show a low sphericity and angular shape. The cement of the rock is siliceous.

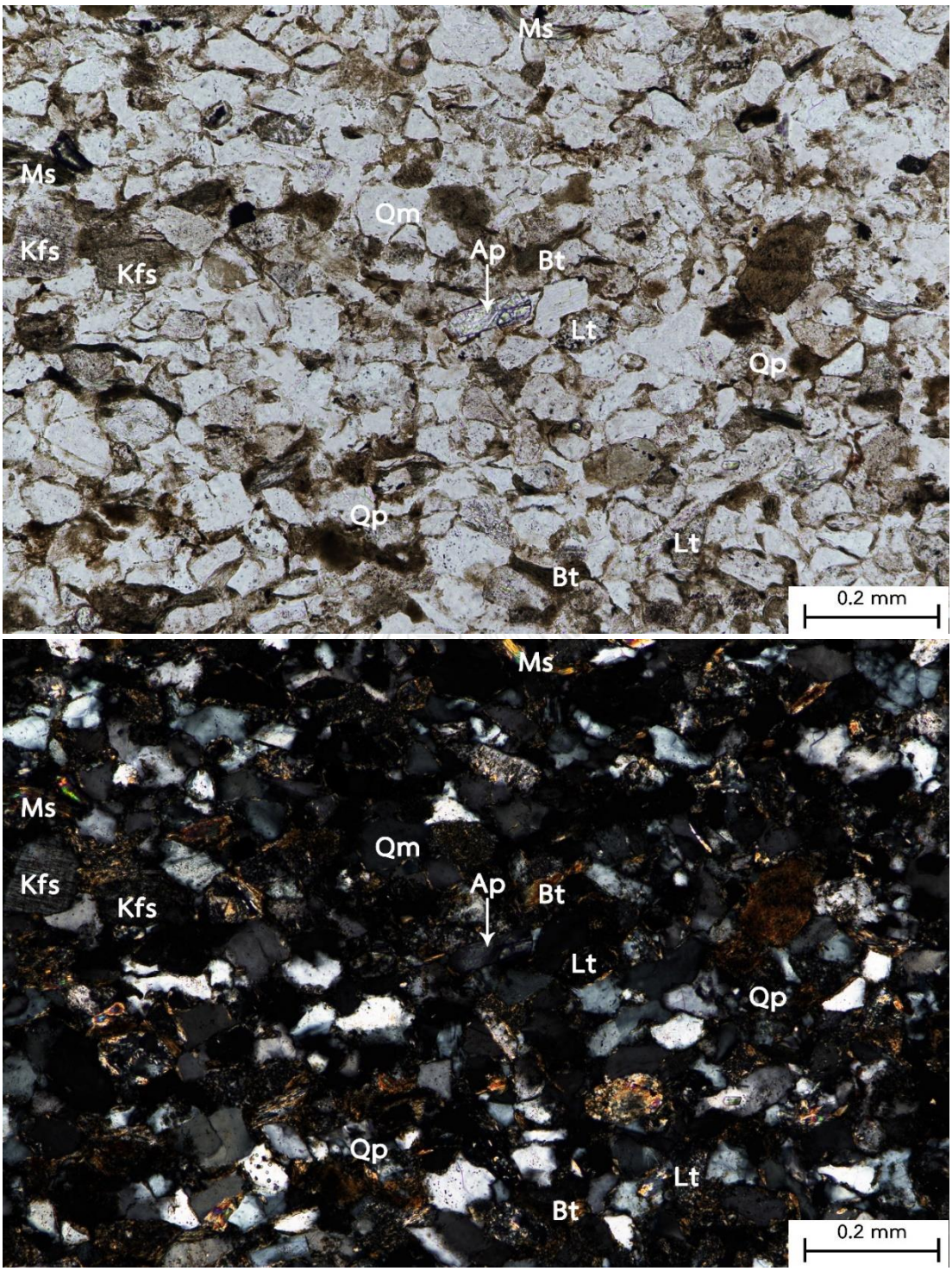

Figure 58 *Photomicrographs of feldspathic litharenite (Sample PTT14) from the Phu Kradung Formation at Phu Phan Mountain Range showing well defined clastic texture and grains of quartz, alkaline feldspar, lithic fragments, muscovite, biotite, and apatite. (top) Ordinary light and (bottom) Cross polar. (Qm = monocrystalline quartz, Qp = polycrystalline quartz, Kfs = alkaline feldspar, Lt = lithic fragment, Ms = muscovite, Bt = biotite, and Ap = apatite)*

Sample no: PTT15

Location: Highway 2358 (Lat: 16°54'12"N Long: 104°10'56"E)

Rock name: Sublitharenite

Type of outcrop: Natural **Outcrop size:** 5x20 m

Rock units: Phu Phan Formation (Khorat Group)

Figure 59 *Natural outcrop of sandstone of the Phu Phan Formation along Highway 2358, Tao Ngoi District, Sakhon Nakhon Province (Right person-Mr. Sitichok Kumrangwat, 180 cm-tall, is to scale). White rectangle is the sampling site.*

Macroscopic description

The red rock sample is very fine-grain and shows a clastic texture. It is a reddish-brown weathering surfaces. The grains are made up mostly of quartz (colorless), feldspar (white), and less opaque minerals and lithic fragments.

Figure 60 *Reddish brown fine-grained sandstone of the Phu Phan Formation (sample no. PTT15).*

Microscopic description

The weathered rock sample shows a clastic texture. The rock compositions are composed of largely of quartz (including monocrystalline quartz and polycrystalline quartz) (86 modal %), with small amount of feldspar (5 modal %) and lithic fragment (9 modal %). The rock sample are also included of muscovite, biotite, and apatite. The size of mineral is up to 0.05 to 0.2 mm with moderate well sorted. The grains show a low sphericity and angular shape. The cement of the rock is calcareous.

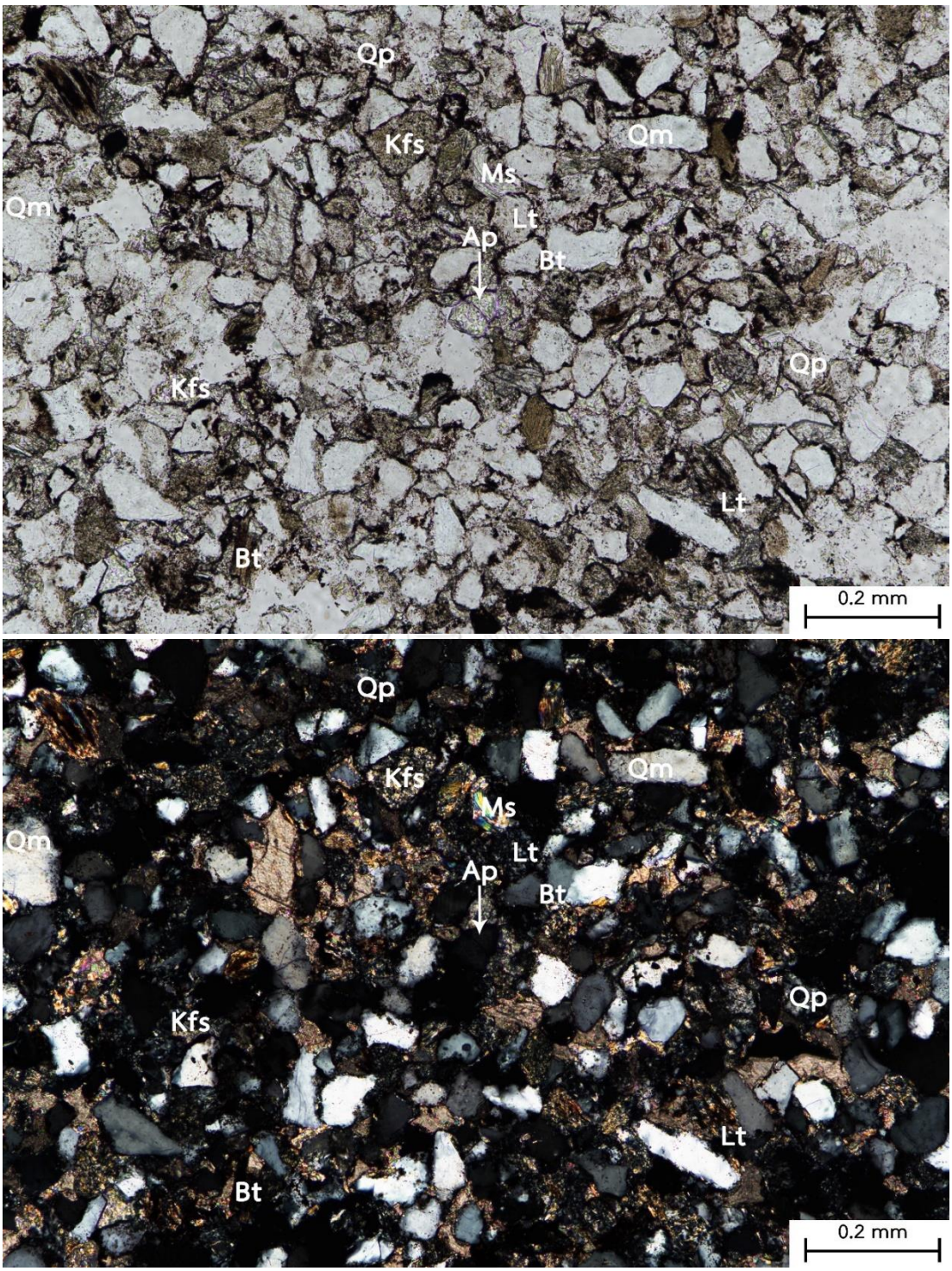

Figure 61 *Photomicrographs of sublitharenite (sample PTT15) from the Phu Phan Formation at Phu Phan Mountain Range showing well defined clastic texture and grains of quartz, alkaline feldspar, lithic fragments, muscovite, biotite, and apatite. (top) Ordinary light and (bottom) Cross polar. (Qm = monocrystalline quartz, Qp = polycrystalline quartz, Kfs = alkaline feldspar, Lt = lithic fragment, Ms = muscovite, Bt = biotite, and Ap = apatite)*

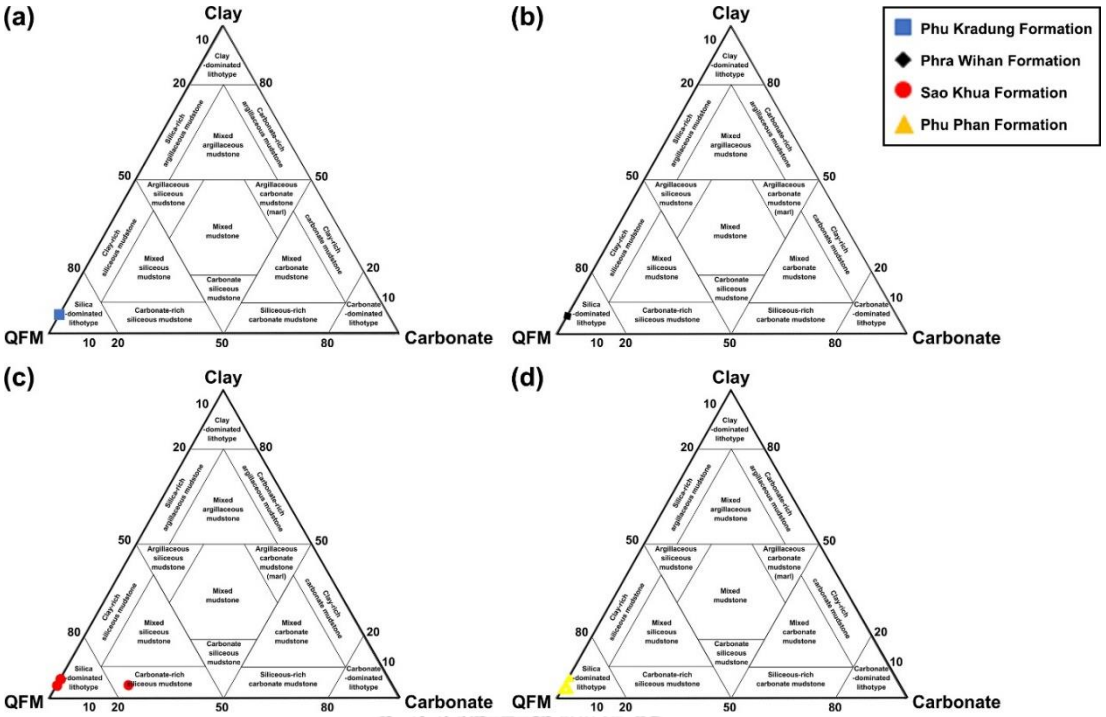

Figure 62 The ternary plot showing the most samples from (a) Phu Kradung Formation, (b) Phra Wihan Formation, (c) Sao Khua Formation, and (d) Phu Phan Formation were dominated by quartz rather than by clay and carbonate (after Gamero-Diaz et al., 2013).

Table 1 Attitude of joint plane in this study

Site	Strike/Dip	Site	Strike/Dip	Site	Strike/Dip	Site	Strike/Dip
PP02	240/80,	**PP02**	193/63,	**PTT14**	065/16,	**PTT14**	310/05,
	190/10,		290/86,		065/80,		175/75,
	351/62,		285/10,		075/05,		163/77,
	257/83,		328/19,		305/50,		083/25,
	295/70,		168/03,		060/08,		177/88,
	115/80,		299/15,		310/19,		133/45
	095/88,		335/14		128/70,	**PTT15**	246/80,
	180/85,	**PP05-3**	279/76,		153/65,		160/88,
	090/78,		188/79		170/85,		345/75,
	170/89,	**PP09**	222/86,		096/25,		190/05,
	153/65,		107/10,		155/50,		170/80
	140/70,		296/84		160/60,		
	150/85,	**PP13**	275/89,		288/80,		
	176/82,		183/80		203/80,		

APPENDIX B: Zoomed cross sections of this study

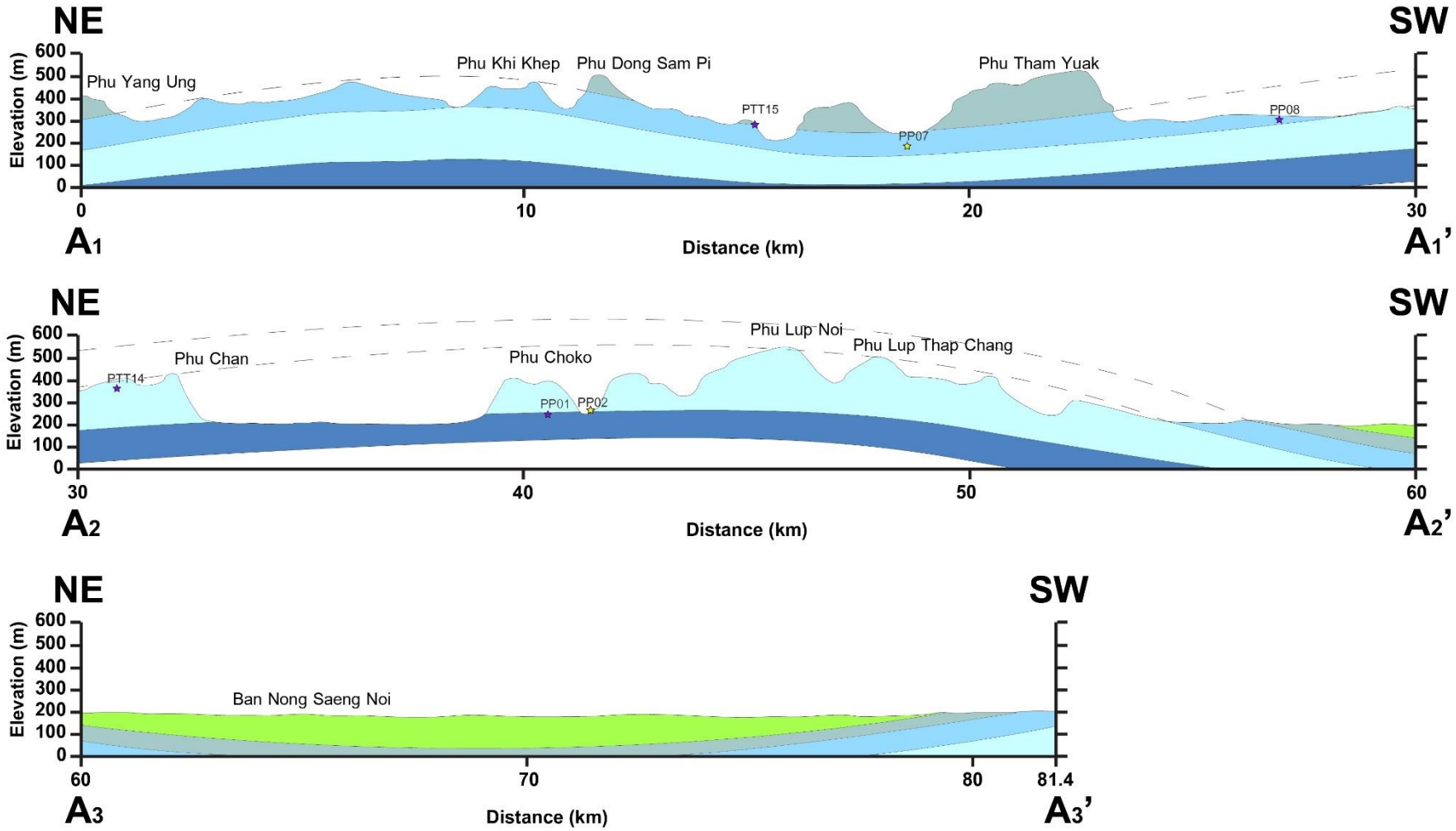

Figure 1 Three subdivided cross sections of AA' cross section line.

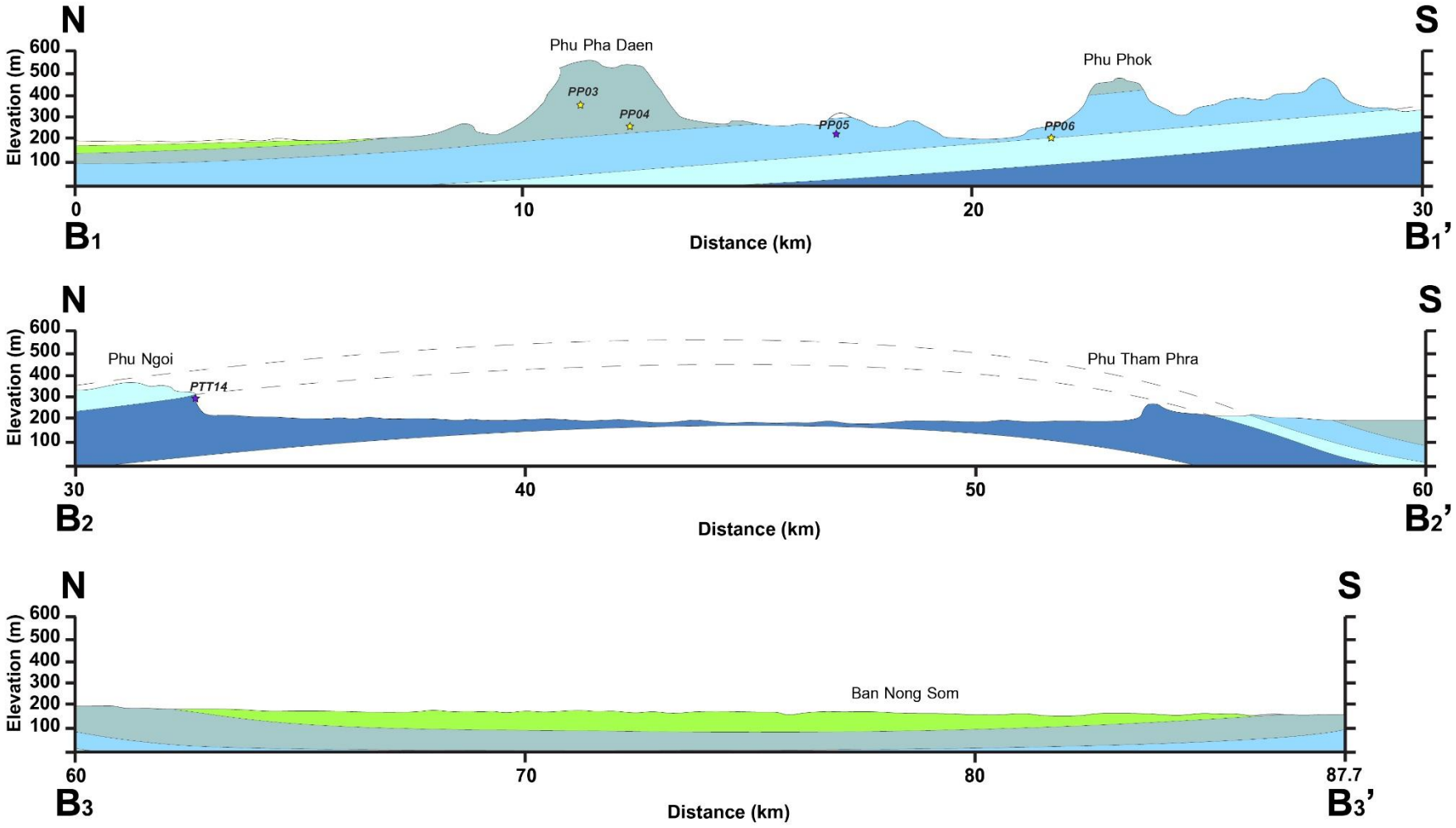

Figure 2 Three subdivided cross sections of BB' cross section line.

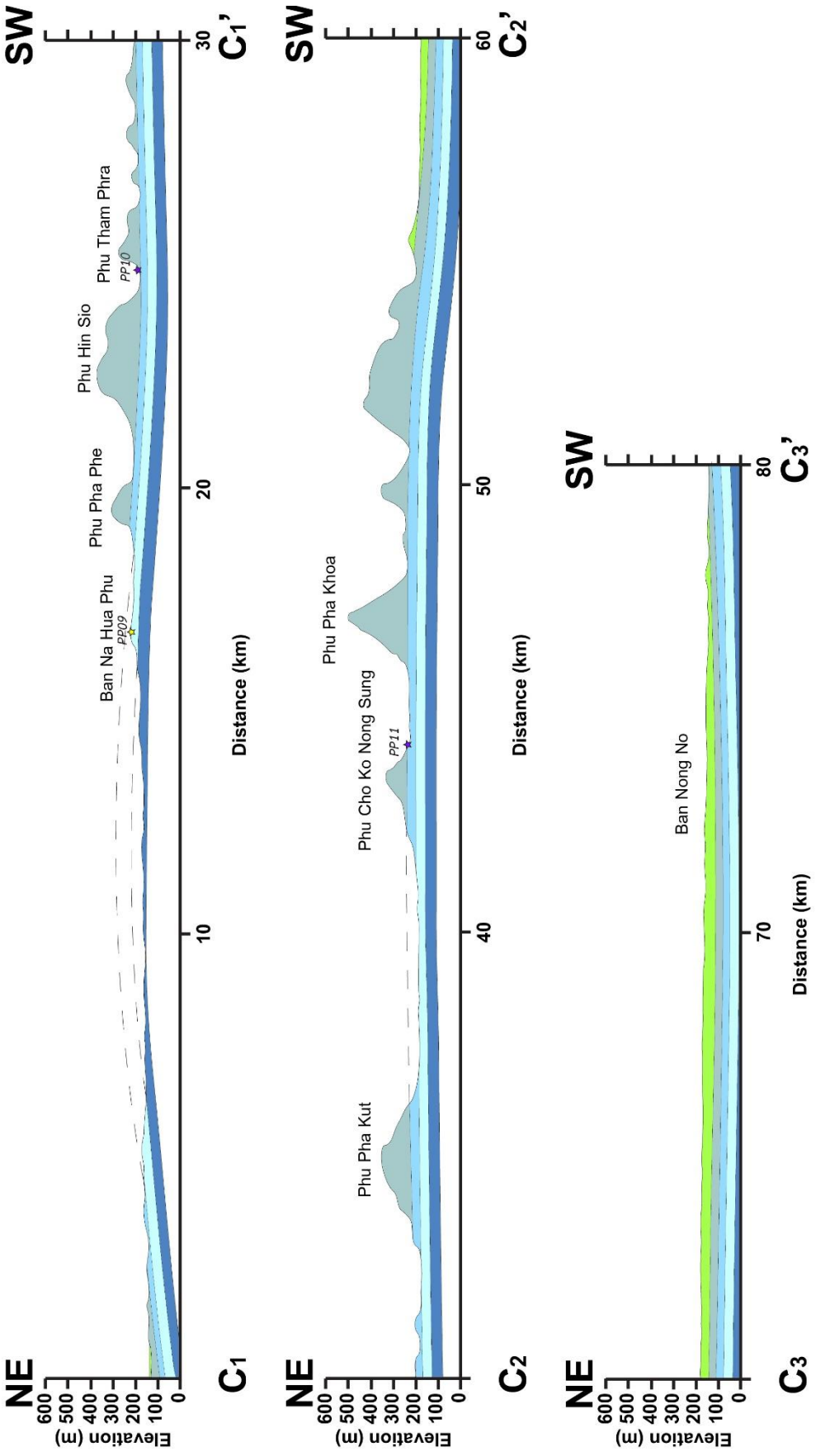

Figure 3 Three subdivided cross sections of CC' cross section line.

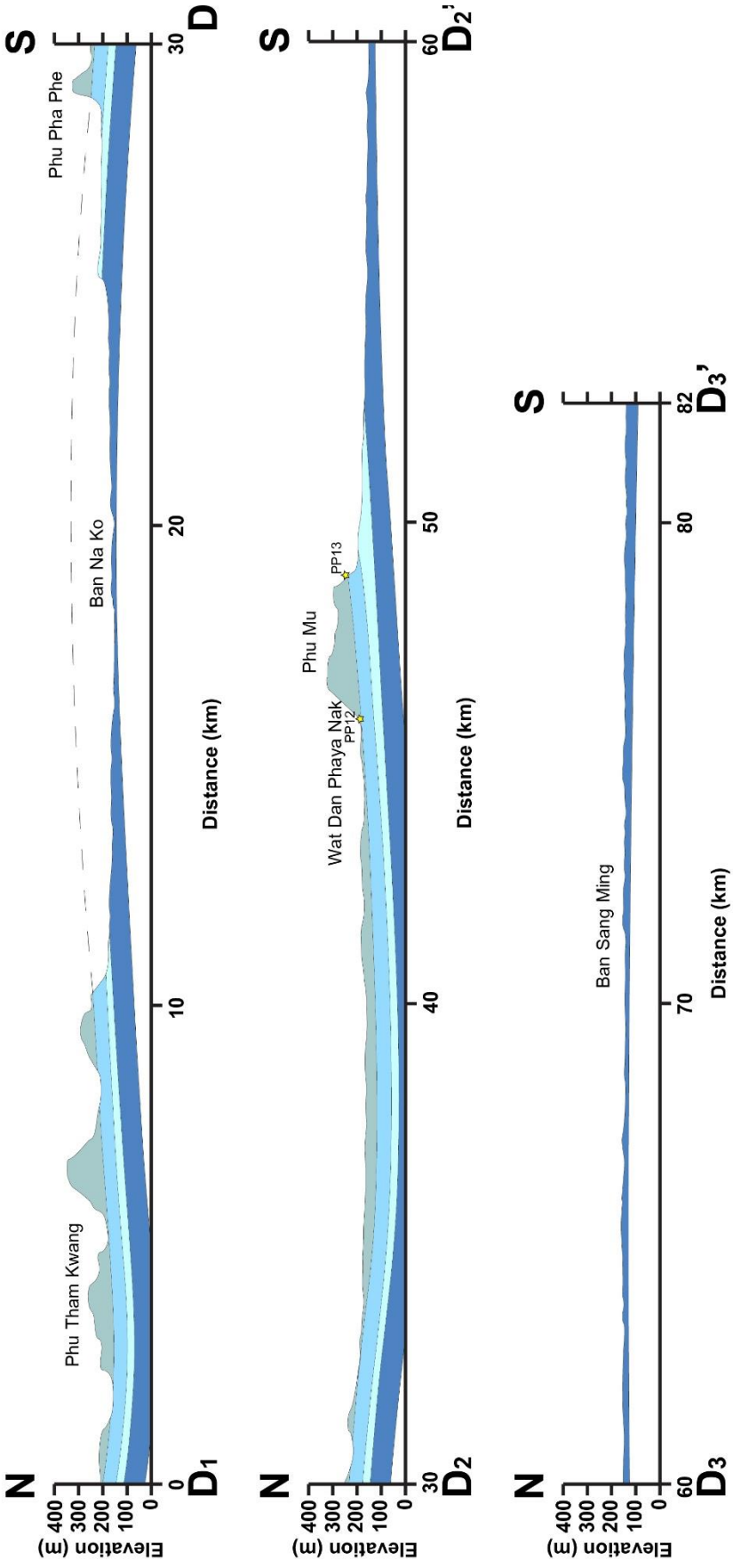

Figure 4 Three subdivided cross sections of DD' cross section line.

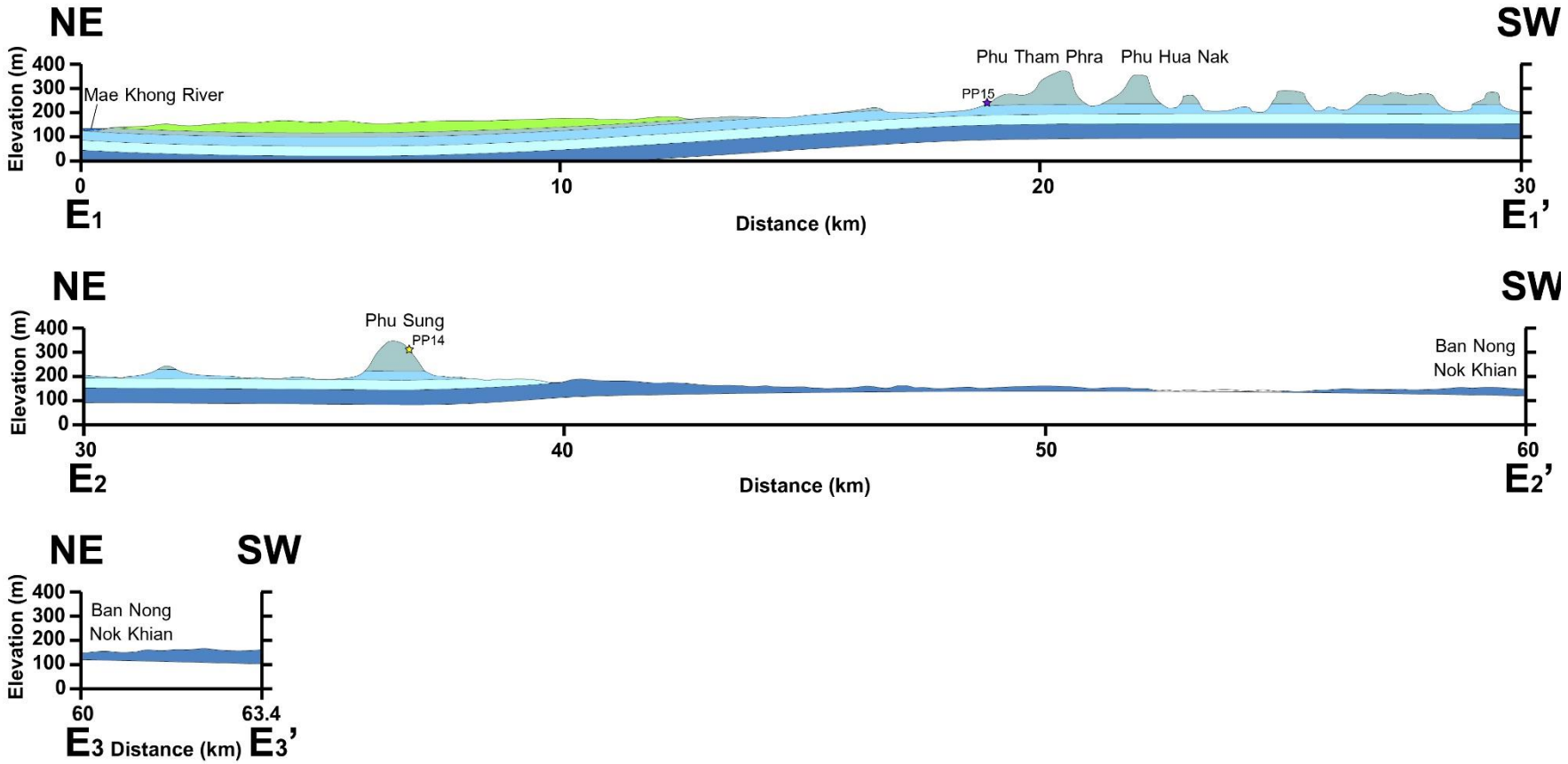

Figure 5 Three sudivided cross sections of EE' cross section line.

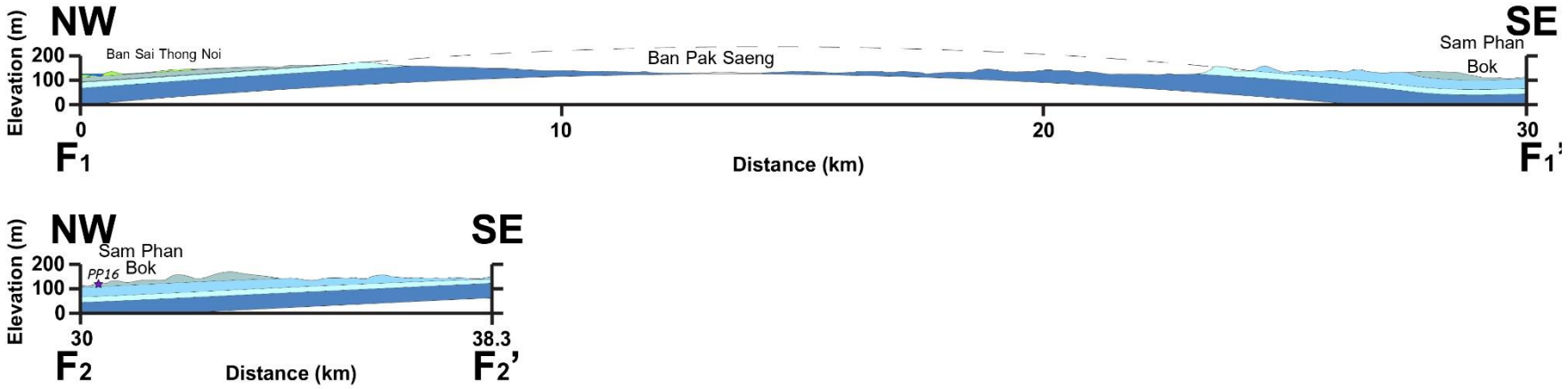

Figure 6 Two subdivided cross sections of FF cross section line.

APPENDIX C: LA-ICP-MS data and pooled AFT age

Table 1 The LA-ICP-MS data and fission track-dating from sample DUR.

DUR grain ID	spot ID	LA-ICP-MS data												FT dating									
		Ap						NIST610						Ap/ NIST610 ($^{238}U/^{43}Ca$)	SE (%)	U (μg/g)	Average Ap/ NIST610	SE (%)	ρ_s (10^6/ cm^2)	Ns	A (μm^2)	T (Ma)	σ (Ma)
		$^{238}U/^{43}Ca$	SE (%)	$^{238}Th/^{43}Ca$	SE (%)	$^{206}Pb/^{238}U$	SE (%)	$^{238}U/^{43}Ca$	SE (%)	$^{238}Th/^{43}Ca$	SE (%)	$^{206}Pb/^{238}U$	SE (%)										
1	a	0.0167	2.0340	0.2389	2.1980	0.0141	10.7899	4.2924	1.9827	3.2744	0.8381	0.2390	0.5985	0.0039	2.84	8.5378	0.0040	1.62	0.1331	84	92500	30.6	3.5
	b	0.0170	1.8584	0.2382	1.6440	0.0086	15.6185	4.2930	3.1033	3.2763	0.8490	0.2389	0.6076	0.0039	3.62	8.6508							
	c	0.0173	1.7088	0.2433	1.2947	0.0102	12.7771	4.2935	4.2239	3.2783	0.8598	0.2389	0.6167	0.0040	4.56	8.8276							
	d	0.0182	1.7492	0.2556	1.7159	0.0098	14.7442	4.2950	7.5856	3.2841	0.8924	0.2387	0.6440	0.0042	7.78	9.2885							
2	a	0.0192	1.8114	0.2345	1.9232	0.0096	13.3278	4.1395	0.8567	3.1836	0.8940	0.2456	0.7383	0.0046	2.00	2.2032	0.0048	1.06	0.1989	184	63100	38.5	3.0
	b	0.0206	2.6241	0.2464	1.8556	0.0074	13.8330	4.1700	0.8578	3.2014	0.8807	0.2443	0.7085	0.0049	2.76	10.8109							
	c	0.0197	2.3948	0.2356	1.7026	0.0077	14.5261	4.2005	0.8589	3.2191	0.8673	0.2430	0.6787	0.0047	2.54	10.2660							
	d	0.0203	1.9312	0.2445	1.9747	0.0085	11.0263	4.2310	0.8599	3.2369	0.8540	0.2417	0.6489	0.0048	2.11	10.4846							
	e	0.0208	2.2786	0.2539	1.6540	0.0089	12.7833	4.2614	0.8610	3.2547	0.8406	0.2404	0.6192	0.0049	2.44	10.7013							
														Weighted mean							35.9	2.3
														Pooled mean			0.0045	0.89	0.1722	268	155600	35.6	2.4

*Pooled AFT age is calculated with ζ_{MS}= 0.928±0.022

Table 2 The LA-ICP-MS data and fission-track dating from sample FCT.

FCT grain ID	spot ID	LA-ICP-MS data												FT dating								
		Ap						NIST610						Ap/ NIST610 ($^{238}U/^{43}Ca$)	SE (%)	U (μg/g)	Average Ap/ NIST610	SE (%)	ρ_s (10^6/ cm^2)	Ns	A (μm^2)	T (Ma)	σ (Ma)
		$^{238}U/^{43}Ca$	SE (%)	$^{238}Th/^{43}Ca$	SE (%)	$^{206}Pb/^{238}U$	SE (%)	$^{238}U/^{43}Ca$	SE (%)	$^{238}Th/^{43}Ca$	SE (%)	$^{206}Pb/^{238}U$	SE (%)										
1	a	0.0293	1.8016	0.0663	1.8297	0.0654	3.7597	4.28623	8.26631	3.2728	0.9413	0.2369	0.7016	0.0068	8.46	14.9487	0.0061	6.25	0.1595	20	12537.99	24.2	5.6
	b	0.0250	1.6921	0.0689	1.6571	0.0722	3.1192	4.28157	8.04635	3.2662	0.9603	0.2361	0.7259	0.0058	8.22	12.7968							
	c	0.0291	2.1784	0.0807	2.1348	0.0665	2.7542	4.27691	7.82639	3.2596	0.9794	0.2353	0.7501	0.0068	8.12	14.9105							
	d	0.0213	1.6126	0.0556	1.7320	0.0842	3.2790	4.27225	7.60643	3.2530	0.9984	0.2344	0.7744	0.0050	7.78	10.9176							
3	a	0.0186	1.7127	0.0501	1.6847	0.0959	2.9679	4.26759	7.38647	3.2464	1.0175	0.2336	0.7987	0.0044	7.58	9.5571	0.0065	14.21	0.2512	27	10747.94	35.5	8.5
	b	0.0302	1.8362	0.0914	1.6041	0.0626	2.5378	4.28011	7.38682	3.2514	1.0168	0.2328	0.7928	0.0071	7.61	15.4660							
	c	0.0352	1.8173	0.0972	1.6822	0.0507	2.5483	4.29729	7.60714	3.2630	0.9972	0.2328	0.7627	0.0082	7.82	17.9668							
4	a	0.0377	1.6944	0.1079	1.6163	0.0489	2.3820	4.31448	7.82745	3.2746	0.9775	0.2328	0.7325	0.0087	8.01	19.1242	0.0087	0.22	0.2733	20	7316.87	29.1	6.5
	b	0.0376	1.6605	0.1114	1.6293	0.0469	3.1411	4.33166	8.04776	3.2863	0.9579	0.2328	0.7024	0.0087	8.22	19.0033							
5	a	0.0161	2.2437	0.0390	2.0008	0.1048	3.7293	4.34884	8.26807	3.2979	0.9382	0.2328	0.6723	0.0037	8.57	8.0975	0.0048	15.94	0.1321	6	4542.06	25.6	10.5
	b	0.0255	2.0022	0.0643	1.7769	0.0710	2.9995	4.36603	8.48838	3.3095	0.9185	0.2328	0.6421	0.0058	8.72	12.8115							
6	a	0.0307	2.1859	0.0854	2.0660	0.0582	4.0618	4.37351	6.47134	3.3206	0.8930	0.2308	0.6677	0.0070	6.83	15.3657	0.0068	4.76	0.2534	35	13814.63	34.3	5.9
	b	0.0324	1.9828	0.0894	2.0141	0.0564	3.5885	4.36866	5.35267	3.3203	0.8900	0.2298	0.6955	0.0074	5.71	16.2332							
	c	0.0265	1.6792	0.0707	1.8207	0.0669	3.0872	4.36381	4.23399	3.3200	0.8870	0.2288	0.7234	0.0061	4.55	13.2922							
8	a	0.0157	1.9492	0.0315	2.0827	0.1103	3.5577	4.35897	3.11532	3.3198	0.8841	0.2279	0.7512	0.0036	3.67	7.8779	0.0035	1.21	0.2347	20	8520.31	61.3	13.8
	b	0.0151	1.7110	0.0325	1.8563	0.1169	3.7148	4.35412	1.99664	3.3195	0.8811	0.2269	0.7791	0.0035	2.63	7.6124							
9	a	0.0361	1.9501	0.0912	1.9735	0.0553	3.6215	4.34605	0.88708	3.3130	0.8723	0.2260	0.7955	0.0083	2.14	18.2119	0.0077	4.66	0.2499	14	5601.73	29.9	8.0
	b	0.0348	2.3487	0.0939	2.2526	0.0584	4.4442	4.34283	0.89619	3.3068	0.8665	0.2262	0.7841	0.0080	2.51	17.5701							
	c	0.0298	1.6006	0.0817	1.5894	0.0613	3.5290	4.33961	0.9053	3.3006	0.8606	0.2263	0.7726	0.0069	1.84	15.0423							
28	a	0.0180	1.8544	0.0409	2.0306	0.0985	3.4331	4.33639	0.91441	3.2943	0.8547	0.2264	0.7612	0.0041	2.07	9.0712	0.0048	9.87	0.2509	12	4782.27	48.2	14.0
	b	0.0238	1.8003	0.0549	1.3107	0.0775	2.9746	4.33317	0.92352	3.2881	0.8489	0.2265	0.7498	0.0055	2.02	12.0139							
33	a	0.0295	1.6841	0.0859	1.7576	0.0595	3.4025	4.32995	0.93263	3.2819	0.8430	0.2266	0.7384	0.0068	1.93	14.8983	0.0078	7.54	0.3406	47	13798.45	40.6	6.0
	b	0.0317	1.8972	0.0905	1.5953	0.0570	2.7507	4.31932	0.96188	3.2844	0.8869	0.2273	0.7147	0.0073	2.13	16.0667							
	c	0.0396	1.5026	0.1077	1.3367	0.0449	3.2676	4.31561	0.97195	3.2888	0.9118	0.2276	0.7085	0.0092	1.79	20.0844							
34	a	0.0150	2.5976	0.0364	2.5159	0.1190	3.1784	4.31191	0.98203	3.2932	0.9366	0.2279	0.7024	0.0035	2.78	7.6048	0.0035	2.78	0.1441	3	2081.41	38.4	22.2
36	a	0.0434	1.8142	0.1213	1.6713	0.0428	3.2270	4.3082	0.9921	3.2976	0.9615	0.2282	0.6962	0.0101	2.07	22.0629	0.0098	2.12	0.3339	16	4791.80	31.6	8.0
	b	0.0408	1.5254	0.1127	1.5823	0.0444	2.6846	4.3045	1.00217	3.3019	0.9864	0.2285	0.6901	0.0095	1.83	20.7770							

*Pooled AFT age is calculated with ζ_{MS}= 0.928±0.022

Table 2 (cont.)

FCT grain ID	spot ID	LA-ICP-MS data												FT dating									
		Ap						NIST610						Ap/ NIST610 ($^{238}U/^{43}Ca$)	SE (%)	U (μg/g)	Average Ap/ NIST610	SE (%)	ρ_s (10^6/ cm^2)	Ns	A (μm^2)	T (Ma)	σ (Ma)
		$^{238}U/^{43}Ca$	SE (%)	$^{238}Th/^{43}Ca$	SE (%)	$^{206}Pb/^{238}U$	SE (%)	$^{238}U/^{43}Ca$	SE (%)	$^{238}Th/^{43}Ca$	SE (%)	$^{206}Pb/^{238}U$	SE (%)										
44	a	0.0025	2.8746	0.0076	2.0852	0.8233	4.3919	3.90872	0.7799	3.1192	0.7841	0.2490	0.6005	0.0006	2.98	1.3760	0.0007	10.25	0.0854	5	5855.22	107.0	47.9
	b	0.0033	2.9336	0.0102	2.4845	0.6064	3.7464	3.90356	0.7747	3.1107	0.7906	0.2482	0.5938	0.0008	3.03	1.8424							
45	a	0.0227	2.3781	0.0581	2.0539	0.0735	3.1504	3.89841	0.76949	3.1022	0.7972	0.2475	0.5870	0.0058	2.50	12.7574	0.0057	1.65	0.1693	8	4726.57	27.5	9.8
	b	0.0216	2.1287	0.0580	1.9382	0.0778	2.9748	3.89326	0.76428	3.0936	0. 8037	0.2467	0.5803	0.0056	2.26	12.1764							
46	a	0.0230	2.4546	0.0592	2.0283	0.0735	3.9709	3.8881	0.75907	3.0851	0.8102	0.2459	0.5736	0.0059	2.57	12.9828	0.0064	3.21	0.2806	56	19954.58	40.4	5.5
	b	0.0260	2.1791	0.0749	2.2091	0.0694	2.8055	3.88542	0.78791	3.0779	0.8129	0.2454	0.5680	0.0067	2.32	14.6827							
	c	0.0259	2.2677	0.0735	2.3617	0.0645	4.3017	3.88788	0.82195	3.0791	0.8090	0.2456	0.5692	0.0067	2.41	14.6087							
48	a	0.0247	2.4502	0.0681	2.0802	0.0672	2.9097	3.89035	0.85599	3.0804	0.8052	0.2459	0.5704	0.0063	2.60	13.8988	0.0072	8.75	0.1993	9	4514.73	25.5	8.5
	b	0.0317	2.1411	0.0925	1.7984	0.0558	3.1872	3.89282	0.89002	3.0817	0.8013	0.2462	0.5716	0.0081	2.32	17.8253							
49	a	0.0262	2.0639	0.0768	2.0721	0.0651	3.4269	3.89528	0.92406	3.0829	0.7974	0.2464	0.5728	0.0067	2.26	14.7417	0.0070	2.94	0.4200	21	5000.34	55.3	12.1
	b	0.0285	2.3777	0.0829	2.4938	0.0617	3.9885	3.89775	0.9581	3.0842	0.7936	0.2467	0.5740	0.0073	2.56	14.9487							
														Weighted mean								37.5	2.7
														Pooled mean			0.0063	0.22	0.2481	319	128,586.90	36.4	2.2

*Pooled AFT age is calculated with ζ_{MS}= 0.928±0.022

Table 3 LA-ICP-MS data and fission-track dating sample PP01, belonging to the Phu Kradung Formation, Phu Phan Mountain Range.

PP01 grain ID	spot ID	LA-ICP-MS data															FT dating								
		Ap						NIST610						Ap/ NIST610	SE	U	Average Ap/ NIST610	SE	ρ_s	Ns	A	T	σ
		$^{238}U/^{43}Ca$	SE (%)	$^{232}Th/^{43}Ca$	SE (%)	$^{208}Pb/^{238}U$	SE (%)	$^{238}U/^{43}Ca$	SE (%)	$^{232}Th/^{43}Ca$	SE (%)	$^{208}Pb/^{238}U$	SE (%)	($^{238}U/^{43}Ca$)	(%)	(μg/g)		(%)	(10^6/ cm^2)		(μm^2)	(Ma)	(Ma)
2	a	0.0108	1.7716	0.0185	1.6706	0.0814	4.8928	4.2708	0.9937	3.2808	0.9524	0.2277	0.6991	0.0025	2.03	5.5266	0.0025	0.79	0.2390	12	5020.58	88.3	25.6
	b	0.0105	2.2366	0.0186	1.8061	0.0768	7.1400	4.2609	0.9876	3.2723	0.9328	0.2273	0.7042	0.0025	2.44	5.4047							
3	a	0.0149	1.7451	0.0292	1.5135	0.0844	3.5111	4.2509	0.9814	3.2638	0.9132	0.2270	0.7093	0.0035	2.00	7.6877	0.0034	3.25	0.2546	14	5498.04	70.0	18.9
	b	0.0136	1.8341	0.0270	1.7196	0.0855	3.2492	4.2409	0.9752	3.2553	0.8936	0.2266	0.7144	0.0032	2.08	7.0127							
6	a	0.0143	1.4326	0.0469	1.2573	0.2198	1.9419	4.2417	0.9103	3.2408	0.8553	0.2246	0.7092	0.0034	1.70	7.4052	0.0036	5.14	0.3991	11	2756.02	100.8	30.9
	b	0.0166	1.7645	0.0559	1.4251	0.2202	2.2598	4.2471	0.8809	3.2377	0.8460	0.2237	0.7041	0.0039	1.97	8.5668							
11	a	0.0111	3.0172	0.0175	2.4366	0.2190	3.4867	4.2525	0.8515	3.2347	0.8366	0.2229	0.6990	0.0026	3.14	5.7019	0.0026	0.59	0.1661	6	3,612	59.4	24.3
	b	0.0109	2.2413	0.0191	2.8529	0.2221	2.5453	4.2579	0.8221	3.2317	0.8273	0.2221	0.6939	0.0026	2.39	5.6070							
13	a	0.0579	1.1555	0.1082	1.0807	0.0858	2.0217	4.2633	0.7927	3.2286	0.8180	0.2212	0.6888	0.0136	1.40	29.7520	0.0122	7.88	0.9697	46	4743.85	73.2	12.4
	b	0.0463	1.4053	0.0778	1.2615	0.0951	1.9338	4.2669	2.9495	3.2236	0.8381	0.2200	0.6815	0.0109	3.27	23.7861							
15	a	0.0695	1.3064	0.0050	1.8490	0.3017	1.3386	4.2650	5.1358	3.2216	0.8676	0.2197	0.6794	0.0163	5.30	35.7169	0.0157	2.07	0.9449	42	4444.8	55.5	8.7
	b	0.0647	1.5951	0.0049	1.8533	0.3174	1.1382	4.2631	7.3221	3.2195	0.8970	0.2193	0.6773	0.0152	7.49	33.2413							
21	a	0.0108	1.9013	0.0198	2.0263	0.1067	3.8853	4.2594	11.6946	3.2155	0.9559	0.2185	0.6730	0.0025	11.85	5.5491	0.0024	2.96	0.2671	6	2246.73	101.1	41.5
	b	0.0099	2.0685	0.0179	1.9439	0.1171	3.3113	4.2576	13.8809	3.2134	0.9854	0.2182	0.6709	0.0023	14.03	5.1029							
22	a	0.0477	1.1859	0.2156	1.0749	0.0660	2.1076	4.2431	11.7126	3.2144	0.9854	0.2181	0.6672	0.0113	11.77	24.6443	0.0155	20.00	1.0507	68	6472.15	62.8	14.8
	b	0.0975	1.0560	0.2862	1.1156	0.0458	1.9209	4.2368	9.5353	3.2159	0.9708	0.2182	0.6665	0.0230	9.59	50.4121							
	c	0.0512	1.8100	0.1980	1.0644	0.0563	2.0810	4.2306	7.3581	3.2173	0.9561	0.2183	0.6657	0.0121	7.58	26.5210							
26	a	0.0137	1.4977	0.0248	1.6677	0.0781	3.3390	4.2243	5.1808	3.2188	0.9414	0.2185	0.6649	0.0032	5.39	7.0781	0.0032	0.71	0.2514	16	6365.4	73.0	18.3
	b	0.0133	1.5901	0.0247	1.3690	0.0799	3.9100	4.2180	3.0036	3.2203	0.9267	0.2186	0.6641	0.0031	3.40	6.8816							
	c	0.0133	1.6707	0.0244	1.3439	0.0912	3.1653	4.2113	0.8125	3.2202	0.8792	0.2183	0.6551	0.0032	1.86	6.9160							
32	a	0.0174	1.4908	0.0318	1.5794	0.1488	2.4801	4.3102	0.7993	3.2656	0.7441	0.2145	0.5961	0.0040	1.69	8.8652	0.0047	9.90	0.2551	6	2351.69	50.1	21.1
	b	0.0233	1.2195	0.0487	1.0893	0.1122	2.0767	4.3441	0.8224	3.2838	0.7647	0.2142	0.5929	0.0054	1.47	11.7509							
34	a	0.0518	1.3938	0.0787	1.3175	0.0403	1.8455	4.3781	0.8455	3.3020	0.7852	0.2139	0.5897	0.0118	1.63	25.9298	0.0111	4.60	1.1630	33	2837.46	96.4	17.5
	b	0.0458	1.8424	0.0761	1.6263	0.0445	3.3688	4.4120	0.8686	3.3202	0.8058	0.2136	0.5865	0.0104	2.04	22.7603							
37	a	0.0561	1.8903	0.0511	1.9209	0.4214	1.2447	4.4211	3.2741	3.3268	0.8423	0.2132	0.5997	0.0127	3.78	27.8027	0.0130	1.73	0.7311	32	4377.07	51.9	9.3
	b	0.0586	1.4625	0.0616	1.4302	0.4223	1.0973	4.3963	5.6564	3.3151	0.8583	0.2130	0.6161	0.0133	5.84	29.1944							
44	a	0.1047	1.3490	0.0002	10.3316	0.1042	1.4588	4.3714	8.0388	3.3034	0.8742	0.2129	0.6325	0.0240	8.15	52.4760	0.0216	7.66	1.1018	36	3267.38	47.1	8.7
	b	0.0838	1.1103	0.0001	13.8319	0.1186	1.4439	4.3466	10.4212	3.2917	0.8902	0.2127	0.6489	0.0193	10.48	42.2179							
49	a	0.0157	1.6942	0.0312	1.6335	0.0793	2.6532	4.3668	4.5031	3.3070	0.8268	0.2137	0.7186	0.0036	4.81	7.8968	0.0035	1.27	0.3510	27	7692.51	92.0	17.9

*Pooled AFT age is calculated with ζ_{MS}= 0.928±0.022

Table 3 (cont.)

PP01 grain ID	spot ID	LA-ICP-MS data												FT dating									
		Ap						NIST610						Ap/ NIST610 ($^{238}U/^{43}Ca$)	SE (%)	U (μg/g)	Average Ap/ NIST610	SE (%)	ρ_s (10^6/ cm^2)	Ns	A (μm^2)	T (Ma)	σ (Ma)
		$^{238}U/^{43}Ca$	SE (%)	$^{238}Th/^{43}Ca$	SE (%)	$^{206}Pb/^{238}U$	SE (%)	$^{238}U/^{43}Ca$	SE (%)	$^{238}Th/^{43}Ca$	SE (%)	$^{206}Pb/^{238}U$	SE (%)										
	b	0.0152	1.3124	0.0297	1.2551	0.0802	2.8384	4.3784	2.7227	3.3135	0.8109	0.2139	0.7248	0.0035	3.02	7.6039							
	c	0.0153	1.5710	0.0310	1.3231	0.0826	3.0444	4.4097	0.9272	3.3295	0.7913	0.2140	0.7347	0.0035	1.82	7.6033							
														Weighted mean								70.7	5.6
														Pooled mean			0.0081	0.38	0.5755	355	61,686.09	65.4	3.8

*Pooled AFT age is calculated with ζ_{MS}= 0.928±0.022

Table 4 LA-ICP-MS data and fission-track dating sample PTT14, belonging to the Phu Kradung Formation, Phu Phan Mountain Range.

PTT14 grain ID	spot ID	LA-ICP-MS data												FT dating									
		Ap						NIST610						Ap/ NIST610 ($^{238}U/^{43}Ca$)	SE (%)	U (μg/g)	Average Ap/ NIST610	SE (%)	ρ_s (10^6/ cm^2)	Ns	A (μm^2)	T (Ma)	σ (Ma)
		$^{238}U/^{43}Ca$	SE (%)	$^{232}Th/^{43}Ca$	SE (%)	$^{206}Pb/^{238}U$	SE (%)	$^{238}U/^{43}Ca$	SE (%)	$^{232}Th/^{43}Ca$	SE (%)	$^{206}Pb/^{238}U$	SE (%)										
1-2	a	0.0318	2.9556	0.0895	2.8202	0.1430	2.5405	4.4878	0.9928	3.2795	1.0212	0.2598	0.8613	0.0071	3.12	15.5441	0.0071	3.12	0.0000	0	532.53	0.0	0.0
1-4	a	0.2126	2.3320	0.0530	2.3529	0.0491	1.7867	4.5127	1.0237	3.2788	1.0282	0.2598	0.8888	0.0471	2.55	103.177	0.0471	2.55	1.8627	14	751.6	36.6	9.9
1-11	a	0.1946	2.3725	0.0008	3.8745	0.0628	2.0960	4.5376	1.0547	3.2781	1.0353	0.2597	0.9163	0.0429	2.60	93.9602	0.0429	2.60	3.4878	20	573.43	75.0	17.0
1-12	a	0.0053	2.9255	0.0074	2.8761	0.3093	4.1143	4.5625	1.0857	3.2775	1.0424	0.2596	0.9439	0.0012	3.12	2.56157	0.0012	3.12	0.0000	0	889.22	0.0	0.0
1-13	a	0.0901	3.4519	0.0032	4.0490	0.0937	2.9799	4.5874	1.1166	3.2768	1.0494	0.2595	0.9714	0.0196	3.63	43.0125	0.0196	3.63	1.8146	23	1267.53	85.2	18.1
1-14	a	0.1398	2.5676	0.0232	2.3145	0.0602	2.2934	4.5908	1.1573	3.2713	1.0494	0.2593	0.9669	0.0305	2.82	66.72	0.0305	2.82	3.8686	21	542.83	116.8	25.8
1-16	a	0.0160	2.5623	0.0127	2.3458	0.1819	3.5635	4.5694	1.1669	3.2663	1.0423	0.2591	0.9348	0.0035	2.82	7.65245	0.0035	2.82	0.0000	0	717.26	0.0	0.0
1-17	a	0.0129	2.7300	0.0225	2.7018	0.0993	3.8724	4.5479	1.1766	3.2614	1.0351	0.2590	0.9028	0.0028	2.97	6.2017	0.0029	1.38	0.2935	5	1703.63	93.6	42.0
	b	0.0133	2.4991	0.0241	1.7653	0.0991	3.7004	4.5264	1.1863	3.2565	1.0280	0.2589	0.8708	0.0029	2.77	6.44773							
1-21	a	0.0105	2.2752	0.0212	2.5893	0.2571	2.7442	4.5049	1.1959	3.2516	1.0209	0.2587	0.8387	0.0023	2.57	5.10596	0.0023	2.57	0.2697	2	741.49	106.5	75.4
1-22	a	0.0699	3.1529	0.0052	4.5159	0.0751	2.6128	4.4835	1.2056	3.2467	1.0138	0.2586	0.8067	0.0156	3.38	34.1298	0.0156	3.38	1.5325	13	848.27	90.6	25.4
1-23	a	0.0163	2.3075	0.0447	2.0273	0.3397	4.3648	4.4533	1.1798	3.2465	0.9965	0.2570	0.8102	0.0037	2.59	7.99527	0.0037	2.59	0.3190	4	1253.99	80.6	40.4
1-27	a	0.0484	2.5002	0.0101	2.7477	0.1116	2.1239	4.4445	1.1443	3.2513	0.9863	0.2555	0.8457	0.0109	2.75	23.8392	0.0112	2.01	0.5074	11	2168.01	41.9	12.7
	b	0.0511	2.7197	0.0168	2.7944	0.1046	2.1293	4.4402	1.1266	3.2537	0.9812	0.2548	0.8634	0.0115	2.94	25.231							
1-31	a	0.0240	2.2107	0.0170	2.2203	0.1744	2.4259	4.4358	1.1088	3.2561	0.9761	0.2540	0.8812	0.0054	2.47	11.8462	0.0059	5.63	0.5319	6	1128.11	83.5	34.4
	b	0.0281	2.3698	0.0165	2.7473	0.1551	2.7728	4.4304	1.0569	3.2516	0.9603	0.2539	0.8724	0.0063	2.59	13.8967							
1-41	a	0.0034	3.1194	0.0070	2.7204	0.2307	5.8897	4.4273	0.9544	3.2312	0.9283	0.2556	0.7930	0.0008	3.26	1.66101	0.0008	3.26	0.0000	0	833.8	0.0	0.0
1-48	a	0.0582	2.0957	0.2168	2.1862	0.1209	3.0134	4.4262	0.9202	3.2244	0.9176	0.2561	0.7665	0.0131	2.29	28.7864	0.0131	2.29	0.8932	5	559.81	62.8	28.1
1-52	a	0.0121	2.2137	0.0235	2.3239	0.1008	3.8322	4.3849	0.9475	3.2039	0.9016	0.2588	0.7476	0.0028	2.41	6.04077	0.0028	2.41	0.0384	1	2605.8	12.9	12.9
1-55	a	0.0382	2.1094	0.0305	2.4263	0.0773	2.3980	4.3653	0.9953	3.2004	0.9042	0.2595	0.7647	0.0088	2.33	19.1814	0.0088	2.33	0.9336	6	642.68	98.2	40.2
3-42	a	0.0079	2.0338	0.0179	1.7893	0.2109	10.3406	3.9213	0.9451	3.0942	0.8308	0.2463	0.6082	0.0020	2.24	4.39337	0.0020	2.24	0.2996	2	667.52	137.2	97.1
3-61	a	0.0038	2.3023	0.0135	1.9029	0.2905	4.0236	3.9423	0.8981	3.1029	0.8719	0.2457	0.6411	0.0010	2.47	2.13848	0.0010	2.47	0.1496	2	1336.73	140.7	99.6
4-14	a	0.0453	1.5711	0.0004	4.9255	0.1484	1.7117	3.9432	0.8719	3.1045	0.9056	0.2444	0.6880	0.0115	1.80	25.191	0.0115	1.80	1.0244	5	488.11	82.1	36.8
4-21	a	0.0151	1.7791	0.0201	1.3571	0.2075	2.9732	3.9401	0.8666	3.1038	0.9156	0.2439	0.7060	0.0038	1.98	8.40908	0.0038	1.98	0.2498	2	800.5	60.1	42.5
4-31	a	0.0242	1.5868	0.0035	2.0221	0.1034	2.8723	3.9371	0.8613	3.1032	0.9255	0.2434	0.7239	0.0061	1.81	13.4506	0.0061	1.81	0.4737	5	1055.61	71.2	31.9
4-62	a	0.0447	1.7219	0.0025	2.5278	0.1071	2.1696	3.9340	0.8561	3.1025	0.9355	0.2429	0.7419	0.0114	1.92	24.8666	0.0114	1.92	1.6124	9	558.16	130.5	43.7
5-5	a	0.2805	1.7894	0.0349	2.0659	0.0448	2.0457	3.9245	0.8668	3.0934	0.9383	0.2429	0.7437	0.0715	1.99	156.572	0.0715	1.99	6.1147	87	1422.79	78.9	8.8
5-7	a	0.0578	1.8777	0.0308	1.8433	0.0978	1.9284	3.9180	0.8828	3.0849	0.9311	0.2434	0.7277	0.0148	2.07	32.3154	0.0148	2.07	1.1079	11	992.89	69.3	21.0
5-8	a	0.0242	2.3255	0.0214	2.1130	0.0970	3.1254	3.9116	0.8987	3.0764	0.9239	0.2439	0.7116	0.0062	2.49	13.5342	0.0062	2.49	0.5946	6	1009.06	88.7	36.3

*Pooled AFT age is calculated with ζ_{MS}= 0.928±0.022

Table 4 (cont.)

PTT14 grain ID	spot ID	LA-ICP-MS data												FT dating									
		Ap						NIST610						Ap/ NIST610 ($^{238}U/^{43}Ca$)	SE (%)	U (μg/g)	Average Ap/ NIST610	SE (%)	ρ_s (10^6/ cm^2)	Ns	A (μm^2)	T (Ma)	σ (Ma)
		$^{238}U/^{43}Ca$	SE (%)	$^{238}Th/^{43}Ca$	SE (%)	$^{206}Pb/^{238}U$	SE (%)	$^{238}U/^{43}Ca$	SE (%)	$^{238}Th/^{43}Ca$	SE (%)	$^{206}Pb/^{238}U$	SE (%)										
5-16	a	0.0910	2.1651	0.0556	3.7115	0.0672	2.9995	3.9052	0.9147	3.0679	0.9166	0.2444	0.6956	0.0233	2.35	51.0527	0.0233	2.35	2.5498	21	823.61	100.7	22.2
5-19	a	0.0494	2.1275	0.0357	1.8324	0.3654	1.5556	3.8923	0.9467	3.0509	0.9022	0.2454	0.6634	0.0127	2.33	27.794	0.0127	2.33	0.8601	6	697.58	62.6	25.6
5-20	a	0.0222	2.1640	0.0697	1.8867	0.1259	3.6817	3.8858	0.9626	3.0424	0.8950	0.2459	0.6474	0.0057	2.37	12.5069	0.0057	2.37	0.3651	2	547.82	59.1	41.8
5-22	a	0.0090	2.3047	0.0104	2.8035	0.2483	2.9098	3.8800	0.9438	3.0363	0.8539	0.2450	0.6411	0.0023	2.49	5.07992	0.0023	2.49	0.0000	0	425.95	0.0	0.0
5-28	a	0.0052	2.2905	0.0138	2.0167	0.2381	3.4600	3.8804	0.9264	3.0375	0.8370	0.2443	0.6460	0.0013	2.47	2.94591	0.0013	2.47	0.0000	0	550.83	0.0	0.0
5-31	a	0.0051	3.1294	0.0111	2.7204	0.4847	5.6149	3.8807	0.9089	3.0387	0.8201	0.2436	0.6509	0.0013	3.26	2.86974	0.0013	3.26	0.2225	1	449.53	155.7	155.8
5-36	a	0.0133	2.2195	0.0282	2.1534	0.1627	3.0685	3.8811	0.8915	3.0399	0.8032	0.2429	0.6557	0.0034	2.39	7.50827	0.0034	2.39	0.4486	4	891.63	120.3	60.3
5-41	a	0.0386	2.1023	0.0623	2.4106	0.0911	3.0255	3.8814	0.8741	3.0411	0.7862	0.2421	0.6606	0.0099	2.28	21.7606	0.0094	3.71	0.6060	9	1485.19	59.3	19.9
	b	0.0348	2.0418	0.0470	2.3472	0.0957	3.1797	3.8866	0.8662	3.0425	0.7688	0.2409	0.6762	0.0089	2.22	19.5926							
5-45	a	0.0174	2.6790	0.0008	4.2902	1.0528	2.3526	3.8914	0.8757	3.0427	0.7683	0.2403	0.6870	0.0045	2.82	9.76778	0.0045	2.82	0.3584	6	1674.2	74.2	30.4
5-53	a	0.0786	2.4222	0.1661	1.9268	0.1032	1.7683	3.8963	0.8853	3.0429	0.7678	0.2398	0.6977	0.0202	2.58	44.2135	0.0202	2.58	1.2742	9	706.32	58.3	19.5
														Weighted mean								79.9	7.1
														Pooled mean			0.0118	0.61	0.9259	318	34,344.02	72.6	4.4

*Pooled AFT age is calculated with ζ_{MS}= 0.928±0.022

Table 5 The LA-ICP-MS data and fission-track dating from sample PP10, belonging to the Phu Phan Formation, Phu Phan Mountain Range.

PP10 grain ID	spot ID	LA-ICP-MS data												FT dating								
		Ap						NIST610						Ap/ NIST610 ($^{238}U/^{43}Ca$)	SE (%)	U (μg/g)	Average Ap/ NIST610	SE (%)	ρ_s (10^6/ cm^2)	Ns	A (μm^2)	T (Ma)	σ (Ma)
		$^{238}U/^{43}Ca$	SE (%)	$^{238}Th/^{43}Ca$	SE (%)	$^{206}Pb/^{238}U$	SE (%)	$^{238}U/^{43}Ca$	SE (%)	$^{238}Th/^{43}Ca$	SE (%)	$^{206}Pb/^{238}U$	SE (%)									
1	a	0.0961	1.8214	0.0761	1.6609	0.0636	1.7261	4.4294	0.9122	3.3391	0.7876	0.2138	0.7385	0.0217	2.04	47.5392	0.0232	4.68	1.4256	88	6172.91	56.7	6.7
	b	0.1102	1.6029	0.0894	1.7620	0.0582	1.9809	4.4491	0.8972	3.3486	0.7839	0.2137	0.7424	0.0248	1.84	54.2726							
4	a	0.0064	1.8006	0.0097	1.8683	0.3409	2.8695	4.4688	0.8822	3.3582	0.7802	0.2136	0.7462	0.0014	2.01	3.1578	0.0104	60.95	0.8994	51	5670.66	79.5	49.7
	b	0.0872	2.3831	0.1250	2.2252	0.0617	2.0741	4.4885	0.8671	3.3678	0.7766	0.2135	0.7500	0.0194	2.54	42.5760							
5	a	0.0529	2.3010	0.0022	2.5652	0.0713	3.9182	4.5081	0.8521	3.3774	0.7729	0.2133	0.7538	0.0117	2.45	25.7180	0.0123	3.23	0.5778	41	7096.05	43.4	7.0
	b	0.0575	1.8814	0.0024	2.7548	0.0677	2.1087	4.4701	0.8375	3.3543	0.8061	0.2132	2.7576	0.0129	2.06	28.1800							
6	a	0.0216	2.3890	0.0596	1.9874	0.1965	2.2892	4.4412	0.8376	3.3379	0.8246	0.2132	3.7576	0.0049	2.53	10.6366	0.0033	19.83	0.1884	21	11144.7	53.2	15.7
	B	0.0116	2.6665	0.0270	2.1240	0.3407	3.6395	4.4124	0.8378	3.3216	0.8431	0.2132	4.7576	0.0026	2.80	5.7544							
	c	0.0103	2.4088	0.0244	2.1582	0.3555	2.2467	4.3835	0.8380	3.3052	0.8616	0.2132	5.7576	0.0023	2.55	5.1249							
7	a	0.0215	1.9822	0.0020	2.9811	0.1877	2.3720	4.3546	0.8382	3.2889	0.8800	0.2132	6.7576	0.0049	2.15	10.8027	0.0052	3.06	0.5362	22	4102.76	95.8	20.8
	b	0.0233	1.8965	0.0020	2.4641	0.1768	2.4268	4.3380	0.8525	3.2801	0.8895	0.2133	8.7576	0.0054	2.08	11.7796							
8	a	0.0073	1.9920	0.0000	22.5831	0.2728	3.2247	4.3503	0.8667	3.2876	0.8804	0.2135	0.7170	0.0017	2.17	3.6532	0.0017	2.17	0.1092	7	6409.16	60.5	22.9
9	a	0.0729	1.5501	0.0001	14.2775	0.2338	3.8598	4.3748	0.8950	3.2952	0.8714	0.2136	0.7120	0.0167	1.79	36.5091	0.0166	7.81	0.8209	68	8283.33	45.6	6.7
	b	0.0608	1.7757	0.0017	2.5113	0.0718	2.3431	4.3871	0.9091	3.3027	0.8624	0.2138	0.7070	0.0139	1.99	30.3689							
	c	0.0852	1.7507	0.0014	3.3037	0.0806	1.7685	4.3993	0.9233	3.3102	0.8534	0.2139	0.7020	0.0194	1.98	42.4401							
14	a	0.0071	1.9432	0.0023	2.6129	0.0660	1.8712	4.4099	0.9546	3.3178	0.8443	0.2141	0.6970	0.0016	2.17	3.5302	0.0016	2.76	0.1555	25	16080.18	89.6	18.2
	b	0.0066	2.4294	0.0164	1.9766	0.2304	3.3690	4.4091	0.9631	3.3232	0.8312	0.2134	0.7007	0.0015	2.61	3.2850							
	c	0.0074	1.8379	0.0182	2.1991	0.2442	2.9274	4.4083	0.9717	3.3221	0.8292	0.2130	0.7050	0.0017	2.08	3.6923							
15	a	0.0303	2.0258	0.0199	1.9104	0.2283	2.9309	4.4074	0.9802	3.3211	0.8271	0.2126	0.7094	0.0069	2.25	15.0683	0.0033	43.47	0.1471	25	16993.03	40.7	19.5
	b	0.0055	2.3068	0.0237	2.2851	0.1284	2.2021	4.4066	0.9888	3.3200	0.8251	0.2122	0.7137	0.0013	2.51	2.7520							
	c	0.0083	2.1082	0.0028	2.4454	0.5093	2.6896	4.3867	1.0145	3.3190	0.8230	0.2118	0.7181	0.0019	2.34	4.1310							
18	a	0.0220	2.0231	0.0026	2.4185	0.3504	2.4838	4.3676	1.0316	3.3044	0.8479	0.2113	0.6978	0.0050	2.27	11.0113	0.0042	7.64	0.2361	43	18211.88	51.5	8.9
	b	0.0169	1.9215	0.0546	1.9872	0.4013	1.7647	4.3485	1.0488	3.2909	0.8748	0.2111	0.6731	0.0039	2.19	8.5141							
	c	0.0164	2.3191	0.0510	1.5181	0.5864	1.8701	4.3294	1.0659	3.2773	0.9018	0.2109	0.6485	0.0038	2.55	8.3095							
19	a	0.0127	2.9369	0.0509	1.9726	0.6148	2.2017	4.3103	1.0831	3.2638	0.9287	0.2107	0.6238	0.0030	3.13	6.4646	0.0030	3.13	0.4614	17	3684.63	143.5	35.2
20	a	0.0129	1.8877	0.0349	2.2277	0.2055	2.6430	4.2912	1.1002	3.2503	0.9556	0.2105	0.5992	0.0030	2.18	6.6035	0.0028	4.58	0.2936	19	6470.83	95.5	22.5
	b	0.0114	3.3798	0.0179	1.7597	0.1699	2.8036	4.3051	1.1378	3.2367	0.9826	0.2103	0.5745	0.0026	3.57	5.7994							
24	a	0.0783	2.2330	0.0154	4.8114	0.2275	4.2668	4.3160	1.1446	3.2401	0.9811	0.2096	0.5473	0.0181	2.51	39.7454	0.0155	11.23	0.8265	79	9558.13	49.3	7.9
	b	0.0488	1.9448	0.0128	3.8673	0.1962	5.2057	4.3270	1.1514	3.2486	0.9668	0.2094	0.5460	0.0113	2.26	24.6982							

*Pooled AFT age is calculated with ζ_{MS}= 0.928±0.022

Table 5 (cont.)

PP10 grain ID	spot ID	LA-ICP-MS data												FT dating									
		Ap						NIST610						Ap/ NIST610 ($^{238}U/^{43}Ca$)	SE (%)	U (μg/g)	Average Ap/ NIST610	SE (%)	ρ_s (10^6/ cm^2)	Ns	A (μm^2)	T (Ma)	σ (Ma)
		$^{238}U/^{43}Ca$	SE (%)	$^{238}Th/^{43}Ca$	SE (%)	$^{206}Pb/^{238}U$	SE (%)	$^{238}U/^{43}Ca$	SE (%)	$^{238}Th/^{43}Ca$	SE (%)	$^{206}Pb/^{238}U$	SE (%)										
	c	0.0740	2.4631	0.0012	3.9582	0.0606	1.9377	4.3380	1.1582	3.2570	0.9526	0.2091	0.5447	0.0171	2.72	37.3601								
														Weighted mean								58.2	3.6
														Pooled mean			0.0070	1.26	0.4221	506	119,878.25	56.1	2.9

*Pooled AFT age is calculated with ζ_{MS}= 0.928±0.022

Table 6 The LA-ICP-MS data and fission-track dating from sample PP15, belonging to the Phu Phan Formation, Phu Phan Mountain Range.

PP15 grain ID	spot ID	LA-ICP-MS data												FT dating								
		Ap						NIST610						Ap/ NIST610 ($^{238}U/^{43}Ca$)	SE (%)	U (μg/g)	Average Ap/ NIST610	SE (%)	ρ_s (10^6/ cm^2)	Ns	A (μm^2)	T (Ma)	σ (Ma)
		$^{238}U/^{43}Ca$	SE (%)	$^{232}Th/^{43}Ca$	SE (%)	$^{206}Pb/^{238}U$	SE (%)	$^{238}U/^{43}Ca$	SE (%)	$^{232}Th/^{43}Ca$	SE (%)	$^{206}Pb/^{238}U$	SE (%)										
1	a	0.1597	1.6324	0.0036	2.6129	0.0586	1.5702	3.9087	0.7799	3.1192	0.7841	0.2490	0.6005	0.0409	1.81	89.5152	0.0413	0.78	2.1719	139	6400	48.6	4.3
	b	0.1631	2.0512	0.0033	3.0498	0.0603	1.4366	3.9036	0.7747	3.1107	0.7906	0.2482	0.5938	0.0418	2.19	91.5233							
2	a	0.0073	1.9886	0.0137	1.7652	0.2204	3.0327	3.8984	0.7695	3.1022	0.7972	0.2475	0.5870	0.0019	2.13	4.0801	0.0018	2.05	0.1771	17	9600	90.2	22.0
	b	0.0068	1.8743	0.0089	1.6006	0.2252	3.6832	3.8933	0.7643	3.0936	0.8037	0.2467	0.5803	0.0018	2.02	3.8496							
3	a	0.0094	1.7799	0.0023	3.0556	0.3152	2.4522	3.8881	0.7591	3.0851	0.8102	0.2459	0.5736	0.0024	1.93	5.2711	0.0024	1.93	0.2464	17	6900	94.3	23.1
5	a	0.1372	1.5430	0.0039	2.6249	0.0626	1.6923	3.8854	0.7879	3.0779	0.8129	0.2454	0.5680	0.0353	1.73	77.3653	0.0353	1.73	1.8400	92	5000	48.2	5.2
6	a	0.0279	1.8849	0.0276	1.8540	0.2267	1.9263	3.8879	0.8219	3.0791	0.8090	0.2456	0.5692	0.0072	2.06	15.7094	0.0072	2.06	0.7500	21	2800	96.3	21.2
13	a	0.0020	3.1237	0.0065	2.1885	0.3824	7.3952	3.8953	0.9241	3.0829	0.7974	0.2464	0.5728	0.0005	3.26	1.1115	0.0005	4.06	0.0364	2	5500	69.9	49.6
	b	0.0018	3.3115	0.0052	2.1822	0.3581	5.1483	3.8978	0.9581	3.0842	0.7936	0.2467	0.5740	0.0005	3.45	0.9908							
15	a	0.1130	1.1661	0.0007	4.5620	0.1720	1.3647	3.9353	0.9137	3.1000	0.8582	0.2459	0.6301	0.0287	1.48	62.9001	0.0277	2.59	1.0811	80	7400	36.1	4.2
	b	0.1052	1.4361	0.0006	4.3602	0.1877	1.0911	3.9423	0.8981	3.1029	0.8719	0.2457	0.6411	0.0267	1.69	58.4570							
16	a	0.0101	1.4305	0.0281	1.3783	0.1923	3.3263	3.9463	0.8771	3.1052	0.8956	0.2450	0.6701	0.0026	1.68	5.6108	0.0018	16.70	0.0984	6	6100	49.6	21.9
	b	0.0064	1.6784	0.0132	1.4963	0.3093	2.6440	3.9432	0.8719	3.1045	0.9056	0.2444	0.6880	0.0016	1.89	3.5397							
	c	0.0052	1.9306	0.0095	1.8825	0.3556	3.9694	3.9401	0.8666	3.1038	0.9156	0.2439	0.7060	0.0013	2.12	2.8889							
19	a	0.0327	1.8183	0.0632	1.9076	0.1563	2.4538	3.9371	0.8613	3.1032	0.9255	0.2434	0.7239	0.0083	2.01	18.1735	0.0083	2.01	0.3500	14	4000	39.0	10.5
20	a	0.0911	1.7256	0.0207	1.8645	0.0656	2.1767	3.9340	0.8561	3.1025	0.9355	0.2429	0.7419	0.0232	1.93	50.7216	0.0232	1.93	1.4500	29	2000	57.9	10.9
22	a	0.0550	1.4109	0.0107	1.9974	0.1314	1.9726	3.9116	0.8987	3.0764	0.9239	0.2439	0.7116	0.0141	1.67	30.8222	0.0141	1.67	0.6207	54	8700	40.8	5.7
23	a	0.0029	2.8260	0.0000	24.8496	0.5233	4.1468	3.8346	1.0455	2.9204	0.9349	0.2348	0.7901	0.0008	3.01	1.6510	0.0008	3.01	0.0000	0	6600	0.0	0.0
25	a	0.0371	1.6142	0.0097	1.7947	0.0990	2.3623	3.8923	0.9467	3.0509	0.9022	0.2454	0.6634	0.0095	1.87	20.8814	0.0051	62.63	0.1023	9	8800	18.7	13.3
	b	0.0022	3.0045	0.0001	21.3568	0.3972	5.9309	3.8797	0.9612	3.0351	0.8709	0.2457	0.6362	0.0006	3.15	1.2655							
29	a	0.0543	1.5456	0.0015	3.1037	0.0954	1.6747	3.8804	0.9264	3.0375	0.8370	0.2443	0.6460	0.0140	1.80	30.6533	0.0140	1.80	0.5797	40	6900	38.3	6.2
30	a	0.0559	1.5744	0.0013	3.1837	0.1707	38.6431	3.8807	0.9089	3.0387	0.8201	0.2436	0.6509	0.0144	1.82	31.5649	0.0144	1.82	0.7778	28	3600	49.9	9.5
31	a	0.0205	1.5835	0.0283	1.6679	0.2941	1.9445	3.8811	0.8915	3.0399	0.8032	0.2429	0.6557	0.0053	1.82	11.5842	0.0060	8.58	0.5385	14	2600	82.5	23.2
	b	0.0262	1.8030	0.0297	1.8717	0.2695	2.0345	3.8814	0.8741	3.0411	0.7862	0.2421	0.6606	0.0067	2.00	14.7847							
33	a	0.0950	1.8144	0.0015	3.5119	0.0916	1.7679	3.8914	0.8757	3.0427	0.7683	0.2403	0.6870	0.0244	2.01	53.4590	0.0260	4.39	1.6500	66	4000	58.6	7.8
	b	0.1077	1.7559	0.0017	3.7676	0.0851	1.6189	3.8963	0.8853	3.0429	0.7678	0.2398	0.6977	0.0276	1.97	60.5342							
34	a	0.0278	2.1370	0.0145	2.1391	0.1312	2.1103	3.8255	1.0610	2.9102	0.9074	0.2363	0.8095	0.0073	2.39	15.9362	0.0049	35.33	0.1795	7	3900	34.2	17.7
	b	0.0093	2.0440	0.0028	2.9092	0.2566	3.6793	3.8301	1.0533	2.9153	0.9212	0.2355	0.7998	0.0024	2.30	5.3181							
37	a	0.0101	2.1381	0.0294	1.7450	0.1898	3.1427	3.8392	1.0378	2.9255	0.9486	0.2340	0.7804	0.0026	2.38	5.7719	0.0026	2.38	0.0000	0	2300	0.0	0.0

*Pooled AFT age is calculated with ζ_{MS}= 0.928±0.022

Table 6 (cont.)

PP15 grain ID	spot ID	LA-ICP-MS data												FT dating								
		Ap						NIST610						Ap/ NIST610 ($^{238}U/^{43}Ca$)	SE (%)	U (μg/g)	Average Ap/ NIST610	SE (%)	ρ_s (10^6/ cm^2)	Ns	A (μm^2)	T (Ma)	σ (Ma)
		$^{238}U/^{43}Ca$	SE (%)	$^{238}Th/^{43}Ca$	SE (%)	$^{206}Pb/^{238}U$	SE (%)	$^{238}U/^{43}Ca$	SE (%)	$^{238}Th/^{43}Ca$	SE (%)	$^{206}Pb/^{238}U$	SE (%)										
44	a	0.0041	2.5947	0.0119	2.6904	0.4269	2.8199	3.9358	0.9295	2.9305	0.9624	0.2332	0.7707	0.0010	2.76	2.2542	0.0014	18.31	0.0667	8	12000	44.4	17.7
	b	0.0069	2.5388	0.0078	2.1985	0.3712	2.8225	3.9634	0.9011	2.9622	0.8541	0.2283	0.6893	0.0017	2.69	3.8293							
46	a	0.0232	1.6515	0.0227	2.3468	0.2359	2.9506	3.9911	0.8727	2.9693	0.8089	0.2272	0.6687	0.0058	1.87	12.7291	0.0056	2.34	0.3947	45	11400	64.8	9.9
	b	0.0219	1.8291	0.0601	1.4392	0.2079	1.9419	4.0204	0.8549	2.9765	0.7637	0.2260	0.6480	0.0054	2.02	11.9127							
47	a	0.0576	2.3443	0.0571	1.8487	0.2105	2.6193	4.0221	0.8655	2.9860	0.7400	0.2247	1.6274	0.0143	2.50	31.3855	0.0112	12.02	0.7225	164	22700	59.8	8.7
	b	0.0417	2.3517	0.0538	2.2325	0.0755	2.0796	4.0238	0.8760	2.9883	0.7615	0.2244	2.6274	0.0104	2.51	22.6814							
	c	0.0355	2.4727	0.0463	2.5380	0.0899	1.9511	4.0256	0.8866	2.9907	0.7830	0.2242	3.6274	0.0088	2.63	19.2977							
48	a	0.0852	1.9352	0.0476	2.3767	0.0958	2.4865	4.0290	0.9077	2.9930	0.8045	0.2239	4.6274	0.0211	2.14	46.2995	0.0211	2.14	0.7442	32	4300	32.6	5.9
49	a	0.0266	2.1901	0.0014	3.3915	0.0912	1.6560	4.0307	0.9182	2.9977	0.8476	0.2234	6.6274	0.0066	2.37	14.4315	0.0066	2.37	0.3400	17	5000	47.7	11.7
														Weighted mean								50.1	2.2
														Pooled mean			0.0108	0.48	0.5685	901	158,500	48.5	2.0

*Pooled AFT age is calculated with ζ_{MS}= 0.928±0.022

Table 7 The LA-ICP-MS data and fission-track dating from sample PP16, belonging to the Phu Phan Formation, Phu Phan Mountain Range.

PP16 grain ID	spot ID	LA-ICP-MS data												FT dating									
		Ap						NIST610						Ap/ NIST610 ($^{238}U/^{43}Ca$)	SE (%)	U (μg/g)	Average Ap/ NIST610	SE (%)	ρ_s (10^6/ cm^2)	Ns	A (μm^2)	T (Ma)	σ (Ma)
		$^{238}U/^{43}Ca$	SE (%)	$^{238}Th/^{43}Ca$	SE (%)	$^{206}Pb/^{238}U$	SE (%)	$^{238}U/^{43}Ca$	SE (%)	$^{238}Th/^{43}Ca$	SE (%)	$^{206}Pb/^{238}U$	SE (%)										
2	a	0.0172	1.9967	0.0011	3.6518	0.1682	2.6547	3.9059	0.9043	3.0433	0.7668	0.2387	0.7191	0.0044	2.19	9.6385	0.0046	2.37	0.3342	42	12569.19	67.8	10.7
	b	0.0184	1.9540	0.0012	3.7870	0.1614	2.8506	3.9108	0.9138	3.0435	0.7663	0.2382	0.7299	0.0047	2.16	10.3070							
3	a	0.0461	2.1451	0.0009	3.8409	0.0818	1.9788	3.9191	0.9190	3.0386	0.7660	0.2374	0.7265	0.0118	2.33	25.7939	0.0114	2.62	0.7161	32	4468.88	58.3	10.5
	b	0.0429	2.5148	0.0008	3.7351	0.0842	2.0271	3.9225	0.9147	3.0334	0.7662	0.2373	0.7123	0.0109	2.68	23.9529							
4	a	0.0967	2.1239	0.0026	2.8203	0.0454	2.2531	3.9259	0.9104	3.0283	0.7664	0.2371	0.6982	0.0246	2.31	53.9702	0.0296	11.92	1.6172	154	9522.35	50.4	7.4
	b	0.1361	2.0698	0.0041	2.9128	0.0412	1.6657	3.9294	0.9061	3.0231	0.7666	0.2369	0.6841	0.0346	2.26	75.8477							
10	a	0.0042	2.4507	0.0135	2.0997	0.3568	3.0868	3.9328	0.9017	3.0180	0.7668	0.2367	0.6699	0.0011	2.61	2.3158	0.0011	0.75	0.0278	1	3599.53	24.1	24.1
	b	0.0043	2.2734	0.0144	2.4395	0.3481	3.1050	3.9363	0.8974	3.0129	0.7670	0.2365	0.6558	0.0011	2.44	2.3653							
15	a	0.2715	2.0098	0.0030	2.3093	0.0523	1.8882	3.9351	0.8974	3.0062	0.7843	0.2362	0.6526	0.0690	2.20	151.1035	0.0704	0.88	3.2423	350	10,795	42.6	2.5
	b	0.2812	2.1991	0.0039	2.7562	0.0529	1.8600	3.9304	0.9017	3.0047	0.8013	0.2360	0.6636	0.0716	2.38	156.7307							
	c	0.2778	1.9719	0.0032	2.6376	0.0537	1.8500	3.9258	0.9060	3.0033	0.8184	0.2358	0.6746	0.0708	2.17	154.9790							
17	a	0.2150	2.0723	0.0013	3.9413	0.0540	1.6943	3.9212	0.9103	3.0018	0.8354	0.2356	0.6855	0.0548	2.26	120.0850	0.0575	1.92	2.7460	492	17917.06	44.1	2.4
	b	0.2306	2.1238	0.0016	3.2266	0.0524	1.8871	3.9165	0.9146	3.0003	0.8525	0.2355	0.6965	0.0589	2.31	128.9447							
	c	0.2304	2.1377	0.0019	3.2013	0.0502	2.0244	3.9119	0.9189	2.9988	0.8695	0.2353	0.7075	0.0589	2.33	128.9837							
25	a	0.1237	2.2162	0.0012	4.0533	0.0686	1.7448	3.9219	0.9230	3.0052	0.8525	0.2339	0.6994	0.0315	2.40	69.0716	0.0287	2.31	1.4338	317	22109.32	46.1	3.0
	b	0.1140	1.8490	0.0008	3.8603	0.0685	2.0104	3.9292	0.9229	3.0091	0.8355	0.2333	0.6899	0.0290	2.07	63.5308							
	c	0.1083	2.2213	0.0008	4.1876	0.0700	1.5935	3.9365	0.9228	3.0131	0.8184	0.2327	0.6804	0.0275	2.41	60.2535							
	d	0.1096	2.2315	0.0012	3.5572	0.0731	1.8798	3.9438	0.9226	3.0170	0.8014	0.2321	0.6709	0.0278	2.41	60.8515							
	e	0.1102	1.8956	0.0010	3.1995	0.0732	1.6596	3.9511	0.9225	3.0209	0.7844	0.2314	0.6614	0.0279	2.11	61.0673							
														Weighted mean								45.9	1.5
														Pooled mean			0.0348	0.51	1.7140	1,388	80,981.03	45.5	1.6

*Pooled AFT age is calculated with ζ_{MS}= 0.928±0.022

Table 8 The LA-ICP-MS data and fission-track dating from sample PTT15, belonging to the Phu Phan Formation, Phu Phan Mountain Range.

PTT15 grain ID	spot ID	LA-ICP-MS data												FT dating								
		Ap						NIST610						Ap/ NIST610 ($^{238}U/^{43}Ca$)	SE (%)	U (μg/g)	Average Ap/ NIST610	SE (%)	ρ_s (10^6/ cm^2)	Ns	A (μm^2)	T (Ma)	σ (Ma)
		$^{238}U/^{43}Ca$	SE (%)	$^{238}Th/^{43}Ca$	SE (%)	$^{206}Pb/^{238}U$	SE (%)	$^{238}U/^{43}Ca$	SE (%)	$^{238}Th/^{43}Ca$	SE (%)	$^{206}Pb/^{238}U$	SE (%)										
1-15	a	0.1423	1.7211	0.0098	2.0983	0.0504	1.8039	3.9653	0.9263	3.0281	0.7639	0.2307	0.6549	0.0359	1.95	78.6303	0.0311	10.79	1.5995	101	6314.64	47.5	7.1
p	b	0.1048	2.0339	0.0087	2.3887	0.0540	1.8365	3.9721	0.9302	3.0313	0.7605	0.2307	0.6578	0.0264	2.24	57.8183							
2-26	a	0.0777	1.3205	0.0175	1.4291	0.0535	2.2152	3.9925	0.9420	3.0408	0.7503	0.2304	0.6666	0.0195	1.62	42.6489	0.0195	1.62	1.9160	11	574.12	90.7	27.5
2-28	a	0.0360	2.3864	0.0180	2.8764	0.0695	2.4681	3.9857	0.9381	3.0376	0.7537	0.2305	0.6637	0.0090	2.56	19.8038	0.0090	2.56	0.8510	8	940.08	86.8	30.8
3-1	a	0.0936	1.4075	0.0127	1.6289	0.2017	1.4492	3.9964	0.8865	2.9993	0.8176	0.2223	0.7938	0.0234	1.66	51.2865	0.0212	7.21	1.5843	42	2651.00	68.8	11.8
	b	0.0759	1.6280	0.0107	2.1560	0.1761	1.3132	3.9784	0.8653	2.9978	0.7811	0.2219	0.7591	0.0191	1.84	41.7945							
5-26	a	0.0805	1.3640	0.0442	1.4514	0.0479	1.8476	4.0432	1.0003	3.0411	0.7907	0.2211	0.8057	0.0199	1.69	43.6058	0.0199	1.69	1.2247	24	1959.61	56.8	11.7
														Weighted mean								61.7	5.6
														Pooled mean			0.0251	1.05	1.4952	186	12,439.45	55.1	4.3

*Pooled AFT age is calculated with ζ_{MS}= 0.928±0.022

APPENDIX D Uranium concentration comparing with single grain age

The uranium concentration comparing with single grain age by using IsoPlotR program (Vermeesch, 2018)

Following the analytical process and result from Glorie et al. (2017) to compare with optional variable will use an “other” option that is provided in program. There are 3 necessary columns to fill the value, are t – a column of AFT age, s[t] – the standard errors of AFT age, and [C] – an optional value which in this topic will use the value of $^{238}U/^{43}Ca$ ratio of their single-grain apatites. In case of central FT age of this method is a slightly different from a direct “fission track” method, but in this study, will use the central FT age results obtained only from direct method which has actual values for calculating. Therefore, in this part will show some interested result that related to the single-grain apatite plot in radial plot.

The results show that the high precision value (t/**σ**) has more red color which means it has more uranium content (see Figure 4.48). At the same time, the apatite grain which has younger age will have more uranium content than the older grain (see clearly in sample PP10, Figure 4.48).

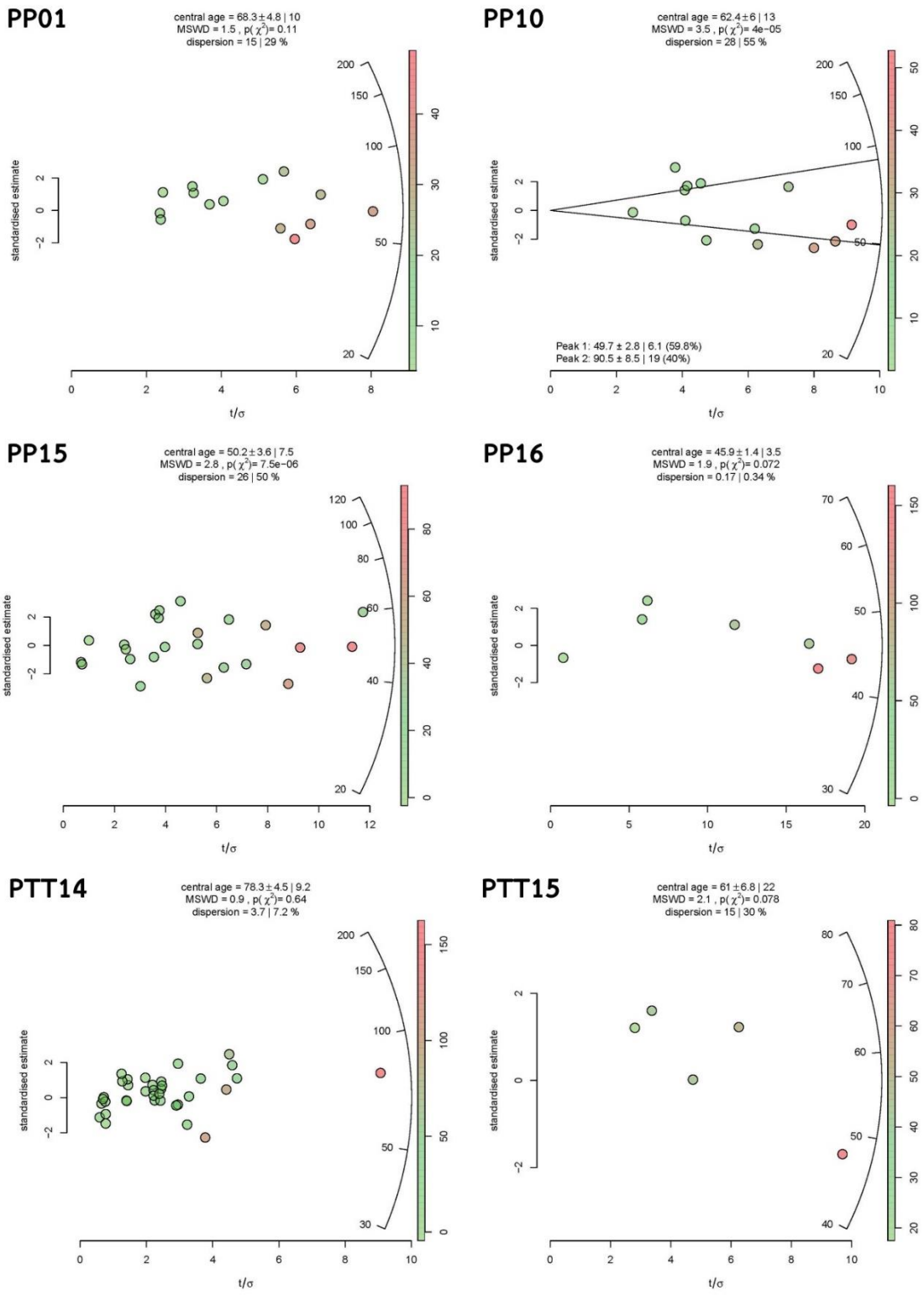

Figure 1 *Apatite fission track results illustrated on radial plots (Galbraith, 1990) for the Phu Phan Mountain Range. The plots were drawn using IsoPlotR[beta] (Vermeesch, 2017). The colour code displays uranium concentrations*

VITA

Mr. Apivut Veeravinantanakul was born in Bangkok in 1992. He studied at Suankularb Wittayalai School in Bangkok from 2004-2010. He graduated with a Bachelor Degree of Science (Geology) from Chulalongkorn University in 2014. After his graduation, he has continued his study in Master Degree of Science in Geology at Chulalongkorn University since July 2018.